

CO-OP AGREEMENT

UNIV. OF IDAHO

THESIS/
REPORTS

MILLER,

S.M

FINAL REPORT FOR COOPERATIVE AGREEMENT NO.
INT-88295-COA with
UNIVERSITY OF IDAHO
FS Contact: Carol J. Hammond
Co-op Contact: Dr. Stanley M. Miller

Development of Probabilistic Methods for a Three-Level Landslide Analysis System

Summary of Groundwater Modeling Studies

Summary Completion Report

Cooperative Research Agreement No. INT-88295

U.S.D.A.-Forest Service Intermountain Research Station

Moscow, Idaho

and

Department of Geology and Geological Engineering

University of Idaho

Stanley M. Miller

James G. Cuthbertson

K. Scott Kendall

November 1990

Development of Probabilistic Methods for a Three-Level Landslide Analysis System

Summary Completion Report

Cooperative Research Agreement No. INT-88295

U.S.D.A.-Forest Service Intermountain Research Station

Moscow, Idaho

and

Department of Geology and Geological Engineering

University of Idaho

Stanley M. Miller

James G. Cuthbertson

K. Scott Kendall

November 1990

Section 1

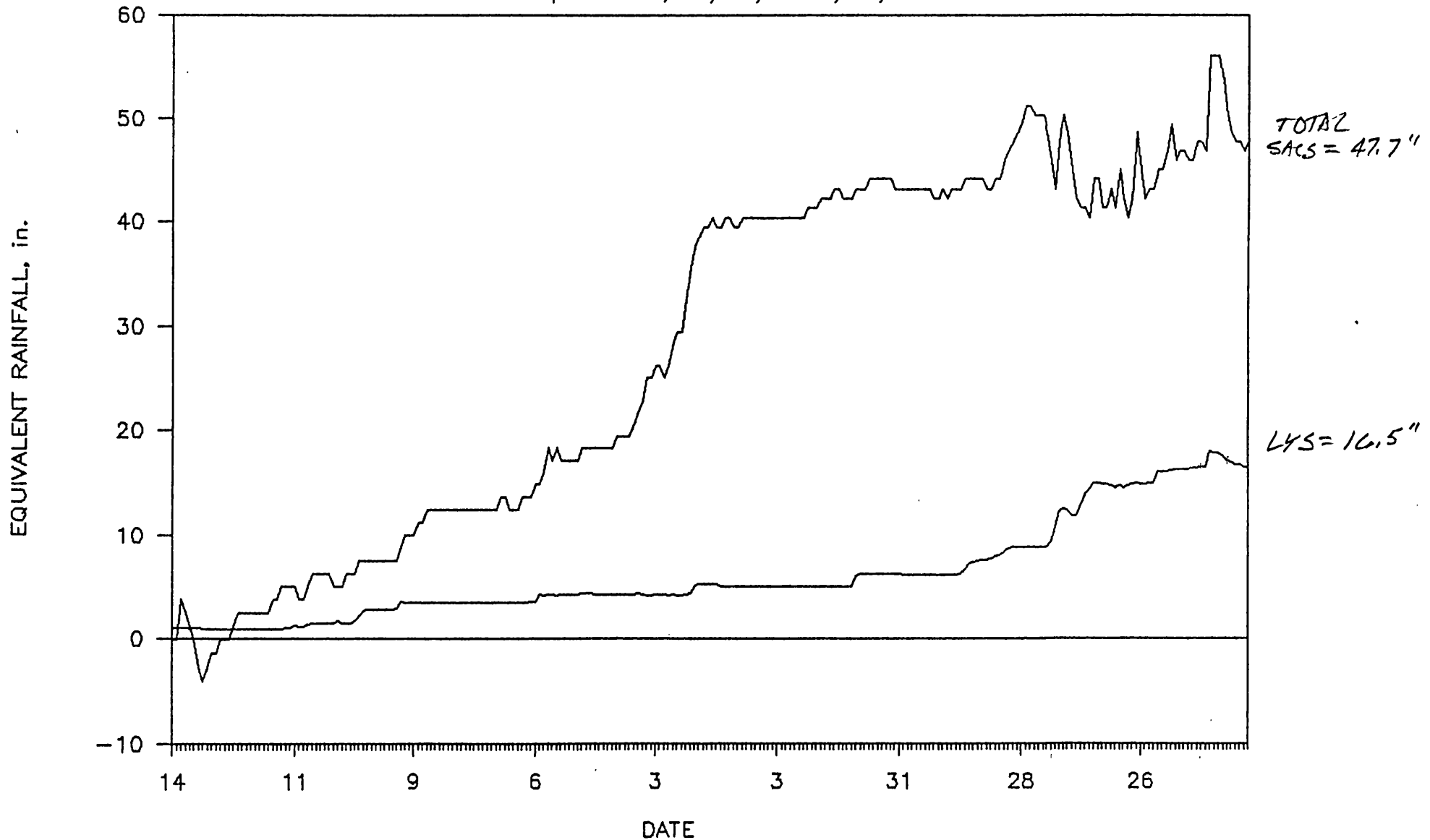
Summary of Groundwater Modeling Studies

Hydrologic Monitoring of Dan Lee Site, 1989

	Drill Holes with Piezometric Data*									
	2	3	4	8	11	17	22	32	35	37
Maximum net rise in piez. level (ft)	2.9	0.5	4.2	6.1	0.4	1.3	5.3	0.7	3.2	4.5
Seasonal accum. of equiv. precip. when maximum piez. level was observed (in.)	46.0	51.2	46.0	46.0	46.0	46.0	47.7	46.5	46.0	46.0
Seasonal accum. of water infiltration (in.):										
- - when maximum piez. level observed (in.)	8.5	8.3	8.5	8.5	8.5	8.5	16.7	9.8	8.5	8.5
- - six days prior to max. observed piez. level	7.5	7.5	7.5	7.5	7.5	7.5	16.3	9.0	7.5	7.5
- - six days after max. observed piez. level	9.0	8.8	9.0	9.0	9.0	9.0	17.3	10.2	9.0	9.0
Time interval of significant rise in piez. level (days)	92	57	88	80	55	84	87	58	103	92

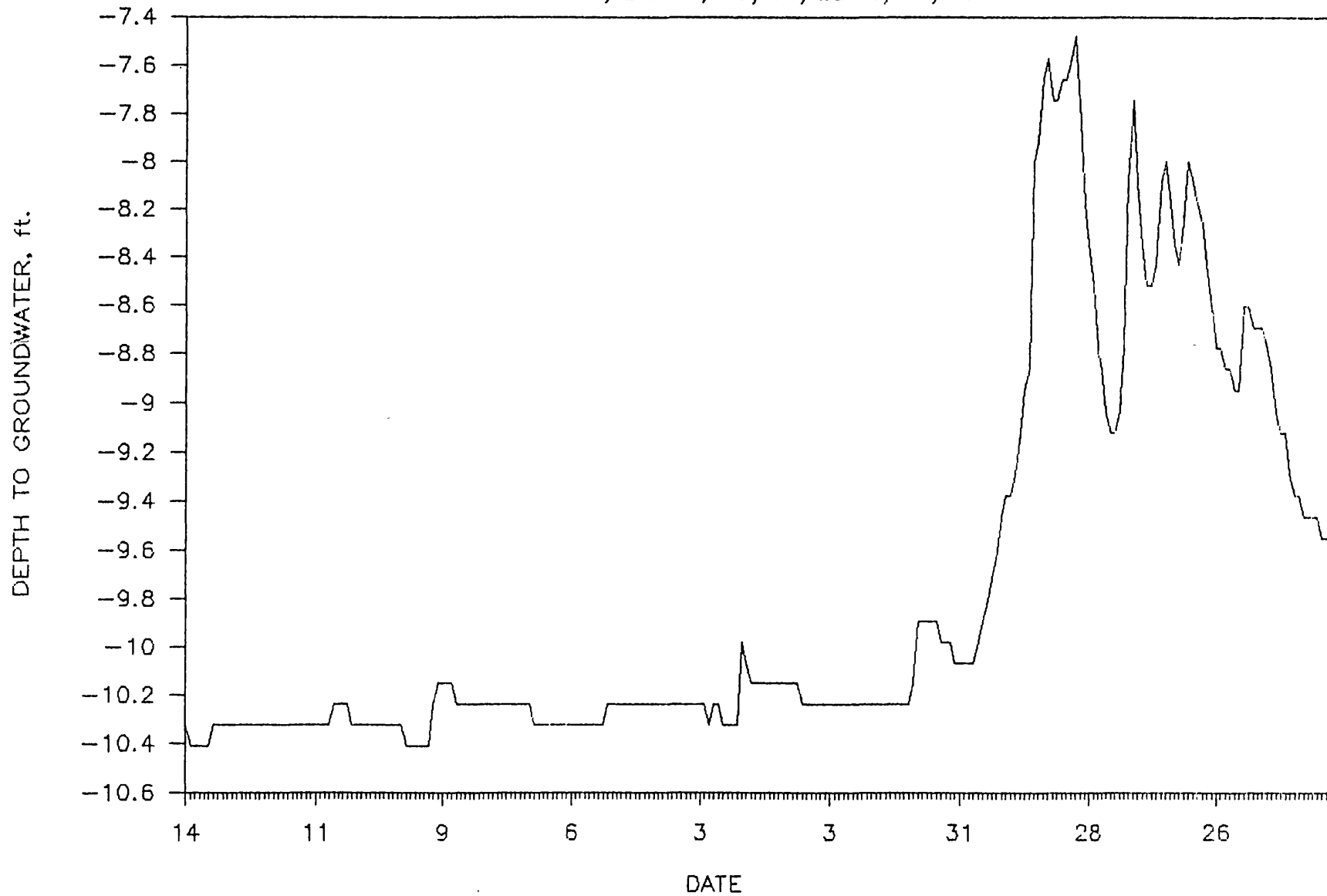
* Holes 13, 28, and 30 also were monitored, but no significant change in piezometric level was recorded.

CLEARWATER, DAN LEE,
Lower Precip. Station, 10/14/89-6/20/90



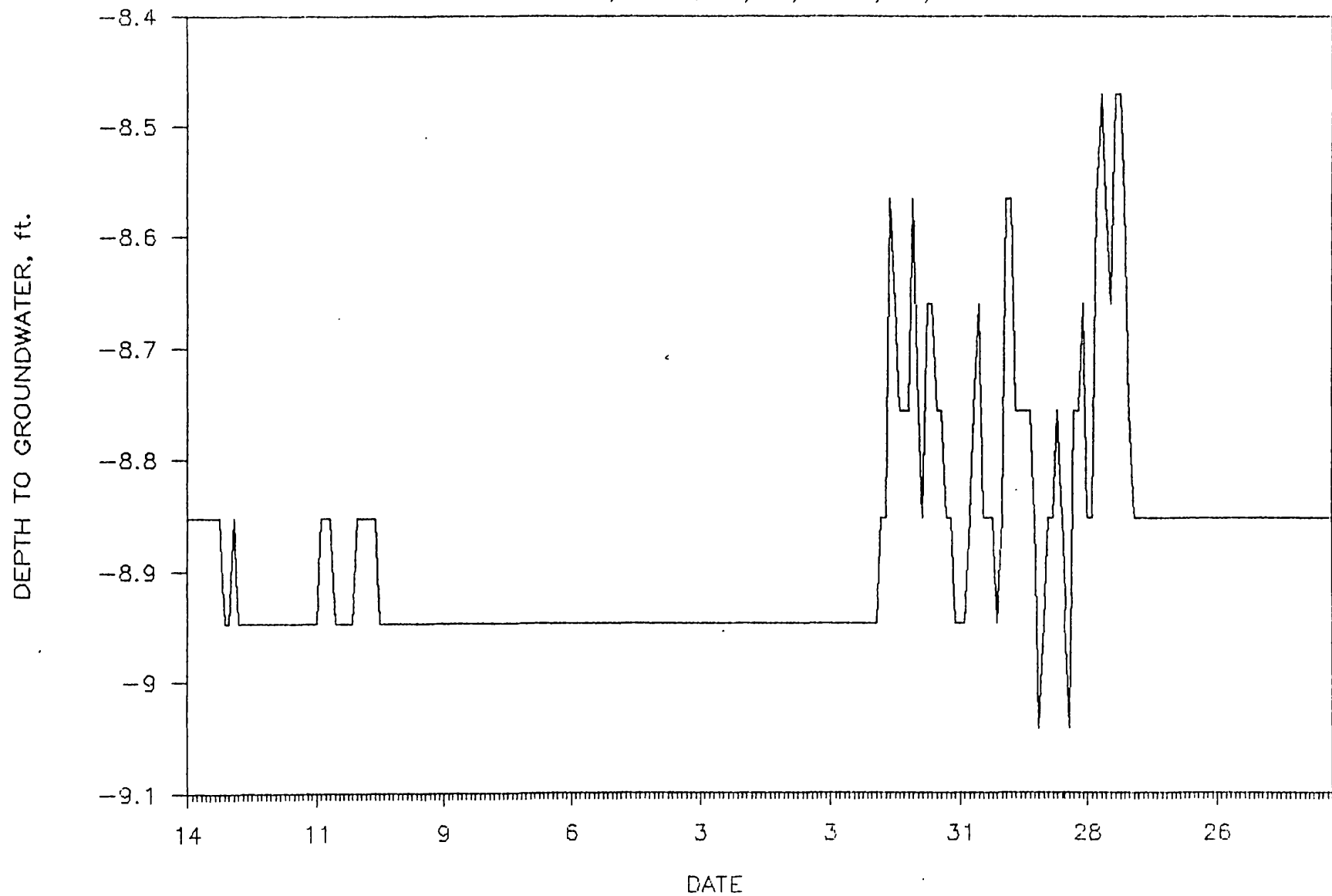
CLEARWATER, DAN LEE,

Groundwater, DH 02, 10/14/89-6/20/90

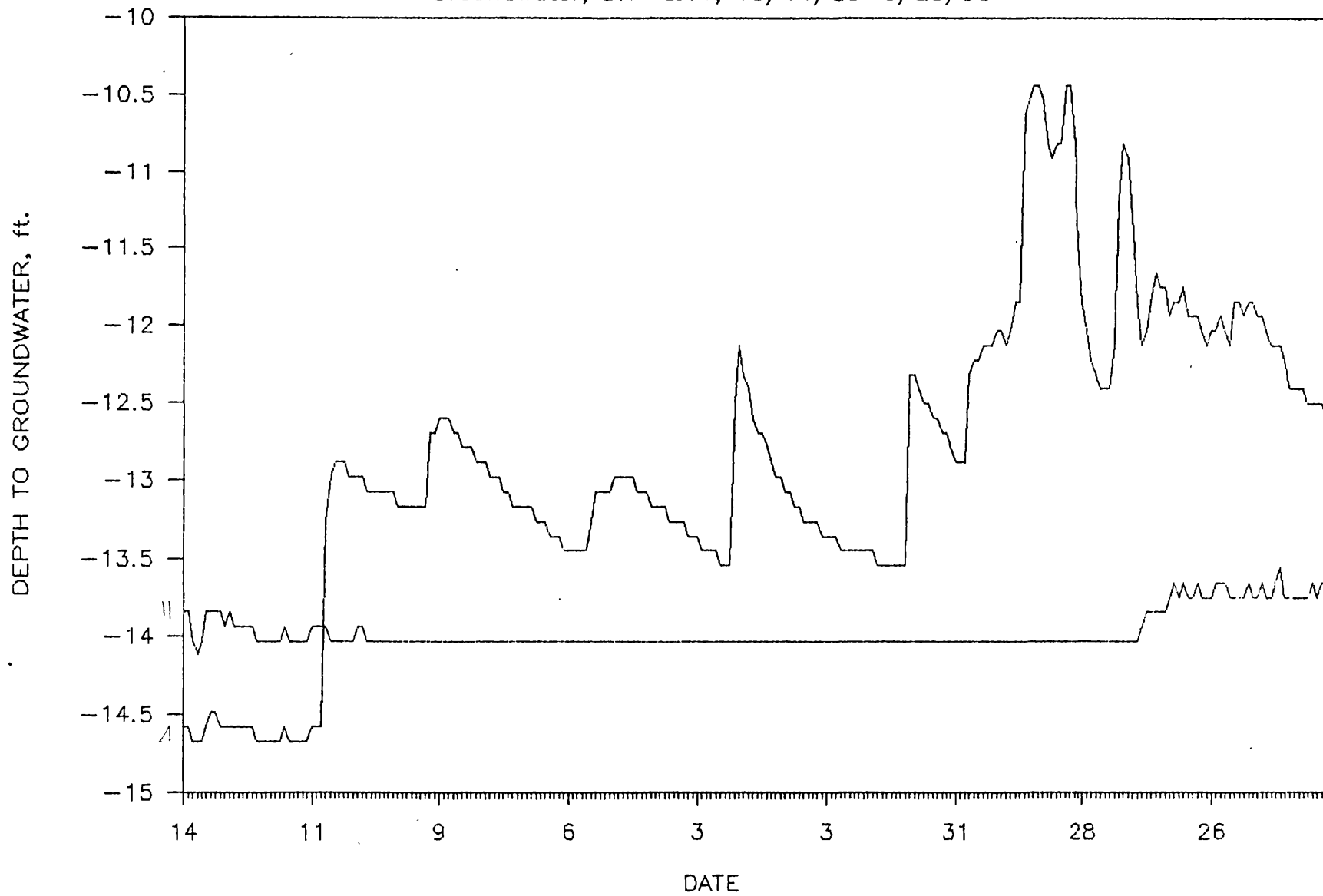


CLEARWATER, DAN LEE,

Groundwater, DH03, 10/14/89-6/20/90

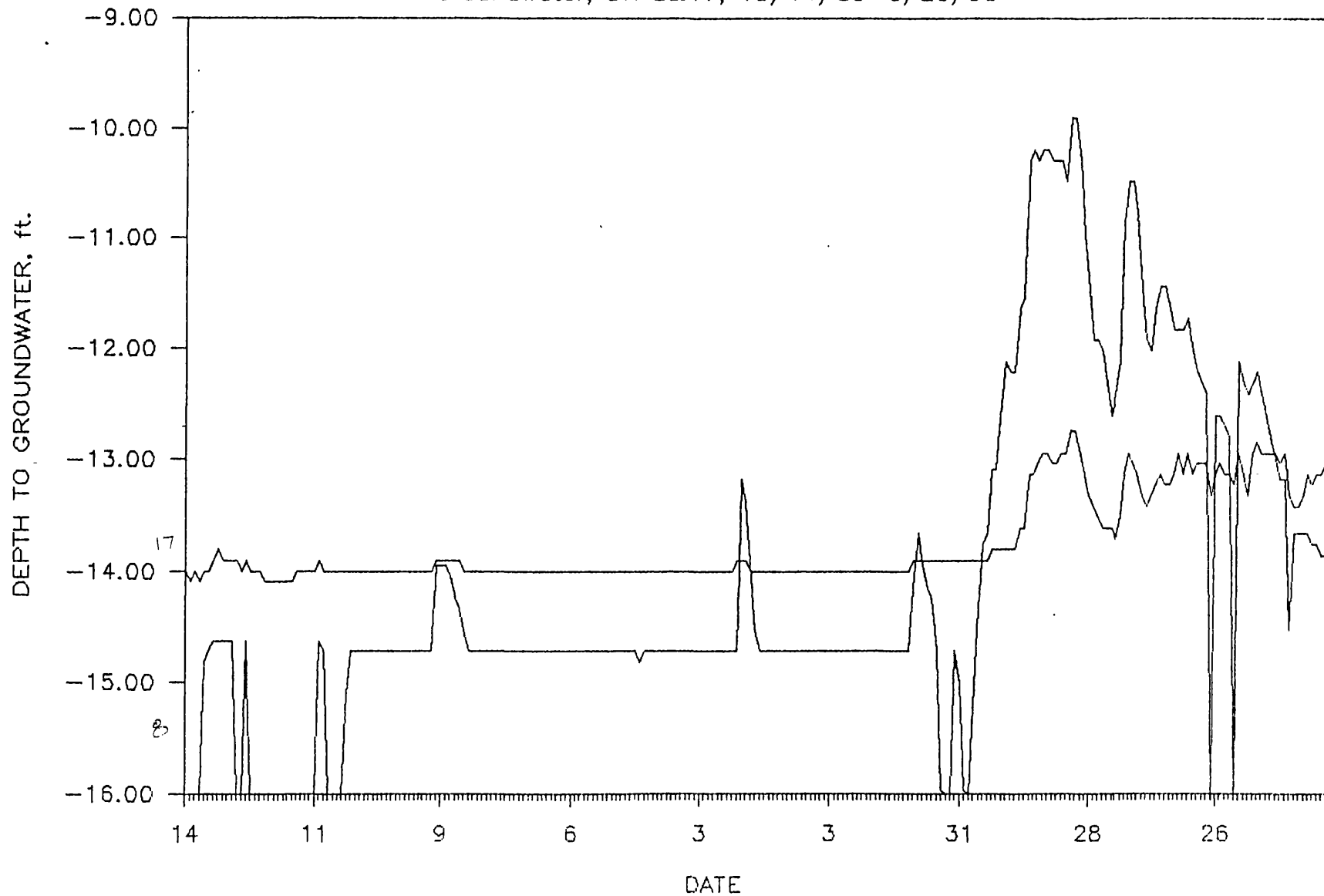


CLEARWATER, DAN LEE,
Groundwater, DH 4&11, 10/14/89-6/20/90

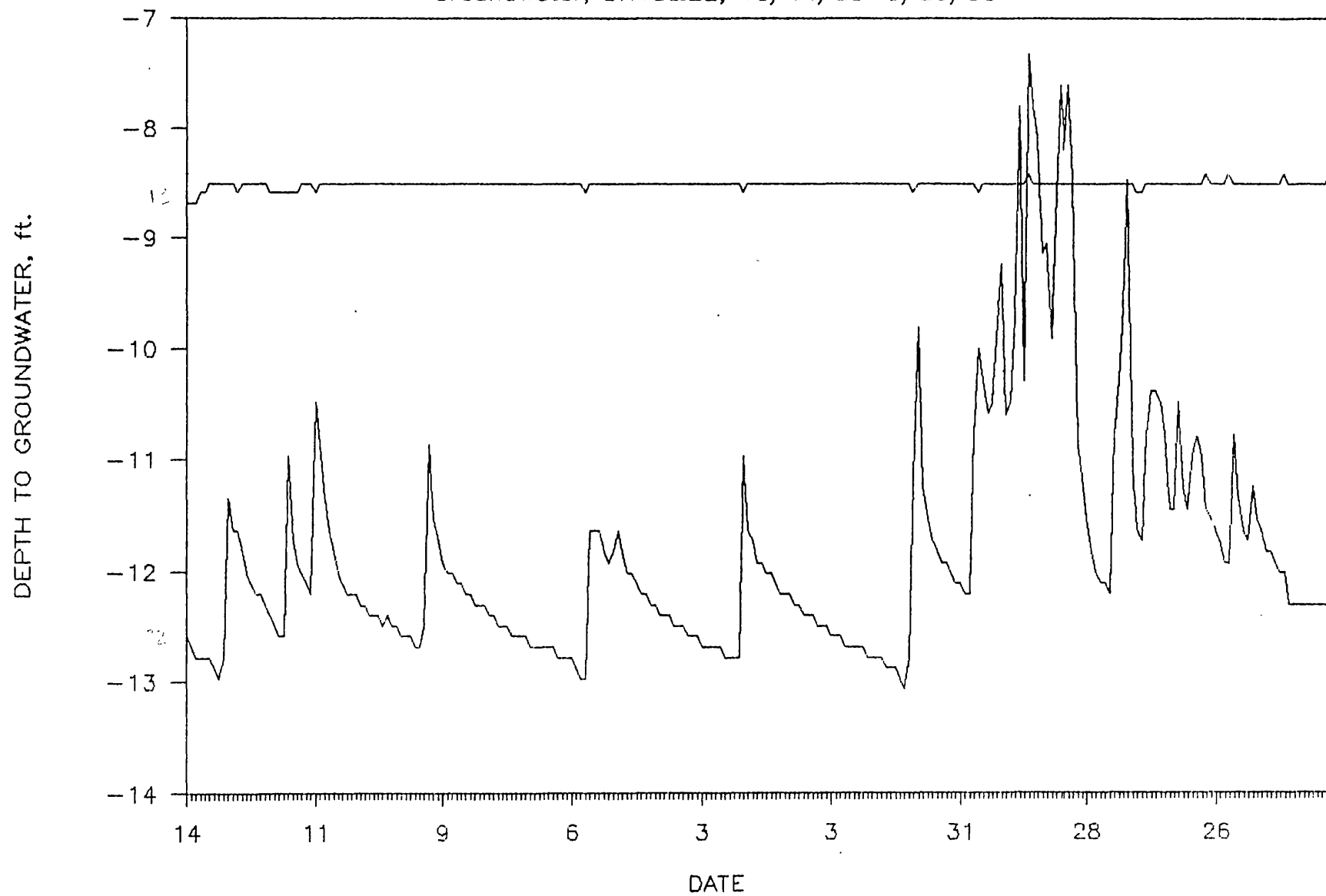


CLEARWATER, DAN LEE,

Groundwater, DH 8&17, 10/14/89-6/20/90

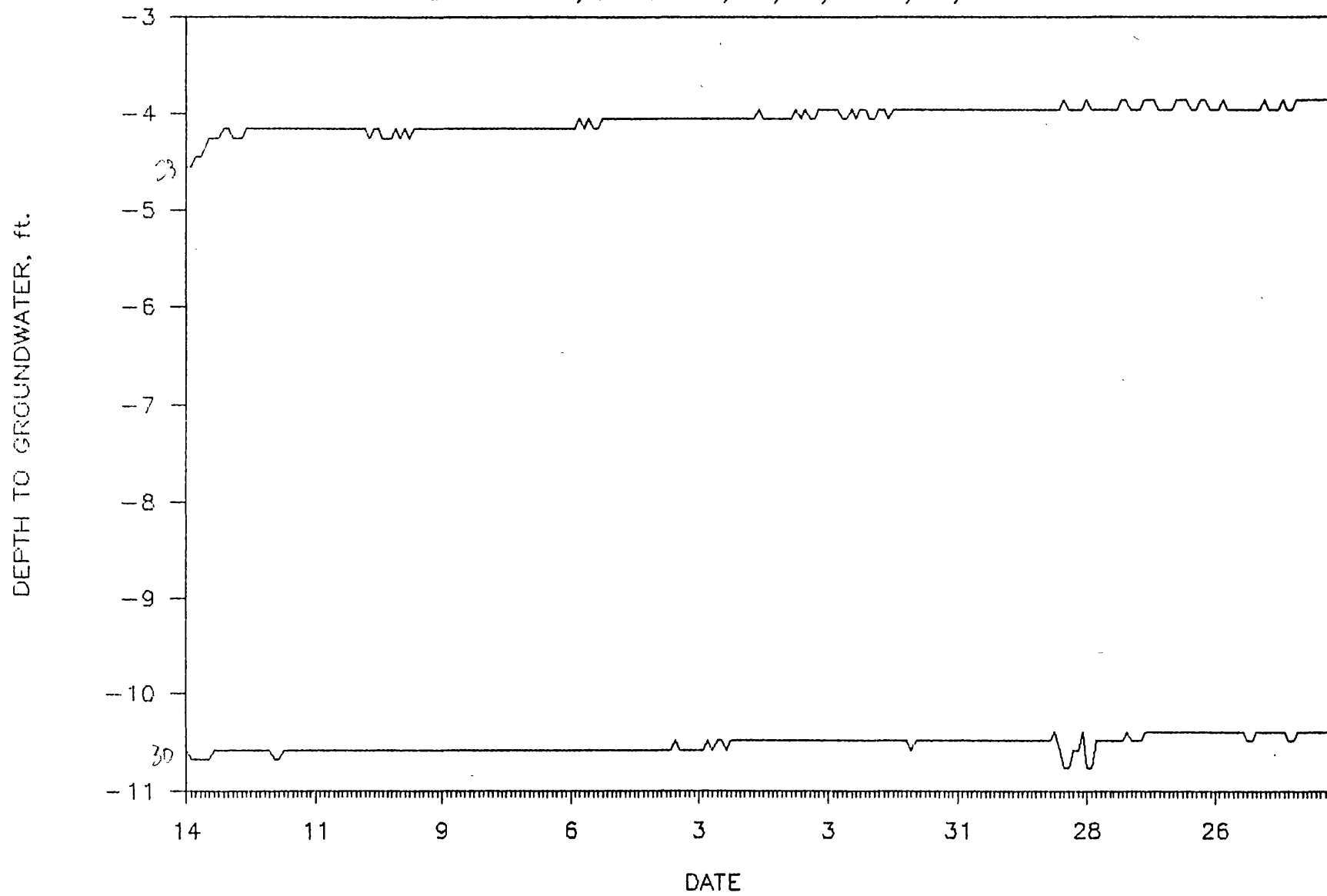


CLEARWATER, DAN LEE,
Groundwater, DH13&22, 10/14/89-6/20/90



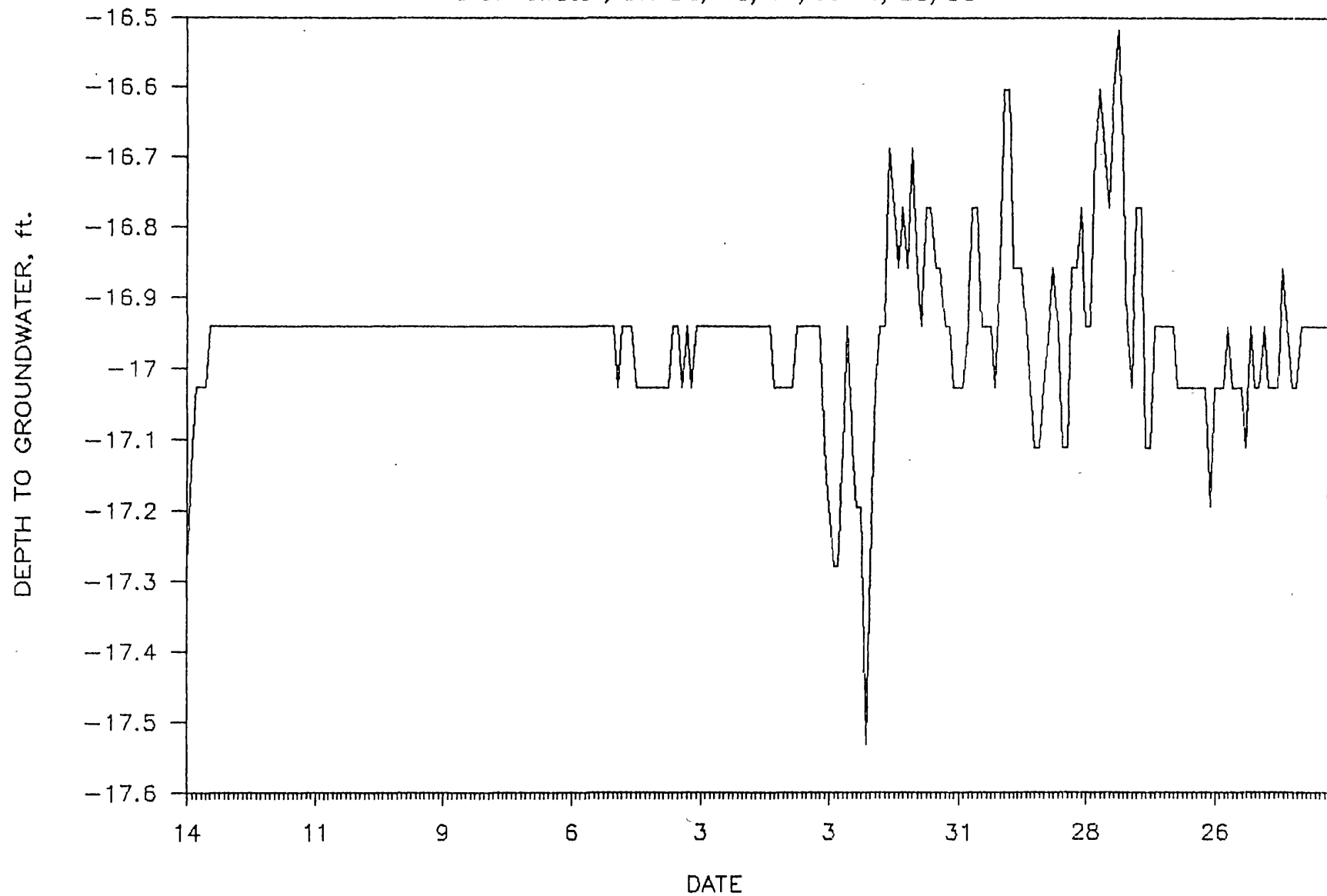
CLEARWATER, DAN LEE,

Groundwater, DH 28&30, 10/14/89-6/20/90



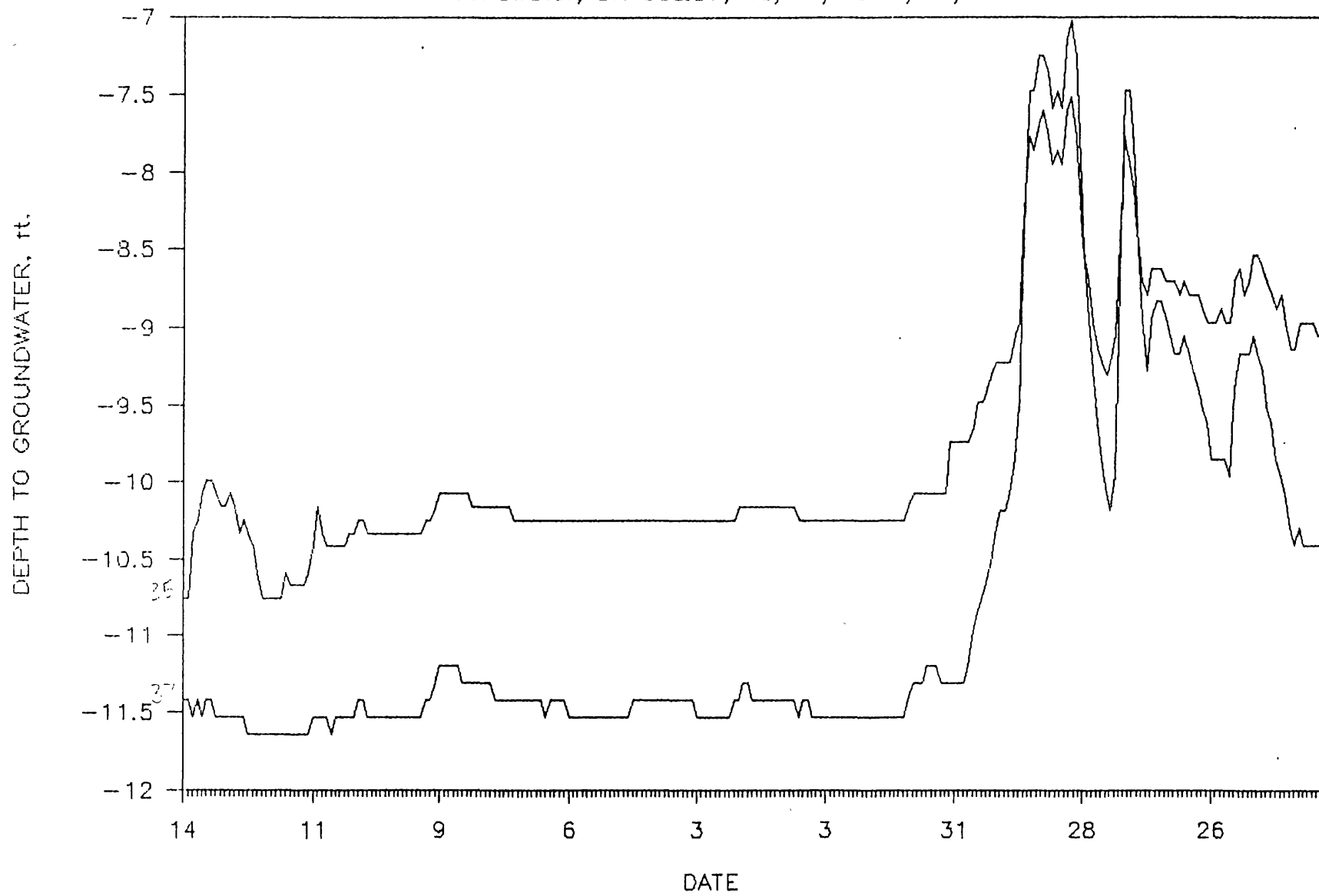
CLEARWATER, DAN LEE,

Groundwater, DH 32, 10/14/89-6/20/90



CLEARWATER, DAN LEE,

Groundwater, DH 35&37, 10/14/89-6/20/90



Hydrogeological Modeling
of
Two Drainage Basins,
Oregon Coast Range

J. Cuthbertson

CONTENTS

	Page
1. INTRODUCTION	1
1.1 Purpose of Project	1
1.2 Hydrogeologic Setting of the Coast Range, Oregon ..	1
2. HYDROGEOLOGICAL MODELING	2
2.1 Selection of a Groundwater Model	2
2.2 Description of the MODFLOW Model	4
2.3 Conceptual Model of a Hypothetical Coast Range Slope	5
3. MODELING PROBLEMS	10
3.1 Dry Nodes	10
3.2 Steady-State Conflicts with the Conceptual Model ..	11
4. CONCLUSIONS	15
5. UNSATURATED FLOW MODELS	15
5.1 UNSAT2	15
5.2 POREFLOW	16
REFERENCES	17
APPENDIX A; NARROW BASIN COMPUTER OUTPUT	18
APPENDIX B; WIDE BASIN COMPUTER OUTPUT	34

LIST OF FIGURES

Figure		Page
2.1	Description of the hypothetical slope used to evaluate the three computer models for the US Forest Service.	3
2.2	Contour plot of the narrow basin used for the simulations.	6
2.3	Three-dimensional plot with 10 foot contour lines superimposed showing the narrow basin geometry.	7
2.4	Contour plot of the wide basin used for the simulations.	8
2.5	Three-dimensional plot with 10 foot contour lines superimposed showing the wide basin geometry.	9
3.1	Plot of the steady-state heads along the central axis of the narrow basin.	12
3.2	Plot of the steady-state heads along the central axis of the wide basin.	13
3.3	Plot of the changes in head from the initial value of four feet calculated by MODFLOW for the steady-state conditions along the central axis.	14

1. INTRODUCTION

1.1 Purpose of Project

Increased pore-water pressure within soils on a steeply dipping slope will reduce the effective stress, decreasing the stability and possibly inducing failure of the soil mass. Increases in pore-water pressure are due primarily to the pressure head associated with water table fluctuations and to seepage forces caused by the velocity head associated with inclined groundwater flow.

Therefore, the purpose of this project was to model groundwater fluctuations (i.e., changes in hydraulic head) occurring within the soil profiles of two first-order drainage basins with two different soil depths and with varying storm intensities. The idea was to simulate conditions similar to those occurring during winter and spring in regions of the Oregon Coast Range. Principally, the simulations were used to estimate the storm intensity required to increase the hydraulic head to the point where the head was equal to or slightly more than the ground surface elevation.

1.2 Hydrogeologic Setting of the Coast Range

The Coast Range of Oregon, located in the western part of the state, extends from slightly south of Coos Bay northward to the Oregon/Washington border. Typical terrain includes steeply dipping, high-relief slopes ranging from 30° to 55° with thin soil mantles covered by dense understory brush and thick overstory stands of mixed timber. Stream valleys are narrow and separated by narrow ridges. Second-order and Higher-order streams actively downcut in the region.

Bedrock in the area is principally Tyee Formation, a 4,900 ft thick sequence of massive sandstone with interbeds of siltstone. Bedding seldom dips more than 20° and joints within the unit are widely spaced and tight (Pierson, 1977). Sills of basalt, doirite, nepheline syenite, gabbro, and camptonite intrude into the Tyee Formation in many places and frequently cap the higher peaks in the Coast Range.

Soils in the coast range are basically of two types, residual and colluvial. Residual soils are derived from the Tyee Formation and are found on relatively flat surfaces such as ridge crests, benches, and valley bottoms. Steep hillslopes have colluvial soils, which are the focus of this project.

The colluvial soils range in thickness from a minimum of several inches to a maximum of approximately 10 ft, with a typical range of 2 to 6 ft. Soil classifications for the colluvial soils range from GP to ML in the Unified Soil Classification system, hydraulic conductivity estimates are from one to ten feet per day.

The climate of the coast range is maritime with warm dry summers and wet mild winters. Annual rainfall is from 60 to 140 in at the higher inland elevations, with approximately 90% of the yearly precipitation occurring between October and May in the form of rain (Pierson, 1977). Snow accumulates only occasionally in the higher elevations and does not persist. Winter storms are typically long duration, low intensity events with 2-year, 24-hour design storms ranging from 3 to 5 inches, and 25-year, 24-hour design storms ranging from 5 to 9 inches.

2. HYDROGEOLOGICAL MODELING

2.1 Selection of a Groundwater Model

Previous modeling of slopes similar to those in the Coast Range has been conducted for the USDA-FS (Cooperative Agreement No. INT-88295, 1988) by the Department of Geology and Geological Engineering at the University of Idaho. The modeling was done as an overview of selected groundwater flow models for their later use in modeling steep slopes. Two saturated flow models, MODFLOW and PLASM, and one unsaturated flow model, UNSAT2, were evaluated.

The three computer models were used to model a simple soil slope with a two-dimensional flow regime characterized by down-slope flow with horizontal and vertical components (Figure 2.1). Results of the preliminary simulations indicated that both MODFLOW and PLASM can simulate 20 to 40 ft thick aquifers on slopes as steep as 63° without numerical instabilities developing. However, steep slopes require a finer grid and smaller time steps for satisfactory model performance. It should be noted that even though the simulations were two-dimensional, both MODFLOW and PLASM are capable of modeling three-dimensional flow.

The third model evaluated was UNSAT2. This model is a variably saturated two-dimensional flow model capable of modeling unsaturated flow conditions. This capability requires significantly more data in order for the

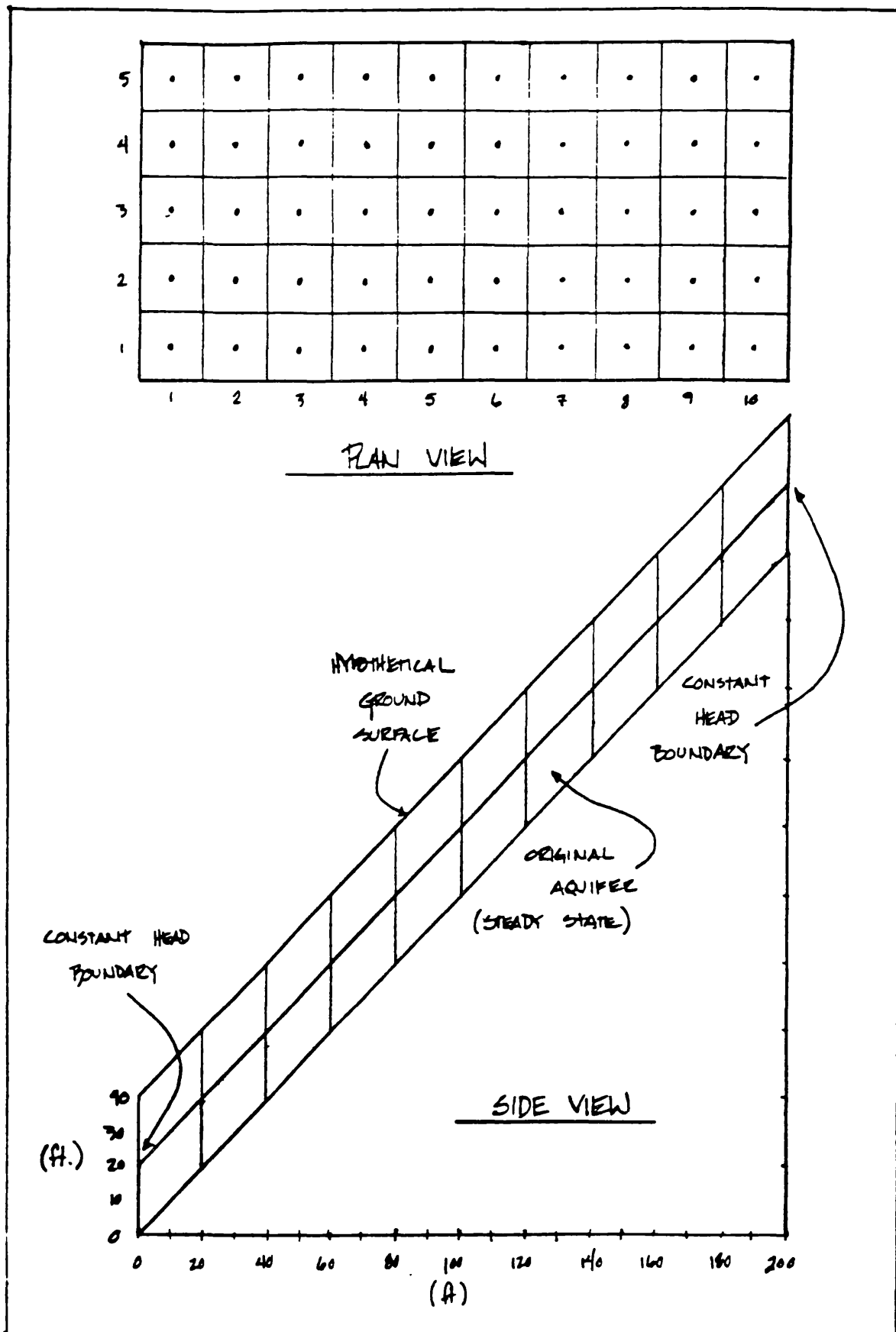


Figure 2.1. Description of the hypothetical slope used to evaluate the three computer models for the US Forest Service.

model to be effective. Often these data are unavailable without laboratory testing. Also, this model is a two-dimensional model which limits its use to a single vertical plane for a steeply dipping slope. For these reasons, this model was considered to be generally inappropriate for modeling slopes in the Coast Range. Therefore, one of the saturated flow models seemed to offer the most promise for successfully modeling soil hydraulics on steep slopes.

MODFLOW was selected for use over PLASM because of the pre-processor and post-processor programs available for the MODFLOW program. Both PLASM and MODFLOW require extensive data files, and the capability of a program to create and alter data files is a definite advantage.

2.2 Description of the MODFLOW Model

MODFLOW is a three-dimensional, block centered, saturated flow model, which uses finite-difference techniques to solve groundwater flow problems. McDonald and Harbaugh (1984) developed the model for the United States Geological Survey (USGS).

The model is modular in format. Similar program functions are grouped together while specific computational and hydrogeological options remain independent of other options. Using this format, a hydraulic model is constructed by adding the necessary components to describe the hydrogeology to the basic components describing the discretization of space and time. The components available to describe the hydrogeology include the following descriptive packages:

1. Well package, both recharge and discharge wells.
2. River package.
3. Drain package.
4. Areal recharge package.
5. Evapotranspiration package.
6. General head boundary package.

The computer model uses these components with the general three-dimensional groundwater flow equation to solve both two-dimensional and three-dimensional flow problems for multiple layers, confined aquifers, unconfined aquifers, or any combination. The model can use two different solution algorithms to solve the general groundwater flow equation, enabling the program to run on a stand personal computer:

1. Strongly implicit solution (SIP).
2. Slice successive over-relaxation method (SSOR).

Data required for use by the program during the simulation include:

1. Definition of boundary nodes.
2. Initial head values.
3. Length of stress periods.
4. Number of stress periods.
5. Time step multiplier.
6. Anisotropy ratios.
7. Cell lengths and widths.
8. Storativity/specific yield.
9. Hydraulic conductivity along rows and columns.
10. Vertical hydraulic conductivity.
11. Aquifer bottom elevation.
12. Recharge rates.

Several output options are available for the model, including printouts of the initial head values, final head values, drawdown at each node, and cell-by-cell flow terms at each time step. In addition, the head values also can be stored on a disk for use in other graphics programs.

2.3 Conceptual Model of a Hypothetical Coast Range Slope

One basic hillslope was used to simulate groundwater flow on steep slopes in the coast Range. The basic hillslope was designed to simulate a narrow first-order catchment basin commonly found slightly below ridge crests in the Coast Range. these catchment basins typically are inclined at 45° to 55° along their axis perpendicular to the ridge crest and have side slopes which dip into the central or drainage axis at approximately 15° to 30°, forming a bowl-shaped depression.

Our basic hillslope model represents a narrow basin with a maximum side slope of 25° and an average axis inclination of 45° (Figures 2.2 and 2.3). Nodes spaced at 4 ft intervals in both the X-direction and Y-direction were used to discretize the slope for the model. Changing the X-axis nodal spacing in the MODFLOW model from 4 ft to 8 ft reduces the side-slope angle to 15° while preserving the axis angle of 45°, thus modeling a wide basin (Figures 2.4 and 2.5). Both slopes are symmetrical about the drainage axis. Therefore, the MODFLOW model requires only one half of the basin for the simulations.

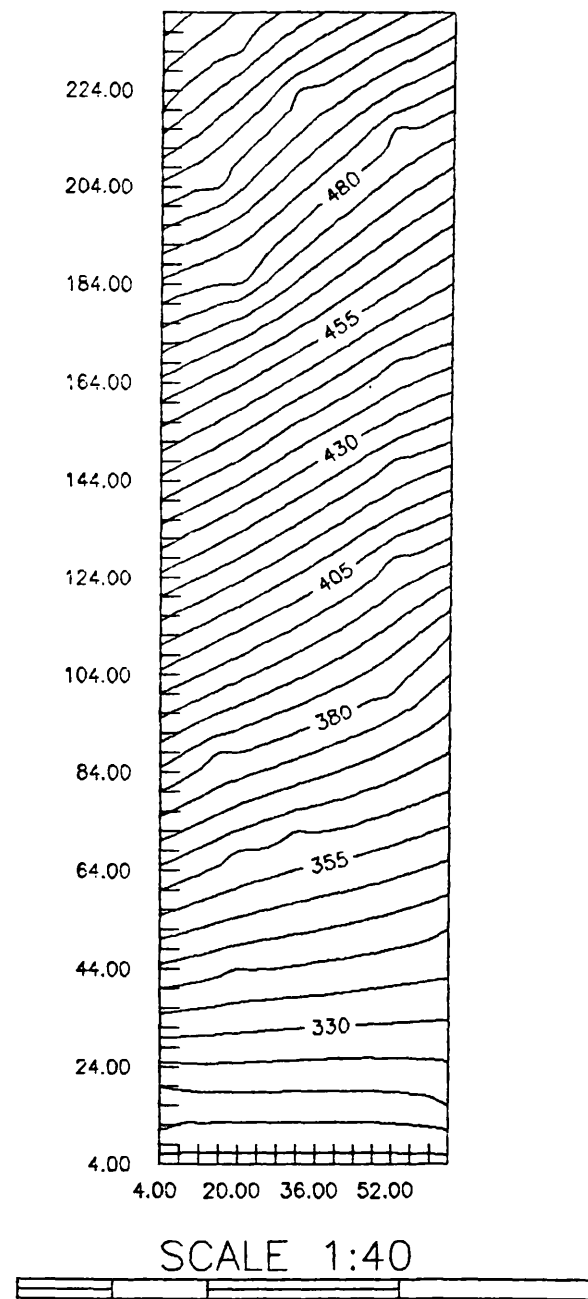


Figure 2.2. Contour plot of the narrow basin used for the simulations.

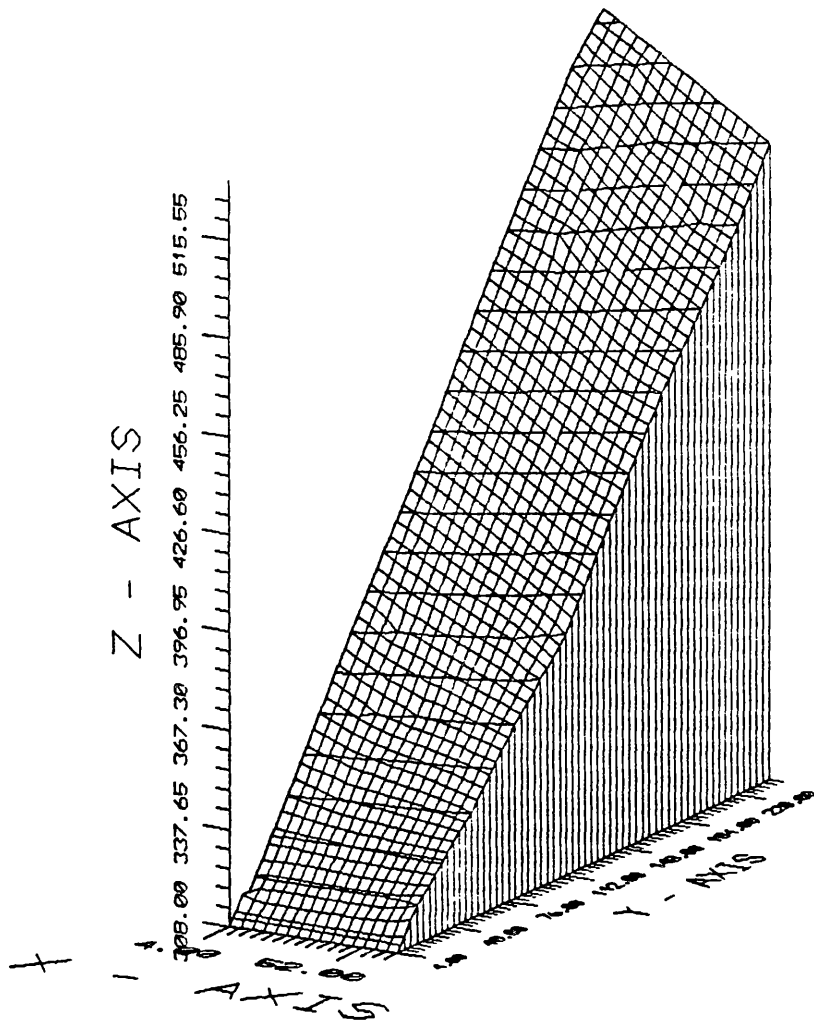


Figure 2.3. Three-dimensional plot with 10 foot contour lines superimposed showing the narrow basin geometry.

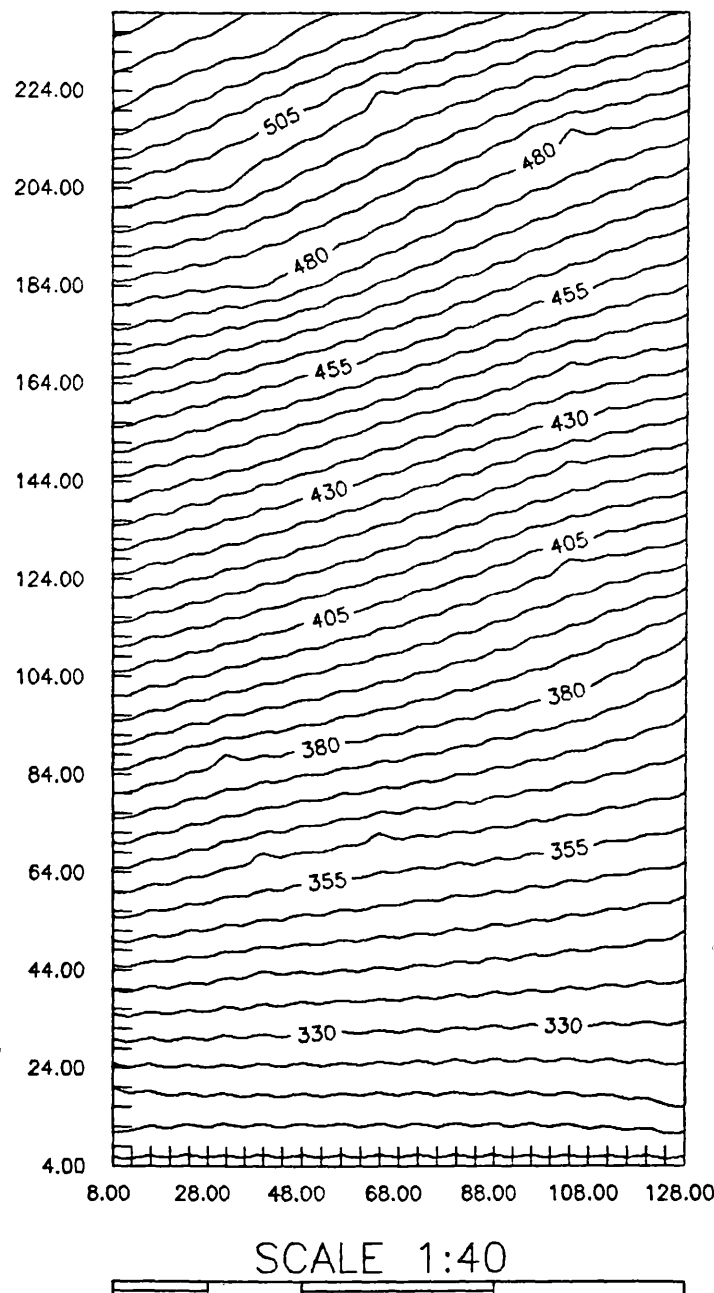


Figure 2.4. Contour plot of the wide basin used for the simulations.

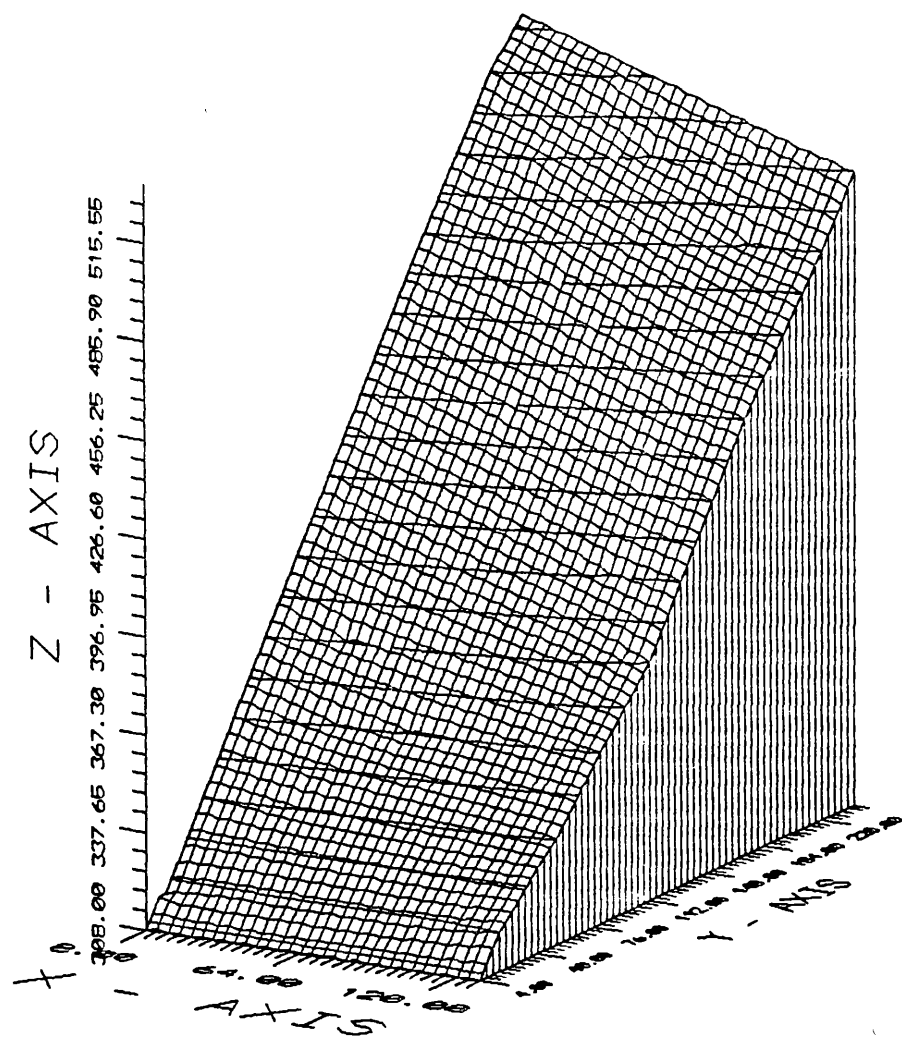


Figure 2.5. Three-dimensional plot with 10 foot contour lines superimposed showing the wide basin geometry.

The basic catchment basin model used for the simulation is 16 nodes wide by 60 nodes long. this nodal arrangement models one half of the basin, which would actually be 32 by 60 nodes in size. The narrow basin model has a nodal spacing of 4 ft, making the total horizontal area of the narrow catchment basin 64 by 240 ft. The wide basin has nodal spacing of 8 ft perpendicular to the basin axis and 4 ft parallel to the drainage axis, making the horizontal area 128 by 240 ft.

Soil properties are consistent with the colluvial soils of the area, primarily a gravel-sand-silt mixture with a hydraulic conductivity of 5 ft per day. Soil depths of 5 ft and 10 ft are considered representative soil depths for the model, because a depth of 5 ft is roughly in the middle of the soil depth range and 10 ft is typically the maximum value encountered.

MODFLOW models an unconfined aquifer as the saturated portion of an infinitely thick soil profile. The saturated zone does not have an upper elevation limitation, and the soil thicknesses modeled on the slope by the MODFLOW program are the same as the hydraulic head of the water in the slope. The model requires an initial head value as a seed for its calculations. The initial heads used in the simulation were 4 ft above the impermeable layer, (bedrock, in this case), making the initial model soil thickness 4 ft. Consequently, a rise in head of 2 ft would be equivalent to having 6 ft of saturated soil on the slope.

Steady-state flow conditions are required as a reference point to which the head fluctuations due to a storm event can be compared. Without the steady-state conditions the fluctuations due to a storm event are meaningless. It is in defining the steady-state flow conditions that problems occur with the model. Appendices A and B contain the output from two steady-state simulations.

3. MODELING PROBLEMS

3.1 Dry Nodes

The MODFLOW program is a saturated flow model. this requires that any particular node maintains a head value in excess of the node elevation (i.e., all nodes must contain water). After the water is drained from any node, that

node becomes inactive; all flow into and out of the node is halted. This sets up a "domino effect", and the nodes immediately surrounding the dry node subsequently become inactive.

The Coast Range basin simulations had severe problems with the nodes becoming dry. Many of the nodes became dry within minutes after the start of the simulation. This problem is due to two directions of flow, high hydraulic conductivity, and shallow soils with little storage capacity.

Two methods can be used to solve the problem of dry nodes. First, the hydraulic conductivity can be decreased by several orders of magnitude to prevent rapid draining of the node, thus altering the conceptual model significantly. Secondly, enough water must be supplied to keep the system saturated. To achieve this, it is necessary to place constant-head nodes around three sides of the model. Consequently, two sides of the model have an infinite source of water flowing into the slope, and the bottom of the slope has an infinitely deep bucket into which water can drain.

Both methods have advantages and disadvantages. Altering the hydraulic conductivity changes the aspect of the model. A model with a much lower hydraulic conductivity will not accurately simulate the gravelly/sandy soils of the Coast Range, and therefore, this method was eliminated as a possible solution. Conversely, providing an infinite source of water also creates problems. However, it was hoped that these problems would be minimal and that the conceptual model of a saturated slope could be used.

3.2 Steady-State Conflicts with the Conceptual Model

With an infinite source of water, the model remains saturated, but the steady-state head values along the central axis exceed the conceptual model's ground surface elevations of 5 ft and 10 ft for both basin configurations. Figures 3.1 and 3.2 show the values of the steady-state heads in relation to the soil profiles for both basins. Note that dividing the basin into two halves along the central axis causes the head changes calculated by the model in achieving steady-state to be the minimum head changes which could occur (see Figure 3.3). The maximum head changes along the axis could be twice the value determined by the simulation due to lateral water flow from the other half of the basin.

STEADY STATE HEADS
FOR NARROW BASIN GEOMETRY
ALONG CENTRAL AXIS

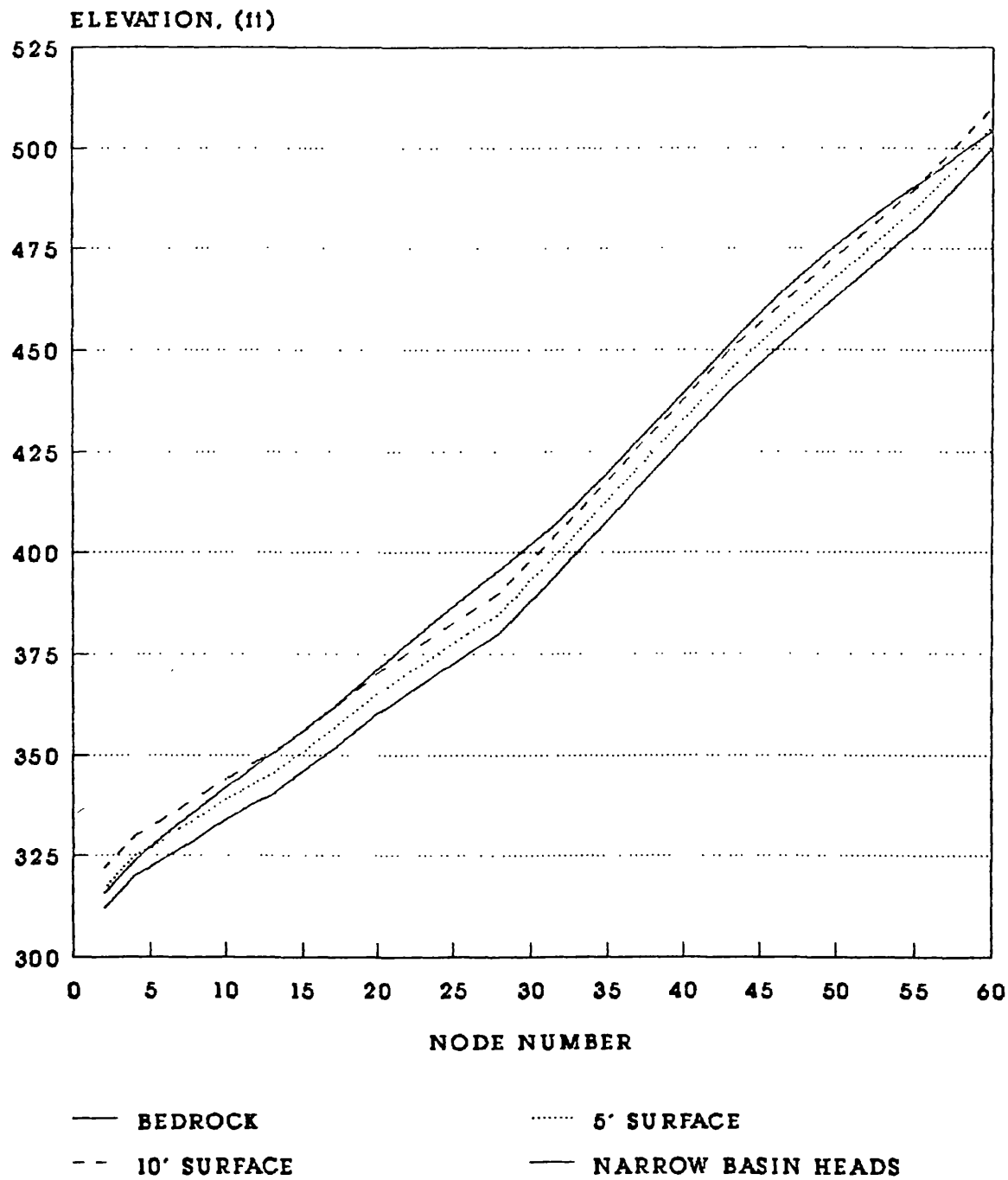


Figure 3.1. Plot of the steady-state heads along the central axis of the narrow basin.

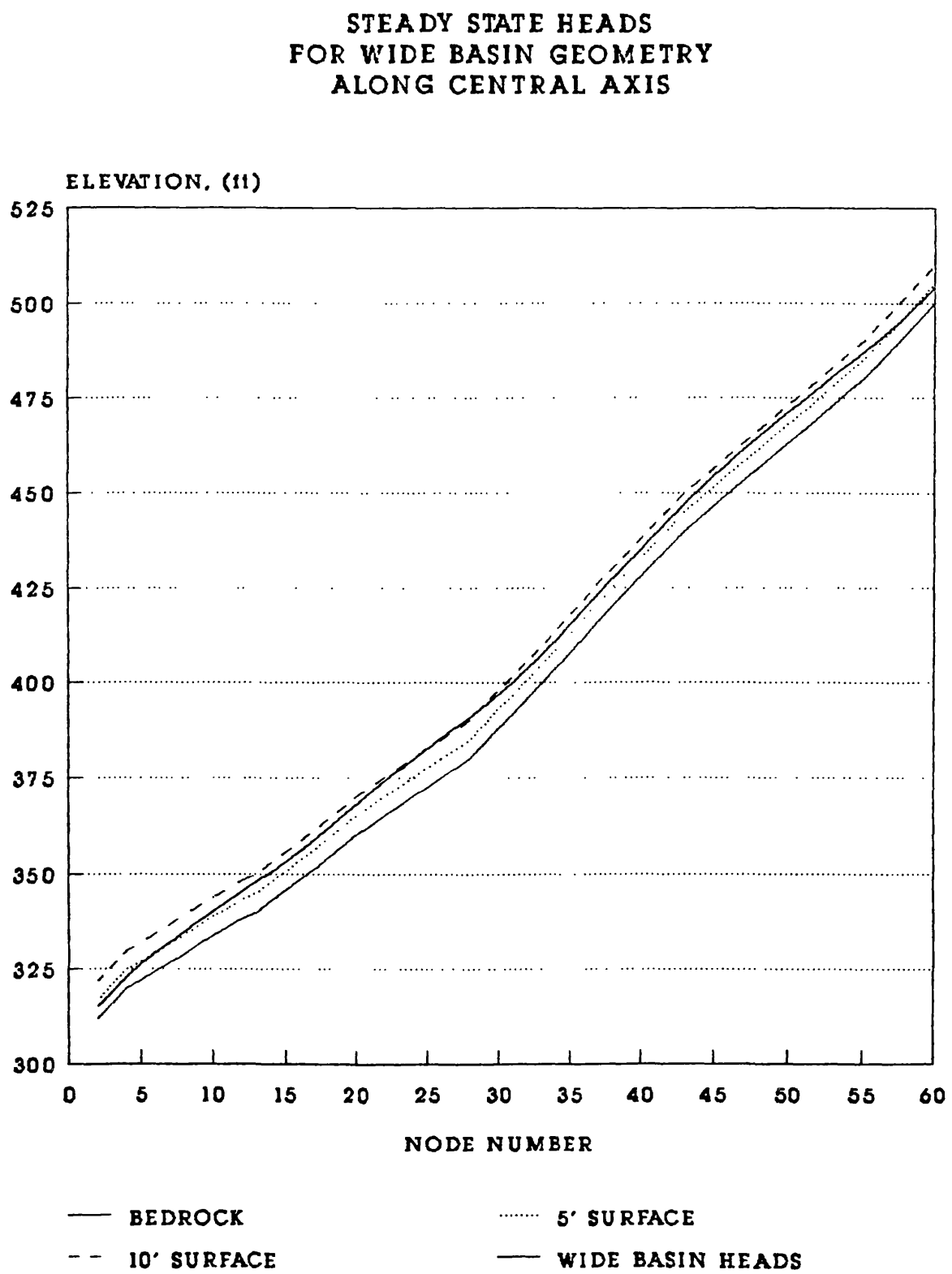


Figure 3.2. Plot of the steady-state heads along the central axis of the wide basin.

HEAD FLUCTUATIONS FROM FOUR FEET
TO ACHIEVE STEADY STATE

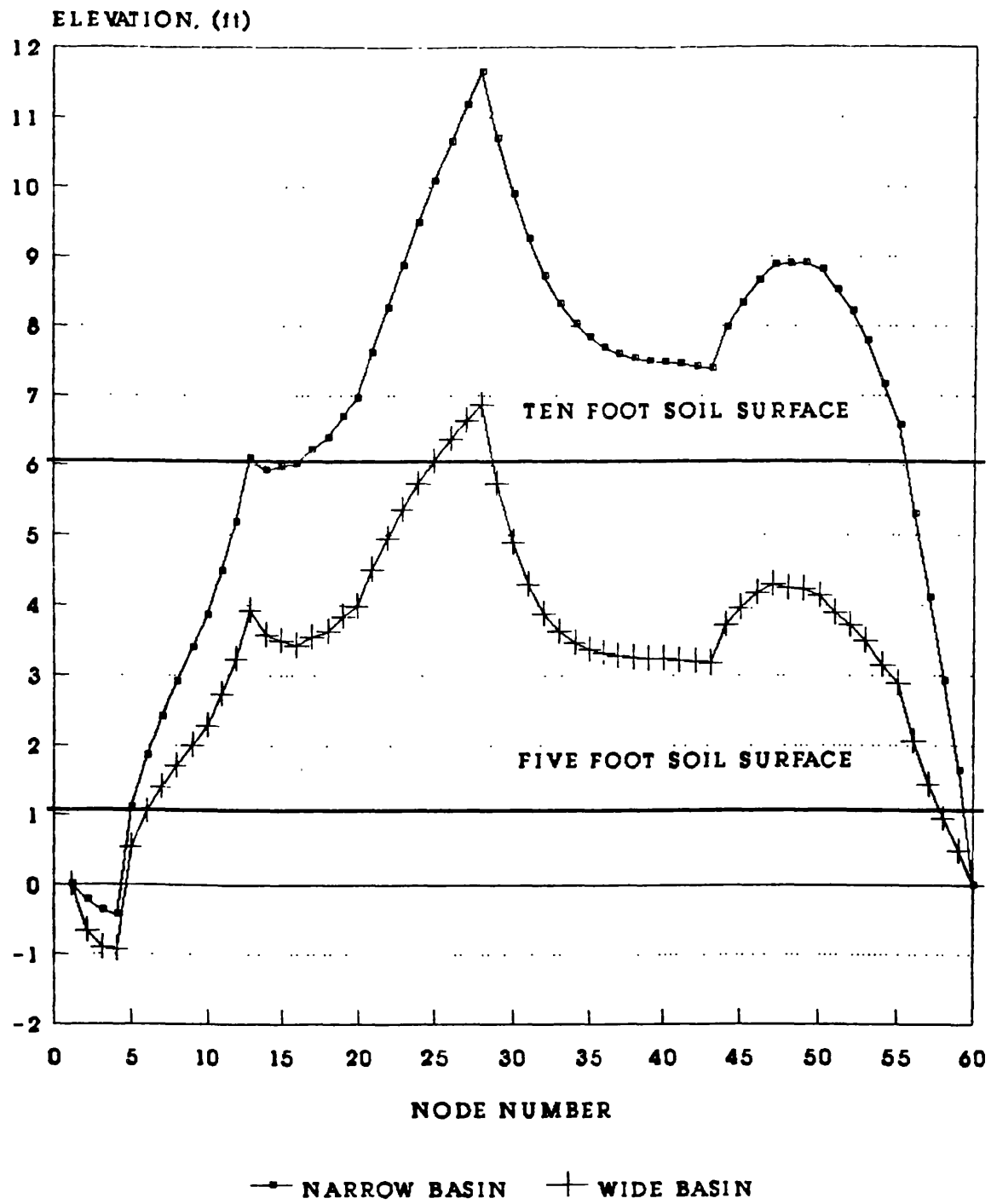


Figure 3.3. Plot of the changes in head from the initial value of four feet calculated by MODFLOW for the steady-state conditions along the central axis.

Having the head values greater than 10 ft would be acceptable if the simulated conceptual model had greater than 10 ft of soil. With 20 ft of soil the constant-head node solution may be acceptable (and thus, the success of previous studies at the University of Idaho that show promise for using MODFLOW). However, the slopes in the Coast Range usually have a maximum of 10 ft of soil on them. Typically, soil thicknesses range from 2 to 6 ft. Therefore, providing an infinite source of water is not acceptable, and the steady-state conditions determined for soils less than 10 ft thick are not useful.

4. CONCLUSIONS

In overcoming the limitations of this MODFLOW application by using constant-head nodes to force a saturated model, the conceptual model is altered. The steady-state conditions estimated by MODFLOW in this project are unsatisfactory for use in modeling the head response due to storm events in the shallow soils of the Coast Range.

The MODFLOW model itself is not at fault. The program would probably be satisfactory if the soils in the Coast Range were thicker. The problem arises in trying to force a model to simulated conditions which in all likelihood do not exist. Conceptually, the slopes of the Coast Range are not saturated between storm events due to coarse, well-drained soils on steeply dipping slopes. The only time that a slope could possibly remain saturated between storm events separated by several days or weeks would be if springs were present. The MODFLOW model supported this hypothesis by running itself dry while trying to simulate steady-state conditions in the early runs of the model. As a result, an unsaturated three-dimensional flow model may be best suited to model the slopes of the Coast Range.

5. UNSATURATED FLOW MODELS

5.1 UNSAT2

DeGroot (1987) developed a method that uses sectional partitioning to model three-dimensional flow using the two-dimensional UNSAT2 model. The method uses convergent, divergent, and parallel sections to divide the

watershed into manageable pieces. The parallel sections have two-dimensional flow fields and are modeled as usual by the two-dimensional UNSAT2 model. The width of the seepage face, horizontal planar area, and average horizontal flow path for the divergent and convergent sections are mathematically related to the geometric properties of circular sectors. The flow within the sections then is simulated using radial flow assumptions and the equivalent circular sector. De Groot successfully used this method to simulate the outflow from a first-order watershed in central Idaho, and this method also may be successful in modeling the head fluctuations due to storm events.

5.2 POREFLOW

POREFLOW is a three-dimensional unsaturated flow model currently under development by Battelle, Pacific Northwest Division (Smoot, 1990). The program is currently proprietary and access to it is limited. However, this program may be satisfactory for modeling the slopes of the Coast Range and may warrant further inquiries.

REFERENCES

DeGroot, Philip H., 1987, *Simulation of Variably Saturated Subsurface Flow by Sectional Partitioning (Idaho)*: Ph.D. Dissertation, Utah State University, 148 p.

Department of Geology and Geological Engineering, University of Idaho, 1988, *Progress Report for USDA-FS Cooperative Agreement Number INT-88295, Development of Probabilistic Methodologies for Three-Level Landslide Analysis System*, unpublished paper.

Huyakorn, P. S., Jones, G. B., and Andersen, P. F., 1986, *Finite Element Algorithms for Simulating Three-Dimensional Groundwater Flow and Solute Transport in Multilayer Systems*, Water Resources Research, v. 22, no. 3, pp. 361-374.

Huyakorn, P. S., Springer, E. P., Guvansen, Varut, and Wadsworth, 1986, *A Three-Dimensional Finite-Element Model for Simulating Water Flow in Variably Saturated Porous Media*, Water Resources Research, v. 22, no. 13, pp. 1790-1808.

McDonald, M. G., and Harbough, A. W., 1988, *A Modular Three-Dimensional Finite-Difference Ground-Water Flow Model*, Techniques of Water-Resources Investigations of the United States Geological Survey, Book 6, Chapter A1; US Geological Survey Groundwater Branch, Reston, Virginia.

Pierson, T. C., 1977, *Factors Controlling Debris-Flow Initiation on Forested Hillslopes in the Oregon Coast Range*, Ph.D. Dissertation, University of Washington, 166 p.

Smoot, John, 1990, Personal communication concerning POREFLOW, Battelle, Pacific Northwest Division, Richland, WA.

APPENDIX A
NARROW BASIN COMPUTER OUTPUT


```

94 -1 1 1 1 1 1 1 1 1 1 1 1 1 1 1 1
0 25 -1 1 1 1 1 1 1 1 1 1 1 1 1 1 1 1
^ 26 -1 1 1 1 1 1 1 1 1 1 1 1 1 1 1 1
^ 27 -1 1 1 1 1 1 1 1 1 1 1 1 1 1 1 1
v 28 -1 1 1 1 1 1 1 1 1 1 1 1 1 1 1 1
0 29 -1 1 1 1 1 1 1 1 1 1 1 1 1 1 1 1
^ 30 -1 1 1 1 1 1 1 1 1 1 1 1 1 1 1 1
^ 31 -1 1 1 1 1 1 1 1 1 1 1 1 1 1 1 1
0 32 -1 1 1 1 1 1 1 1 1 1 1 1 1 1 1 1
^ 33 -1 1 1 1 1 1 1 1 1 1 1 1 1 1 1 1
^ 34 -1 1 1 1 1 1 1 1 1 1 1 1 1 1 1 1
0 35 -1 1 1 1 1 1 1 1 1 1 1 1 1 1 1 1
^ 36 -1 1 1 1 1 1 1 1 1 1 1 1 1 1 1 1
^ 37 -1 1 1 1 1 1 1 1 1 1 1 1 1 1 1 1
^ 38 -1 1 1 1 1 1 1 1 1 1 1 1 1 1 1 1
0 39 -1 1 1 1 1 1 1 1 1 1 1 1 1 1 1 1
^ 40 -1 1 1 1 1 1 1 1 1 1 1 1 1 1 1 1
^ 41 -1 1 1 1 1 1 1 1 1 1 1 1 1 1 1 1
0 42 -1 1 1 1 1 1 1 1 1 1 1 1 1 1 1 1
^ 43 -1 1 1 1 1 1 1 1 1 1 1 1 1 1 1 1
^ 44 -1 1 1 1 1 1 1 1 1 1 1 1 1 1 1 1
v 45 -1 1 1 1 1 1 1 1 1 1 1 1 1 1 1 1
^ 46 -1 1 1 1 1 1 1 1 1 1 1 1 1 1 1 1
^ 47 -1 1 1 1 1 1 1 1 1 1 1 1 1 1 1 1
^ 48 -1 1 1 1 1 1 1 1 1 1 1 1 1 1 1 1
0 49 -1 1 1 1 1 1 1 1 1 1 1 1 1 1 1 1
^ 50 -1 1 1 1 1 1 1 1 1 1 1 1 1 1 1 1
^ 51 -1 1 1 1 1 1 1 1 1 1 1 1 1 1 1 1
0 52 -1 1 1 1 1 1 1 1 1 1 1 1 1 1 1 1
^ 53 -1 1 1 1 1 1 1 1 1 1 1 1 1 1 1 1
^ 54 -1 1 1 1 1 1 1 1 1 1 1 1 1 1 1 1
v 55 -1 1 1 1 1 1 1 1 1 1 1 1 1 1 1 1
^ 56 -1 1 1 1 1 1 1 1 1 1 1 1 1 1 1 1
^ 57 -1 1 1 1 1 1 1 1 1 1 1 1 1 1 1 1
^ 58 -1 1 1 1 1 1 1 1 1 1 1 1 1 1 1 1
0 59 -1 1 1 1 1 1 1 1 1 1 1 1 1 1 1 1
^ 60 -1 -1 -1 -1 -1 -1 -1 -1 -1 -1 -1 -1 -1 -1 -1 -1

```

QUIFER HEAD WILL BE SET TO .00000 AT ALL NO-FLOW NODES (IBOUND=0).

0

INITIAL HEAD FOR LAYER 1 WILL BE READ ON UNIT 1 USING FORMAT: (7G11.4)

	1	2	3	4	5	6	7	8	9	10
	11	12	13	14	15	16				
1	537.3	535.1	532.9	530.7	528.4	526.2	524.0	521.8	519.5	517.3
	515.1	512.9	510.7	508.0	506.2	504.0				
^ 2	534.7	532.4	530.2	528.0	525.9	523.2	520.0	517.9	515.5	513.2
	510.9	508.5	506.4	504.0	502.1	500.0				
3	532.0	529.6	527.3	525.3	524.0	520.0	516.0	513.9	511.5	509.1
	506.7	504.0	502.2	500.0	498.1	496.0				
4	529.3	526.8	524.2	521.8	519.4	516.1	512.0	509.5	507.3	505.1
	502.7	500.3	498.2	496.0	494.1	492.0				
0 5	526.7	523.8	521.0	518.3	515.5	512.3	508.0	504.0	503.1	501.2

0 6	498.8	496.4	494.0	492.0	490.0	488.0				
	524.0	520.7	517.8	515.0	512.1	509.0	505.0	502.4	500.0	497.6
	495.1	492.3	489.5	487.0	486.1	484.0				
1 7	520.0	517.2	514.5	511.7	508.8	505.8	502.0	499.7	497.0	494.3
	491.5	488.3	484.0	483.0	482.4	480.7				
0 8	516.0	513.6	511.1	508.6	505.7	502.7	499.0	496.7	493.9	491.1
	488.3	485.5	482.6	480.0	479.1	477.3				
1 9	512.0	509.9	507.9	505.8	502.7	499.6	496.0	493.6	490.7	488.0
	485.3	482.6	480.0	477.0	476.0	474.0				
1 10	508.0	506.2	504.7	504.0	499.8	496.5	493.0	490.4	487.5	484.8
	482.1	479.5	477.1	474.0	472.7	470.7				
v 11	504.0	502.3	500.6	498.8	496.0	493.1	490.0	487.1	484.0	481.5
	478.9	476.4	474.0	471.0	469.5	467.3				
1 12	500.0	498.3	496.6	494.7	492.4	489.7	486.0	484.0	481.0	478.2
	475.6	473.1	470.7	468.0	466.2	464.0				
0 13	496.0	494.4	492.7	491.0	489.0	486.6	483.0	480.5	477.6	474.8
	472.2	469.7	467.4	465.0	462.8	460.7				
1 14	492.0	490.5	488.9	487.5	486.1	484.0	480.0	477.0	474.1	471.3
	468.7	466.2	463.9	461.0	459.5	457.3				
1 15	488.0	486.5	485.1	484.0	484.0	479.8	476.0	473.2	470.4	467.6
	465.1	462.6	460.3	458.0	456.0	454.0				
v 16	484.0	482.4	480.8	479.3	477.8	475.0	472.0	469.2	466.5	463.8
	461.3	458.9	456.6	454.0	452.6	450.7				
1 17	480.0	478.3	476.5	474.8	472.8	470.4	467.0	465.1	462.5	459.9
	457.4	455.0	452.8	450.0	449.0	447.3				
0 18	476.0	474.2	472.3	470.4	468.3	465.9	463.0	460.9	458.4	455.9
	453.4	451.0	448.7	446.0	445.4	444.0				
1 19	472.0	470.1	468.1	466.1	464.0	461.6	459.0	456.8	454.3	451.9
	449.4	446.9	444.0	442.0	441.5	440.0				
1 20	468.0	466.0	464.0	461.9	459.7	457.4	455.0	452.6	450.2	447.8
	445.5	443.1	440.9	439.0	437.6	436.0				
v 21	464.0	462.0	459.9	457.8	455.6	453.3	450.0	448.4	446.1	443.8
	441.5	439.3	437.1	435.0	433.6	432.0				
1 22	460.0	458.0	455.9	453.7	451.5	449.2	446.0	444.0	442.0	439.8
	437.5	435.3	433.1	431.0	429.6	428.0				
0 23	456.0	454.0	451.9	449.8	447.6	445.3	442.0	440.4	438.1	435.8
	433.5	431.1	428.9	427.0	425.6	424.0				
1 24	452.0	450.0	447.9	445.9	444.0	441.4	438.0	436.5	434.2	431.8
	429.5	427.0	424.0	423.0	421.5	420.0				
1 25	448.0	446.0	443.9	441.8	439.7	437.4	435.0	432.6	430.3	427.9
	425.6	423.2	420.9	419.0	417.6	416.0				
- 26	444.0	442.0	439.9	437.8	435.6	433.4	431.0	428.8	426.4	424.0
	421.7	419.4	417.3	415.0	413.7	412.0				
1 27	440.0	438.0	435.9	433.8	431.7	429.4	427.0	424.9	422.5	420.2
	417.9	415.5	413.3	411.0	409.7	408.0				
0 28	436.0	434.0	431.9	429.9	427.8	425.5	423.0	421.0	418.7	416.4
	414.0	411.5	409.0	407.0	405.7	404.0				
1 29	432.0	430.0	428.0	426.0	424.0	421.7	419.0	417.2	414.9	412.6
	410.1	407.4	404.0	403.0	401.7	400.0				
1 30	428.0	426.0	424.0	422.0	419.9	417.8	415.0	413.4	411.2	408.9
	406.6	404.1	401.6	399.0	397.9	396.0				
31	424.0	422.0	420.0	418.0	416.0	413.9	411.0	409.7	407.5	405.3
	403.1	400.8	398.5	396.0	394.2	392.0				
1 32	420.0	418.0	416.0	414.0	412.0	410.0	408.0	406.0	403.9	401.8
	399.7	397.5	395.3	393.0	390.6	388.0				
0 33	416.0	414.0	412.1	410.1	408.1	406.2	404.0	402.3	400.3	398.3

0 34	396.3	394.2	392.1	389.0	387.1	384.0	400.0	398.6	396.8	394.9
35	412.0	410.0	408.1	406.1	404.2	402.3	400.0	398.6	396.8	394.9
	393.0	391.1	389.0	386.0	384.2	381.5				
	408.0	406.0	404.1	402.1	400.3	398.5	396.0	395.0	393.2	391.5
	389.7	388.0	386.2	383.0	381.5	379.0				
0 36	404.0	402.0	400.0	398.1	396.3	394.6	392.0	391.3	389.6	388.0
	386.5	385.0	384.0	381.0	378.8	376.5				
37	400.0	397.9	395.8	393.9	392.2	390.7	389.0	387.6	386.0	384.5
	383.1	381.6	380.1	378.0	376.0	374.0				
38	396.0	393.8	391.6	389.4	388.1	386.7	385.0	383.9	382.5	381.0
	379.6	378.2	376.7	375.0	373.3	371.5				
v 39	392.0	389.7	387.2	384.0	384.0	382.8	381.0	380.1	378.8	377.5
	376.2	374.9	373.5	372.0	370.5	369.0				
40	388.0	385.9	383.6	381.5	380.3	379.0	377.0	376.4	375.2	374.0
	372.9	371.6	370.4	369.0	367.8	366.5				
0 41	384.0	382.0	380.0	378.1	376.6	375.2	373.0	372.6	371.5	370.5
	369.5	368.4	367.3	366.0	365.0	364.0				
42	380.0	378.1	376.2	374.4	372.8	371.3	370.0	368.6	367.9	367.1
	366.2	365.2	364.2	363.0	362.2	361.1				
43	376.0	374.2	372.4	370.5	368.7	367.5	366.0	364.0	364.2	363.7
	363.0	362.1	361.2	360.0	359.3	358.3				
v 44	372.0	370.3	368.5	366.6	364.0	363.7	362.0	361.7	361.2	360.6
	359.9	359.1	358.2	357.0	356.4	355.4				
45	368.0	366.5	364.9	363.2	361.6	360.7	359.0	358.9	358.2	357.5
	356.8	356.1	355.3	354.0	353.5	352.6				
0 46	364.0	362.6	361.2	359.8	358.6	357.6	356.0	355.9	355.2	354.5
	353.9	353.1	352.4	351.0	350.6	349.7				
47	360.0	358.8	357.5	356.4	355.3	354.4	353.0	352.9	352.2	351.6
	350.9	350.2	349.5	348.0	347.9	346.9				
48	356.0	354.9	353.8	352.8	351.8	351.0	350.0	349.7	349.1	348.6
	348.0	347.4	346.7	346.0	345.2	344.0				
v 49	352.0	351.0	350.1	349.1	348.1	347.6	347.0	346.6	346.1	345.6
	345.1	344.6	344.0	343.0	342.8	342.2				
50	348.0	347.2	346.3	345.3	344.0	344.1	343.0	343.4	343.0	342.6
	342.2	341.8	341.4	340.0	340.5	340.1				
0 51	344.0	343.4	342.7	342.0	341.3	340.9	340.0	340.3	340.0	339.7
	339.3	339.0	338.7	338.0	338.1	337.9				
52	340.0	339.5	339.1	338.6	338.1	337.8	337.0	337.2	337.0	336.7
	336.4	336.2	336.0	335.0	335.6	335.5				
53	336.0	335.8	335.5	335.1	334.8	334.6	334.0	334.1	333.9	333.7
	333.5	333.4	333.3	333.0	333.1	333.1				
54	332.0	332.0	331.9	331.7	331.5	331.3	331.0	331.0	330.8	330.7
	330.6	330.5	330.5	330.0	330.6	330.7				
55	328.0	328.2	328.3	328.3	328.2	328.1	328.0	327.9	327.8	327.7
	327.6	327.6	327.7	327.0	328.0	328.3				
0 56	324.0	324.6	324.9	324.9	324.9	324.9	324.0	324.7	324.6	324.6
	324.6	324.7	324.8	325.0	325.5	326.0				
57	320.0	321.3	321.6	321.7	321.7	321.6	321.0	321.5	321.5	321.5
	321.5	321.6	321.8	322.0	322.7	324.0				
58	320.0	318.8	318.6	318.5	318.5	318.4	318.0	318.4	318.4	318.4
	318.4	318.5	318.6	318.0	319.3	320.0				
59	316.0	315.5	315.4	315.3	315.2	315.2	315.0	315.2	315.2	315.2
	315.2	315.3	315.3	315.0	315.7	316.0				
60	312.0	312.0	312.0	312.0	312.0	312.0	312.0	312.0	312.0	312.0
	312.0	312.0	312.0	312.0	312.0	312.0				

0HEAD PRINT FORMAT IS FORMAT NUMBER -4

DRAWDOWN PRINT FORMAT IS FORMAT NUMBER -4

HEADS WILL BE SAVED ON UNIT 0 DRAWDOWNS WILL BE SAVED ON UNIT 0

OUTPUT CONTROL IS SPECIFIED EVERY TIME STEP

COLUMN TO ROW ANISOTROPY = 1.000000
DELR = 4.000000
DELC = 4.000000
HYD. COND. ALONG ROWS = 5.000000 FOR LAYER 1

BOTTOM FOR LAYER 1 WILL BE READ ON UNIT 11 USING FORMAT: (7G11.4)

	1	2	3	4	5	6	7	8	9	10
	11	12	13	14	15	16				
0 1	533.3	531.1	528.9	526.7	524.4	522.2	520.0	517.8	515.6	513.3
	511.1	508.9	506.7	504.4	502.2	500.0				
2	530.7	528.4	526.1	524.0	521.9	519.2	516.5	513.9	511.5	509.2
	506.9	504.6	502.4	500.3	498.2	496.0				
3	528.0	525.6	523.3	521.3	520.0	516.0	512.8	509.9	507.5	505.1
	502.7	500.0	498.2	496.2	494.1	492.0				
4	525.3	522.7	520.2	517.8	515.4	512.1	508.8	505.5	503.3	501.1
	498.7	496.3	494.2	492.1	490.1	488.0				
5	522.7	519.8	517.0	514.3	511.5	508.3	504.7	500.0	499.1	497.2
	494.8	492.4	490.0	488.0	486.0	484.0				
6	520.0	516.7	513.8	511.0	508.1	505.0	501.7	498.3	496.0	493.7
	491.1	488.3	485.6	483.9	482.1	480.0				
7	516.0	513.2	510.5	507.7	504.8	501.8	498.7	495.7	493.0	490.3
	487.5	484.3	480.0	479.8	478.4	476.7				
8	512.0	509.6	507.1	504.6	501.7	498.7	495.7	492.7	489.9	487.1
	484.3	481.5	478.6	476.9	475.1	473.3				
9	508.0	505.9	503.9	501.8	498.7	495.6	492.6	489.6	486.7	484.0
	481.2	478.6	476.1	473.9	472.0	470.0				
10	504.0	502.2	500.7	500.0	495.8	492.5	489.4	486.4	483.5	480.8
	478.1	475.5	473.1	470.9	468.7	466.7				
11	500.0	498.3	496.6	494.8	492.0	489.1	486.1	483.1	480.0	477.5
	474.9	472.4	470.0	467.7	465.5	463.3				
12	496.0	494.3	492.6	490.7	488.4	485.7	482.8	480.0	477.0	474.2
	471.6	469.1	466.7	464.4	462.2	460.0				
13	492.0	490.4	488.7	487.0	485.0	482.6	479.5	476.5	473.6	470.8
	468.2	465.7	463.3	461.1	458.8	456.7				
14	488.0	486.5	484.9	483.5	482.1	480.0	476.2	473.0	470.1	467.3
	464.7	462.2	459.9	457.6	455.5	453.3				
15	484.0	482.5	481.1	480.0	480.0	475.8	472.4	469.2	466.4	463.6
	461.1	458.6	456.3	454.1	452.0	450.0				
16	480.0	478.4	476.8	475.3	473.8	471.0	468.1	465.2	462.5	459.8
	457.3	454.9	452.6	450.5	448.6	446.7				
17	476.0	474.3	472.5	470.8	468.8	466.4	463.8	461.1	458.5	455.9
	453.4	451.0	448.8	446.8	445.0	443.3				
18	472.0	470.2	468.3	466.4	464.3	461.9	459.5	456.9	454.4	451.9
	449.4	447.0	444.7	442.9	441.4	440.0				
19	468.0	466.1	464.1	462.1	460.0	457.6	455.2	452.8	450.3	447.9
	445.4	442.9	440.0	438.9	437.4	436.0				
20	464.0	462.0	460.0	457.9	455.7	453.4	451.0	448.6	446.2	443.8
	441.5	439.1	436.9	435.2	433.6	432.0				
21	460.0	458.0	455.9	453.8	451.6	449.3	446.8	444.4	442.1	439.8

0 22	437.5	435.3	433.1	431.3	429.6	428.0				
	456.0	454.0	451.9	449.7	447.5	445.2	442.7	440.0	438.0	435.8
	433.5	431.3	429.2	427.3	425.6	424.0				
23	452.0	450.0	447.9	445.8	443.6	441.3	438.8	436.4	434.1	431.8
	429.5	427.1	424.9	423.2	421.6	420.0				
24	448.0	446.0	443.9	441.9	440.0	437.4	434.9	432.5	430.2	427.8
	425.5	423.0	420.0	419.0	417.6	416.0				
25	444.0	442.0	439.9	437.8	435.7	433.4	431.0	428.6	426.3	423.9
	421.6	419.2	416.9	415.2	413.6	412.0				
26	440.0	438.0	435.9	433.8	431.6	429.4	427.1	424.7	422.4	420.0
	417.7	415.4	413.3	411.4	409.7	408.0				
27	436.0	434.0	431.9	429.8	427.7	425.4	423.2	420.9	418.5	416.2
	413.8	411.5	409.3	407.4	405.7	404.0				
28	432.0	430.0	427.9	425.9	423.8	421.6	419.3	417.0	414.7	412.4
	410.0	407.5	405.0	403.3	401.7	400.0				
29	428.0	426.0	424.0	421.9	420.0	417.7	415.5	413.2	410.9	408.6
	406.1	403.4	400.0	399.2	397.7	396.0				
30	424.0	422.0	420.0	418.0	415.9	413.8	411.6	409.4	407.2	404.9
	402.6	400.1	397.6	395.8	393.9	392.0				
31	420.0	418.0	416.0	414.0	412.0	409.9	407.8	405.7	403.5	401.3
	399.1	396.8	394.5	392.4	390.2	388.0				
v 32	416.0	414.0	412.0	410.0	408.0	406.0	404.0	402.0	399.9	397.8
	395.7	393.5	391.3	389.0	386.6	384.0				
33	412.0	410.0	408.1	406.1	404.1	402.2	400.2	398.3	396.3	394.3
	392.3	390.2	388.1	385.7	383.1	380.0				
34	408.0	406.0	404.1	402.1	400.2	398.3	396.5	394.6	392.8	390.9
	389.0	387.1	385.0	382.7	380.2	377.5				
35	404.0	402.0	400.1	398.1	396.3	394.5	392.7	390.9	389.2	387.5
	385.7	384.0	382.2	379.9	377.5	375.0				
36	400.0	398.0	396.0	394.1	392.3	390.6	388.9	387.3	385.6	384.0
	382.5	381.0	380.0	377.2	374.8	372.5				
v 37	396.0	393.9	391.8	389.9	388.2	386.7	385.1	383.6	382.0	380.5
	379.1	377.6	376.1	374.1	372.0	370.0				
38	392.0	389.8	387.6	385.4	384.1	382.7	381.3	379.9	378.4	377.0
	375.6	374.2	372.7	371.0	369.3	367.5				
39	388.0	385.7	383.2	380.0	380.0	378.8	377.5	376.1	374.8	373.5
	372.2	370.9	369.5	368.0	366.5	365.0				
40	384.0	381.9	379.6	377.5	376.3	375.0	373.7	372.4	371.2	370.0
	368.8	367.6	366.4	365.1	363.8	362.5				
41	380.0	378.0	376.0	374.1	372.6	371.2	369.9	368.6	367.6	366.5
	365.5	364.4	363.3	362.2	361.0	360.0				
42	376.0	374.1	372.2	370.4	368.7	367.3	366.0	364.6	363.9	363.1
	362.2	361.2	360.2	359.2	358.2	357.1				
43	372.0	370.2	368.4	366.5	364.7	363.5	362.1	360.0	360.2	359.7
	359.0	358.1	357.2	356.2	355.3	354.3				
44	368.0	366.3	364.5	362.6	360.0	359.7	358.8	357.7	357.2	356.6
	355.9	355.1	354.2	353.3	352.4	351.4				
45	364.0	362.4	360.8	359.2	357.6	356.7	355.8	354.9	354.2	353.5
	352.8	352.1	351.3	350.4	349.5	348.6				
46	360.0	358.6	357.2	355.8	354.6	353.6	352.7	351.9	351.2	350.5
	349.9	349.1	348.4	347.5	346.7	345.7				
47	356.0	354.8	353.5	352.4	351.3	350.4	349.6	348.9	348.2	347.6
	346.9	346.2	345.5	344.7	343.9	342.9				
48	352.0	350.9	349.8	348.8	347.8	347.0	346.4	345.7	345.2	344.6
	344.0	343.4	342.7	342.0	341.2	340.0				
49	348.0	347.0	346.1	345.1	344.1	343.6	343.1	342.6	342.1	341.6

	341.1	340.6	340.0	339.5	338.8	338.2			
0 50	344.0	343.2	342.3	341.3	340.0	340.1	339.8	339.4	339.0
	338.2	337.8	337.4	336.9	336.5	336.1			338.6
1	340.0	339.4	338.7	338.0	337.3	336.9	336.6	336.3	336.0
	335.3	335.0	334.7	334.4	334.1	333.9			335.7
0 52	336.0	335.5	335.1	334.6	334.1	333.8	333.5	333.2	333.0
	332.4	332.2	332.0	331.8	331.6	331.5			332.7
0 53	332.0	331.7	331.4	331.1	330.8	330.6	330.3	330.1	329.9
	329.5	329.4	329.3	329.2	329.1	329.1			329.7
0 54	328.0	328.0	327.9	327.7	327.5	327.3	327.2	327.0	326.8
	326.6	326.5	326.5	326.5	326.6	326.7			326.7
0 55	324.0	324.2	324.3	324.3	324.2	324.1	324.0	323.9	323.8
	323.6	323.6	323.7	323.8	324.0	324.3			323.7
0 56	320.0	320.6	320.9	320.9	320.9	320.9	320.8	320.7	320.6
	320.6	320.7	320.8	321.0	321.4	322.0			320.6
0 57	316.0	317.3	317.6	317.7	317.7	317.6	317.6	317.5	317.5
	317.5	317.6	317.8	318.1	318.7	320.0			317.5
0 58	316.0	314.8	314.6	314.5	314.5	314.4	314.4	314.4	314.4
	314.4	314.5	314.6	314.9	315.3	316.0			314.4
0 59	312.0	311.5	311.3	311.3	311.2	311.2	311.2	311.2	311.2
	311.2	311.3	311.3	311.5	311.7	312.0			311.2
0 60	308.0	308.0	308.0	308.0	308.0	308.0	308.0	308.0	308.0
	308.0	308.0	308.0	308.0	308.0	308.0			308.0

SOLUTION BY SLICE-SUCCESSIVE OVERRELAXATION

MAXIMUM ITERATIONS ALLOWED FOR CLOSURE = 100
 ACCELERATION PARAMETER = 1.0000
 HEAD CHANGE CRITERION FOR CLOSURE = .10000E+01
 SOR HEAD CHANGE PRINTOUT INTERVAL = 1
 STRESS PERIOD NO. 1, LENGTH = 1.000000

NUMBER OF TIME STEPS = 24

MULTIPLIER FOR DELT = 1.000

INITIAL TIME STEP SIZE = .4166667E-01

3 ITERATIONS FOR TIME STEP 1 IN STRESS PERIOD 1

MAXIMUM HEAD CHANGE FOR EACH ITERATION:

HEAD CHANGE	LAYER,ROW,COL						
-2.562	(1, 15, 5)	1.162	(1, 34, 16)	.8891	(1, 33, 16)		

HEAD/DRAWDOWN PRINTOUT FLAG = 0 TOTAL BUDGET PRINTOUT FLAG = 0 CELL-BY-CELL FLOW TERM FLAG = 0

OUTPUT FLAGS FOR ALL LAYERS ARE THE SAME:

HEAD DRAWDOWN HEAD DRAWDOWN
 RINTOUT PRINTOUT SAVE SAVE

0 0 0 0

1 ITERATIONS FOR TIME STEP 2 IN STRESS PERIOD 1

MAXIMUM HEAD CHANGE FOR EACH ITERATION:

HEAD CHANGE	LAYER,ROW,COL						
-------------	---------------	-------------	---------------	-------------	---------------	-------------	---------------

.7371 (1, 33, 16)

HEAD/DRAWDOWN PRINTOUT FLAG = 0 TOTAL BUDGET PRINTOUT FLAG = 0 CELL-BY-CELL FLOW TERM FLAG = 0

OUTPUT FLAGS FOR ALL LAYERS ARE THE SAME:

HEAD DRAWDOWN HEAD DRAWDOWN

PRINTOUT PRINTOUT SAVE SAVE

0 0 0 0

1 ITERATIONS FOR TIME STEP 3 IN STRESS PERIOD 1

MAXIMUM HEAD CHANGE FOR EACH ITERATION:

0 HEAD CHANGE LAYER,ROW,COL HEAD CHANGE LAYER,ROW,COL HEAD CHANGE LAYER,ROW,COL HEAD CHANGE LAYER,ROW,COL

.6355 (1, 33, 16)

HEAD/DRAWDOWN PRINTOUT FLAG = 0 TOTAL BUDGET PRINTOUT FLAG = 0 CELL-BY-CELL FLOW TERM FLAG = 0

OUTPUT FLAGS FOR ALL LAYERS ARE THE SAME:

HEAD DRAWDOWN HEAD DRAWDOWN

PRINTOUT PRINTOUT SAVE SAVE

0 0 0 0

1 ITERATIONS FOR TIME STEP 4 IN STRESS PERIOD 1

MAXIMUM HEAD CHANGE FOR EACH ITERATION:

0 HEAD CHANGE LAYER,ROW,COL HEAD CHANGE LAYER,ROW,COL HEAD CHANGE LAYER,ROW,COL HEAD CHANGE LAYER,ROW,COL

.5601 (1, 33, 16)

HEAD/DRAWDOWN PRINTOUT FLAG = 0 TOTAL BUDGET PRINTOUT FLAG = 0 CELL-BY-CELL FLOW TERM FLAG = 0

OUTPUT FLAGS FOR ALL LAYERS ARE THE SAME:

HEAD DRAWDOWN HEAD DRAWDOWN

PRINTOUT PRINTOUT SAVE SAVE

0 0 0 0

1 ITERATIONS FOR TIME STEP 5 IN STRESS PERIOD 1

MAXIMUM HEAD CHANGE FOR EACH ITERATION:

0 HEAD CHANGE LAYER,ROW,COL HEAD CHANGE LAYER,ROW,COL HEAD CHANGE LAYER,ROW,COL HEAD CHANGE LAYER,ROW,COL

.5019 (1, 33, 16)

HEAD/DRAWDOWN PRINTOUT FLAG = 0 TOTAL BUDGET PRINTOUT FLAG = 0 CELL-BY-CELL FLOW TERM FLAG = 0

OUTPUT FLAGS FOR ALL LAYERS ARE THE SAME:

HEAD DRAWDOWN HEAD DRAWDOWN

PRINTOUT PRINTOUT SAVE SAVE

0 0 0 0

1 ITERATIONS FOR TIME STEP 6 IN STRESS PERIOD 1

MAXIMUM HEAD CHANGE FOR EACH ITERATION:

0 HEAD CHANGE LAYER,ROW,COL HEAD CHANGE LAYER,ROW,COL HEAD CHANGE LAYER,ROW,COL HEAD CHANGE LAYER,ROW,COL

.4553 (1, 33, 16)

HEAD/DRAWDOWN PRINTOUT FLAG = 0 TOTAL BUDGET PRINTOUT FLAG = 0 CELL-BY-CELL FLOW TERM FLAG = 0

OUTPUT FLAGS FOR ALL LAYERS ARE THE SAME:

HEAD DRAWDOWN HEAD DRAWDOWN

PRINTOUT PRINTOUT SAVE SAVE

0 0 0 0

1 ITERATIONS FOR TIME STEP 7 IN STRESS PERIOD 1

MAXIMUM HEAD CHANGE FOR EACH ITERATION:

HEAD CHANGE LAYER,ROW,COL HEAD CHANGE LAYER,ROW,COL HEAD CHANGE LAYER,ROW,COL HEAD CHANGE LAYER,ROW,COL

.4167 (1, 33, 16)

HEAD/DRAWDOWN PRINTOUT FLAG = 0 TOTAL BUDGET PRINTOUT FLAG = 0 CELL-BY-CELL FLOW TERM FLAG = 0

OUTPUT FLAGS FOR ALL LAYERS ARE THE SAME:

HEAD DRAWDOWN HEAD DRAWDOWN
PRINTOUT PRINTOUT SAVE SAVE

0 0 0 0

1 ITERATIONS FOR TIME STEP 8 IN STRESS PERIOD 1

MAXIMUM HEAD CHANGE FOR EACH ITERATION:

HEAD CHANGE LAYER,ROW,COL HEAD CHANGE LAYER,ROW,COL HEAD CHANGE LAYER,ROW,COL HEAD CHANGE LAYER,ROW,COL

.3837 (1, 33, 16)

0

HEAD/DRAWDOWN PRINTOUT FLAG = 0 TOTAL BUDGET PRINTOUT FLAG = 0 CELL-BY-CELL FLOW TERM FLAG = 0

OUTPUT FLAGS FOR ALL LAYERS ARE THE SAME:

HEAD DRAWDOWN HEAD DRAWDOWN
PRINTOUT PRINTOUT SAVE SAVE

0 0 0 0

1 ITERATIONS FOR TIME STEP 9 IN STRESS PERIOD 1

MAXIMUM HEAD CHANGE FOR EACH ITERATION:

HEAD CHANGE LAYER,ROW,COL HEAD CHANGE LAYER,ROW,COL HEAD CHANGE LAYER,ROW,COL HEAD CHANGE LAYER,ROW,COL

.3548 (1, 33, 16)

HEAD/DRAWDOWN PRINTOUT FLAG = 0 TOTAL BUDGET PRINTOUT FLAG = 0 CELL-BY-CELL FLOW TERM FLAG = 0

OUTPUT FLAGS FOR ALL LAYERS ARE THE SAME:

HEAD DRAWDOWN HEAD DRAWDOWN
PRINTOUT PRINTOUT SAVE SAVE

0 0 0 0

1 ITERATIONS FOR TIME STEP 10 IN STRESS PERIOD 1

MAXIMUM HEAD CHANGE FOR EACH ITERATION:

HEAD CHANGE LAYER,ROW,COL HEAD CHANGE LAYER,ROW,COL HEAD CHANGE LAYER,ROW,COL HEAD CHANGE LAYER,ROW,COL

.3290 (1, 33, 16)

0

HEAD/DRAWDOWN PRINTOUT FLAG = 0 TOTAL BUDGET PRINTOUT FLAG = 0 CELL-BY-CELL FLOW TERM FLAG = 0

OUTPUT FLAGS FOR ALL LAYERS ARE THE SAME:

HEAD DRAWDOWN HEAD DRAWDOWN
PRINTOUT PRINTOUT SAVE SAVE

0 0 0 0

1 ITERATIONS FOR TIME STEP 11 IN STRESS PERIOD 1

MAXIMUM HEAD CHANGE FOR EACH ITERATION:

HEAD CHANGE LAYER,ROW,COL HEAD CHANGE LAYER,ROW,COL HEAD CHANGE LAYER,ROW,COL HEAD CHANGE LAYER,ROW,COL

.3059 (1, 33, 16)

HEAD/DRAWDOWN PRINTOUT FLAG = 0 TOTAL BUDGET PRINTOUT FLAG = 0 CELL-BY-CELL FLOW TERM FLAG = 0

INPUT FLAGS FOR ALL LAYERS ARE THE SAME:

HEAD DRAWDOWN HEAD DRAWDOWN
PRINTOUT PRINTOUT SAVE SAVE

0 0 0 0

1 ITERATIONS FOR TIME STEP 12 IN STRESS PERIOD 1

MAXIMUM HEAD CHANGE FOR EACH ITERATION:

HEAD CHANGE LAYER,ROW,COL HEAD CHANGE LAYER,ROW,COL HEAD CHANGE LAYER,ROW,COL HEAD CHANGE LAYER,ROW,COL

.2850 (1, 33, 16)

HEAD/DRAWDOWN PRINTOUT FLAG = 0 TOTAL BUDGET PRINTOUT FLAG = 0 CELL-BY-CELL FLOW TERM FLAG = 0

INPUT FLAGS FOR ALL LAYERS ARE THE SAME:

HEAD DRAWDOWN HEAD DRAWDOWN
PRINTOUT PRINTOUT SAVE SAVE

0 0 0 0

1 ITERATIONS FOR TIME STEP 13 IN STRESS PERIOD 1

MAXIMUM HEAD CHANGE FOR EACH ITERATION:

HEAD CHANGE LAYER,ROW,COL HEAD CHANGE LAYER,ROW,COL HEAD CHANGE LAYER,ROW,COL HEAD CHANGE LAYER,ROW,COL

.2661 (1, 33, 16)

HEAD/DRAWDOWN PRINTOUT FLAG = 0 TOTAL BUDGET PRINTOUT FLAG = 0 CELL-BY-CELL FLOW TERM FLAG = 0

INPUT FLAGS FOR ALL LAYERS ARE THE SAME:

HEAD DRAWDOWN HEAD DRAWDOWN
PRINTOUT PRINTOUT SAVE SAVE

0 0 0 0

1 ITERATIONS FOR TIME STEP 14 IN STRESS PERIOD 1

MAXIMUM HEAD CHANGE FOR EACH ITERATION:

HEAD CHANGE LAYER,ROW,COL HEAD CHANGE LAYER,ROW,COL HEAD CHANGE LAYER,ROW,COL HEAD CHANGE LAYER,ROW,COL

.2493 (1, 33, 16)

HEAD/DRAWDOWN PRINTOUT FLAG = 0 TOTAL BUDGET PRINTOUT FLAG = 0 CELL-BY-CELL FLOW TERM FLAG = 0

INPUT FLAGS FOR ALL LAYERS ARE THE SAME:

HEAD DRAWDOWN HEAD DRAWDOWN
PRINTOUT PRINTOUT SAVE SAVE

0 0 0 0

1 ITERATIONS FOR TIME STEP 15 IN STRESS PERIOD 1

MAXIMUM HEAD CHANGE FOR EACH ITERATION:

HEAD CHANGE LAYER,ROW,COL HEAD CHANGE LAYER,ROW,COL HEAD CHANGE LAYER,ROW,COL HEAD CHANGE LAYER,ROW,COL

.2345 (1, 34, 16)

HEAD/DRAWDOWN PRINTOUT FLAG = 0 TOTAL BUDGET PRINTOUT FLAG = 0 CELL-BY-CELL FLOW TERM FLAG = 0

INPUT FLAGS FOR ALL LAYERS ARE THE SAME:

HEAD DRAWDOWN HEAD DRAWDOWN
PRINTOUT PRINTOUT SAVE SAVE

0 0 0 0

1 ITERATIONS FOR TIME STEP 16 IN STRESS PERIOD 1

MAXIMUM HEAD CHANGE FOR EACH ITERATION:

HEAD CHANGE LAYER,ROW,COL HEAD CHANGE LAYER,ROW,COL HEAD CHANGE LAYER,ROW,COL HEAD CHANGE LAYER,ROW,COL

.2215 (1, 34, 16)

HEAD/DRAWDOWN PRINTOUT FLAG = 0 TOTAL BUDGET PRINTOUT FLAG = 0 CELL-BY-CELL FLOW TERM FLAG = 0

OUTPUT FLAGS FOR ALL LAYERS ARE THE SAME:

HEAD DRAWDOWN HEAD DRAWDOWN

RINTOUT PRINTOUT SAVE SAVE

0 0 0 0

1 ITERATIONS FOR TIME STEP 17 IN STRESS PERIOD 1

MAXIMUM HEAD CHANGE FOR EACH ITERATION:

HEAD CHANGE LAYER,ROW,COL HEAD CHANGE LAYER,ROW,COL HEAD CHANGE LAYER,ROW,COL HEAD CHANGE LAYER,ROW,COL

.2100 (1, 34, 16)

HEAD/DRAWDOWN PRINTOUT FLAG = 0 TOTAL BUDGET PRINTOUT FLAG = 0 CELL-BY-CELL FLOW TERM FLAG = 0

OUTPUT FLAGS FOR ALL LAYERS ARE THE SAME:

HEAD DRAWDOWN HEAD DRAWDOWN

RINTOUT PRINTOUT SAVE SAVE

0 0 0 0

1 ITERATIONS FOR TIME STEP 18 IN STRESS PERIOD 1

MAXIMUM HEAD CHANGE FOR EACH ITERATION:

HEAD CHANGE LAYER,ROW,COL HEAD CHANGE LAYER,ROW,COL HEAD CHANGE LAYER,ROW,COL HEAD CHANGE LAYER,ROW,COL

.1999 (1, 34, 16)

HEAD/DRAWDOWN PRINTOUT FLAG = 0 TOTAL BUDGET PRINTOUT FLAG = 0 CELL-BY-CELL FLOW TERM FLAG = 0

OUTPUT FLAGS FOR ALL LAYERS ARE THE SAME:

HEAD DRAWDOWN HEAD DRAWDOWN

RINTOUT PRINTOUT SAVE SAVE

0 0 0 0

1 ITERATIONS FOR TIME STEP 19 IN STRESS PERIOD 1

MAXIMUM HEAD CHANGE FOR EACH ITERATION:

HEAD CHANGE LAYER,ROW,COL HEAD CHANGE LAYER,ROW,COL HEAD CHANGE LAYER,ROW,COL HEAD CHANGE LAYER,ROW,COL

.1911 (1, 33, 16)

HEAD/DRAWDOWN PRINTOUT FLAG = 0 TOTAL BUDGET PRINTOUT FLAG = 0 CELL-BY-CELL FLOW TERM FLAG = 0

OUTPUT FLAGS FOR ALL LAYERS ARE THE SAME:

HEAD DRAWDOWN HEAD DRAWDOWN

RINTOUT PRINTOUT SAVE SAVE

0 0 0 0

1 ITERATIONS FOR TIME STEP 20 IN STRESS PERIOD 1

MAXIMUM HEAD CHANGE FOR EACH ITERATION:

HEAD CHANGE LAYER,ROW,COL HEAD CHANGE LAYER,ROW,COL HEAD CHANGE LAYER,ROW,COL HEAD CHANGE LAYER,ROW,COL

.1836 (1, 33, 16)

HEAD/DRAWDOWN PRINTOUT FLAG = 0 TOTAL BUDGET PRINTOUT FLAG = 0 CELL-BY-CELL FLOW TERM FLAG = 0

OUTPUT FLAGS FOR ALL LAYERS ARE THE SAME:

HEAD DRAWDOWN HEAD DRAWDOWN

RINTOUT PRINTOUT SAVE SAVE

0 0 0 0

1 ITERATIONS FOR TIME STEP 21 IN STRESS PERIOD 1

MAXIMUM HEAD CHANGE FOR EACH ITERATION:

HEAD CHANGE LAYER,ROW,COL HEAD CHANGE LAYER,ROW,COL HEAD CHANGE LAYER,ROW,COL HEAD CHANGE LAYER,ROW,COL

.1770 (1, 33, 16)

HEAD/DRAWDOWN PRINTOUT FLAG = 0 TOTAL BUDGET PRINTOUT FLAG = 0 CELL-BY-CELL FLOW TERM FLAG = 0

OUTPUT FLAGS FOR ALL LAYERS ARE THE SAME:

HEAD DRAWDOWN HEAD DRAWDOWN
PRINTOUT PRINTOUT SAVE SAVE

0 0 0 0

1 ITERATIONS FOR TIME STEP 22 IN STRESS PERIOD 1

MAXIMUM HEAD CHANGE FOR EACH ITERATION:

HEAD CHANGE LAYER,ROW,COL HEAD CHANGE LAYER,ROW,COL HEAD CHANGE LAYER,ROW,COL HEAD CHANGE LAYER,ROW,COL

.1712 (1, 33, 16)

HEAD/DRAWDOWN PRINTOUT FLAG = 0 TOTAL BUDGET PRINTOUT FLAG = 0 CELL-BY-CELL FLOW TERM FLAG = 0

OUTPUT FLAGS FOR ALL LAYERS ARE THE SAME:

HEAD DRAWDOWN HEAD DRAWDOWN
PRINTOUT PRINTOUT SAVE SAVE

0 0 0 0

1 ITERATIONS FOR TIME STEP 23 IN STRESS PERIOD 1

MAXIMUM HEAD CHANGE FOR EACH ITERATION:

HEAD CHANGE LAYER,ROW,COL HEAD CHANGE LAYER,ROW,COL HEAD CHANGE LAYER,ROW,COL HEAD CHANGE LAYER,ROW,COL

.1660 (1, 33, 16)

HEAD/DRAWDOWN PRINTOUT FLAG = 0 TOTAL BUDGET PRINTOUT FLAG = 0 CELL-BY-CELL FLOW TERM FLAG = 0

OUTPUT FLAGS FOR ALL LAYERS ARE THE SAME:

HEAD DRAWDOWN HEAD DRAWDOWN
PRINTOUT PRINTOUT SAVE SAVE

0 0 0 0

1 ITERATIONS FOR TIME STEP 24 IN STRESS PERIOD 1

MAXIMUM HEAD CHANGE FOR EACH ITERATION:

HEAD CHANGE LAYER,ROW,COL HEAD CHANGE LAYER,ROW,COL HEAD CHANGE LAYER,ROW,COL HEAD CHANGE LAYER,ROW,COL

.1616 (1, 32, 16)

HEAD/DRAWDOWN PRINTOUT FLAG = 1 TOTAL BUDGET PRINTOUT FLAG = 1 CELL-BY-CELL FLOW TERM FLAG = 1

OUTPUT FLAGS FOR ALL LAYERS ARE THE SAME:

HEAD DRAWDOWN HEAD DRAWDOWN
PRINTOUT PRINTOUT SAVE SAVE

1 1 0 0

HEAD IN LAYER 1 AT END OF TIME STEP 24 IN STRESS PERIOD 1

1 2 3 4 5 6 7 8 9 10 11 12 13 14 15 16

0 1	537.30	535.10	532.90	530.70	528.40	526.20	524.00	521.80	519.50	517.30	515.10	512.90	510.70	508.00	506.20	504.00
0 2	534.70	532.37	530.10	527.89	525.61	522.90	520.31	517.85	515.49	513.22	510.96	508.72	506.60	504.45	502.80	501.64

3	532.00	529.57	527.20	524.88	522.08	519.02	516.31	513.77	511.47	509.21	506.95	504.80	502.82	500.98	499.65	498.93
0	529.30	526.69	524.08	521.41	518.22	515.19	512.34	509.75	507.61	505.42	503.20	501.14	499.22	497.66	496.61	496.11
5	526.70	523.75	520.91	518.02	514.84	511.71	508.80	506.41	504.28	501.97	499.68	497.58	495.79	494.50	493.68	493.30
6	524.00	520.66	517.69	514.74	511.64	508.58	505.79	503.46	501.10	498.66	496.32	494.25	492.60	491.55	490.88	490.57
0	520.00	517.15	514.34	511.50	508.51	505.52	502.76	500.29	497.84	495.41	493.14	491.23	489.82	488.84	488.17	487.86
8	516.00	513.50	510.99	508.36	505.41	502.44	499.64	497.05	494.57	492.22	490.10	488.39	487.13	486.10	485.41	485.09
9	512.00	509.83	507.66	505.38	502.27	499.24	496.39	493.74	491.27	489.00	487.01	485.39	484.16	483.18	482.53	482.21
0	508.00	506.07	504.15	501.48	498.37	495.63	492.92	490.33	487.89	485.71	483.81	482.26	481.05	480.13	479.51	479.22
11	504.00	502.10	500.03	497.18	494.58	492.01	489.41	486.88	484.51	482.37	480.52	479.00	477.82	476.95	476.39	476.12
12	500.00	498.13	496.06	493.58	491.12	488.59	485.97	483.42	481.05	478.92	477.10	475.62	474.48	473.67	473.15	472.91
13	496.00	494.20	492.26	490.15	487.98	485.43	482.55	479.85	477.46	475.35	473.57	472.14	471.05	470.29	469.81	469.59
0	492.00	490.28	488.53	486.82	485.36	482.17	478.89	476.10	473.71	471.63	469.91	468.54	467.51	466.80	466.37	466.18
15	488.00	486.30	484.63	483.10	480.57	477.19	474.48	471.98	469.73	467.75	466.11	464.81	463.85	463.20	462.82	462.66
16	484.00	482.23	480.40	478.52	475.15	472.39	469.95	467.69	465.60	463.74	462.18	460.96	460.07	459.49	459.16	459.02
0	480.00	478.13	476.16	474.00	470.93	468.08	465.61	463.39	461.39	459.64	458.16	457.01	456.18	455.67	455.39	455.27
18	476.00	474.02	471.95	469.66	466.87	464.02	461.43	459.18	457.21	455.52	454.11	453.01	452.21	451.76	451.50	451.39
19	472.00	469.94	467.79	465.46	462.80	460.04	457.41	455.08	453.08	451.41	450.08	449.06	448.35	447.88	447.57	447.42
20	468.00	465.89	463.70	461.34	458.77	456.11	453.45	451.04	449.01	447.37	446.10	445.15	444.49	443.96	443.62	443.46
0	464.00	461.87	459.65	457.30	454.80	452.17	449.52	447.05	445.03	443.39	442.10	441.16	440.47	439.96	439.63	439.48
22	460.00	457.86	455.64	453.32	450.88	448.29	445.67	443.26	441.21	439.47	438.12	437.11	436.40	435.93	435.64	435.50
23	456.00	453.87	451.67	449.41	447.05	444.47	441.91	439.57	437.41	435.58	434.17	433.10	432.34	431.92	431.66	431.53
0	452.00	449.87	447.69	445.46	443.07	440.54	438.08	435.75	433.60	431.74	430.29	429.23	428.50	428.04	427.74	427.60
25	448.00	445.87	443.69	441.43	439.03	436.61	434.22	431.92	429.78	427.93	426.49	425.45	424.75	424.20	423.86	423.70
26	444.00	441.88	439.70	437.45	435.11	432.73	430.38	428.11	425.98	424.15	422.69	421.62	420.88	420.34	420.00	419.84
0	440.00	437.88	435.72	433.51	431.23	428.89	426.56	424.31	422.21	420.39	418.91	417.79	416.99	416.49	416.18	416.03
28	436.00	433.90	431.77	429.59	427.36	425.06	422.76	420.53	418.47	416.67	415.18	414.03	413.22	412.76	412.46	412.32
29	432.00	429.92	427.81	425.67	423.45	421.18	418.95	416.78	414.78	413.02	411.59	410.52	409.77	409.26	408.90	408.72
30	428.00	425.93	423.84	421.71	419.52	417.33	415.16	413.08	411.15	409.48	408.16	407.17	406.48	405.88	405.46	405.25
0	424.00	421.95	419.87	417.76	415.63	413.50	411.42	409.42	407.58	406.01	404.77	403.83	403.12	402.53	402.12	401.90
32	420.00	417.96	415.92	413.85	411.76	409.71	407.70	405.79	404.06	402.59	401.41	400.51	399.82	399.27	398.89	398.69
33	416.00	413.99	411.97	409.93	407.91	405.92	404.01	402.19	400.57	399.20	398.10	397.26	396.62	396.13	395.80	395.64
0	412.00	410.00	407.99	405.99	404.05	402.14	400.32	398.60	397.09	395.83	394.82	394.06	393.49	393.05	392.78	392.67
35	408.00	406.00	403.99	402.04	400.16	398.34	396.61	395.02	393.61	392.44	391.53	390.86	390.38	389.97	389.74	389.64
36	404.00	401.96	399.94	398.02	396.21	394.51	392.90	391.42	390.11	389.03	388.20	387.57	387.11	386.80	386.64	386.58
0	397.91	395.86	393.94	392.26	390.68	389.19	387.81	386.60	385.61	384.82	384.22	383.79	383.60	383.51	383.48	
38	396.00	393.86	391.78	389.88	388.40	386.92	385.51	384.21	383.11	382.19	381.47	380.94	380.59	380.43	380.38	380.37
39	392.00	389.91	387.92	386.26	384.79	383.29	381.90	380.66	379.64	378.81	378.16	377.71	377.43	377.30	377.25	
40	388.00	386.07	384.30	382.80	381.21	379.69	378.32	377.15	376.21	375.46	374.90	374.51	374.27	374.16	374.12	
0	384.00	382.20	380.56	379.05	377.51	376.06	374.76	373.65	372.82	372.18	371.69	371.34	371.12	371.01	370.97	
42	380.00	378.31	376.72	375.23	373.77	372.46	371.27	370.25	369.54	368.98	368.54	368.22	368.01	367.88	367.80	
43	376.00	374.41	372.89	371.45	370.11	369.02	368.01	367.17	366.50	365.92	365.48	365.15	364.93	364.79	364.72	
0	372.00	370.52	369.14	367.88	366.79	365.85	364.98	364.26	363.54	362.93	362.46	362.13	361.90	361.75	361.66	
45	368.00	366.70	365.52	364.48	363.61	362.72	361.90	361.20	360.53	359.94	359.48	359.14	358.91	358.75	358.66	
46	364.00	362.89	361.88	361.00	360.23	359.45	358.73	358.08	357.47	356.95	356.51	356.18	355.95	355.81	355.72	
0	360.00	359.05	358.19	357.43	356.73	356.08	355.48	354.91	354.39	353.92	353.54	353.25	353.05	352.93	352.86	
48	356.00	355.19	354.46	353.79	353.18	352.66	352.17	351.70	351.27	350.88	350.57	350.35	350.19	350.12	350.08	
49	352.00	351.34	350.73	350.15	349.64	349.25	348.87	348.49	348.14	347.84	347.60	347.44	347.35	347.32	347.33	
50	348.00	347.52	347.05	346.64	346.27	345.94	345.61	345.31	345.03	344.80	344.62	344.52	344.48	344.49	344.54	
0	344.00	343.69	343.42	343.18	342.97	342.68	342.40	342.14	341.93	341.75	341.63	341.58	341.59	341.64	341.70	
52	340.00	339.87	339.76	339.66	339.54	339.36	339.15	338.96	338.80	338.68	338.62	338.66	338.74	338.83	338.89	
53	336.00	336.07	336.12	336.13	336.10	336.00	335.89	335.76	335.65	335.59	335.58	335.61	335.70	335.81	335.93	
0	332.00	332.28	332.48	332.61	332.66	332.65	332.60	332.54	332.48	332.46	332.49	332.56	332.68	332.83	332.99	
55	328.00	328.51	328.88	329.11	329.24	329.30	329.29	329.28	329.27	329.30	329.35	329.46	329.61	329.79	329.99	
56	324.00	324.87	325.39	325.69	325.86	325.94	325.98	326.00	326.03	326.08	326.16	326.27	326.43	326.63	326.87	
0	320.00	321.50	322.06	322.34	322.51	322.59	322.66	322.71	322.76	322.81	322.88	322.98	323.10	323.26	323.42	
58	320.00	319.03	318.94	319.04	319.14	319.23	319.30	319.36	319.41	319.46	319.51	319.58	319.63	319.69	319.70	

1

59 316.00 315.68 315.60 315.64 315.71 315.78 315.83 315.87 315.91 315.94 315.97 316.00 316.01 315.98 315.90 315.77

60 312.00 312.00 312.00 312.00 312.00 312.00 312.00 312.00 312.00 312.00 312.00 312.00 312.00 312.00 312.00 312.00

DRAWDOWN IN LAYER 1 AT END OF TIME STEP 24 IN STRESS PERIOD 1

	1	2	3	4	5	6	7	8	9	10	11	12	13	14	15	16
1	.00	.00	.00	.00	.00	.00	.00	.00	.00	.00	.00	.00	.00	.00	.00	0.00
2	.00	.03	.10	.11	.29	.30	-.31	.05	.01	-.02	-.06	-.22	-.20	-.45	-.70	-1.64
3	.00	.03	.10	.42	1.92	.98	-.31	.13	.03	-.11	-.25	-.80	-.62	-.98	-1.55	-2.93
4	.00	.11	.12	.39	1.18	.91	-.34	-.25	-.31	-.32	-.50	-.84	-1.02	-1.66	-2.51	-4.11
5	.00	.05	.09	.28	.66	.59	-.80	-2.41	-1.18	-.77	-.88	-1.18	-1.79	-2.50	-3.68	-5.30
6	.00	.04	.11	.26	.46	.42	-.79	-1.06	-1.10	-1.06	-1.22	-1.95	-3.10	-4.55	-4.78	-6.57
7	.00	.05	.16	.20	.29	.28	-.76	-.59	-.84	-1.11	-1.64	-2.93	-5.82	-5.84	-5.77	-7.16
8	.00	.10	.11	.24	.29	.26	-.64	-.35	-.67	-1.12	-1.80	-2.89	-4.53	-6.10	-6.31	-7.79
9	.00	.07	.24	.42	.43	.36	-.39	-.14	-.57	-1.00	-1.71	-2.79	-4.16	-6.18	-6.53	-8.21
10	.00	.13	.55	2.52	1.43	.87	.08	.07	-.39	-.91	-1.71	-2.76	-3.95	-6.13	-6.81	-8.52
11	.00	.20	.57	1.62	1.42	1.09	.59	.22	-.51	-.87	-1.62	-2.60	-3.82	-5.95	-6.89	-8.82
12	.00	.17	.54	1.12	1.28	1.11	.03	.58	-.05	-.72	-1.50	-2.52	-3.78	-5.67	-6.95	-8.91
13	.00	.20	.44	.85	1.02	1.17	.45	.65	.14	-.55	-1.37	-2.44	-3.65	-5.29	-7.01	-8.89
14	.00	.22	.37	.68	.74	1.83	1.11	.90	.39	-.33	-1.21	-2.34	-3.61	-5.80	-6.87	-8.88
15	.00	.20	.47	.90	3.43	2.61	1.52	1.22	.67	-.15	-1.01	-2.21	-3.55	-5.20	-6.82	-8.66
16	.00	.17	.40	.78	2.65	2.61	2.05	1.51	.90	.06	-.88	-2.06	-3.47	-5.49	-6.56	-8.32
17	.00	.17	.34	.80	1.87	2.32	1.39	1.71	1.11	.26	-.76	-2.01	-3.38	-5.67	-6.39	-7.97
18	.00	.18	.35	.74	1.43	1.88	1.57	1.72	1.19	.38	-.71	-2.01	-3.51	-5.76	-6.10	-7.39
19	.00	.16	.31	.64	1.20	1.56	1.59	1.72	1.22	.49	-.68	-2.16	-4.35	-5.88	-6.07	-7.42
20	.00	.11	.30	.56	.93	1.29	1.55	1.56	1.19	.43	-.60	-2.05	-3.59	-4.96	-6.02	-7.46
21	.00	.13	.25	.50	.80	1.13	.48	1.35	1.07	.41	-.60	-1.86	-3.37	-4.96	-6.03	-7.48
22	.00	.14	.26	.38	.62	.91	.33	.74	.79	.33	-.62	-1.81	-3.30	-4.93	-6.04	-7.50
23	.00	.13	.23	.39	.55	.83	.09	.83	.69	.22	-.67	-2.00	-3.44	-4.92	-6.06	-7.53
24	.00	.13	.21	.44	.93	.86	-.08	.75	.60	.06	-.79	-2.23	-4.50	-5.04	-6.24	-7.60
25	.00	.13	.21	.37	.67	.79	.78	.68	.52	-.03	-.89	-2.25	-3.85	-5.20	-6.26	-7.70
26	.00	.12	.20	.35	.49	.67	.62	.69	.42	-.15	-.99	-2.22	-3.58	-5.34	-6.30	-7.84
27	.00	.12	.18	.29	.47	.51	.44	.59	.29	-.19	-1.01	-2.29	-3.69	-5.49	-6.48	-8.03
28	.00	.10	.13	.31	.44	.44	.24	.47	.23	-.27	-1.18	-2.53	-4.22	-5.76	-6.76	-8.32
29	.00	.08	.19	.33	.55	.52	.05	.42	.12	-.42	-1.49	-3.12	-5.77	-6.26	-7.20	-8.72
30	.00	.07	.16	.29	.38	.47	-.16	.32	.05	-.58	-1.56	-3.07	-4.88	-6.88	-7.56	-9.25
31	.00	.05	.13	.24	.37	.40	-.42	.28	-.08	-.71	-1.67	-3.03	-4.62	-6.53	-7.92	-9.90
32	.00	.04	.08	.16	.24	.29	.30	.21	-.16	-.79	-1.71	-3.01	-4.52	-6.27	-8.29	-10.69
33	.00	.01	.13	.17	.19	.28	-.01	.11	-.27	-.90	-1.80	-3.06	-4.52	-7.13	-8.70	-11.64
34	.00	.00	.11	.11	.15	.16	-.32	-.00	-.29	-.93	-1.82	-2.96	-4.49	-7.05	-8.58	-11.17
35	.00	.00	.11	.06	.14	.16	-.61	-.02	-.41	-.94	-1.83	-2.86	-4.18	-6.97	-8.24	-10.64
36	.00	.04	.06	.08	.09	.09	-.90	-.12	-.51	-1.03	-1.70	-2.57	-3.11	-5.80	-7.84	-10.08
37	.00	-.01	-.06	-.04	-.06	.02	-.19	-.21	-.60	-1.11	-1.72	-2.62	-3.69	-5.60	-7.51	-9.48
38	.00	-.06	-.18	-.48	-.30	-.22	-.51	-.31	-.61	-1.19	-1.87	-2.74	-3.89	-5.43	-7.08	-8.87
39	.00	-.21	-.72	-2.26	-.79	-.49	-.90	-.56	-.84	-1.31	-1.96	-2.81	-3.93	-5.30	-6.75	-8.25
40	.00	-.17	-.70	-1.30	-.91	-.69	-1.32	-.75	-1.01	-1.46	-2.00	-2.91	-3.87	-5.16	-6.32	-7.62
41	.00	-.20	-.56	-.95	-.91	-.86	-1.76	-1.05	-1.32	-1.68	-2.19	-2.94	-3.82	-5.01	-5.97	-6.96
42	.00	-.21	-.52	-.83	-.97	-1.16	-1.27	-1.65	-1.64	-1.88	-2.34	-3.02	-3.81	-4.88	-5.63	-6.70
43	.00	-.21	-.49	-.95	-1.41	-1.52	-2.01	-3.17	-2.30	-2.22	-2.48	-3.05	-3.73	-4.79	-5.42	-6.39
44	.00	-.22	-.64	-1.28	-2.79	-2.15	-2.98	-2.56	-2.34	-2.33	-2.56	-3.03	-3.70	-4.75	-5.26	-6.22
45	.00	-.20	-.62	-1.28	-2.01	-2.02	-2.90	-2.30	-2.33	-2.44	-2.68	-3.04	-3.61	-4.75	-5.16	-6.01
46	.00	-.29	-.68	-1.20	-1.63	-1.85	-2.73	-2.18	-2.27	-2.45	-2.61	-3.08	-3.55	-4.81	-5.12	-5.97
47	.00	-.25	-.69	-1.03	-1.43	-1.68	-2.48	-2.01	-2.19	-2.32	-2.64	-3.05	-3.55	-4.93	-4.96	-5.92

48	.00	-.29	-.66	-.99	-1.38	-1.66	-2.17	-2.00	-2.17	-2.28	-2.57	-2.95	-3.49	-4.12	-4.88	-6.09
0 49	.00	-.34	-.63	-1.05	-1.54	-1.65	-1.87	-1.89	-2.04	-2.24	-2.50	-2.84	-3.35	-4.32	-4.53	-5.18
50	.00	-.32	-.75	-1.34	-2.27	-1.84	-2.61	-1.91	-2.03	-2.20	-2.42	-2.72	-3.08	-4.49	-4.04	-4.49
51	.00	-.29	-.72	-1.18	-1.67	-1.78	-2.40	-1.84	-1.93	-2.05	-2.33	-2.58	-2.89	-3.64	-3.60	-3.86
0 52	.00	-.37	-.66	-1.06	-1.44	-1.56	-2.15	-1.76	-1.80	-1.98	-2.22	-2.42	-2.66	-3.74	-3.23	-3.39
53	.00	-.27	-.62	-1.03	-1.30	-1.40	-1.89	-1.66	-1.75	-1.89	-2.08	-2.21	-2.40	-2.81	-2.83	-2.91
54	.00	-.28	-.58	-.91	-1.16	-1.35	-1.60	-1.54	-1.68	-1.76	-1.89	-2.06	-2.18	-2.83	-2.39	-2.40
55	.00	-.31	-.58	-.81	-1.04	-1.20	-1.29	-1.38	-1.47	-1.60	-1.75	-1.86	-1.91	-2.79	-1.99	-1.86
0 56	.00	-.27	-.49	-.79	-.96	-1.04	-1.98	-1.30	-1.43	-1.48	-1.56	-1.57	-1.63	-1.63	-1.37	-1.12
57	.00	-.20	-.46	-.64	-.81	-.99	-1.66	-1.21	-1.26	-1.31	-1.38	-1.38	-1.30	-1.26	-.72	0.44
58	.00	-.23	-.34	-.54	-.64	-.83	-1.30	-.96	-1.01	-1.06	-1.11	-1.08	-1.03	-1.69	-.40	0.38
0 59	.00	-.18	-.20	-.34	-.51	-.58	-.83	-.67	-.71	-.74	-.77	-.70	-.71	-.98	-.20	0.23
60	.00	.00	.00	.00	.00	.00	.00	.00	.00	.00	.00	.00	.00	.00	.00	.00

VOLUMETRIC BUDGET FOR ENTIRE MODEL AT END OF TIME STEP 24 IN STRESS PERIOD 1

CUMULATIVE VOLUMES	L**3	RATES FOR THIS TIME STEP	L**3/T
IN:		IN:	
---		---	
STORAGE = .00000		STORAGE = .00000	
CONSTANT HEAD = 2999.7		CONSTANT HEAD = 2975.6	
TOTAL IN = 2999.7		TOTAL IN = 2975.6	
OUT:		OUT:	
---		---	
STORAGE = .00000		STORAGE = .00000	
CONSTANT HEAD = 1094.6		CONSTANT HEAD = 1279.1	
TOTAL OUT = 1094.6		TOTAL OUT = 1279.1	
IN - OUT = 1905.2		IN - OUT = 1696.5	
PERCENT DISCREPANCY = 93.06		PERCENT DISCREPANCY = 79.75	

TIME SUMMARY AT END OF TIME STEP 24 IN STRESS PERIOD 1

	SECONDS	MINUTES	HOURS	DAYS	YEARS
TIME STEP LENGTH	3600.00	60.0000	1.00000	.416667E-01	.114077E-03
STRESS PERIOD TIME	86400.0	1440.00	24.0000	1.00000	.273785E-02
TOTAL SIMULATION TIME	86400.0	1440.00	24.0000	1.00000	.273785E-02

APPENDIX B
WIDE BASIN COMPUTER OUTPUT

U.S. GEOLOGICAL SURVEY MODULAR FINITE-DIFFERENCE GROUND-WATER MODEL

HYDRAULIC BASIN RESPONSE

1 LAYERS 60 ROWS 16 COLUMNS

1 STRESS PERIOD(S) IN SIMULATION

MODEL TIME UNIT IS DAYS

I/O UNITS:

ELEMENT OF IUNIT: 1 2 3 4 5 6 7 8 9 10 11 12 13 14 15 16 17 18 19 20 21 22 23 24
I/O UNIT: 11 0 0 0 0 0 0 0 0 21 22 0 0 0 0 0 0 0 0 0 0 0 0 0 0 0

OBAS1 -- BASIC MODEL PACKAGE, VERSION 1, 9/1/87 INPUT READ FROM UNIT 1

ARRAYS RHS AND BUFF WILL SHARE MEMORY.

START HEAD WILL BE SAVED

8720 ELEMENTS IN X ARRAY ARE USED BY BAS

8720 ELEMENTS OF X ARRAY USED OUT OF 100000

BCF1 -- BLOCK-CENTERED FLOW PACKAGE, VERSION 1, 9/1/87 INPUT READ FROM UNIT 11

STEADY-STATE SIMULATION

LAYER AQUIFER TYPE

1

1921 ELEMENTS IN X ARRAY ARE USED BY BCF

10641 ELEMENTS OF X ARRAY USED OUT OF 100000

SOR1 -- SLICE-SUCCESSIVE OVERRELAXATION PACKAGE, VERSION 1, 9/1/87 INPUT READ FROM UNIT 21

100 ITERATIONS ALLOWED FOR SOR CLOSURE

464 ELEMENTS IN X ARRAY ARE USED BY SOR

11105 ELEMENTS OF X ARRAY USED OUT OF 100000

HYDRAULIC BASIN RESPONSE

BOUNDARY ARRAY FOR LAYER 1 WILL BE READ ON UNIT 1 USING FORMAT: (40I2)

1 2 3 4 5 6 7 8 9 10 11 12 13 14 15 16

```

-24 -1 1 1 1 1 1 1 1 1 1 1 1 1 1 1 1
0 25 -1 1 1 1 1 1 1 1 1 1 1 1 1 1 1 1
-26 -1 1 1 1 1 1 1 1 1 1 1 1 1 1 1 1
-27 -1 1 1 1 1 1 1 1 1 1 1 1 1 1 1 1
0 28 -1 1 1 1 1 1 1 1 1 1 1 1 1 1 1 1
-29 -1 1 1 1 1 1 1 1 1 1 1 1 1 1 1 1
-30 -1 1 1 1 1 1 1 1 1 1 1 1 1 1 1 1
0 31 -1 1 1 1 1 1 1 1 1 1 1 1 1 1 1 1
-0 32 -1 1 1 1 1 1 1 1 1 1 1 1 1 1 1 1
-33 -1 1 1 1 1 1 1 1 1 1 1 1 1 1 1 1
-34 -1 1 1 1 1 1 1 1 1 1 1 1 1 1 1 1
0 35 -1 1 1 1 1 1 1 1 1 1 1 1 1 1 1 1
-36 -1 1 1 1 1 1 1 1 1 1 1 1 1 1 1 1
-37 -1 1 1 1 1 1 1 1 1 1 1 1 1 1 1 1
0 38 -1 1 1 1 1 1 1 1 1 1 1 1 1 1 1 1
-39 -1 1 1 1 1 1 1 1 1 1 1 1 1 1 1 1
-40 -1 1 1 1 1 1 1 1 1 1 1 1 1 1 1 1
-41 -1 1 1 1 1 1 1 1 1 1 1 1 1 1 1 1
-0 42 -1 1 1 1 1 1 1 1 1 1 1 1 1 1 1 1
-43 -1 1 1 1 1 1 1 1 1 1 1 1 1 1 1 1
-44 -1 1 1 1 1 1 1 1 1 1 1 1 1 1 1 1
0 45 -1 1 1 1 1 1 1 1 1 1 1 1 1 1 1 1
-46 -1 1 1 1 1 1 1 1 1 1 1 1 1 1 1 1
-47 -1 1 1 1 1 1 1 1 1 1 1 1 1 1 1 1
0 48 -1 1 1 1 1 1 1 1 1 1 1 1 1 1 1 1
-49 -1 1 1 1 1 1 1 1 1 1 1 1 1 1 1 1
-50 -1 1 1 1 1 1 1 1 1 1 1 1 1 1 1 1
-51 -1 1 1 1 1 1 1 1 1 1 1 1 1 1 1 1
0 52 -1 1 1 1 1 1 1 1 1 1 1 1 1 1 1 1
-53 -1 1 1 1 1 1 1 1 1 1 1 1 1 1 1 1
-54 -1 1 1 1 1 1 1 1 1 1 1 1 1 1 1 1
0 55 -1 1 1 1 1 1 1 1 1 1 1 1 1 1 1 1
-56 -1 1 1 1 1 1 1 1 1 1 1 1 1 1 1 1
-57 -1 1 1 1 1 1 1 1 1 1 1 1 1 1 1 1
0 58 -1 1 1 1 1 1 1 1 1 1 1 1 1 1 1 1
-59 -1 1 1 1 1 1 1 1 1 1 1 1 1 1 1 1
-0 60 -1 -1 -1 -1 -1 -1 -1 -1 -1 -1 -1 -1 -1 -1 -1 -1

```

AQUIFER HEAD WILL BE SET TO .00000 AT ALL NO-FLOW NODES (IBOUND=0).

0

INITIAL HEAD FOR LAYER 1 WILL BE READ ON UNIT 1 USING FORMAT: (7G11.4)

	1	2	3	4	5	6	7	8	9	10
	11	12	13	14	15	16				
1	537.3	535.1	532.9	530.7	528.4	526.2	524.0	521.8	519.5	517.3
	515.1	512.9	510.7	508.0	506.2	504.0				
2	534.7	532.4	530.2	528.0	525.9	523.2	520.0	517.9	515.5	513.2
	510.9	508.5	506.4	504.0	502.1	500.0				
3	532.0	529.6	527.3	525.3	524.0	520.0	516.0	513.9	511.5	509.1
	506.7	504.0	502.2	500.0	498.1	496.0				
4	529.3	526.8	524.2	521.8	519.4	516.1	512.0	509.5	507.3	505.1
	502.7	500.3	498.2	496.0	494.1	492.0				
5	526.7	523.8	521.0	518.3	515.5	512.3	508.0	504.0	503.1	501.2

0 6	498.8	496.4	494.0	492.0	490.0	488.0	505.0	502.4	500.0	497.6
1 7	524.0	520.7	517.8	515.0	512.1	509.0	505.0	502.4	500.0	497.6
2 8	495.1	492.3	489.5	487.0	486.1	484.0	508.8	505.8	502.0	499.7
3 9	520.0	517.2	514.5	511.7	508.8	505.8	483.0	480.7	497.0	494.3
4 10	491.5	488.3	484.0	482.4	480.7	480.7	479.1	477.3	493.9	491.1
5 11	516.0	513.6	511.1	508.6	505.7	502.7	480.0	477.3	496.7	488.0
6 12	488.3	485.5	482.6	480.0	479.1	474.0	479.1	474.0	490.7	488.0
7 13	512.0	509.9	507.9	505.8	502.7	499.6	496.0	493.6	490.4	487.5
8 14	485.3	482.6	480.0	477.0	476.0	474.0	479.5	477.1	490.4	484.8
9 15	508.0	506.2	504.7	504.0	499.8	496.5	493.0	490.4	487.5	484.8
10 16	482.1	479.5	477.1	474.0	472.7	470.7	479.5	477.1	484.0	481.5
11 17	504.0	502.3	500.6	498.8	496.0	493.1	490.0	487.1	484.0	481.5
12 18	478.9	476.4	474.0	471.0	469.5	467.3	476.4	474.0	481.0	478.2
13 19	500.0	498.3	496.6	494.7	492.4	489.7	486.0	484.0	481.0	478.2
14 20	475.6	473.1	470.7	468.0	466.2	464.0	473.1	470.7	477.6	474.8
15 21	496.0	494.4	492.7	491.0	489.0	486.6	483.0	480.5	477.6	474.8
16 22	472.2	469.7	467.4	465.0	462.8	460.7	469.7	467.4	474.1	471.3
17 23	492.0	490.5	488.9	487.5	486.1	484.0	480.0	477.0	474.1	471.3
18 24	468.7	466.2	463.9	461.0	459.5	457.3	466.2	463.9	466.5	463.8
19 25	488.0	486.5	485.1	484.0	484.0	479.8	476.0	473.2	470.4	467.6
20 26	465.1	462.6	460.3	458.0	456.0	454.0	462.6	460.3	466.5	463.8
21 27	484.0	482.4	480.8	479.3	477.8	475.0	472.0	469.2	466.5	463.8
22 28	461.3	458.9	456.6	454.0	452.6	450.7	458.9	456.6	454.3	451.9
23 29	480.0	478.3	476.5	474.8	472.8	470.4	467.0	465.1	462.5	459.9
24 30	457.4	455.0	452.8	450.0	449.0	447.3	455.0	452.8	458.4	455.9
25 31	476.0	474.2	472.3	470.4	468.3	465.9	463.0	460.9	458.4	455.9
26 32	453.4	451.0	448.7	446.0	445.4	444.0	451.0	448.7	454.3	451.9
27 33	472.0	470.1	468.1	466.1	464.0	461.6	459.0	456.8	454.3	451.9
28 0	449.4	446.9	444.0	442.0	441.5	440.0	449.4	446.9	444.0	447.8
29 1	468.0	466.0	464.0	461.9	459.7	457.4	455.0	452.6	450.2	447.8
30 2	445.5	443.1	440.9	439.0	437.6	436.0	443.1	440.9	442.0	439.8
31 3	480.0	478.3	476.5	474.8	472.8	470.4	467.0	465.1	462.5	459.9
32 4	457.4	455.0	452.8	450.0	449.0	447.3	455.0	452.8	458.4	455.9
33 5	476.0	474.2	472.3	470.4	468.3	465.9	463.0	460.9	458.4	455.9
34 6	453.4	451.0	448.7	446.0	445.4	444.0	451.0	448.7	454.3	451.9
35 7	472.0	470.1	468.1	466.1	464.0	461.6	459.0	456.8	454.3	451.9
36 8	449.4	446.9	444.0	442.0	441.5	440.0	449.4	446.9	444.0	447.8
37 9	468.0	466.0	464.0	461.9	459.7	457.4	455.0	452.6	450.2	447.8
38 10	445.5	443.1	440.9	439.0	437.6	436.0	443.1	440.9	442.0	439.8
39 11	480.0	478.3	476.5	474.8	472.8	470.4	467.0	465.1	462.5	459.9
40 12	457.4	455.0	452.8	450.0	449.0	447.3	455.0	452.8	458.4	455.9
41 13	476.0	474.2	472.3	470.4	468.3	465.9	463.0	460.9	458.4	455.9
42 14	453.4	451.0	448.7	446.0	445.4	444.0	451.0	448.7	454.3	451.9
43 15	472.0	470.1	468.1	466.1	464.0	461.6	459.0	456.8	454.3	451.9
44 16	449.4	446.9	444.0	442.0	441.5	440.0	449.4	446.9	444.0	447.8
45 17	468.0	466.0	464.0	461.9	459.7	457.4	455.0	452.6	450.2	447.8
46 18	445.5	443.1	440.9	439.0	437.6	436.0	443.1	440.9	442.0	439.8
47 19	480.0	478.3	476.5	474.8	472.8	470.4	467.0	465.1	462.5	459.9
48 20	457.4	455.0	452.8	450.0	449.0	447.3	455.0	452.8	458.4	455.9
49 21	476.0	474.2	472.3	470.4	468.3	465.9	463.0	460.9	458.4	455.9
50 22	453.4	451.0	448.7	446.0	445.4	444.0	451.0	448.7	454.3	451.9
51 23	472.0	470.1	468.1	466.1	464.0	461.6	459.0	456.8	454.3	451.9
52 24	449.4	446.9	444.0	442.0	441.5	440.0	449.4	446.9	444.0	447.8
53 25	468.0	466.0	464.0	461.9	459.7	457.4	455.0	452.6	450.2	447.8
54 26	445.5	443.1	440.9	439.0	437.6	436.0	443.1	440.9	442.0	439.8
55 27	480.0	478.3	476.5	474.8	472.8	470.4	467.0	465.1	462.5	459.9
56 28	457.4	455.0	452.8	450.0	449.0	447.3	455.0	452.8	458.4	455.9
57 29	476.0	474.2	472.3	470.4	468.3	465.9	463.0	460.9	458.4	455.9
58 30	453.4	451.0	448.7	446.0	445.4	444.0	451.0	448.7	454.3	451.9
59 31	472.0	470.1	468.1	466.1	464.0	461.6	459.0	456.8	454.3	451.9
60 32	449.4	446.9	444.0	442.0	441.5	440.0	449.4	446.9	444.0	447.8
61 33	468.0	466.0	464.0	461.9	459.7	457.4	455.0	452.6	450.2	447.8
62 34	445.5	443.1	440.9	439.0	437.6	436.0	443.1	440.9	442.0	439.8
63 35	480.0	478.3	476.5	474.8	472.8	470.4	467.0	465.1	462.5	459.9
64 36	457.4	455.0	452.8	450.0	449.0	447.3	455.0	452.8	458.4	455.9
65 37	476.0	474.2	472.3	470.4	468.3	465.9	463.0	460.9	458.4	455.9
66 38	453.4	451.0	448.7	446.0	445.4	444.0	451.0	448.7	454.3	451.9
67 39	472.0	470.1	468.1	466.1	464.0	461.6	459.0	456.8	454.3	451.9
68 40	449.4	446.9	444.0	442.0	441.5	440.0	449.4	446.9	444.0	447.8
69 41	468.0	466.0	464.0	461.9	459.7	457.4	455.0	452.6	450.2	447.8
70 42	445.5	443.1	440.9	439.0	437.6	436.0	443.1	440.9	442.0	439.8
71 43	480.0	478.3	476.5	474.8	472.8	470.4	467.0	465.1	462.5	459.9
72 44	457.4	455.0	452.8	450.0	449.0	447.3	455.0	452.8	458.4	455.9
73 45	476.0	474.2	472.3	470.4	468.3	465.9	463.0	460.9	458.4	455.9
74 46	453.4	451.0	448.7	446.0	445.4	444.0	451.0	448.7	454.3	451.9
75 47	472.0	470.1	468.1	466.1	464.0	461.6	459.0	456.8	454.3	451.9
76 48	449.4	446.9	444.0	442.0	441.5	440.0	449.4	446.9	444.0	447.8
77 49	468.0	466.0	464.0	461.9	459.7	457.4	455.0	452.6	450.2	447.8
78 50	445.5	443.1	440.9	439.0	437.6	436.0	443.1	440.9	442.0	439.8
79 51	480.0	478.3	476.5	474.8	472.8	470.4	467.0	465.1	462.5	459.9
80 52	457.4	455.0	452.8	450.0	449.0	447.3	455.0	452.8	458.4	455.9
81 53	476.0	474.2	472.3	470.4	468.3	465.9	463.0	460.9	458.4	455.9
82 54	453.4	451.0	448.7	446.0	445.4	444.0	451.0	448.7	454.3	451.9
83 55	472.0	470.1	468.1	466.1	464.0	461.6	459.0	456.8	454.3	451.9
84 56	449.4	446.9	444.0	442.0	441.5	440.0	449.4	446.9	444.0	447.8
85 57	468.0	466.0	464.0	461.9	459.7	457.4	455.0	452.6	450.2	447.8
86 58	445.5	443.1	440.9	439.0	437.6	436.0	443.1	440.9	442.0	439.8
87 59	480.0	478.3	476.5	474.8	472.8	470.4	467.0	465.1	462.5	459.9
88 60	457.4	455.0	452.8	450.0	449.0	447.3	455.0	452.8	458.4	455.9
89 61	476.0	474.2	472.3	470.4	468.3	465.9	463.0	460.9	458.4	455.9
90 62	453.4	451.0	448.7	446.0	445.4	444.0	451.0	448.7	454.3	451.9
91 63	472.0	470.1	468.1	466.1	464.0	461.6	459.0	456.8	454.3	451.9
92 64	449.4	446.9	444.0	442.0	441.5	440.0	449.4	446.9	444.0	447.8
93 65	468.0	466.0	464.0	461.9	459.7	457.4	455.0	452.6	450.2	447.8
94 66	445.5	443.1	440.9	439.0	437.6	436.0	443.1	440.9	442.0	439.8
95 67	480.0	478.3	476.5	474.8	472.8	470.4	467.0	465.1	462.5	459.9
96 68	457.4	455.0	452.8	450.0	449.0	447.3	455.0	452.8	458.4	455.9
97 69	476.0	474.2	472.3	470.4	468.3	465.9	463.0	460.9	458.4	455.9
98 70	453.4	451.0	448.7	446.0	445.4	444.0	451.0	448.7	454.3	451.9
99 71	472.0	470.1	468.1	466.1	464.0	461.6	459.0	456.8	454.3	451.9
100 72	449.4	446.9	444.0	442.0	441.5	440.0	449.4	446.9	444.0	447.8
101 73	468.0	466.0	464.0	461.9	459.7	457.4	455.0	452.6	450.2	447.8
102 74	445.5	443.1	440.9	439.0	437.6	436.0	443.1	440.9	442.0	439.8
103 75	480.0	478.3	476.5	474.8	472.8	470.4	467.0	465.1	462.5	459.9
104 76	457.4	455.0	452.8	450.0	449.0	447.3	455.0	452.8	458.4	455.9
105 77	476.0	474.2	472.3	470.4	468.3	465.9	463.0	460.9	4	

	396.3	394.2	392.1	389.0	387.1	384.0			
0 34	412.0	410.0	408.1	406.1	404.2	402.3	400.0	398.6	396.8
	393.0	391.1	389.0	386.0	384.2	381.5			394.9
35	408.0	406.0	404.1	402.1	400.3	398.5	396.0	395.0	393.2
	389.7	388.0	386.2	383.0	381.5	379.0			391.5
36	404.0	402.0	400.0	398.1	396.3	394.6	392.0	391.3	389.6
	386.5	385.0	384.0	381.0	378.8	376.5			388.0
37	400.0	397.9	395.8	393.9	392.2	390.7	389.0	387.6	386.0
	383.1	381.6	380.1	378.0	376.0	374.0			384.5
38	396.0	393.8	391.6	389.4	388.1	386.7	385.0	383.9	382.5
	379.6	378.2	376.7	375.0	373.3	371.5			381.0
0 39	392.0	389.7	387.2	384.0	384.0	382.8	381.0	380.1	378.8
	376.2	374.9	373.5	372.0	370.5	369.0			377.5
40	388.0	385.9	383.6	381.5	380.3	379.0	377.0	376.4	375.2
	372.9	371.6	370.4	369.0	367.8	366.5			374.0
41	384.0	382.0	380.0	378.1	376.6	375.2	373.0	372.6	371.5
	369.5	368.4	367.3	366.0	365.0	364.0			370.5
42	380.0	378.1	376.2	374.4	372.8	371.3	370.0	368.6	367.9
	366.2	365.2	364.2	363.0	362.2	361.1			367.1
43	376.0	374.2	372.4	370.5	368.7	367.5	366.0	364.0	364.2
	363.0	362.1	361.2	360.0	359.3	358.3			363.7
0 44	372.0	370.3	368.5	366.6	364.0	363.7	362.0	361.7	361.2
	359.9	359.1	358.2	357.0	356.4	355.4			360.6
45	368.0	366.5	364.9	363.2	361.6	360.7	359.0	358.9	358.2
	356.8	356.1	355.3	354.0	353.5	352.6			357.5
46	364.0	362.6	361.2	359.8	358.6	357.6	356.0	355.9	355.2
	353.9	353.1	352.4	351.0	350.6	349.7			354.5
47	360.0	358.8	357.5	356.4	355.3	354.4	353.0	352.9	352.2
	350.9	350.2	349.5	348.0	347.9	346.9			351.6
48	356.0	354.9	353.8	352.8	351.8	351.0	350.0	349.7	349.1
	348.0	347.4	346.7	346.0	345.2	344.0			348.6
0 49	352.0	351.0	350.1	349.1	348.1	347.6	347.0	346.6	346.1
	345.1	344.6	344.0	343.0	342.8	342.2			345.6
50	348.0	347.2	346.3	345.3	344.0	344.1	343.0	343.4	343.0
	342.2	341.8	341.4	340.0	340.5	340.1			342.6
51	344.0	343.4	342.7	342.0	341.3	340.9	340.0	340.3	340.0
	339.3	339.0	338.7	338.0	338.1	337.9			339.7
52	340.0	339.5	339.1	338.6	338.1	337.8	337.0	337.2	337.0
	336.4	336.2	336.0	335.0	335.6	335.5			336.7
53	336.0	335.8	335.5	335.1	334.8	334.6	334.0	334.1	333.9
	333.5	333.4	333.3	333.0	333.1	333.1			333.7
0 54	332.0	332.0	331.9	331.7	331.5	331.3	331.0	331.0	330.8
	330.6	330.5	330.5	330.0	330.6	330.7			330.7
55	328.0	328.2	328.3	328.3	328.2	328.1	328.0	327.9	327.8
	327.6	327.6	327.7	327.0	328.0	328.3			327.7
0 56	324.0	324.6	324.9	324.9	324.9	324.9	324.0	324.7	324.6
	324.6	324.7	324.8	325.0	325.5	326.0			324.6
57	320.0	321.3	321.6	321.7	321.7	321.6	321.0	321.5	321.5
	321.5	321.6	321.8	322.0	322.7	324.0			321.5
58	320.0	318.8	318.6	318.5	318.5	318.4	318.0	318.4	318.4
	318.4	318.5	318.6	318.0	319.3	320.0			318.4
0 59	316.0	315.5	315.4	315.3	315.2	315.2	315.0	315.2	315.2
	315.2	315.3	315.3	315.0	315.7	316.0			315.2
60	312.0	312.0	312.0	312.0	312.0	312.0	312.0	312.0	312.0
	312.0	312.0	312.0	312.0	312.0	312.0			312.0

0HEAD PRINT FORMAT IS FORMAT NUMBER -4

DRAWDOWN PRINT FORMAT IS FORMAT NUMBER -4

HEADS WILL BE SAVED ON UNIT 0 DRAWDOWNS WILL BE SAVED ON UNIT 0
OUTPUT CONTROL IS SPECIFIED EVERY TIME STEP

COLUMN TO ROW ANISOTROPY = 1.000000
DELR = 8.000000
DELC = 4.000000
HYD. COND. ALONG ROWS = 5.000000 FOR LAYER 1

BOTTOM FOR LAYER 1 WILL BE READ ON UNIT 11 USING FORMAT: (7G11.4)

	1	2	3	4	5	6	7	8	9	10
	11	12	13	14	15	16				

1	533.3	531.1	528.9	526.7	524.4	522.2	520.0	517.8	515.6	513.3
	511.1	508.9	506.7	504.4	502.2	500.0				
2	530.7	528.4	526.1	524.0	521.9	519.2	516.5	513.9	511.5	509.2
	506.9	504.6	502.4	500.3	498.2	496.0				
3	528.0	525.6	523.3	521.3	520.0	516.0	512.8	509.9	507.5	505.1
	502.7	500.0	498.2	496.2	494.1	492.0				
4	525.3	522.7	520.2	517.8	515.4	512.1	508.8	505.5	503.3	501.1
	498.7	496.3	494.2	492.1	490.1	488.0				
5	522.7	519.8	517.0	514.3	511.5	508.3	504.7	500.0	499.1	497.2
	494.8	492.4	490.0	488.0	486.0	484.0				
6	520.0	516.7	513.8	511.0	508.1	505.0	501.7	498.3	496.0	493.7
	491.1	488.3	485.6	483.9	482.1	480.0				
7	516.0	513.2	510.5	507.7	504.8	501.8	498.7	495.7	493.0	490.3
	487.5	484.3	480.0	479.8	478.4	476.7				
8	512.0	509.6	507.1	504.6	501.7	498.7	495.7	492.7	489.9	487.1
	484.3	481.5	478.6	476.9	475.1	473.3				
9	508.0	505.9	503.9	501.8	498.7	495.6	492.6	489.6	486.7	484.0
	481.2	478.6	476.1	473.9	472.0	470.0				
10	504.0	502.2	500.7	500.0	495.8	492.5	489.4	486.4	483.5	480.8
	478.1	475.5	473.1	470.9	468.7	466.7				
11	500.0	498.3	496.6	494.8	492.0	489.1	486.1	483.1	480.0	477.5
	474.9	472.4	470.0	467.7	465.5	463.3				
12	496.0	494.3	492.6	490.7	488.4	485.7	482.8	480.0	477.0	474.2
	471.6	469.1	466.7	464.4	462.2	460.0				
13	492.0	490.4	488.7	487.0	485.0	482.6	479.5	476.5	473.6	470.8
	468.2	465.7	463.3	461.1	458.8	456.7				
14	488.0	486.5	484.9	483.5	482.1	480.0	476.2	473.0	470.1	467.3
	464.7	462.2	459.9	457.6	455.5	453.3				
15	484.0	482.5	481.1	480.0	480.0	475.8	472.4	469.2	466.4	463.6
	461.1	458.6	456.3	454.1	452.0	450.0				
16	480.0	478.4	476.8	475.3	473.8	471.0	468.1	465.2	462.5	459.8
	457.3	454.9	452.6	450.5	448.6	446.7				
17	476.0	474.3	472.5	470.8	468.8	466.4	463.8	461.1	458.5	455.9
	453.4	451.0	448.8	446.8	445.0	443.3				
18	472.0	470.2	468.3	466.4	464.3	461.9	459.5	456.9	454.4	451.9
	449.4	447.0	444.7	442.9	441.4	440.0				
19	468.0	466.1	464.1	462.1	460.0	457.6	455.2	452.8	450.3	447.9
	445.4	442.9	440.0	438.9	437.4	436.0				
20	464.0	462.0	460.0	457.9	455.7	453.4	451.0	448.6	446.2	443.8
	441.5	439.1	436.9	435.2	433.6	432.0				
21	460.0	458.0	455.9	453.8	451.6	449.3	446.8	444.4	442.1	439.8

0 22	437.5	435.3	433.1	431.3	429.6	428.0				
	456.0	454.0	451.9	449.7	447.5	445.2	442.7	440.0	438.0	435.8
	433.5	431.3	429.2	427.3	425.6	424.0				
23	452.0	450.0	447.9	445.8	443.6	441.3	438.8	436.4	434.1	431.8
	429.5	427.1	424.9	423.2	421.6	420.0				
24	448.0	446.0	443.9	441.9	440.0	437.4	434.9	432.5	430.2	427.8
	425.5	423.0	420.0	419.0	417.6	416.0				
25	444.0	442.0	439.9	437.8	435.7	433.4	431.0	428.6	426.3	423.9
	421.6	419.2	416.9	415.2	413.6	412.0				
26	440.0	438.0	435.9	433.8	431.6	429.4	427.1	424.7	422.4	420.0
	417.7	415.4	413.3	411.4	409.7	408.0				
0 27	436.0	434.0	431.9	429.8	427.7	425.4	423.2	420.9	418.5	416.2
	413.8	411.5	409.3	407.4	405.7	404.0				
28	432.0	430.0	427.9	425.9	423.8	421.6	419.3	417.0	414.7	412.4
	410.0	407.5	405.0	403.3	401.7	400.0				
29	428.0	426.0	424.0	421.9	420.0	417.7	415.5	413.2	410.9	408.6
	406.1	403.4	400.0	399.2	397.7	396.0				
30	424.0	422.0	420.0	418.0	415.9	413.8	411.6	409.4	407.2	404.9
	402.6	400.1	397.6	395.8	393.9	392.0				
31	420.0	418.0	416.0	414.0	412.0	409.9	407.8	405.7	403.5	401.3
	399.1	396.8	394.5	392.4	390.2	388.0				
0 32	416.0	414.0	412.0	410.0	408.0	406.0	404.0	402.0	399.9	397.8
	395.7	393.5	391.3	389.0	386.6	384.0				
33	412.0	410.0	408.1	406.1	404.1	402.2	400.2	398.3	396.3	394.3
	392.3	390.2	388.1	385.7	383.1	380.0				
34	408.0	406.0	404.1	402.1	400.2	398.3	396.5	394.6	392.8	390.9
	389.0	387.1	385.0	382.7	380.2	377.5				
35	404.0	402.0	400.1	398.1	396.3	394.5	392.7	390.9	389.2	387.5
	385.7	384.0	382.2	379.9	377.5	375.0				
36	400.0	398.0	396.0	394.1	392.3	390.6	388.9	387.3	385.6	384.0
	382.5	381.0	380.0	377.2	374.8	372.5				
0 37	396.0	393.9	391.8	389.9	388.2	386.7	385.1	383.6	382.0	380.5
	379.1	377.6	376.1	374.1	372.0	370.0				
38	392.0	389.8	387.6	385.4	384.1	382.7	381.3	379.9	378.4	377.0
	375.6	374.2	372.7	371.0	369.3	367.5				
39	388.0	385.7	383.2	380.0	380.0	378.8	377.5	376.1	374.8	373.5
	372.2	370.9	369.5	368.0	366.5	365.0				
40	384.0	381.9	379.6	377.5	376.3	375.0	373.7	372.4	371.2	370.0
	368.8	367.6	366.4	365.1	363.8	362.5				
41	380.0	378.0	376.0	374.1	372.6	371.2	369.9	368.6	367.6	366.5
	365.5	364.4	363.3	362.2	361.0	360.0				
0 42	376.0	374.1	372.2	370.4	368.7	367.3	366.0	364.6	363.9	363.1
	362.2	361.2	360.2	359.2	358.2	357.1				
43	372.0	370.2	368.4	366.5	364.7	363.5	362.1	360.0	360.2	359.7
	359.0	358.1	357.2	356.2	355.3	354.3				
0 44	368.0	366.3	364.5	362.6	360.0	359.7	358.8	357.7	357.2	356.6
	355.9	355.1	354.2	353.3	352.4	351.4				
45	364.0	362.4	360.8	359.2	357.6	356.7	355.8	354.9	354.2	353.5
	352.8	352.1	351.3	350.4	349.5	348.6				
46	360.0	358.6	357.2	355.8	354.6	353.6	352.7	351.9	351.2	350.5
	349.9	349.1	348.4	347.5	346.7	345.7				
0 47	356.0	354.8	353.5	352.4	351.3	350.4	349.6	348.9	348.2	347.6
	346.9	346.2	345.5	344.7	343.9	342.9				
48	352.0	350.9	349.8	348.8	347.8	347.0	346.4	345.7	345.2	344.6
	344.0	343.4	342.7	342.0	341.2	340.0				
0 49	348.0	347.0	346.1	345.1	344.1	343.6	343.1	342.6	342.1	341.6

	341.1	340.6	340.0	339.5	338.8	338.2			
0 50	344.0	343.2	342.3	341.3	340.0	340.1	339.8	339.4	339.0
	338.2	337.8	337.4	336.9	336.5	336.1			
51	340.0	339.4	338.7	338.0	337.3	336.9	336.6	336.3	336.0
	335.3	335.0	334.7	334.4	334.1	333.9			
52	336.0	335.5	335.1	334.6	334.1	333.8	333.5	333.2	333.0
	332.4	332.2	332.0	331.8	331.6	331.5			
53	332.0	331.7	331.4	331.1	330.8	330.6	330.3	330.1	329.9
	329.5	329.4	329.3	329.2	329.1	329.1			
54	328.0	328.0	327.9	327.7	327.5	327.3	327.2	327.0	326.8
	326.6	326.5	326.5	326.5	326.6	326.7			
0 55	324.0	324.2	324.3	324.3	324.2	324.1	324.0	323.9	323.8
	323.6	323.6	323.7	323.8	324.0	324.3			
56	320.0	320.6	320.9	320.9	320.9	320.9	320.8	320.7	320.6
	320.6	320.7	320.8	321.0	321.4	322.0			
57	316.0	317.3	317.6	317.7	317.7	317.6	317.6	317.5	317.5
	317.5	317.6	317.8	318.1	318.7	320.0			
58	316.0	314.8	314.6	314.5	314.5	314.4	314.4	314.4	314.4
	314.4	314.5	314.6	314.9	315.3	316.0			
59	312.0	311.5	311.3	311.3	311.2	311.2	311.2	311.2	311.2
	311.2	311.3	311.3	311.5	311.7	312.0			
0 60	308.0	308.0	308.0	308.0	308.0	308.0	308.0	308.0	308.0
	308.0	308.0	308.0	308.0	308.0	308.0			

SOLUTION BY SLICE-SUCCESSIVE OVERRELAXATION

MAXIMUM ITERATIONS ALLOWED FOR CLOSURE = 100
 ACCELERATION PARAMETER = 1.0000
 HEAD CHANGE CRITERION FOR CLOSURE = .10000E+01
 SOR HEAD CHANGE PRINTOUT INTERVAL = 1
 STRESS PERIOD NO. 1, LENGTH = 1.000000

NUMBER OF TIME STEPS = 24

MULTIPLIER FOR DELT = 1.000

INITIAL TIME STEP SIZE = .4166667E-01

2 ITERATIONS FOR TIME STEP 1 IN STRESS PERIOD 1

MAXIMUM HEAD CHANGE FOR EACH ITERATION:

HEAD CHANGE LAYER,ROW,COL HEAD CHANGE LAYER,ROW,COL HEAD CHANGE LAYER,ROW,COL HEAD CHANGE LAYER,ROW,COL

-2.089 (1, 15, 5) -.8952 (1, 16, 5)

HEAD/DRAWDOWN PRINTOUT FLAG = 0 TOTAL BUDGET PRINTOUT FLAG = 0 CELL-BY-CELL FLOW TERM FLAG = 0

OUTPUT FLAGS FOR ALL LAYERS ARE THE SAME:

HEAD DRAWDOWN HEAD DRAWDOWN
PRINTOUT PRINTOUT SAVE SAVE

0 0 0 0

1 ITERATIONS FOR TIME STEP 2 IN STRESS PERIOD 1

MAXIMUM HEAD CHANGE FOR EACH ITERATION:

HEAD CHANGE LAYER,ROW,COL HEAD CHANGE LAYER,ROW,COL HEAD CHANGE LAYER,ROW,COL HEAD CHANGE LAYER,ROW,COL

.5100 (1, 34, 16)

HEAD/DRAWDOWN PRINTOUT FLAG = 0 TOTAL BUDGET PRINTOUT FLAG = 0 CELL-BY-CELL FLOW TERM FLAG = 0

OUTPUT FLAGS FOR ALL LAYERS ARE THE SAME:

HEAD DRAWDOWN HEAD DRAWDOWN

PRINTOUT PRINTOUT SAVE SAVE

0 0 0 0

1 ITERATIONS FOR TIME STEP 3 IN STRESS PERIOD 1

MAXIMUM HEAD CHANGE FOR EACH ITERATION:

0 HEAD CHANGE LAYER,ROW,COL HEAD CHANGE LAYER,ROW,COL HEAD CHANGE LAYER,ROW,COL HEAD CHANGE LAYER,ROW,COL

.4296 (1, 34, 16)

0

HEAD/DRAWDOWN PRINTOUT FLAG = 0 TOTAL BUDGET PRINTOUT FLAG = 0 CELL-BY-CELL FLOW TERM FLAG = 0

OUTPUT FLAGS FOR ALL LAYERS ARE THE SAME:

HEAD DRAWDOWN HEAD DRAWDOWN

PRINTOUT PRINTOUT SAVE SAVE

0 0 0 0

1 ITERATIONS FOR TIME STEP 4 IN STRESS PERIOD 1

MAXIMUM HEAD CHANGE FOR EACH ITERATION:

0 HEAD CHANGE LAYER,ROW,COL HEAD CHANGE LAYER,ROW,COL HEAD CHANGE LAYER,ROW,COL HEAD CHANGE LAYER,ROW,COL

.3745 (1, 34, 16)

HEAD/DRAWDOWN PRINTOUT FLAG = 0 TOTAL BUDGET PRINTOUT FLAG = 0 CELL-BY-CELL FLOW TERM FLAG = 0

OUTPUT FLAGS FOR ALL LAYERS ARE THE SAME:

HEAD DRAWDOWN HEAD DRAWDOWN

PRINTOUT PRINTOUT SAVE SAVE

0 0 0 0

1 ITERATIONS FOR TIME STEP 5 IN STRESS PERIOD 1

MAXIMUM HEAD CHANGE FOR EACH ITERATION:

0 HEAD CHANGE LAYER,ROW,COL HEAD CHANGE LAYER,ROW,COL HEAD CHANGE LAYER,ROW,COL HEAD CHANGE LAYER,ROW,COL

.3345 (1, 34, 16)

0

HEAD/DRAWDOWN PRINTOUT FLAG = 0 TOTAL BUDGET PRINTOUT FLAG = 0 CELL-BY-CELL FLOW TERM FLAG = 0

OUTPUT FLAGS FOR ALL LAYERS ARE THE SAME:

HEAD DRAWDOWN HEAD DRAWDOWN

PRINTOUT PRINTOUT SAVE SAVE

0 0 0 0

1 ITERATIONS FOR TIME STEP 6 IN STRESS PERIOD 1

MAXIMUM HEAD CHANGE FOR EACH ITERATION:

0 HEAD CHANGE LAYER,ROW,COL HEAD CHANGE LAYER,ROW,COL HEAD CHANGE LAYER,ROW,COL HEAD CHANGE LAYER,ROW,COL

.3034 (1, 35, 16)

HEAD/DRAWDOWN PRINTOUT FLAG = 0 TOTAL BUDGET PRINTOUT FLAG = 0 CELL-BY-CELL FLOW TERM FLAG = 0

OUTPUT FLAGS FOR ALL LAYERS ARE THE SAME:

HEAD DRAWDOWN HEAD DRAWDOWN

PRINTOUT PRINTOUT SAVE SAVE

0 0 0 0

1 ITERATIONS FOR TIME STEP 7 IN STRESS PERIOD 1

MAXIMUM HEAD CHANGE FOR EACH ITERATION:

HEAD CHANGE LAYER,ROW,COL HEAD CHANGE LAYER,ROW,COL HEAD CHANGE LAYER,ROW,COL HEAD CHANGE LAYER,ROW,COL

.2785 (1, 35, 16)

HEAD/DRAWDOWN PRINTOUT FLAG = 0 TOTAL BUDGET PRINTOUT FLAG = 0 CELL-BY-CELL FLOW TERM FLAG = 0

OUTPUT FLAGS FOR ALL LAYERS ARE THE SAME:

HEAD DRAWDOWN HEAD DRAWDOWN

PRINTOUT PRINTOUT SAVE SAVE

0 0 0 0

1 ITERATIONS FOR TIME STEP 8 IN STRESS PERIOD 1

MAXIMUM HEAD CHANGE FOR EACH ITERATION:

HEAD CHANGE LAYER,ROW,COL HEAD CHANGE LAYER,ROW,COL HEAD CHANGE LAYER,ROW,COL HEAD CHANGE LAYER,ROW,COL

.2575 (1, 35, 16)

HEAD/DRAWDOWN PRINTOUT FLAG = 0 TOTAL BUDGET PRINTOUT FLAG = 0 CELL-BY-CELL FLOW TERM FLAG = 0

OUTPUT FLAGS FOR ALL LAYERS ARE THE SAME:

HEAD DRAWDOWN HEAD DRAWDOWN

PRINTOUT PRINTOUT SAVE SAVE

0 0 0 0

1 ITERATIONS FOR TIME STEP 9 IN STRESS PERIOD 1

MAXIMUM HEAD CHANGE FOR EACH ITERATION:

HEAD CHANGE LAYER,ROW,COL HEAD CHANGE LAYER,ROW,COL HEAD CHANGE LAYER,ROW,COL HEAD CHANGE LAYER,ROW,COL

.2394 (1, 35, 16)

HEAD/DRAWDOWN PRINTOUT FLAG = 0 TOTAL BUDGET PRINTOUT FLAG = 0 CELL-BY-CELL FLOW TERM FLAG = 0

OUTPUT FLAGS FOR ALL LAYERS ARE THE SAME:

HEAD DRAWDOWN HEAD DRAWDOWN

PRINTOUT PRINTOUT SAVE SAVE

0 0 0 0

1 ITERATIONS FOR TIME STEP 10 IN STRESS PERIOD 1

MAXIMUM HEAD CHANGE FOR EACH ITERATION:

HEAD CHANGE LAYER,ROW,COL HEAD CHANGE LAYER,ROW,COL HEAD CHANGE LAYER,ROW,COL HEAD CHANGE LAYER,ROW,COL

.2236 (1, 35, 16)

HEAD/DRAWDOWN PRINTOUT FLAG = 0 TOTAL BUDGET PRINTOUT FLAG = 0 CELL-BY-CELL FLOW TERM FLAG = 0

OUTPUT FLAGS FOR ALL LAYERS ARE THE SAME:

HEAD DRAWDOWN HEAD DRAWDOWN

PRINTOUT PRINTOUT SAVE SAVE

0 0 0 0

1 ITERATIONS FOR TIME STEP 11 IN STRESS PERIOD 1

MAXIMUM HEAD CHANGE FOR EACH ITERATION:

HEAD CHANGE LAYER,ROW,COL HEAD CHANGE LAYER,ROW,COL HEAD CHANGE LAYER,ROW,COL HEAD CHANGE LAYER,ROW,COL

.2096 (1, 35, 16)

HEAD/DRAWDOWN PRINTOUT FLAG = 0 TOTAL BUDGET PRINTOUT FLAG = 0 CELL-BY-CELL FLOW TERM FLAG = 0

OUTPUT FLAGS FOR ALL LAYERS ARE THE SAME:

HEAD DRAWDOWN HEAD DRAWDOWN
PRINTOUT PRINTOUT SAVE SAVE

0 0 0 0

1 ITERATIONS FOR TIME STEP 12 IN STRESS PERIOD 1

MAXIMUM HEAD CHANGE FOR EACH ITERATION:

0 HEAD CHANGE LAYER,ROW,COL HEAD CHANGE LAYER,ROW,COL HEAD CHANGE LAYER,ROW,COL HEAD CHANGE LAYER,ROW,COL

.1972 (1, 36, 16)

HEAD/DRAWDOWN PRINTOUT FLAG = 0 TOTAL BUDGET PRINTOUT FLAG = 0 CELL-BY-CELL FLOW TERM FLAG = 0

OUTPUT FLAGS FOR ALL LAYERS ARE THE SAME:

HEAD DRAWDOWN HEAD DRAWDOWN
PRINTOUT PRINTOUT SAVE SAVE

0 0 0 0

1 ITERATIONS FOR TIME STEP 13 IN STRESS PERIOD 1

MAXIMUM HEAD CHANGE FOR EACH ITERATION:

0 HEAD CHANGE LAYER,ROW,COL HEAD CHANGE LAYER,ROW,COL HEAD CHANGE LAYER,ROW,COL HEAD CHANGE LAYER,ROW,COL

.1863 (1, 36, 16)

HEAD/DRAWDOWN PRINTOUT FLAG = 0 TOTAL BUDGET PRINTOUT FLAG = 0 CELL-BY-CELL FLOW TERM FLAG = 0

OUTPUT FLAGS FOR ALL LAYERS ARE THE SAME:

HEAD DRAWDOWN HEAD DRAWDOWN
PRINTOUT PRINTOUT SAVE SAVE

0 0 0 0

1 ITERATIONS FOR TIME STEP 14 IN STRESS PERIOD 1

MAXIMUM HEAD CHANGE FOR EACH ITERATION:

0 HEAD CHANGE LAYER,ROW,COL HEAD CHANGE LAYER,ROW,COL HEAD CHANGE LAYER,ROW,COL HEAD CHANGE LAYER,ROW,COL

.1764 (1, 36, 16)

HEAD/DRAWDOWN PRINTOUT FLAG = 0 TOTAL BUDGET PRINTOUT FLAG = 0 CELL-BY-CELL FLOW TERM FLAG = 0

OUTPUT FLAGS FOR ALL LAYERS ARE THE SAME:

HEAD DRAWDOWN HEAD DRAWDOWN
PRINTOUT PRINTOUT SAVE SAVE

0 0 0 0

1 ITERATIONS FOR TIME STEP 15 IN STRESS PERIOD 1

MAXIMUM HEAD CHANGE FOR EACH ITERATION:

0 HEAD CHANGE LAYER,ROW,COL HEAD CHANGE LAYER,ROW,COL HEAD CHANGE LAYER,ROW,COL HEAD CHANGE LAYER,ROW,COL

.1675 (1, 36, 16)

HEAD/DRAWDOWN PRINTOUT FLAG = 0 TOTAL BUDGET PRINTOUT FLAG = 0 CELL-BY-CELL FLOW TERM FLAG = 0

OUTPUT FLAGS FOR ALL LAYERS ARE THE SAME:

HEAD DRAWDOWN HEAD DRAWDOWN
PRINTOUT PRINTOUT SAVE SAVE

0 0 0 0

1 ITERATIONS FOR TIME STEP 16 IN STRESS PERIOD 1

MAXIMUM HEAD CHANGE FOR EACH ITERATION:

0 HEAD CHANGE LAYER,ROW,COL HEAD CHANGE LAYER,ROW,COL HEAD CHANGE LAYER,ROW,COL HEAD CHANGE LAYER,ROW,COL

.1594 (1, 36, 16)

HEAD/DRAWDOWN PRINTOUT FLAG = 0 TOTAL BUDGET PRINTOUT FLAG = 0 CELL-BY-CELL FLOW TERM FLAG = 0
OUTPUT FLAGS FOR ALL LAYERS ARE THE SAME:

HEAD DRAWDOWN HEAD DRAWDOWN
PRINTOUT PRINTOUT SAVE SAVE

0 0 0 0

1 ITERATIONS FOR TIME STEP 17 IN STRESS PERIOD 1

MAXIMUM HEAD CHANGE FOR EACH ITERATION:

0 HEAD CHANGE LAYER,ROW,COL HEAD CHANGE LAYER,ROW,COL HEAD CHANGE LAYER,ROW,COL HEAD CHANGE LAYER,ROW,COL

.1520 (1, 36, 16)

0

HEAD/DRAWDOWN PRINTOUT FLAG = 0 TOTAL BUDGET PRINTOUT FLAG = 0 CELL-BY-CELL FLOW TERM FLAG = 0

OUTPUT FLAGS FOR ALL LAYERS ARE THE SAME:

HEAD DRAWDOWN HEAD DRAWDOWN
PRINTOUT PRINTOUT SAVE SAVE

0 0 0 0

1 ITERATIONS FOR TIME STEP 18 IN STRESS PERIOD 1

MAXIMUM HEAD CHANGE FOR EACH ITERATION:

0 HEAD CHANGE LAYER,ROW,COL HEAD CHANGE LAYER,ROW,COL HEAD CHANGE LAYER,ROW,COL HEAD CHANGE LAYER,ROW,COL

.1454 (1, 36, 16)

HEAD/DRAWDOWN PRINTOUT FLAG = 0 TOTAL BUDGET PRINTOUT FLAG = 0 CELL-BY-CELL FLOW TERM FLAG = 0

OUTPUT FLAGS FOR ALL LAYERS ARE THE SAME:

HEAD DRAWDOWN HEAD DRAWDOWN
PRINTOUT PRINTOUT SAVE SAVE

0 0 0 0

1 ITERATIONS FOR TIME STEP 19 IN STRESS PERIOD 1

MAXIMUM HEAD CHANGE FOR EACH ITERATION:

0 HEAD CHANGE LAYER,ROW,COL HEAD CHANGE LAYER,ROW,COL HEAD CHANGE LAYER,ROW,COL HEAD CHANGE LAYER,ROW,COL

.1394 (1, 36, 16)

0

HEAD/DRAWDOWN PRINTOUT FLAG = 0 TOTAL BUDGET PRINTOUT FLAG = 0 CELL-BY-CELL FLOW TERM FLAG = 0

OUTPUT FLAGS FOR ALL LAYERS ARE THE SAME:

HEAD DRAWDOWN HEAD DRAWDOWN
PRINTOUT PRINTOUT SAVE SAVE

0 0 0 0

1 ITERATIONS FOR TIME STEP 20 IN STRESS PERIOD 1

MAXIMUM HEAD CHANGE FOR EACH ITERATION:

0 HEAD CHANGE LAYER,ROW,COL HEAD CHANGE LAYER,ROW,COL HEAD CHANGE LAYER,ROW,COL HEAD CHANGE LAYER,ROW,COL

.1340 (1, 35, 16)

HEAD/DRAWDOWN PRINTOUT FLAG = 0 TOTAL BUDGET PRINTOUT FLAG = 0 CELL-BY-CELL FLOW TERM FLAG = 0

OUTPUT FLAGS FOR ALL LAYERS ARE THE SAME:

HEAD DRAWDOWN HEAD DRAWDOWN
PRINTOUT PRINTOUT SAVE SAVE

0 0 0 0

1 ITERATIONS FOR TIME STEP 21 IN STRESS PERIOD 1

MAXIMUM HEAD CHANGE FOR EACH ITERATION:

HEAD CHANGE LAYER,ROW,COL HEAD CHANGE LAYER,ROW,COL HEAD CHANGE LAYER,ROW,COL HEAD CHANGE LAYER,ROW,COL

.1299 (1, 33, 16)

HEAD/DRAWDOWN PRINTOUT FLAG = 0 TOTAL BUDGET PRINTOUT FLAG = 0 CELL-BY-CELL FLOW TERM FLAG = 0

OUTPUT FLAGS FOR ALL LAYERS ARE THE SAME:

HEAD DRAWDOWN HEAD DRAWDOWN

PRINTOUT PRINTOUT SAVE SAVE

0 0 0 0

1 ITERATIONS FOR TIME STEP 22 IN STRESS PERIOD 1

MAXIMUM HEAD CHANGE FOR EACH ITERATION:

HEAD CHANGE LAYER,ROW,COL HEAD CHANGE LAYER,ROW,COL HEAD CHANGE LAYER,ROW,COL HEAD CHANGE LAYER,ROW,COL

.1264 (1, 33, 16)

HEAD/DRAWDOWN PRINTOUT FLAG = 0 TOTAL BUDGET PRINTOUT FLAG = 0 CELL-BY-CELL FLOW TERM FLAG = 0

OUTPUT FLAGS FOR ALL LAYERS ARE THE SAME:

HEAD DRAWDOWN HEAD DRAWDOWN

PRINTOUT PRINTOUT SAVE SAVE

0 0 0 0

1 ITERATIONS FOR TIME STEP 23 IN STRESS PERIOD 1

MAXIMUM HEAD CHANGE FOR EACH ITERATION:

HEAD CHANGE LAYER,ROW,COL HEAD CHANGE LAYER,ROW,COL HEAD CHANGE LAYER,ROW,COL HEAD CHANGE LAYER,ROW,COL

.1232 (1, 33, 16)

HEAD/DRAWDOWN PRINTOUT FLAG = 0 TOTAL BUDGET PRINTOUT FLAG = 0 CELL-BY-CELL FLOW TERM FLAG = 0

OUTPUT FLAGS FOR ALL LAYERS ARE THE SAME:

HEAD DRAWDOWN HEAD DRAWDOWN

PRINTOUT PRINTOUT SAVE SAVE

0 0 0 0

1 ITERATIONS FOR TIME STEP 24 IN STRESS PERIOD 1

MAXIMUM HEAD CHANGE FOR EACH ITERATION:

HEAD CHANGE LAYER,ROW,COL HEAD CHANGE LAYER,ROW,COL HEAD CHANGE LAYER,ROW,COL HEAD CHANGE LAYER,ROW,COL

.1203 (1, 33, 16)

HEAD/DRAWDOWN PRINTOUT FLAG = 1 TOTAL BUDGET PRINTOUT FLAG = 1 CELL-BY-CELL FLOW TERM FLAG = 1

OUTPUT FLAGS FOR ALL LAYERS ARE THE SAME:

HEAD DRAWDOWN HEAD DRAWDOWN

PRINTOUT PRINTOUT SAVE SAVE

1 1 0 0

HEAD IN LAYER 1 AT END OF TIME STEP 24 IN STRESS PERIOD 1

	1	2	3	4	5	6	7	8	9	10	11	12	13	14	15	16	
1	537.30	535.10	532.90	530.70	528.40	526.20	524.00	521.80	519.50	517.30	515.10	512.90	510.70	508.00	506.20	504.00	
0	2	534.70	532.32	530.03	527.84	525.73	522.92	520.31	517.82	515.48	513.23	510.95	508.63	506.48	504.05	502.20	500.49

3	532.00	529.47	527.04	524.68	522.13	519.19	516.42	513.75	511.47	509.24	506.93	504.62	502.43	500.11	498.30	496.95
0	529.30	526.56	523.90	521.23	518.08	515.35	512.54	509.76	507.63	505.44	503.10	500.80	498.43	496.22	494.52	493.45
5	526.70	523.55	520.69	517.85	514.63	511.84	509.08	506.54	504.29	501.91	499.44	496.96	494.47	492.46	490.93	490.07
6	524.00	520.34	517.43	514.57	511.43	508.62	506.01	503.72	501.18	498.57	495.95	493.32	490.78	488.99	487.62	486.90
0	520.00	516.86	514.10	511.40	508.34	505.49	502.92	500.60	498.00	495.31	492.66	490.10	487.79	485.95	484.53	483.85
8	516.00	513.27	510.81	508.41	505.32	502.40	499.78	497.35	494.75	492.11	489.51	487.13	485.08	483.04	481.54	480.80
9	512.00	509.62	507.50	505.64	502.26	499.23	496.54	494.05	491.46	488.87	486.35	484.04	482.02	480.01	478.49	477.73
10	508.00	505.85	503.84	501.67	498.66	495.87	493.22	490.69	488.10	485.56	483.11	480.83	478.80	476.86	475.36	474.60
11	504.00	501.93	499.82	497.11	494.91	492.44	489.85	487.33	484.75	482.21	479.78	477.52	475.47	473.59	472.17	471.44
12	500.00	498.01	495.90	493.39	491.44	489.13	486.49	483.89	481.34	478.77	476.35	474.09	472.05	470.24	468.89	468.23
13	496.00	494.10	492.08	489.92	488.33	486.00	483.06	480.30	477.75	475.21	472.81	470.57	468.56	466.81	465.56	464.94
0	492.00	490.15	488.27	486.50	485.69	482.46	479.34	476.54	474.01	471.52	469.16	466.94	464.96	463.29	462.15	461.60
15	488.00	486.13	484.25	482.48	481.02	477.84	475.15	472.55	470.10	467.69	465.37	463.20	461.26	459.69	458.65	458.18
16	484.00	482.05	480.01	477.94	475.20	473.04	470.76	468.41	466.07	463.75	461.47	459.33	457.44	455.99	455.07	454.67
0	480.00	477.97	475.81	473.53	470.53	468.44	466.38	464.19	461.96	459.73	457.48	455.36	453.49	452.17	451.36	451.02
18	476.00	473.89	471.65	469.23	466.26	464.03	462.03	459.97	457.81	455.66	453.46	451.35	449.45	448.28	447.51	447.18
19	472.00	469.82	467.54	465.04	462.10	459.80	457.75	455.75	453.66	451.56	449.45	447.41	445.66	444.44	443.61	443.20
20	468.00	465.79	463.47	460.94	458.04	455.67	453.53	451.51	449.51	447.48	445.45	443.54	441.94	440.58	439.67	439.22
0	464.00	461.79	459.44	456.91	454.08	451.61	449.39	447.28	445.39	443.43	441.43	439.56	437.96	436.59	435.68	435.24
22	460.00	457.79	455.45	452.95	450.21	447.67	445.39	443.30	441.38	439.39	437.39	435.46	433.81	432.54	431.68	431.25
23	456.00	453.80	451.48	449.06	446.47	443.83	441.51	439.47	437.44	435.38	433.37	431.37	429.60	428.48	427.68	427.26
0	452.00	449.80	447.50	445.10	442.54	439.92	437.61	435.55	433.50	431.42	429.39	427.43	425.76	424.56	423.71	423.29
25	448.00	445.81	443.51	441.09	438.45	435.97	433.72	431.63	429.57	427.50	425.47	423.60	422.09	420.71	419.78	419.32
26	444.00	441.81	439.53	437.12	434.54	432.05	429.83	427.75	425.66	423.62	421.58	419.71	418.14	416.78	415.85	415.38
0	440.00	437.82	435.55	433.20	430.70	428.22	425.96	423.88	421.80	419.78	417.72	415.78	414.08	412.82	411.92	411.47
28	436.00	433.83	431.61	429.28	426.87	424.42	422.14	420.04	418.00	415.97	413.91	411.91	410.12	408.97	408.09	407.63
29	432.00	429.85	427.66	425.36	422.97	420.57	418.33	416.25	414.25	412.24	410.24	408.33	406.69	405.42	404.41	403.89
30	428.00	425.86	423.68	421.43	419.04	416.73	414.53	412.52	410.56	408.62	406.75	405.01	403.54	402.06	400.90	400.30
0	424.00	421.87	419.71	417.47	415.15	412.90	410.78	408.84	406.93	405.09	403.32	401.69	400.25	398.73	397.55	396.90
32	420.00	417.89	415.76	413.55	411.28	409.11	407.06	405.17	403.36	401.62	399.95	398.40	396.98	395.51	394.37	393.74
33	416.00	413.90	411.80	409.62	407.43	405.33	403.36	401.53	399.83	398.19	396.62	395.18	393.81	392.44	391.40	390.87
0	412.00	409.91	407.81	405.66	403.57	401.54	399.66	397.90	396.31	394.79	393.33	392.01	390.76	389.47	388.55	388.14
35	408.00	405.91	403.77	401.67	399.66	397.74	395.93	394.30	392.77	391.35	390.04	388.83	387.75	386.52	385.71	385.37
36	404.00	401.86	399.66	397.59	395.66	393.89	392.21	390.69	389.23	387.90	386.69	385.54	384.46	383.45	382.81	382.56
0	400.00	397.78	395.53	393.37	391.65	390.02	388.48	387.04	385.68	384.44	383.27	382.15	381.04	380.33	379.89	379.73
38	396.00	393.74	391.41	389.15	387.70	386.18	384.75	383.37	382.14	380.98	379.86	378.82	377.86	377.27	376.96	376.86
39	392.00	389.80	387.55	385.54	383.98	382.45	381.04	379.72	378.59	377.53	376.51	375.56	374.74	374.26	374.01	373.95
40	388.00	385.94	383.94	382.23	380.38	378.76	377.34	376.07	375.05	374.10	373.20	372.36	371.66	371.24	371.04	371.01
41	384.00	382.05	380.22	378.56	376.68	375.07	373.65	372.39	371.53	370.74	369.95	369.20	368.58	368.21	368.04	367.99
42	380.00	378.17	376.43	374.76	372.93	371.43	370.06	368.84	368.14	367.47	366.77	366.09	365.54	365.17	365.01	364.95
43	376.00	374.28	372.62	370.98	369.24	367.97	366.78	365.77	365.03	364.34	363.67	363.05	362.53	362.18	362.00	361.93
0	372.00	370.41	368.88	367.41	365.98	364.80	363.76	362.96	362.08	361.32	360.64	360.05	359.56	359.22	359.03	358.95
45	368.00	366.58	365.24	364.00	362.92	361.73	360.73	359.96	359.10	358.33	357.66	357.08	356.63	356.30	356.12	356.03
46	364.00	362.76	361.58	360.54	359.59	358.54	357.63	356.89	356.10	355.37	354.72	354.16	353.73	353.44	353.28	353.20
47	360.00	358.91	357.89	356.98	356.11	355.22	354.45	353.76	353.06	352.39	351.78	351.29	350.90	350.67	350.54	350.48
48	356.00	355.04	354.18	353.34	352.54	351.85	351.20	350.60	349.99	349.39	348.86	348.44	348.13	347.97	347.90	347.93
49	352.00	351.21	350.46	349.71	348.99	348.48	347.95	347.44	346.90	346.39	345.94	345.60	345.38	345.29	345.32	345.43
50	348.00	347.39	346.79	346.22	345.69	345.21	344.74	344.29	343.83	343.40	343.02	342.75	342.62	342.60	342.70	342.84
0	344.00	343.56	343.18	342.81	342.49	342.01	341.57	341.16	340.77	340.40	340.09	339.90	339.83	339.89	340.03	340.19
52	340.00	339.75	339.55	339.35	339.14	338.78	338.39	338.03	337.68	337.37	337.14	337.02	337.02	337.13	337.32	337.50
53	336.00	336.00	335.96	335.89	335.77	335.49	335.19	334.88	334.57	334.33	334.17	334.10	334.16	334.34	334.59	334.81
54	332.00	332.27	332.42	332.46	332.40	332.20	331.97	331.71	331.46	331.27	331.15	331.13	331.25	331.49	331.81	332.10
55	328.00	328.62	328.94	329.06	329.06	328.93	328.72	328.51	328.31	328.16	328.09	328.13	328.28	328.56	328.96	329.36
56	324.00	325.16	325.57	325.72	325.74	325.63	325.47	325.29	325.13	325.02	324.98	325.04	325.20	325.52	325.98	326.54
57	320.00	321.95	322.31	322.43	322.43	322.33	322.21	322.08	321.96	321.86	321.82	321.87	322.01	322.30	322.66	323.06
0	320.00	318.99	319.03	319.10	319.08	319.02	318.92	318.83	318.73	318.64	318.61	318.71	318.90	319.07	319.09	319.09

59	316.00	315.59	315.61	315.66	315.66	315.63	315.56	315.50	315.43	315.37	315.34	315.34	315.37	315.43	315.45	315.33
60	312.00	312.00	312.00	312.00	312.00	312.00	312.00	312.00	312.00	312.00	312.00	312.00	312.00	312.00	312.00	312.00

1 DRAWDOWN IN LAYER 1 AT END OF TIME STEP 24 IN STRESS PERIOD 1

	1	2	3	4	5	6	7	8	9	10	11	12	13	14	15	16
1	.00	.00	.00	.00	.00	.00	.00	.00	.00	.00	.00	.00	.00	.00	.00	.00
2	.00	.08	.17	.16	.18	.28	-.31	.08	.02	-.03	-.05	-.13	-.08	-.05	-.10	-.049
3	.00	.13	.26	.62	1.87	.81	-.42	.15	.03	-.14	-.23	-.62	-.23	-.11	-.20	-.095
4	.00	.24	.30	.57	1.32	.75	-.54	-.26	-.33	-.34	-.40	-.50	-.23	-.22	-.42	-.145
5	.00	.25	.31	.45	.87	.46	-1.08	-2.54	-1.19	-.71	-.64	-.56	-.47	-.46	-.93	-.207
6	.00	.36	.37	.43	.67	.38	-1.01	-1.32	-1.18	-.97	-.85	-1.02	-1.28	-1.99	-1.52	-2.90
7	.00	.34	.40	.30	.46	.31	-.92	-.90	-1.00	-1.01	-1.16	-1.80	-3.79	-2.95	-2.13	-3.15
8	.00	.33	.29	.19	.38	.30	-.78	-.65	-.85	-1.01	-1.21	-1.63	-2.48	-3.04	-2.44	-3.50
9	.00	.28	.40	.16	.44	.37	-.54	-.45	-.76	-.87	-1.05	-1.43	-2.02	-3.01	-2.49	-3.73
10	.00	.35	.86	2.33	1.14	.63	-.22	-.29	-.60	-.76	-1.01	-1.33	-1.70	-2.86	-2.66	-3.90
11	.00	.37	.78	1.69	1.09	.66	.15	-.23	-.75	-.71	-.88	-1.12	-1.47	-2.59	-2.67	-4.14
12	.00	.29	.70	1.31	.96	.57	-.49	.11	-.34	-.57	-.75	-.99	-1.35	-2.24	-2.69	-4.23
13	.00	.30	.62	1.08	.67	.60	-.06	.20	-.15	-.41	-.61	-.87	-1.16	-1.81	-2.76	-4.24
14	.00	.35	.63	1.00	.41	1.54	.66	.46	.09	-.22	-.46	-.74	-1.06	-2.29	-2.65	-4.30
15	.00	.37	.85	1.52	2.98	1.96	.85	.65	.30	-.09	-.27	-.60	-.96	-1.69	-2.65	-4.18
16	.00	.35	.79	1.36	2.60	1.96	1.24	.79	.43	.05	-.17	-.43	-.84	-1.99	-2.47	-3.97
17	.00	.33	.69	1.27	2.27	1.96	.62	.91	.54	.17	-.08	-.36	-.69	-2.17	-2.36	-3.72
18	.00	.31	.65	1.17	2.04	1.87	.97	.93	.59	.24	-.06	-.35	-.75	-2.28	-2.11	-3.18
19	.00	.28	.56	1.06	1.90	1.80	1.25	1.05	.64	.34	-.05	-.51	-1.66	-2.44	-2.11	-3.20
20	.00	.21	.53	.96	1.66	1.73	1.47	1.09	.69	.32	.05	-.44	-1.04	-1.58	-2.07	-3.22
21	.00	.21	.46	.89	1.52	1.69	.61	1.12	.71	.37	.07	-.26	-.86	-1.59	-2.08	-3.24
22	.00	.21	.45	.75	1.29	1.53	.61	.70	.62	.41	.11	-.16	-.71	-1.54	-2.08	-3.25
23	.00	.20	.42	.74	1.13	1.47	.49	.93	.66	.42	.13	-.27	-.70	-1.48	-2.08	-3.26
24	.00	.20	.40	.80	1.46	1.48	.39	.95	.70	.38	.11	-.43	-1.76	-1.56	-2.21	-3.29
25	.00	.19	.39	.71	1.25	1.43	1.28	.97	.73	.40	.13	-.40	-1.19	-1.71	-2.18	-3.32
26	.00	.19	.37	.68	1.06	1.35	1.17	1.05	.74	.38	.12	-.31	-.84	-1.78	-2.15	-3.38
27	.00	.18	.35	.60	1.00	1.18	1.04	1.02	.70	.42	.18	-.28	-.78	-1.82	-2.22	-3.47
28	.00	.17	.29	.62	.93	1.08	.86	.96	.70	.43	.09	-.41	-1.12	-1.97	-2.39	-3.63
29	.00	.15	.34	.64	1.03	1.13	.67	.95	.65	.36	-.14	-.93	-2.69	-2.42	-2.71	-3.89
30	.00	.14	.32	.57	.86	1.07	.47	.88	.64	.28	-.15	-.91	-1.94	-3.06	-3.00	-4.30
31	.00	.13	.29	.53	.85	1.00	.22	.86	.57	.21	-.22	-.89	-1.75	-2.73	-3.35	-4.90
32	.00	.11	.24	.45	.72	.89	.94	.83	.54	.18	-.25	-.90	-1.68	-2.51	-3.77	-5.74
33	.00	.10	.30	.48	.67	.87	.64	.77	.47	.11	-.32	-.98	-1.71	-3.44	-4.30	-6.87
34	.00	.09	.29	.44	.63	.76	.34	.70	.49	.11	-.33	-.91	-1.76	-3.47	-4.35	-6.64
35	.00	.09	.33	.43	.64	.76	.07	.70	.43	.15	-.34	-.83	-1.55	-3.52	-4.21	-6.37
36	.00	.14	.34	.51	.64	.71	-.21	.61	.37	.10	-.19	-.54	-.46	-2.45	-4.01	-6.06
37	.00	.12	.27	.53	.55	.68	.52	.56	.32	.06	-.17	-.55	-.94	-2.33	-3.89	-5.73
38	.00	.06	.19	.25	.40	.52	.25	.53	.36	.02	-.26	-.62	-1.16	-2.27	-3.66	-5.36
39	.00	-.10	-.35	-1.54	.02	.35	-.04	.38	.21	-.03	-.31	-.66	-1.25	-2.26	-3.51	-4.95
40	.00	-.04	-.34	-.73	-.08	.24	-.34	.33	.15	-.10	-.30	-.76	-1.26	-2.24	-3.24	-4.51
41	.00	-.05	-.22	-.46	-.08	.13	-.65	.21	-.03	-.24	-.45	-.80	-1.28	-2.21	-3.04	-3.99
42	.00	-.07	-.23	-.36	-.13	-.13	-.06	-.24	-.24	-.37	-.57	-.89	-1.34	-2.17	-2.81	-3.85
43	.00	-.08	-.22	-.48	-.54	-.47	-.78	-.177	-.83	-.64	-.67	-.95	-1.33	-2.18	-2.70	-3.63
44	.00	-.11	-.38	-.81	-1.98	-1.10	-1.76	-1.26	-.88	-.72	-.74	-.95	-1.36	-2.22	-2.63	-3.55
45	.00	-.08	-.34	-.80	-1.32	-1.03	-1.73	-1.06	-.90	-.83	-.86	-.98	-1.33	-2.30	-2.62	-3.43
46	.00	-.16	-.38	-.74	-.99	-.94	-1.63	-.99	-.90	-.87	-.82	-1.06	-1.33	-2.44	-2.66	-3.50
47	.00	-.11	-.39	-.58	-.81	-.82	-1.45	-.86	-.86	-.79	-.88	-1.09	-1.40	-2.67	-2.64	-.358

48	.00	-.14	-.38	-.54	-.74	-.85	-1.20	-.90	-.89	-.79	-.86	-1.04	-1.43	-1.97	-2.70	-3.93
0 49	.00	-.21	-.36	-.61	-.89	-.88	-.95	-.84	-.80	-.79	-.84	-1.00	-1.38	-2.29	-2.52	-3.23
50	.00	-.19	-.49	-.92	-1.69	-1.11	-1.74	-.89	-.83	-.80	-.82	-.95	-1.22	-2.60	-2.20	-2.74
51	.00	-.16	-.48	-.81	-1.19	-1.11	-1.57	-.86	-.77	-.70	-.79	-.90	-1.13	-1.89	-1.93	-2.29
0 52	.00	-.25	-.45	-.75	-1.04	-.98	-1.39	-.83	-.68	-.67	-.74	-.82	-1.02	-2.13	-1.72	-2.00
53	.00	-.20	-.46	-.79	-.97	-.89	-1.19	-.78	-.67	-.63	-.67	-.70	-.86	-1.34	-1.49	-1.71
54	.00	-.27	-.52	-.76	-.90	-.90	-.97	-.71	-.66	-.57	-.55	-.63	-.75	-1.49	-1.21	-1.40
0 55	.00	-.42	-.64	-.76	-.86	-.83	-.72	-.61	-.51	-.46	-.49	-.53	-.58	-1.56	-.96	-1.06
56	.00	-.56	-.67	-.82	-.84	-.73	-1.47	-.59	-.53	-.42	-.38	-.34	-.40	-.52	-.48	-.054
57	.00	-.65	-.71	-.73	-.73	-.73	-1.21	-.58	-.46	-.36	-.32	-.27	-.21	-.30	.04	0.94
58	.00	-.19	-.43	-.60	-.58	-.62	-.92	-.43	-.33	-.24	-.21	-.14	-.11	-.90	.23	0.91
0 59	.00	-.09	-.21	-.36	-.46	-.43	-.56	-.30	-.23	-.17	-.14	-.04	-.07	-.43	.25	0.67
60	.00	.00	.00	.00	.00	.00	.00	.00	.00	.00	.00	.00	.00	.00	.00	0.00

VOLUMETRIC BUDGET FOR ENTIRE MODEL AT END OF TIME STEP 24 IN STRESS PERIOD 1

CUMULATIVE VOLUMES	L**3	RATES FOR THIS TIME STEP	L**3/T
IN:		IN:	
---		---	
STORAGE =	.00000	STORAGE =	.00000
CONSTANT HEAD =	3162.2	CONSTANT HEAD =	3167.0
TOTAL IN =	3162.2	TOTAL IN =	3167.0
OUT:		OUT:	
---		---	
STORAGE =	.00000	STORAGE =	.00000
CONSTANT HEAD =	1972.8	CONSTANT HEAD =	2161.1
TOTAL OUT =	1972.8	TOTAL OUT =	2161.1
IN - OUT =	1189.3	IN - OUT =	1005.9
PERCENT DISCREPANCY =	46.32	PERCENT DISCREPANCY =	37.76

TIME SUMMARY AT END OF TIME STEP 24 IN STRESS PERIOD 1

	SECONDS	MINUTES	HOURS	DAYS	YEARS
TIME STEP LENGTH	3600.00	60.0000	1.00000	.416667E-01	.114077E-03
STRESS PERIOD TIME	86400.0	1440.00	24.0000	1.00000	.273785E-02
TOTAL SIMULATION TIME	86400.0	1440.00	24.0000	1.00000	.273785E-02

Section 2

Overview of Decision Tree Computer Code (DTREE)

**COMPUTERIZED DECISION TREE ANALYSIS
FOR GEOTECHNICAL APPLICATIONS**

A Thesis

Presented in Partial Fulfillment of the Requirements for the

Degree of Master of Science

with a

Major in Geological Engineering

in the

College of Graduate Studies

University of Idaho

by

Kenneth Scott Kendall

September 1990

AUTHORIZATION TO SUBMIT
THESIS

This thesis of Kenneth Scott Kendall, submitted for the degree of Master of Science with a major in Geological Engineering and titled "Computerized Decision Tree Analysis for Geotechnical Applications" has been reviewed in final form, as indicated by the signatures and dates given below. Permission is now granted to submit final copies to the College of Graduate Studies for approval.

Major Professor Stanley M. Miller Date 9-27-90
Committee Members Jerry R. Howard Date 9-27-90
Bethuel I. Judi Date 9-27-90

Department
Administrator _____ Date _____

College Dean _____ Date _____

College of Graduate Studies Final Approval and Acceptance:

_____ Date _____

ABSTRACT

Complex engineering and management problems that involve decision alternatives, uncertainties, and risks can be analyzed systematically using decision trees. Decision trees are used routinely on all drilling projects by engineers in Region 6 of the USDA Forest Service. Decision trees are used to choose whether or not to drill a specific site as well as to prioritize drilling projects. Analyzing large decision trees with pencil, paper, and a hand-calculator can become a long, tedious process. Also, changing one probability value or one benefit/cost outcome usually results in recalculating a significant portion of the tree. To minimize the time involved in constructing and solving decision trees the Forest Service chose to investigate the feasibility of developing a computer program to perform decision tree analysis. The purpose of this study was to develop and demonstrate a computer program for personal computers aimed at solving decision trees for geotechnical problems. Two realistic, hypothetical geotechnical projects were used to illustrate the effectiveness of the decision tree computer program.

ACKNOWLEDGEMENTS

The following thesis would not have been possible without financial and technical support from the USDA Forest Service to write the decision tree analysis program, DTREE. The project coordinator, Carol Hammond of the Intermountain Research Station, was instrumental with her insights and suggestions. The thesis committee of Stan Miller (major professor), Terry Howard, and Behzad Izadi provided valuable guidance and review comments. Merion Kendall made this thesis possible with her encouragement throughout the entire project and with the time she devoted to drafting and editing.

TABLE OF CONTENTS

ABSTRACT	III
ACKNOWLEDGEMENTS	IV
TABLE OF CONTENTS	V
LIST OF FIGURES	VII
LIST OF TABLES	VIII
CHAPTER 1. INTRODUCTION	1
Statement of the Problem	1
Purpose and Objectives	2
Method of Study	2
Scope of Study	3
Previous Investigations	4
CHAPTER 2. DESCRIPTION OF DECISION TREES	6
Introduction	6
Decision Tree Example	10
CHAPTER 3. DECISION TREE ANALYSIS PROGRAM	16
Introduction	16
Edit	18
Create	18
View	22
Conditional	22
Graph - XGraph	24
Solve	26
Save - Load	26
Quit	29
Overview of Programming	29
CHAPTER 4. DECISION TREE ANALYSIS FOR ROCK AGGREGATE SOURCES	32
Introduction	32
Problem Description	32
Decision Tree Results	43
Sensitivity Analysis	44
CHAPTER 5. DECISION TREE ANALYSIS FOR SLOPE DESIGN	49
Introduction	49
Problem Description	49
Decision Tree Results	62

Sensitivity Analysis	62
CHAPTER 6. CONCLUSIONS AND RECOMMENDATIONS	65
REFERENCES	68
APPENDIX A	70
APPENDIX B	71
APPENDIX C	79
APPENDIX D	87
APPENDIX E	95
APPENDIX F	103
APPENDIX G	112
APPENDIX H	121
APPENDIX I	130

LIST OF FIGURES

<u>Figure</u>	<u>Page</u>
2.1 Decision alternatives available to a decision maker and outcomes resulting from an action	8
2.2 Decision tree for rock aggregate analysis.....	13
2.3 Solved rock aggregate decision tree.....	15
3.1 Opening screen displayed by DTREE	17
3.2 First node entered into DTREE.....	20
3.3 Two branches appended to the decision tree.....	21
3.4 Conditional probability calculator.....	23
3.5 Graphical displays of decision tree.....	25
3.6 Save window displayed	27
3.7 Load window displayed	28
3.8 Flow chart describing DTREE's method of solving decision trees.....	30
4.1 Rock aggregate source, site 1.....	38
4.2 Rock aggregate source, site 2.....	40
4.3 Summary decision tree for rock aggregate source problem.....	42
5.1 Slope stabilization decision tree, maintenance alternative.....	56
5.2 Slope stabilization decision tree, buttress alternative.....	57
5.3 Slope stabilization decision tree, flatten slope alternative.....	58
5.4 Slope stabilization decision tree, drainage alternative.....	59
5.5 Summary of slope stabilization decision tree.....	61

LIST OF TABLES

<u>Table</u>	<u>Page</u>
4.1 Definition of Events for Rock Aggregate Problem .	35
4.2 Initial Probability Estimates	36
4.3 Initial Costs for Rock Aggregate Problem	37
4.4 Costs for Site 1 as Primary Source	45
4.5 Conditional Probabilities	47
5.1 Definition of Events	52
5.2 Initial Probabilities	52
5.3 Probabilities of Failure for Slope Design Problem	53
5.4 Initial Costs for Slope Stabilization.....	54

CHAPTER 1

INTRODUCTION

Statement of the Problem

Complex engineering and management problems that involve decision alternatives, uncertainties, and risks can be systematically analyzed using decision analysis. An important tool for such analyses is the decision tree, a branched structure that outlines decision alternatives and risks. Practically any decision problem can be represented with a decision tree. Analyzing large decision trees with pencil, paper, and a hand-calculator can become a long, tedious process. Also, changing one probability value or one benefit/cost outcome usually results in recalculating a significant portion of the tree.

In Region 6 of the USDA Forest Service, decision trees are used routinely on all drilling projects. The reason is to decide whether or not to drill a specific site, as well as to prioritize drilling projects. Construction of decision trees to conduct a realistic analysis becomes time consuming. To minimize the time involved in constructing and solving decision trees, the Forest Service chose to investigate the feasibility of developing a computer program to perform decision tree analysis.

Purpose and Objectives

The purpose of this study was to develop and demonstrate a computer program for personal computers aimed at solving decision trees for geotechnical problems. A major advantage of such a program would be the ease of constructing, modifying, and recalculating decision trees.

Specific objectives of this project were:

1. Review and describe in general the use of decision trees in the process of making engineering decisions under uncertainty.
2. Develop a computer program to construct, edit, and solve decision trees.
3. Demonstrate the decision tree computer program by applying it to different geotechnical problems typical to Forest Service projects.

Method of Study

The main characteristic of decision trees that facilitates writing a program to construct and solve decision trees is the tree structure. Data are represented in many computer applications as trees to reduce search times for desired elements of data. A similar scheme can be used to represent a decision tree with a computer program.

The mechanics of constructing and solving decision trees were studied to see how a computer program could represent a

decision tree's structure and function. The C programming language was used to write the decision tree program because it facilitates dynamic memory allocation and can take advantage of available windowing packages. Because the number of nodes on a planned decision tree is initially unknown, a language that allows dynamic allocation of memory is required. C provides the most straightforward method of using dynamic memory allocation. There are also many third-party C libraries available with windowing functions and input functions. These libraries greatly reduce the time needed to create a user interface.

Two case studies typical to Forest Service geotechnical projects were used as examples of applying decision trees and for demonstrating the decision tree computer program. The first study, an aggregate source development, was chosen because the problem relies on conditional probabilities that result from tests performed to gather additional information. The second study, a slope design problem, was chosen because engineers often face numerous uncertainties in dealing with slope stability related to forest roads. Both case studies illustrate typical projects where decision tree analysis can be valuable.

Scope of Study

The decision tree analysis program was developed to the point where it was possible to construct and solve decision trees by the spring of 1989. Initially, the program was difficult to use, so a user interface was created that let users easily construct and solve decision trees. The major portion of that work was completed by August 1990. Two examples were analyzed over the summer of 1990. The program development platform included a variety of IBM compatible computers; an XT, PS/2 Model 30-286, and a COMPAQ 368 Deskpro. Once the decision tree program was created, examples were necessary for application. The first example, a decision tree for aggregate source development, is from a short course presented in 1987 by Prof. Stan Miller of the University of Idaho. The second example, a slope stability problem, was developed jointly with Carol Hammond from the USDA Forest Service Intermountain Research Station in Moscow, Idaho.

Previous Investigations

Application of decision tree analysis has been described by Benjamin and Cornell (1970), Newendorp (1975), Anderson et al. (1977), and Ali (1987). Benjamin and Cornell applied decision tree analysis to civil engineering problems, such as foundations for bridges. Newendorp applied decision tree analysis to petroleum investigations. Anderson applied

decision tree analysis to agricultural applications. He used a decision tree to evaluate if the purchase and use of a crop forecast (which is not 100% reliable) has a lower net cost than not using a crop forecast. Ali used decision tree analysis to choose the most cost-effective foundation design in an expansive soil.

In a study related to decision tree analysis, Keaton and Eckhoff (1990) followed what they termed a "value engineering" approach to identifying risks, and eliminating or modifying those aspects of a system that add costs without reducing risk. An "event tree" was used to compare the "partial risk" costs of various alternatives. Partial risk costs can be compared to expected monetary value.

Each of these references showed the value of an organized, rational decision making process for problems involving uncertainties and associated risks. The computer program described and demonstrated in this thesis simplifies and automates this process. The computer program also allows a "what-if" analysis (i.e., sensitivity analysis) of the decision trees. This allows more information to be gained from decision tree analysis.

CHAPTER 3
DECISION TREE ANALYSIS PROGRAM

Introduction

The computer program described in this chapter was written using the C programming language (Borland, 1990; Kernighan and Ritchie, 1988; Schildt, 1988). It is designed to run on any IBM PC compatible computer. A graphics adapter that has EGA resolution or better is required to graphically view decision trees.

The decision tree analysis program DTREE simplifies decision tree analysis by automating the construction and solution of decision trees. Such automation allows the decision maker to experiment with various subjective inputs and analyze the results quickly.

To execute DTREE, type "DTREE" at the DOS command line. Once the program is loaded into memory, a menu is displayed in the upper half of the screen (see Figure 3.1). Each option in the menu corresponds to a function performed by DTREE. Below the menu options is a comment identifying the currently highlighted menu option. A menu option is selected by pressing the corresponding highlighted character, or by positioning the highlight bar over that option and pressing ENTER. Use the arrow keys to move the highlight bar.

In addition, some menu options are selected by pressing a function key; these are the two graph functions, Graph and

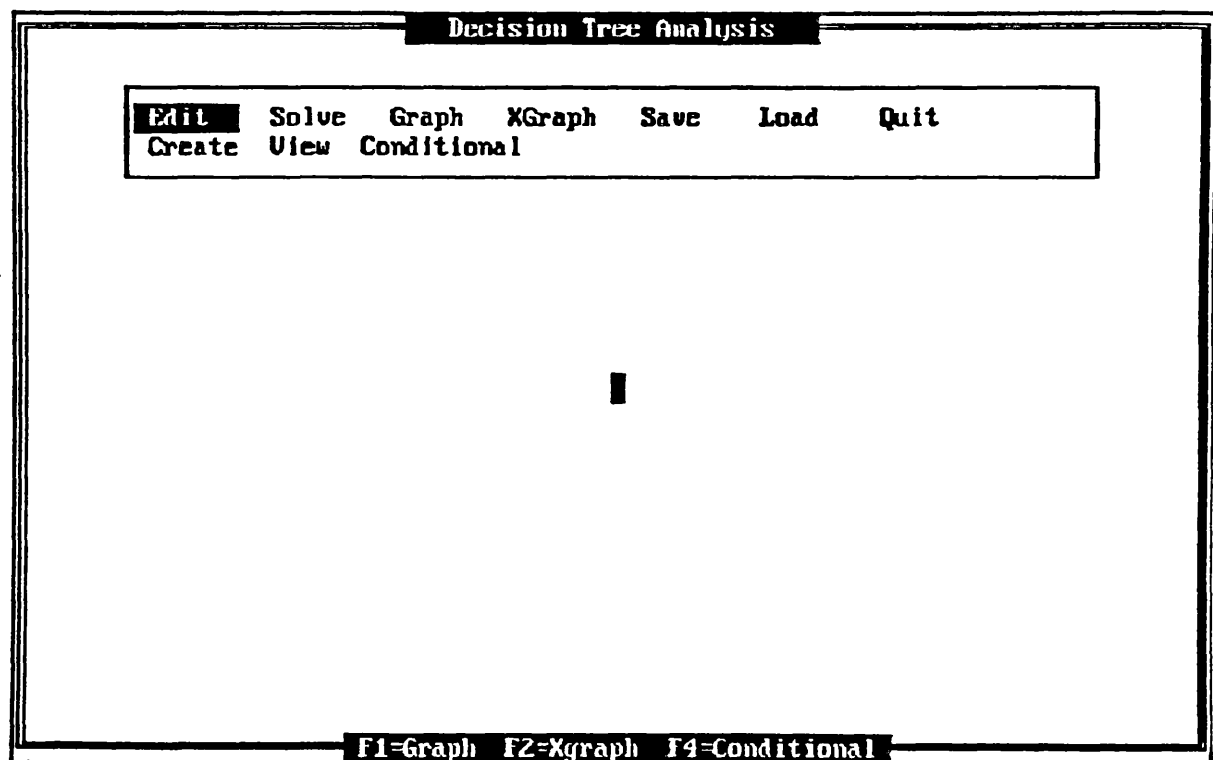


Figure 3.1: Opening screen displayed by DTREE.

Xgraph, and the Conditional option. The function keys allow these options to be selected at any point in the program. Use the ESCAPE key to exit a menu option or menu. Pressing ESCAPE in the main menu exits the program.

Data entry occurs in input fields that allow the user to enter and edit several inputs. An input field is the shaded line on the computer screen which accepts input from the user via the keyboard. In DTREE the input field is grey with black characters. Key strokes available for editing input fields are listed in Appendix A. Only one input field is active at a time. The active input field changes when the active field is completed or the user presses the "TAB" key to move to the next input field.

Any given node on the decision tree is represented in DTREE by a window (a bordered region of the computer screen). The input fields in that window are used to enter the data for that node. Available function keys are displayed on the bottom line of the opening screen. This line changes depending on the location in the menu system.

Edit

Three menu options are available from the Edit option on the main menu; create, modify, conditional.

Create

The "Create" option allows the user to create decision trees and add new nodes to existing decision trees. When the Create menu option is selected prior to loading an existing decision tree, a window with three input fields is displayed on the left half of the screen (Figure 3.2). The first input field is used to select the type of node. Use the arrow keys to scroll through the node type choices, and press ENTER to select one. The node type selected is displayed, then the next input field becomes active. Enter the number of branches for that node in the second input field. The number of branches must be between 1 and 10. The third input field is a short header that describes the node. This input field may contain a string of up to 15 characters.

Only the first node on a tree is entered in the window on the left hand side of the screen. The nodes at the ends of all remaining branches are entered into windows on the right side of the screen, with the window on the left displaying the current parent node (Figure 3.3). As each node is completed the next node appears in an overlapping window. These overlapping windows continue downward until all of the branches for the displayed parent node are filled. When the last node is completed the user is prompted to select from a list the next parent node to which nodes will be appended. If only one parent node needs branches appended, that node is displayed automatically as the parent node and the user is

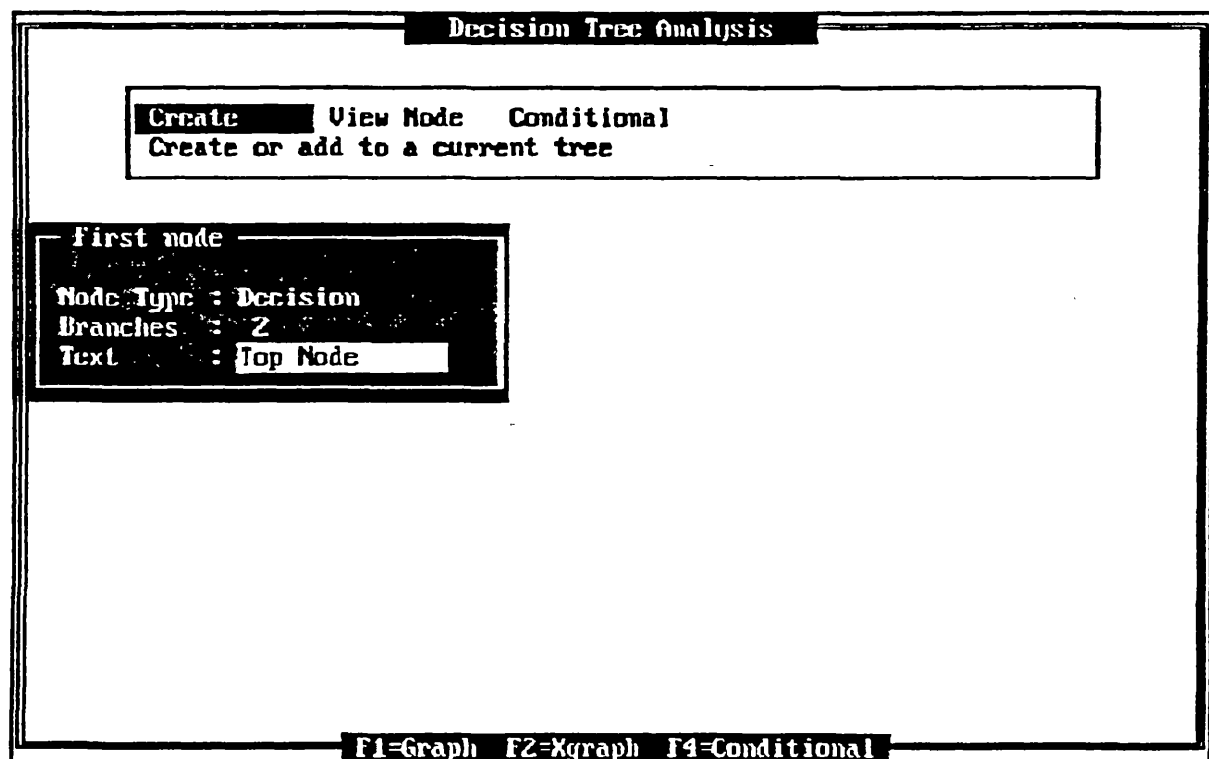


Figure 3.2: First node entered into DTREE.

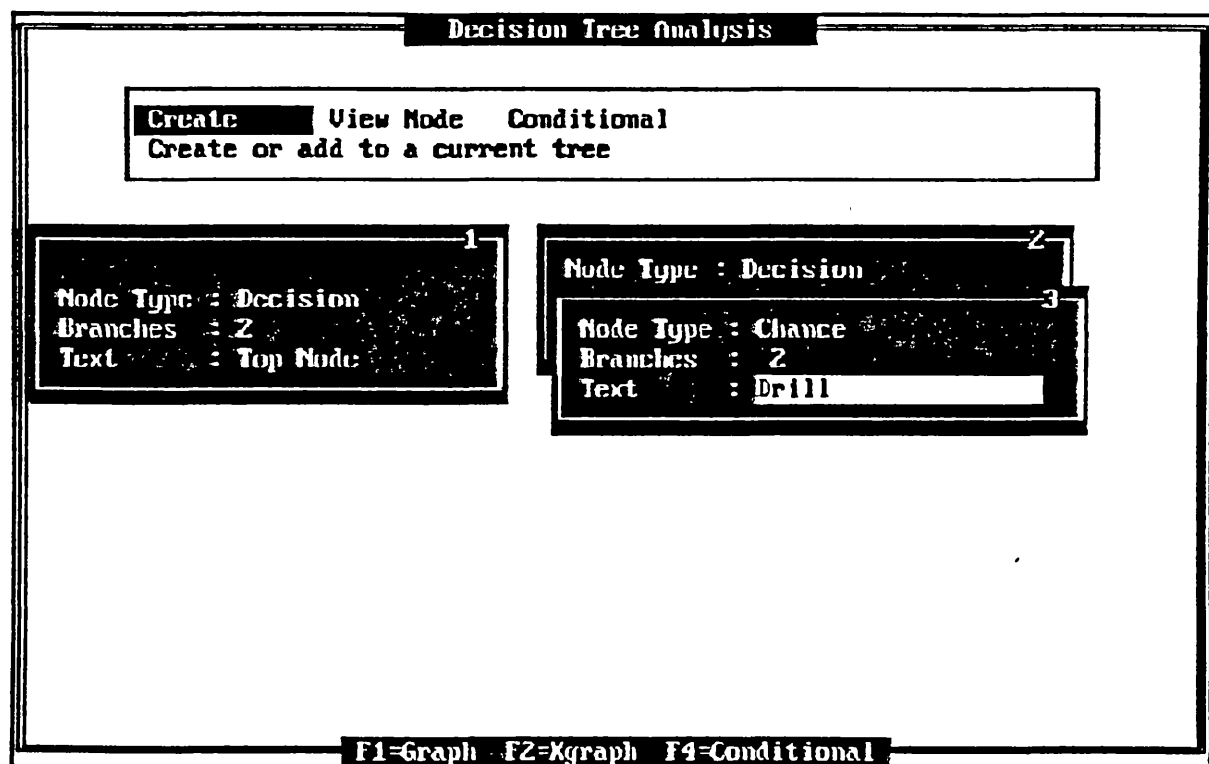


Figure 3.3: Two branches appended to the decision tree.

prompted to complete its branches. If the decision tree is complete, a message indicating so is displayed and the user is returned to the main menu.

View

The "View" option allows the user to modify an existing tree. Nodes can be removed and the contents of nodes can be changed. The user must first select the node to edit by entering the label number of the node or highlighting the desired node from a list of nodes and pressing ENTER. Once a node is selected for editing, a window with the contents of the selected node is displayed. Fields displayed in white are fields that cannot be changed, such as the node type. The TAB key is used to select the input field to be edited. To save the edited node, press enter in the last field or CONTROL-ENTER (press both the CONTROL key and the ENTER key at the same time) in any input field. The ESCAPE key allows the user to exit the edit window, discarding any changes made. The F3 function key is used to delete nodes that have no branches.

Conditional

The "Conditional" option allows the user to calculate conditional probabilities while using the DTREE program. The conditional option can be selected in the menu, or by pressing F6. The conditional calculator can handle up to five events (see Figure 3.4). Enter prior probabilities into the column $P[A_i]$, and the reliabilities ($P[B_j|A_i]$) into the columns A_1

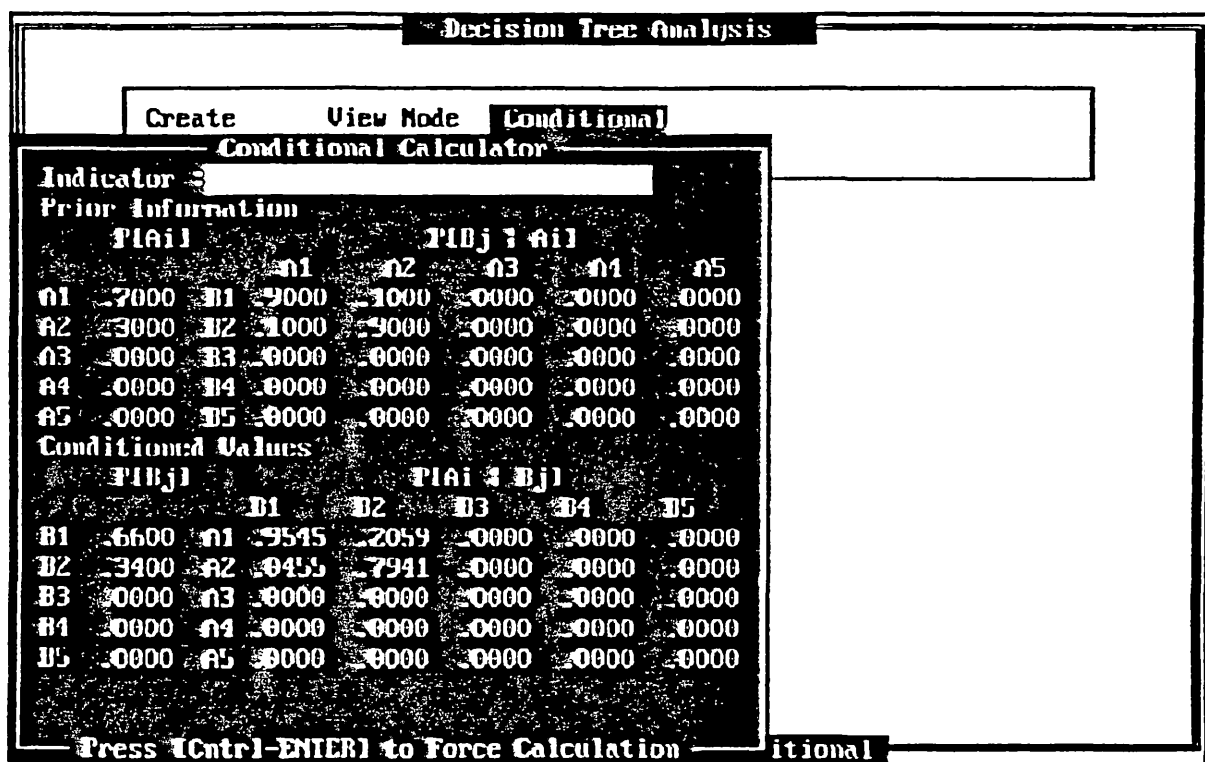


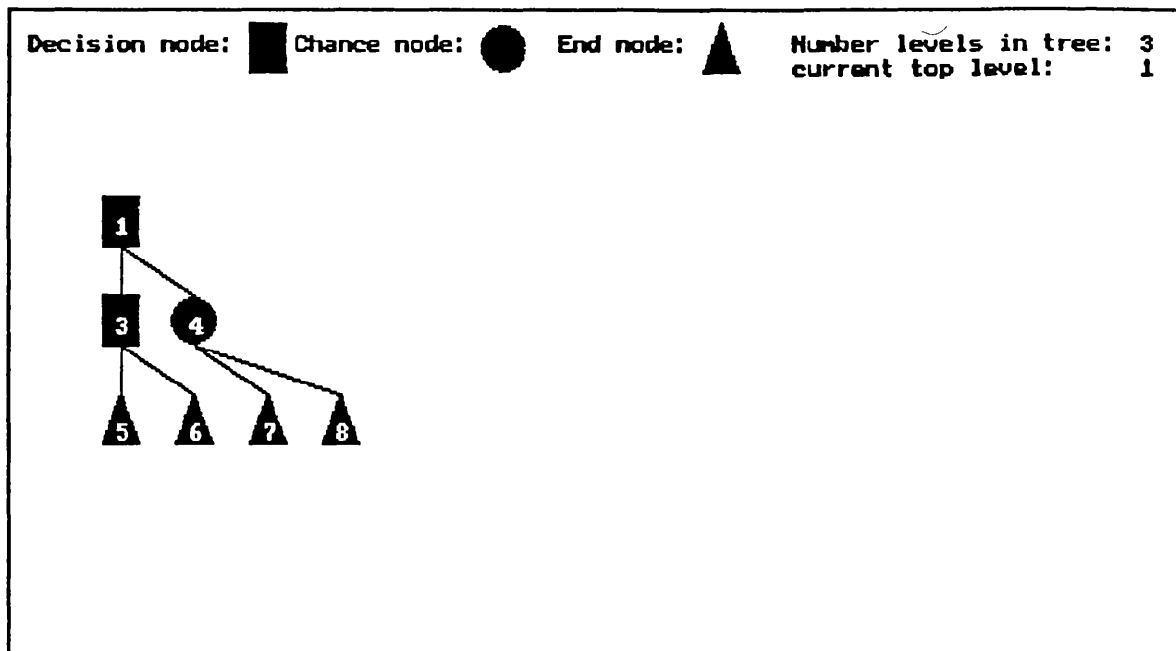
Figure 3.4: Conditional probability calculator.

through A5. The conditional probabilities may be calculated before the entire matrix is filled by pressing CONTROL-ENTER. They also are calculated after pressing ENTER in the lower right hand input field. In either case, if each of the columns and rows do not sum to 1.0, an error message is displayed and the calculations are not made. The conditional probability results are displayed in the lower half of the window. The values in the input fields can be changed and the calculations updated easily. Press ESCAPE to exit the conditional probability calculator. Values in the input fields are not saved, but a hard copy can be made by pressing F10 if a printer is connected to the computer.

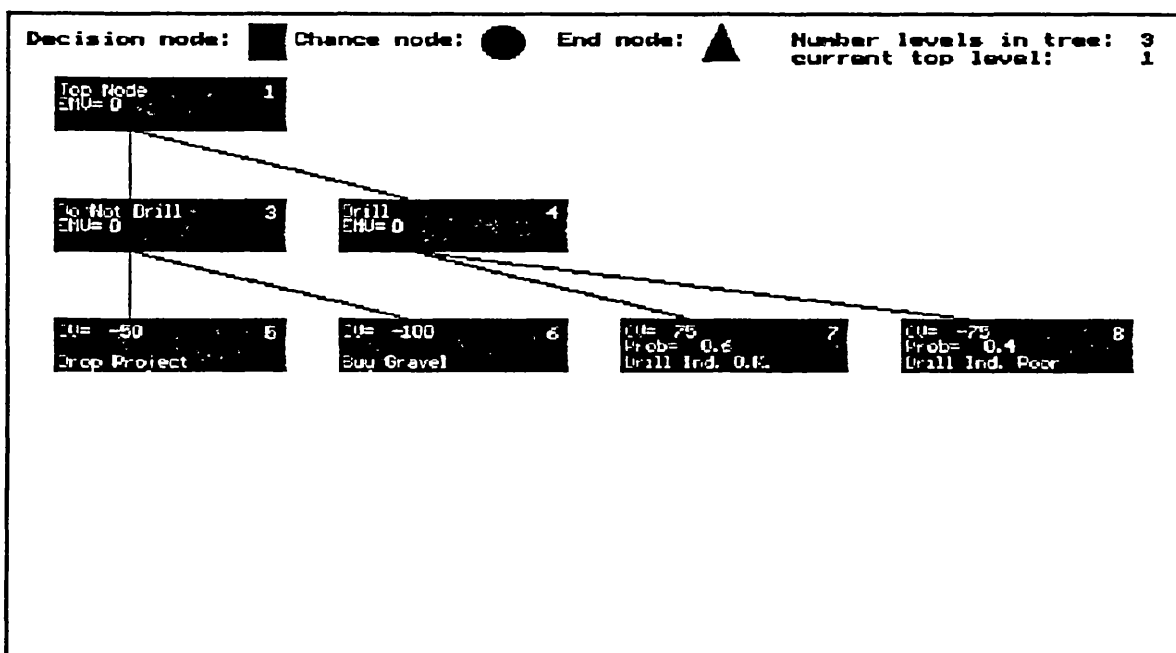
Graph - XGraph

The "Graph" and "Xgraph" options are used to view the decision tree graphically as shown in Figure 3.5. Graph displays the structure of the tree. Each node is represented by a different color and shape: decision, chance and end nodes are represented by squares, circles and triangles, respectively. Each node is assigned a unique number when it is created. This number is displayed in each node and is used as a reference for the user to identify nodes. Use the arrow keys to scroll up and down the tree to view nodes.

XGraph differs from graph in that it displays information about each node in the decision tree, including the node number, the message text, and the EMV after it is calculated.



(a)



(b)

Figure 3.5: Graphical displays of a decision tree, (a) using the Graph option and (b) using the Xgraph option.

For nodes following a chance node, the probability of the node also is displayed. Conditional costs or benefits are displayed for end nodes. Use the arrow keys to view nodes of the tree not displayed. As with Graph, node type is color coded.

Solve

The "Solve" option calculates all of the EMVs in the decision tree. Two options are available after selecting the solve option, the EMV and EMC option. The EMV option is used when conditional values are entered as benefits, and the EMC option is chosen when conditional values are entered as positive costs. If the EMV option is selected, decision nodes are solved by selecting the branch with the greatest EMV; if the EMC option is selected decision nodes are solved by selecting the smallest EMV. A warning is displayed if Solve is selected when the tree is incomplete. The results can be viewed using the Xgraph option.

Save - Load

The "Save" option saves two versions of the decision tree, a DOS text file and a binary file. The text file has a "FDT" extension and the binary file has a "UDT" extension. The current DOS path and filename are displayed in the input field, as shown in Figure 3.6. Press ENTER to accept the

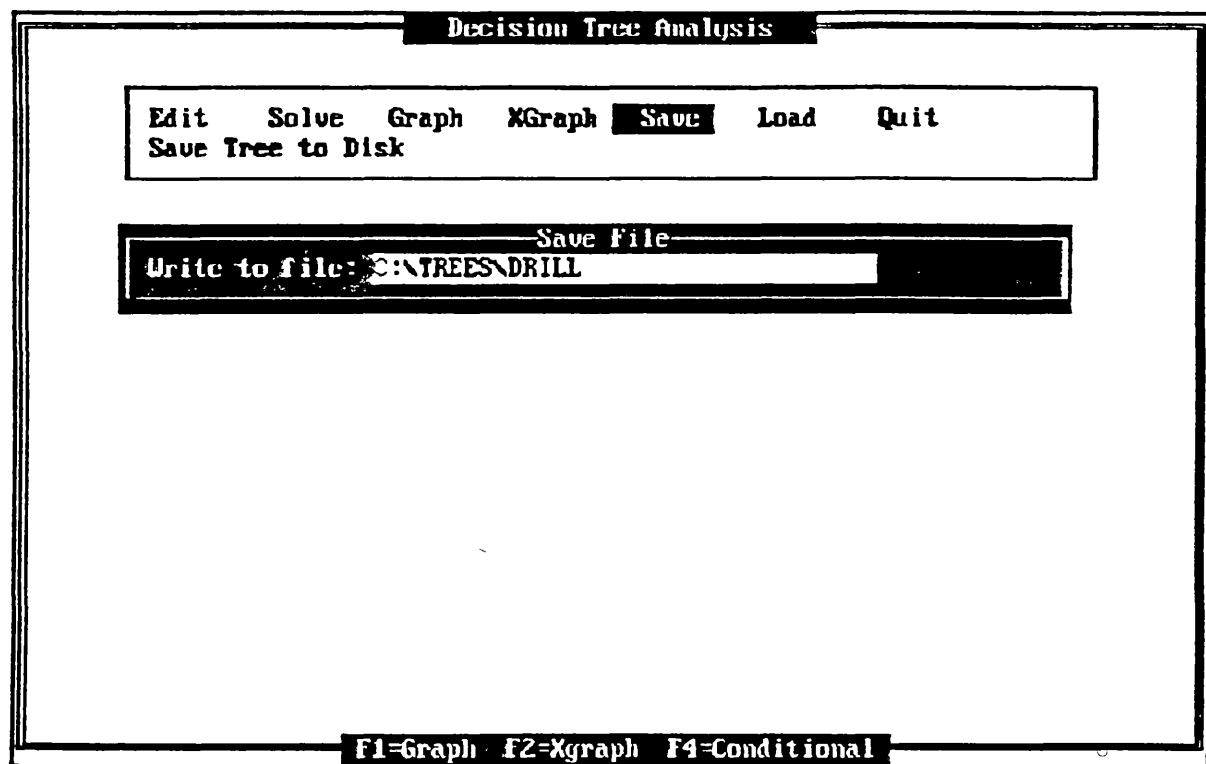


Figure 3.6: Save window displayed.

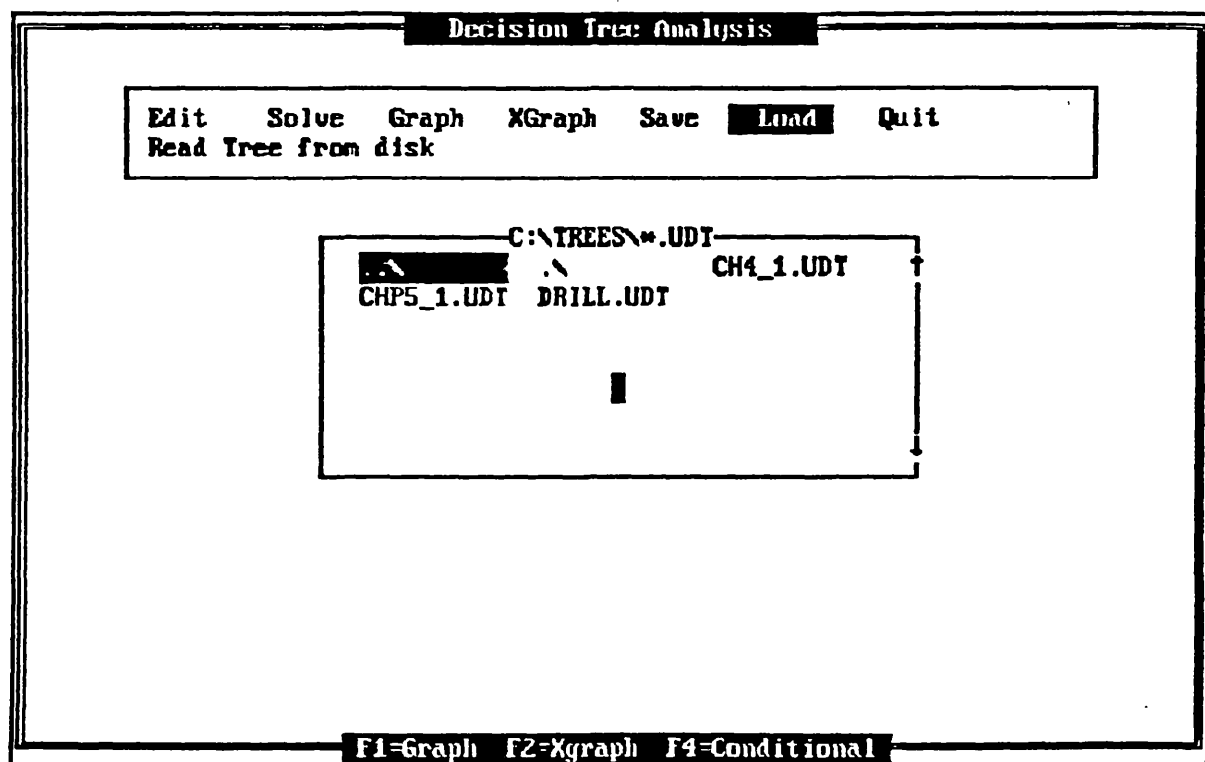


Figure 3.7: Load window displayed.

displayed path, or edit the file name to save the file under a different name or directory.

The "Load" option displays a window that lists the available decision tree files in the current directory (Figure 3.7). A file is loaded into the program by highlighting its name in the window and pressing ENTER.

Quit

Selecting the "Quit" option returns the user to DOS. Pressing ESCAPE in the main menu also exits the program. DTREE prompts the user before exiting the program to confirm the user's intent.

Overview of Programming

DTREE calculates decision trees in a manner slightly different from that used to calculate decision trees by hand. A flow chart illustrating how DTREE solves decision trees is presented in Figure 3.8. DTREE must search for nodes that need to be solved first. This is accomplished by starting at the top of the tree and then searching down the branches.

The solution process begins by calling the SOLVE routine with information about the first node on the tree, (i.e., node 1 in Figure 3.5a). This node is checked to see if it has been solved. If it has been solved then execution of the program returns to the main menu. If the node has not been solved then the branching nodes are searched. In Figure 3.5a, for

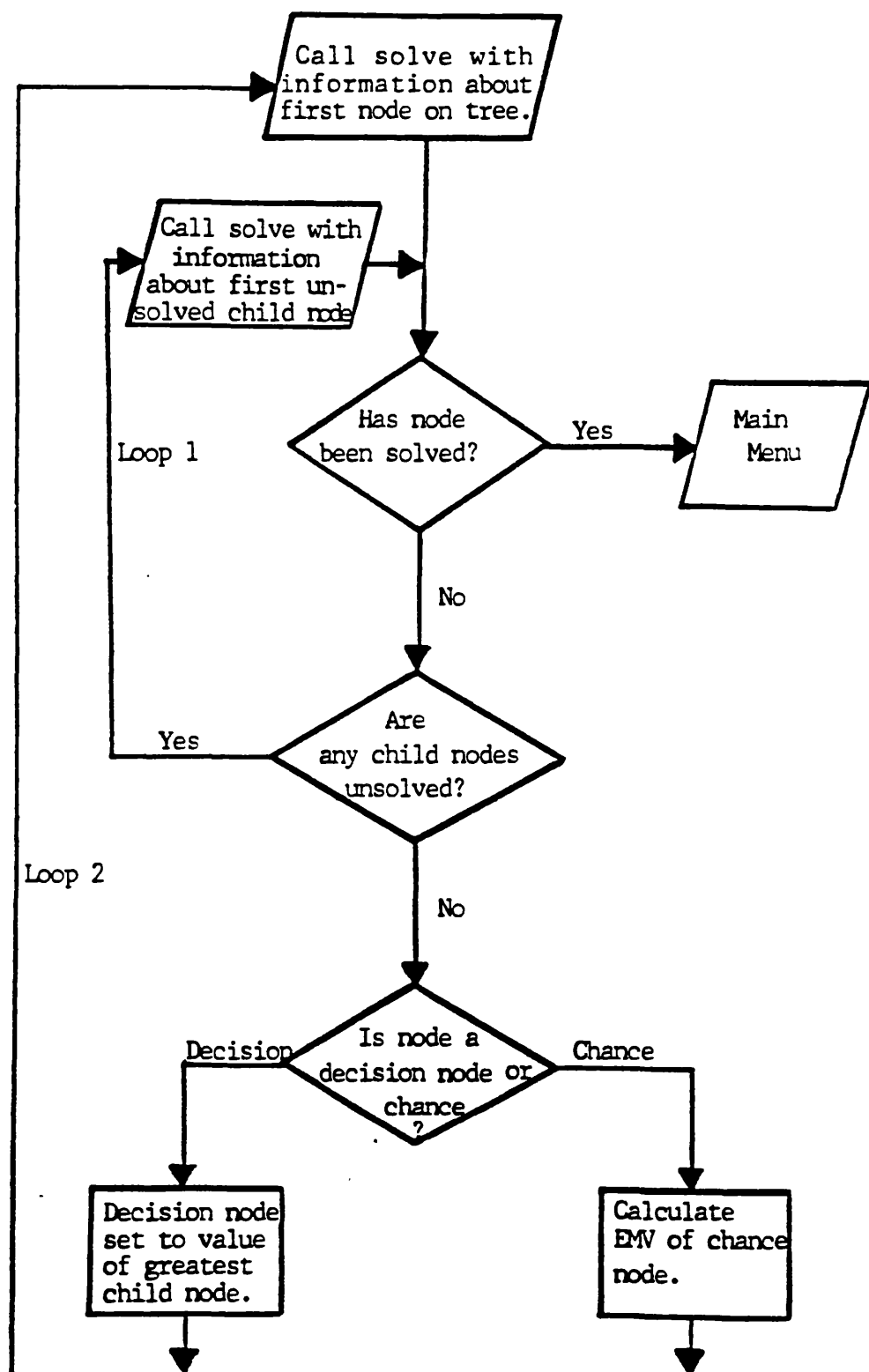


Figure 3.8: Flow chart describing DTREE's method of solving decision trees.

example, the branching nodes of node 1 are nodes 3 and 4. If node 1 is not solved, then nodes 3 and 4 are checked. The first unsolved branch node is checked in the same manner as its parent node. This is loop 1.

Once all the branching nodes are solved, the parent node can be solved. In Figure 3.5a the first node to be solved is node 3. After the node's type is determined the proper code is executed to solve that node. The solution process now begins searching again at the top of the tree, and continues the searching and solving procedure until the tree is completely solved.

CHAPTER 6

CONCLUSIONS AND RECOMMENDATIONS

Decision tree analysis can be a valuable tool in making geotechnical design decisions under uncertainty. The computer program DTREE can aid in the application of decision tree analysis to appropriate geotechnical problems. Important characteristics of DTREE are:

- 1) In addition to creating, solving, and analyzing decision trees, DTREE also allows saving and loading of decision tree files.
- 2) It provides graphical viewing of decision trees.
- 3) DTREE can be used to calculate large decision trees. It is possible to create and manipulate decision trees with as many as 1,400 nodes.
- 4) Because the computer program DTREE allows quick updating and solving of decision trees, a sensitivity analysis can be performed. Costs and probabilities can be updated to see when one design alternative becomes a better choice than another alternative. Chapters 4 and 5 have examples of using sensitivity analysis in geotechnical decision making.
- 5) Care must be taken to avoid misusing the program. The results that DTREE provides are only as credible as the inputs. The reliability of inputs must be tracked so that users can give proper weight to the results.

Outcomes of actions entered into DTREE must be discrete and mutually exclusive and exhaustive. Outcomes of some actions are better represented by probability distributions, for example, the depth at which rock is encountered when drilling. The outcomes of all actions must be discretized when performing decision tree analysis with DTREE. Also, DTREE allows a maximum of 10 branches after a chance or decision node.

Recommendations

Several additions should be made to DTREE to make the manipulation of decision trees even more efficient by computer. Suggestions are as follows:

- 1) These three changes would make the operation of the program more intuitive for the user and allow him/her to concentrate on the problem, not on the solving technique: a) When nodes are created, costs should be entered that apply to that node; then, the program should calculate the conditional costs at the ends of the branches. b) Global variables should be allowed for costs or probabilities that are used more than once in the tree. c) The results from the conditional calculator should be integrated automatically into the decision tree.
- 2) If decision trees become a part of an agency's decision making process, then a data management plan also needs to be included. Information concerning the costs and

outcomes of projects should be recorded so that information can be incorporated into decision trees for future projects. For example, for aggregate source exploration, data concerning prior estimates, quantities, and quality of rock found, as well as geology, location, and costs should be recorded. Decision trees that use results from prior projects will make results from the new decision trees more meaningful.

- 3) Expert systems could be used together with decision trees to identify alternatives that are applicable to a problem. An expert system could be used first to select alternatives that most likely apply to a problem, then the decision tree analysis could be used to select the alternative with the greatest EMV.
- 4) Misuse of DTREE can be avoided by providing training for users. Users not familiar with the concepts of decision tree analysis could easily misinterpret results. Misuse of the program also can occur if more weight is placed on the results than the inputs can justify; this can be avoided only by training users.

REFERENCES

Ali, E. M., 1987, Probabilistic Analysis of Foundations on Expansive Soils; in Proceedings of ICASP5, the Fifth International Conference on Applications of Statistics and Probability in Soil and Structural Engineering, University of British Columbia, Vancouver, B.C., Canada, pp. 775-782.

Anderson, J. R., Dillon, J. L., and Hardaker B., 1977, Agricultural Decision Analysis, McGraw Hill, New York.

Benjamin, J. R., and Cornell, C. A., 1970, Probability, Statistics, and Decision for Civil Engineers, McGraw Hill, New York.

Bloomfield, S. D., 1984, Decisionmaking In The Presence of Risk, in Proceedings of a Workshop on Slope Stability: Problems and Solutions in Forest Management, Seattle, Washington, February, pp. 99-104.

Borland International, Inc., 1990, Turbo C++ Programmer's Guide, Borland International, Inc., California, 264 p.

Hammond, C. J., Miller, S. M., and Prellwitz, R.W., 1988, Estimating the Probability of Landslide Failure Using Monte Carlo Simulation. Proc. 24th Symposium on Engineering Geology and Geotechnical Engineering. Coeur d'Alene, ID, p. 319-331.

Keaton, J. R., and Eckhoff, D. W., 1990, Value Engineering Approach to Geologic Hazard Risk Management, Paper presented at the 69th Annual Meeting of the Transportation Research Board; Washington, DC, January.

Kernighan, B. W., Ritchie, D. M., 1988, The C Programming Language, Second Edition, Prentice Hall, New Jersey.

Luckman, P. G., 1987, Slope Stability Assessment Under Uncertainty: A first Order Stochastic Approach, Ph.D dissertation, Department of Civil Engineering, University of California Berkeley.

Long, M. T., 1990, An Update On Methods and Procedures for Exploration, Design, and Construction of Drain Systems, Prepared for the Fifth International Conference on Low Volume Roads, National Research Council - Tranportation Research Board.

Miller, S. M., 1988, A Temporal Model for Landslide Risk Based on Historical Precipitation. Mathematical Geology, Vol. 20, No. 5.

Miller, S. M., Hammond C., Prellwitz P. R., 1987,
Applications of Probabilistic Methods and Decision
Analysis to Geotechnical Engineering and Resource
Management, Geotechnical Engineering Training Session.
USDA Forest Service, Intermountain Research Station.

Newendorp, P.D., 1975, Decision Analysis for Petroleum
Exploration; Petroleum Publ. Co., Tulsa, OK, 668 p.

Schildt, H., 1988, Turbo C The Complete Reference, McGraw
Hill, Inc., California, 908 p.

Wyllie, D. C.; McCammon, N. R.; Brumund, W. 1979. Planning
Slope Stabilization Programs by Using Decision
Analysis. Transportation Research Record 749, pp. 34-
39.

APPENDIX A

Editing keys available in input fields of DTREE. These keys can be used to move or manipulate text in input fields.

<u>Key</u>	<u>Action</u>
Left Arrow	cursor left
Right Arrow	cursor right
Up Arrow	cursor up
Down Arrow	cursor down
Ctrl-Left Arrow	word left
Ctrl-Right Arrow	word right
Tab	field right
Shift-Tab	field left
Enter	process field
Ctrl-Enter	process all fields
Decimal (.)	move to right side of decimal point
Home	beginning of field
End	end of field line / end of field
Ctrl-Home	beginning of first field
Ctrl-End	end of last field
Ins	toggle insert mode
Del	delete character at cursor
BackSpace	delete character left
Ctrl-BackSpace	delete word left
Ctrl-R	restore field to original contents
Ctrl-T	delete word right
Ctrl-U	delete to end of field
Ctrl-Y	delete to end of last field
Esc	abort data entry

Section 3

Summary of 3D-LISA Model Evaluations

Current Status
of the
3-D LISA Evaluation

J. Cuthbertson
October 30, 1990

Contents

	page
Introduction	1
Field Work	2
Overview of Field Work	2
Soil Sampling and Field Measurement of Soil Density	4
Field Surveying of Failures	7
Laboratory Work	8
Mechanical Grain Size Analysis	8
Test Equipment	8
Test Procedure	8
Test Results and Analyses	9
Soil Strength Parameters	13
Test Equipment	13
Test Procedure	13
Test Results and Analyses	15
Estimation of Saturated Hydraulic Conductivity	16
Test Equipment	16
Test Procedure	17
Test Results and Analyses	18
Bibliography	20

Figures

Figure 2.1. Schematic of the device used to measure the volume of the soil samples gathered in the Coast Range; (A) Planview, (B) Elevation View.	5
Figure 3.1. Plot of the grain size distribution curves for the soils classified as SW.	11
Figure 3.2. Plot of the grain size distribution curves for the soils classified as SP.	11
Figure 3.3. Plot of the grain size distribution curves for the soils classified as GW.	12
Figure 3.4. Plot of the grain size distribution curves for the soils classified as GP.	12
Figure 3.5. Elevation schematic of Tempe cell.	17
Figure 3.6. Constant head permeameter and Tempe cell configuration used for the saturated hydraulic conductivity tests.	18

Tables

Table 2.1. <i>Failure numbers, names, location, and status.</i>	3
Table 2.2. <i>Measured in-situ densities for 11 sample points.</i>	7
Table 3.1. <i>Summary table of mechanical sieve analysis.</i>	10
Table 3.2. <i>Comparison table of soil strength tests performed by Schroeder, Hammond, and Cuthbertson for the soils of the Coast Range.</i>	16
Table 3.3. <i>Measured hydraulic conductivity for the coast range soils.</i>	19

1.0 INTRODUCTION

The University of Idaho in cooperation with the USDA Forest Service Intermountain Research Station, Moscow, Idaho and the Bureau of Land Management, Eugene District, Eugene, Oregon has worked to evaluate the 3-D LISA slope stability model. The current status of their progress is discussed in the following chapters.

2.0 FIELD WORK

2.1 Overview of Field Work

Field work was conducted over a period of three summers starting in 1988 and concluding in 1990. During the first summer's field work in 1988, Jeff Lulitch, a University of Idaho graduate student, located 13 failures which could possibly be used to test the 3-D Lisa model. As part of his field work, he gathered the following information:

1. Soil type/depth
2. Critical block length/width
3. Average slope angle
4. Drainage bearing
5. Alpha angles left/right
6. Tree condition

During the winter of 1988/1989 Jeff decided not to pursue his Master's Degree in Geological Engineering. At that time, I entered the project and completed the remaining field work and evaluation.

During the second field season, 1989, a review of the original 13 sites was conducted. Of the 13 original failures, 2 were side cast failures and dismissed as possible test failures, and 7 were never relocated. The remaining 4 failures were mapped in greater detail, soil samples taken, and 2 new failures added.

During the final summer, 1990, stadia surveys were conducted at 4 sites, and 3 new failures were added to bring the total number of failures for testing the model to 9. Throughout the process of adding failures and removing others from the list, the numbering sequence used to label the failures remained the same and continued consecutively from year to year. Table 2.1 lists all of the failures mapped during the course of the field work, their name, location, and status. Failures which could not be located were typically located in clear cut units older than ten years. The size and thickness of the vegetation in these older units rendered the task of relocating the failures all but impossible.

Table 2.1. Failure numbers, names, location, and status.

No.	Name	Location	Status
1	Neely 78 U-1	NW _{1/4} sec. 29, T.17S., R.10W.	UTL
2	Swisstide U-2	SE _{1/4} sec. 16, T.17S., R.10W.	UTL
3	Turner Cr.	SW _{1/4} SE _{1/4} sec. 14, T.18S., R. 9W.	S
4	Pope Billy	SW _{1/4} NE _{1/4} sec. 25, T.19S., R.11W.	UTL
5	Alma Cemetery	NE _{1/4} SW _{1/4} sec. 4, T.19S., R. 8W.	NS
6	4-Horsemen	NE _{1/4} NW _{1/4} sec. 28, T.16S., R. 8W.	S
7	Taylor Butte	SE _{1/4} SW _{1/4} sec. 17, T.15S., R. 8W.	S
8	Railroad Cr.	NW _{1/4} SW _{1/4} sec. 22, T.20S., R.10W.	UTL
9	Hadsall Cr.	NW _{1/4} NE _{1/4} sec. 25, T.18S., R.10W.	UTL
10	Sawmill	NE _{1/4} SW _{1/4} sec. 31, T.17S., R. 9W.	S
11	Rd. 2680	NE _{1/4} SE _{1/4} sec. 5, T.18S., R. 9W.	UTL
12	Vincent Cr.	NW _{1/4} SW _{1/4} sec. 27, T.20S., R. 9W.	NS
13	Waite Cr.	SW _{1/4} SW _{1/4} sec. 24, T.18S., R. 9W.	UTL
14	Grettle	SE _{1/4} SE _{1/4} sec. 30, T.18S., R. 9W.	S
15	Barber Cr.	SW _{1/4} SE _{1/4} sec. 11, T.18S., R. 9W.	S
16	Bread Crumb	SW _{1/4} NE _{1/4} sec. 30, T.18S., R. 9W.	S
17	Ginger Bread	NE _{1/4} NE _{1/4} sec. 25, T.18S., R. 9W.	S
18	Roy Walker	NW _{1/4} NE _{1/4} sec. 33, T.17S., R.10W.	S

UTL - Unable to locate NS - Not Suitable S - Suitable

Typically, the failures which were mapped by Mr. Lulitch and myself are best described as spoon shaped with the handle lying in the stream channel. They range from 30 to 70 ft at the widest portion and 10 to 25 ft at what could be called the neck of the spoon. The stream channels are scoured to bedrock and have cross-sections which are hyperbolic to almost parabolic in some cases. The bedrock at the bowl of the spoon is usually bowl shaped as well although several failures exist with planar surfaces in the head wall. These failures are typically in large headwalls and may actually be curved but because of the scale the curvature is not discernible in the field.

Within the failures, fresh bedrock is always exposed. Some soil remains in the failures, typically around the scarps and at slope breaks. The bulk of the soil which remains is deposited or left behind as the energy of the failure is dissipated. Also, it is highly possible that some soil from the scarps fails and enters the main failure shortly after the

failure occurs. Several of the failures had sections of the scarps that appeared to have eroded back up slope from the failure.

Soil thicknesses range from several inches up to 10 ft with the majority falling between 2 to 7 ft. In every headwall with a failure there are classic signs of slope instability. These signs include:

1. Hummocky topography
2. Seeps and springs
3. Exposed patches of bedrock
4. Pistol butted trees
5. Windthrow
6. Tension cracks
7. Slope angle near the angle of internal friction

All or only some of these signs may be present, but every failure had at least three signs present.

The majority of the failures occurred on clear-cut slopes. The first winter and then the third through the fifth winters appear to be the most critical to the stability. Several failures occurred during the first winter while others did not fail until the third or a latter winter. Two of the failures occur in un-cut units. Number 18 occurred in the 120 year old fire stand outside of Mapleton and number 14 occurred in a unit which was logged 30 to 50 years ago.

2.2 Soil Sampling and Field Measurement of Soil Density

Soil samples were gathered using two sampling methods. In the first method, a hand trowel was used to fill one or more sealable 1 gallon plastic bags with soil from the base of an existing failure scarp. These samples were gathered primarily for performing grain size analysis.

In the second method, a ledge was excavated into the existing failure scarp upon which a device was used to measure the volume of a small sample removed with a hand trowel and fingers. This device uses both the principals of a balloon densiometer and the common sand cone. It is a plexiglass ring approximately 1 foot in diameter, and in the center of the ring is a 6 inch diameter hole. On the underside of the plexiglass ring and aligned with the hole in the plexiglass, is another ring of soft foam. The foam ring has an inside diameter of 6 inches and an outside diameter of 8 inches (Figure 2.1).

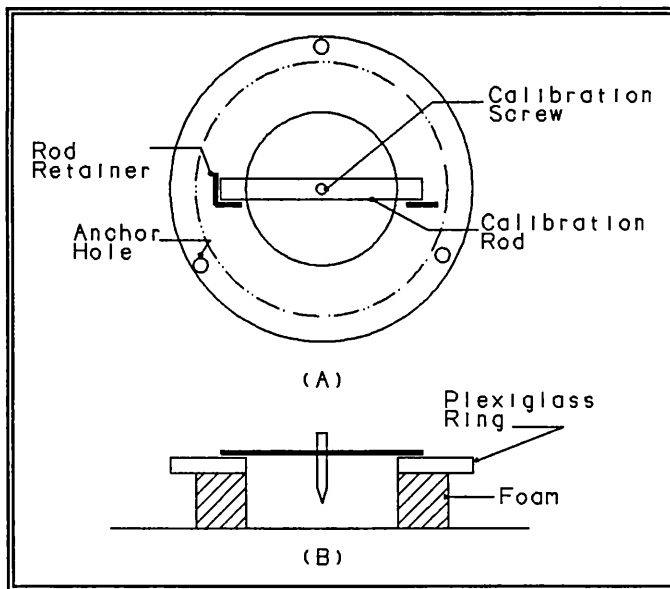


Figure 2.1. Schematic of the device used to measure the volume of the soil samples gathered in the Coast Range; (A) Planview, (B) Elevation View.

Three holes in the plexiglass allow the device to be staked in place on the ground surface. The foam acts as a flexible gasket between the ground surface and the ring. Using threaded stakes with nuts, the device can be securely held in place and leveled by adjusting the position of the nuts. The foam also allows the ring to be leveled upon a sloping surface up to approximately 20°.

Once the ring is in place, a thin plastic bag is placed in the hole of the ring. Water is poured into the bag until the bag has expanded and covers the soil in the bottom of the hole. This procedure measures the volume of the hole in the sample device before the soil sample is taken. After the bag is in place and filled with water a calibration rod is placed across the top of the ring. This rod is guided into position using two pieces of 0.5 inch angle stock. At the center of the rod is a vertical calibration screw which protrudes into the hole in the plexiglass ring. The screw height is adjusted until the screw dimples the surface of the water. This process essentially zeros the device.

Before sampling, the rod is carefully removed along with the bag of water. The bag of water is placed in a safe position where no water can

leak from the bag. The soil sample is removed from the center of the ring and placed in sealable bags. After the soil has been sampled the bag with the water is put back in place along with the calibration rod. A graduated cylinder is used to measure the amount of water which is necessary to bring the water level in the hole back to the original level where the surface is dimpled by the screw. The volume of the water added is the volume of the soil sample removed.

Once the volume of the sample was measured, the first method was used to obtain a larger sample at the same sampling point for some failures. All of the samples were placed in 1 gallon sealable plastic bags to preserve the moisture conditions of the sample. At least one soil sample was gathered at each of the failures during the field work using either method. Out of 9 failures, 6 failures had multiple sample points, and 7 failures had the volume of the soil sample measured to calculate the field density, see Table 2.2.

The samples gathered are numbered using the following procedure:

The first numeral refers to the failure number as described previously. The second number refers to the sample point within the failure. As an example, 6-1 stands for failure number 6 sample point 1, and 6-2 stands for a second sampling point within the same failure. If several sample bags were filled at a single sample point they are further denoted by the letters of the alphabet such as 6-1A and 6-1B.

Multiple samples from a single sample point were eventually mathematically combined into a single sample for classification of the soils and physically for performing the direct shear tests.

Table 2.2. Measured *in-situ* densities for 11 sample points.

Sample No.	Moist Density (g/cm ³)	Dry Density (g/cm ³)	Saturated Density (g/cm ³)	Moist Density (pcf)	Dry Density (pcf)	Saturated Density (pcf)
3-1	1.27	1.14	1.71	79.32	71.05	106.71
6-1	1.74	1.46	1.91	108.71	91.21	119.27
6-2	1.22	0.98	1.61	76.22	61.23	100.60
7-1	1.44	1.26	1.79	90.10	78.99	111.66
15-1	1.20	1.04	1.65	75.19	65.04	102.97
15-2	1.22	1.06	1.66	76.24	66.12	103.64
16-1	1.34	1.13	1.70	83.72	70.60	106.43
16-2	1.45	1.26	1.78	90.59	78.72	111.49
17-1	1.46	1.27	1.79	91.21	79.34	111.88
18-1	1.21	0.93	1.58	75.59	58.10	98.65
18-2	1.38	1.01	1.63	86.22	63.10	101.76

2.2 Field Surveying of Failures

The following 4 failures were surveyed using the stadia method:

1. No. 6, 4-Horsemen
2. No. 16, Bread Crumb
3. No. 17, Ginger Bread
4. No. 18, Roy Walker

The surface topography was surveyed directly, and the subsurface topography was determined using a drive probe at the surface survey points. The locations of the survey points were controlled by the vegetation outside the failure scarps and by footing inside the failures. Thus, the spacing between survey points is random. However, an attempt was made to keep the spacing between points approximately 5 ft with 10 ft as a maximum. Major slope breaks and scarp outlines naturally were surveyed with a greater concentration of survey points.

The accuracy of the survey points is only to the nearest foot. This degree of accuracy seemed appropriate since the surveying was performed mainly to provide a greater understanding of the bedrock geometry and to provide maps which could latter be used to estimate failure block sizes when testing the model.

3.0 LABORATORY WORK

3.1 Mechanical Grain Size Analysis

3.1.1 Test Equipment

The equipment used to determine the grain size distribution consisted of an Ohaus Brainweigh B-5000 mass balance sensitive to 0.1 g, a W.S. Tyler Inc. Ro-Tap mechanical sieve shaker, and the following US standard Sieves:

- A. 3"
- B. 3/4"
- C. No. 4 (0.187")
- D. No. 10 (0.079")
- E. No. 40 (0.017")
- F. No. 200 (0.003")
- G. Pan

3.1.2 Test Procedure

The material was prepared for the sieve analysis using the ASTM D 421-85, Standard Practice for Preparation of Soil Samples for Particle Size Analysis and Determination of Soil Constants, as a guide. The samples were air dried then passed by hand through a No. 4 sieve to separate the gravel fraction from the sand/silt fraction. The process of hand sieving removed the majority of the fines which coated the gravel sized fraction and divided the samples into manageable sizes.

A modified version of the ASTM D 422-63, Standard Method for Particle Size Analysis, was then used as the testing procedure. The standard procedure was modified to decrease the amount of abrasion which occurs to the coarse fraction particles during the mechanical sieving process. A test sample of material larger than a No. 4 sieve (0.187 inches) was sieved and inspected every 5 minutes. After the first five minute period, the material was visually inspected for abrasion and breakage. Significant abrasion and rounding of the particles was noticed after the first five minute period. However, no breakage was observed. Because there was significant abrasion of the particles, the sieve time was decreased to 2.5

minutes for the material larger than a No. 4 sieve. The standard procedure was then followed for the material finer than a No. 4 sieve.

After the 2.5 minute period of sieving the +No. 4 material, the material retained in the pan was added to the -No. 4 material, material smaller than a No. 4 sieve, for a second stage of sieving. Each sieve size used for the sieve analysis corresponds to a particle size division within the Unified Soil Classification System:

coarse gravel	> 3/4"
fine gravel	> No. 4
coarse sand	> No. 10
medium sand	> No. 40
fine sand	> No. 200
silt/clay	< No. 200

A hydrometer analysis to determine the particle size distribution for the material passing the No. 200 sieve was not performed. The maximum amount of material measured passing the No. 200 sieve was 6.9%, and the mean percentage of the material passing the No. 200 sieve was only 2.0%. Coarse grained soils such as these do not require a hydrometer analysis to classify them. Also, these soils are non-plastic, and for the same reasons atterburg limits were not estimated.

3.1.3 Test Results and Analyses

A total of 15 soil samples were sieved from the 9 failures. Three of the failures had only a single sampling point which accounts for the odd number. Table 3.1 lists the parameters used from the sieve analysis to classify the soils using the Unified Soil Classification System (USCS). It also contains the final USCS classification and the field soil classification for the soils from the 9 failures. The grain size distribution curves for the soils are plotted in Figures 3.1, 3.2, 3.3, and 3.4.

Table 3.1. Summary table of mechanical sieve analysis.

Sample	D60	D30	D10	Cu	Cc	%	%	Soil	Soil
No.	(mm)	(mm)	(mm)			Passing No.4	Passing No.200	Class.	Type
3-1	3.40	3.00	0.45	7.6	5.9	37.9	1.5	GP	Bohannon
6-1	7.90	0.90	0.14	56.4	0.7	51.5	4.4	SP	Bohannon
6-2	6.00	1.40	0.20	30.0	1.6	55.2	3.3	SW	Bohannon
7-1	6.60	0.40	0.09	73.3	0.3	57.3	6.9	SP-SM	Jason
7-2	9.50	2.90	0.60	15.8	1.5	41.6	1.2	GW	Jason
10-1	10.00	1.30	0.18	55.6	0.9	47.8	1.1	GP	Digger
10-2	14.00	2.00	0.21	66.7	1.4	49.9	0.4	GW	Digger
14-1	7.40	0.86	0.18	41.1	0.6	54.2	2.5	SP	Bohannon
15-1	2.90	0.56	0.14	20.7	0.8	69.1	3.3	SP	Bohannon
15-2	4.80	0.60	0.14	34.3	0.5	59.9	2.9	SP	Bohannon
16-1	4.00	0.74	0.18	22.2	0.8	63.7	0.5	SP	Umpcoos
16-2	9.00	1.90	0.28	32.1	1.4	43.4	0.2	GW	Umpcoos
17-1	10.05	2.10	0.23	43.7	1.9	41.3	0.6	GW	Jason
18-1	3.40	0.83	0.21	16.2	1.0	66.5	0.3	SW	Preacher
18-2	3.10	0.56	0.14	21.8	0.7	65.4	1.1	SP	Preacher
Max	14.00	3.00	0.60	73.3	5.9	69.1	6.9		
Min	2.90	0.40	0.09	7.6	0.3	37.9	0.2		
Mean	6.80	1.34	0.22	35.8	1.3	53.7	2.0	SW	Bohannon
Std. Dev.	3.17	0.83	0.13	19.2	1.3	9.67	1.8		

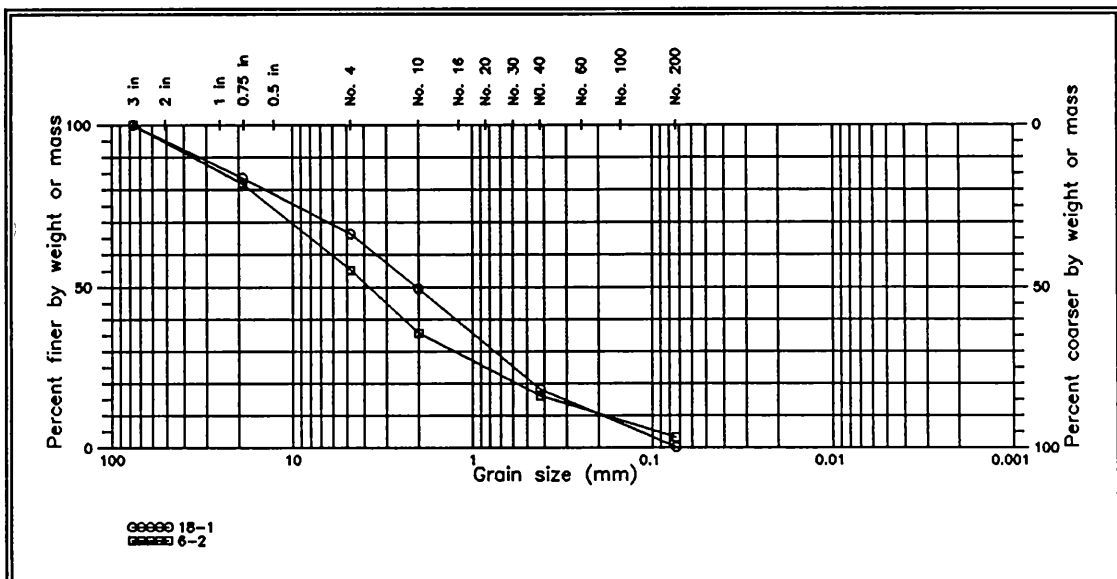


Figure 3.1. Plot of the grain size distribution curves for the soils classified as SW.

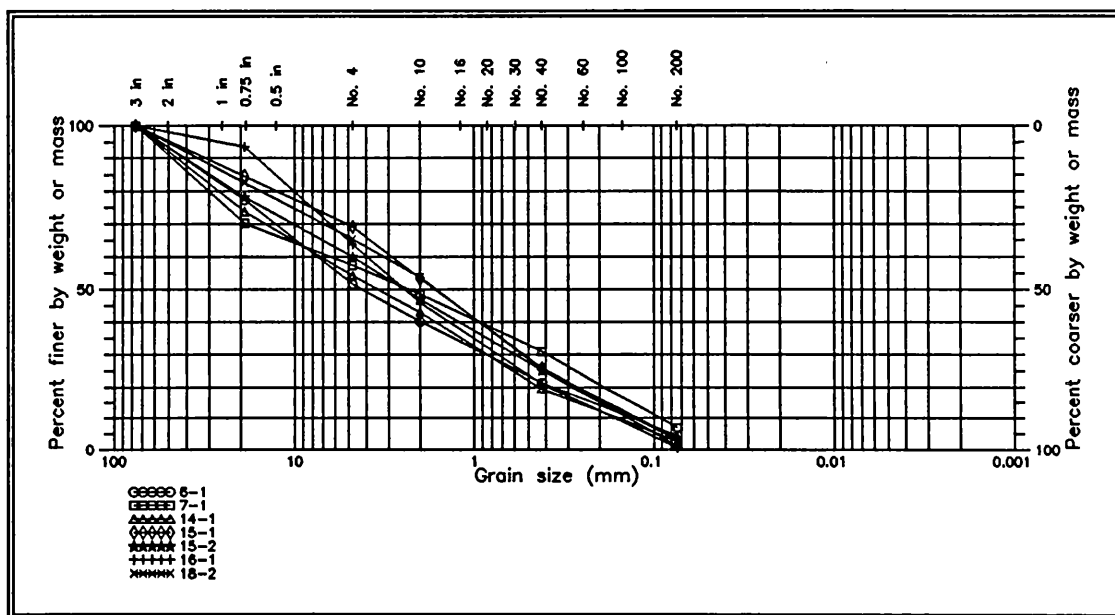


Figure 3.2. Plot of the grain size distribution curves for the soils classified as SP.

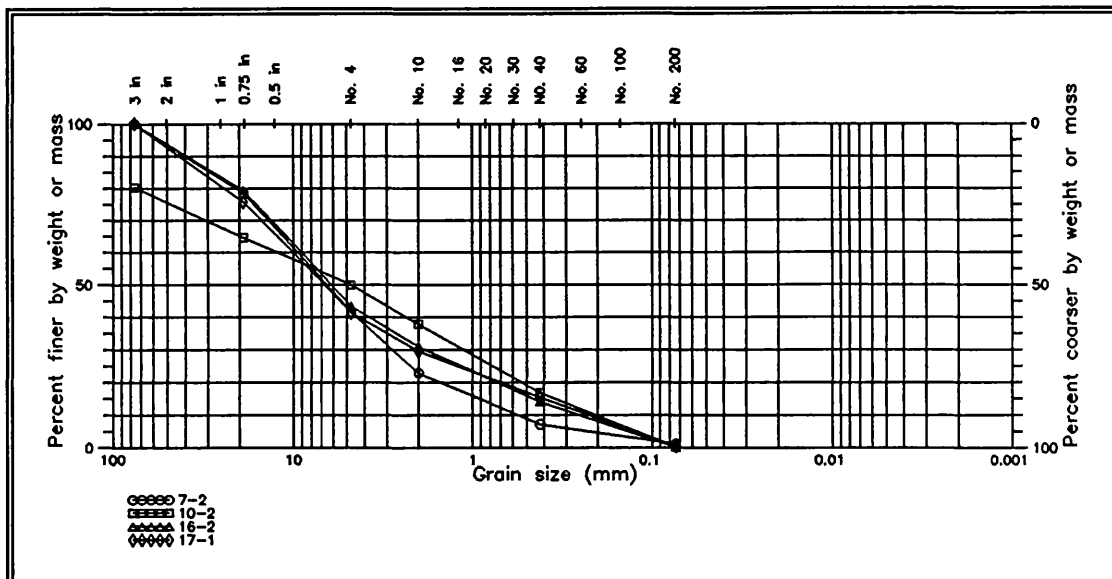


Figure 3.3. Plot of the grain size distribution curves for the soils classified as GW.

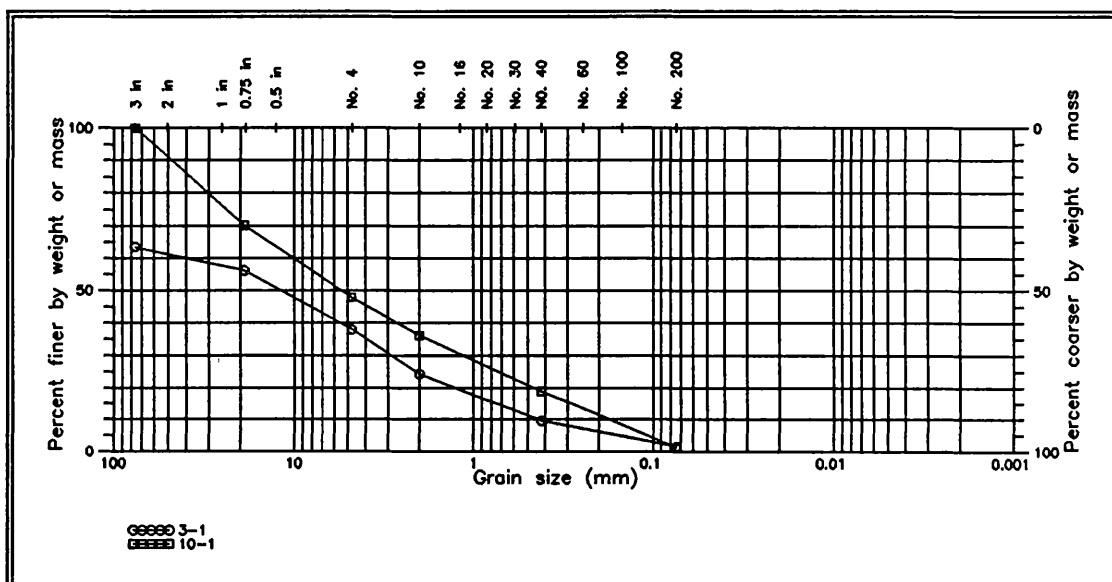


Figure 3.4. Plot of the grain size distribution curves for the soils classified as GP.

3.2 Soil Strength Parameters

3.2.1 Test Equipment

The following test equipment was used for the direct shear tests. A Wykeham Farrance direct shear machine model number 25301 with a sample mold 10 cm square by 5 cm deep was used as the shear device. Also, a Wykeham Farrance analog to digital converter box was used to convert the analog output from the load cell on the shear machine to digital output suitable for input to a computer. The converted output was sent to a Sharp PC-7200 portable computer which used a Basic program to record the horizontal and vertical displacement and average the shear load for five consecutive readings.

3.2.2 Test Procedure

The ASTM D 3080-72, Standard Method for Direct Shear Test of Soils Under Consolidated Drained Conditions, was used as the testing procedure. In compliance with the ASTM procedure, the material larger than a U.S. standard sieve No. 4 (0.187 in) was removed. The test procedure specifies that the ratio of sample thickness to maximum grain size should be no less than 6. The largest direct shear sample mold available with the Wykeham Farrance direct shear machine at the University of Idaho is 3.64 cm thick with a porous stone in the bottom. Therefore, the largest size permissible is $3.64/6$ or 0.607 cm (0.239 in). The process of scalping the +No. 4 material gives a ratio of 7.7:1 which meets the ASTM requirements.

The soils used for the direct shear tests were reconstituted soils. They were re-mixed in the proper grain size proportions, as determined from the grain size analysis, from the air dried soil used for the sieve analysis. Only that fraction of the soil which was less than the No. 4 sieve size was used.

As mentioned earlier, samples that have been scalped should be compacted to a lower density when they are remolded. However, the samples were remolded to field density for the tests for the following reasons:

1. No clear consensus has been reached upon as to the degree to which scalped samples should be under-consolidated.
2. Over-consolidating the scalped samples to field density will over

estimate ϕ . Under this condition, if the 3-D Lisa model computes a high probability of failure then the model will still compute a high probability of failure for a lower ϕ angle, all other factors remaining constant.

3. In the future, it is highly probable that people using the model will not correct for scalping. Therefore, the model should be tested under this condition to see if it computes a low probability of failure for unstable slopes as a result of over estimating ϕ .

The remolded samples were placed in the shear machine and the appropriate normal load was applied in one increment. The samples were allowed to consolidate dry for a period of ten minutes. After the ten minutes of dry consolidation, water was added to the shear box for another ten minute period of consolidation. By the end of the second period of consolidation, the porous stone on top of the sample above the water was saturated from capillary rise, and the consolidation process had slowed to a change in vertical height of 0.001 mm per 1 minute interval or less. This rate of consolidation corresponds to a change in volume of 0.01 cm³ in a one minute period or a change in volume of 0.15 cm³ (0.04% of the sample volume) for the sample over the time it takes to run the test to completion, provided the consolidation rate under the normal load remains constant.

The samples were sheared at a rate of 0.039 in/min (0.999 mm/min) until a total displacement of 0.591 inches (15.0 mm) was achieved. This displacement corresponds to a strain of 0.15 or 15% of the original sample size. A large displacement was used to insure that the residual strength would be reached, but in the final analysis, shear load values occurring at more than 10% strain were not required to determine the strength parameters. After each test was completed, a soil sample of approximately 100 grams was taken from the center of the shear mold to determine the moisture content and ultimately the density of the sample during the test.

Five tests were performed for each soil sample utilizing 5 normal loads. The normal loads used were calculated to correspond to the range of soil depths encountered in the coast range. An assumed density of 105 pcf was used along with various soil depths to calculate the appropriate total normal stress. The value of 105 pcf was determined by calculating the mean

of the saturated densities for the soil samples in which the density was measured. The actual mean is 107 pcf, but 105 pcf was used to simplify the mathematics.

The total normal stress is equal to the density multiplied by the soil depth. For an effective stress analysis, the corresponding pore pressure would be subtracted from the total stress. The total normal stresses used and the equivalent soil depth were:

1. 105.0 psf - 1 ft of soil
2. 210.0 psf - 2 ft of soil
3. 315.0 psf - 3 ft of soil
4. 525.0 psf - 5 ft of soil
5. 840.0 psf - 8 ft of soil

Residual shear strengths were used to determine the Mohr-Coulomb strength envelopes for the soil samples. Linear regression was used to fit a linear line to the five data points determined from the five shear tests.

3.2.3 Test Results and Analyses

After reviewing the available literature, only two other authors have performed shear strength tests on the soils of the Coast Range and reported both c and ϕ values, Schroeder (1983) and Hammond.

Schroeder performed consolidated undrained (CU) triaxial tests upon undisturbed samples. The consolidation pressures he used for the tests and the equivalent soil depth at a density of 105 pcf were:

1. 710 psf - 6.8 ft of soil
2. 1462 psf - 13.9 ft of soil
3. 2151 psf - 20.5 ft of soil

Hammond performed saturated direct shear tests. However, the normal loads used for the tests were not reported. Table 3.2 lists the testing results of Schroeder, Hammond, and myself. The angles of internal friction (ϕ) remain comparable between the authors but the cohesion values vary slightly. The variation is likely attributed to the test procedure used.

Table 3.2. Comparison table of soil strength tests performed by Schroeder, Hammond, and Cuthbertson for the soils of the Coast Range.

Author	Sample No.	USCS Classif	Field	Field	Sat.	Dry	Specific Gravity	c (psf)	ϕ (Degrees)
			Moisture Content (%)	Unit (pcf)	Unit (pcf)	Unit (pcf)			
Schroeder (CU Triax.)	1	SM	35.1	103.67	111.16	76.81	2.73	143.27	35.5
	2	SM	23.8	92.42	109.91	74.94	2.70	20.47	36.9
	3	SM	18.6	83.06	106.16	69.94	2.66	0.00	41.4
	5	SM	30.4	94.92	108.66	73.07	2.74	122.81	37.8
	Linslaw-2	SM	1.4	71.56	108.10	70.60	2.67	244.80	36.8
Hammond (Sat. DS)	Noti-2	SM	1.4	70.35	106.16	69.40	2.63	244.80	33.6
	Buck Cr.	SM	1.2	76.69	105.41	75.80	2.63	230.40	32.5
Cuthbertson (Sat. DS)	6-1	SP	19.0	108.66	119.28	91.18	2.65*	24.20	34.1
	6-2	SW	24.0	76.19	100.54	61.20	2.65*	47.10	34.9
	16-1	SP	19.0	83.68	106.16	70.57	2.65*	6.90	35.1
	16-2	GW	15.0	90.55	111.16	78.69	2.65*	19.80	34.7
	17-1	GW	15.0	91.18	111.78	79.31	2.65*	0.00	38.8
	18-1	SW	30.0	75.56	98.67	58.08	2.65*	3.10	37.1
	18-2	SP	37.0	86.18	101.79	63.07	2.65*	30.60	34.0
	Mean		27.0	93.52	108.97	73.69	2.71	71.64	37.9
Schroeder	Std. Dev.		6.284	7.342	1.849	2.537	0.031	62.249	2.181
	Minimum		18.6	83.06	106.16	69.94	2.66	0.00	35.5
	Maximum		35.1	103.67	111.16	76.81	2.74	143.27	41.4
	Mean		1.3	72.87	106.56	71.93	2.64	240.00	34.3
Hammond	Std. Dev.		0.092	2.748	1.135	2.778	0.019	6.788	1.824
	Minimum		1.2	70.35	105.41	69.40	2.63	230.40	32.5
	Maximum		1.4	76.69	108.10	75.80	2.67	244.80	36.8
	Mean		23.3	83.89	107.06	68.49	2.65	17.92	35.8
Cuthbertson	Std. Dev.		8.055	6.210	6.864	8.329		16.723	1.655
	Minimum		15.0	75.56	98.67	58.08		0.00	34.0
	Maximum		37.0	91.18	119.28	79.31		47.10	38.8
	Mean		19.3	86.05	107.50	72.33	2.67	81.30	35.9
Schroeder	Std. Dev.		11.503	11.191	5.071	8.092	0.033	92.818	2.275
Hammond	Minimum		1.2	70.35	98.67	58.08	2.63	0.00	32.5
	Maximum		37.0	108.66	119.28	91.18	2.74	244.80	41.4

* = Assumed Value

3.3 Estimation of Saturated Hydraulic Conductivity

3.3.1 Test Equipment

The test equipment for the saturated hydraulic conductivity tests consisted of a constant head permeameter, 6 Tempe cells, 6 graduated cylinders with 1 ml divisions, and bottled carbon dioxide. The Tempe cells (Figure 3.5) are brass sample rings with plexiglass caps sealed by O-rings. Water is forced in one cap and flows out of the other cap. Fiberglass mesh and plastic screening is placed between the soil samples and the plexiglass caps to provide support to the soil and allow drainage at the cap soil interface.

3.3.2 Test Procedure

An ASTM test procedure is not defined for performing saturated hydraulic conductivity tests. However, there is a standard practice which the soil scientist at the University of Idaho follow. This practice consists of sieving the test soils to remove particles larger than 2 mm, re-compacting in the Tempe cells to field density, and passing carbon dioxide through the sample for 24 hrs prior to testing.

The carbon dioxide is used to replace the non-soluble air in the voids of the soil. The carbon dioxide which becomes trapped in the voids upon wetting of the soil is readily dissolved into the water allowing full saturation of the sample after a short period of time.

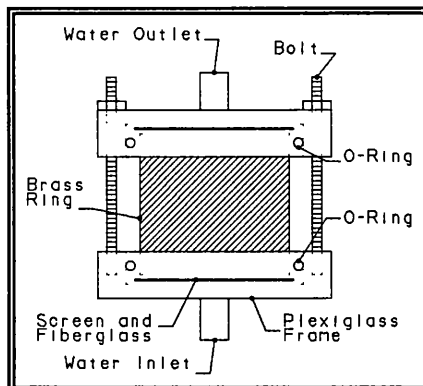


Figure 3.5. Elevation schematic of Tempe cell.

The Tempe cells were connected to a manifold and constant head permeameter which regulated the hydraulic gradient across the samples (Figure 3.6). A change in head of 10 cm between the water outlet and water inlet of the Tempe cells was used for the tests. Three tests per soil sample were run to determine an average hydraulic conductivity for that sample.

Standard tap water at a temperature of 23° C was used for the tests. Many people prefer to use de-aired water to prevent dissolved air from coming out of solution and collecting in the voids, but natural rain water has some amount of dissolved air. Thus, standard tap water was used without considering a correction factor.

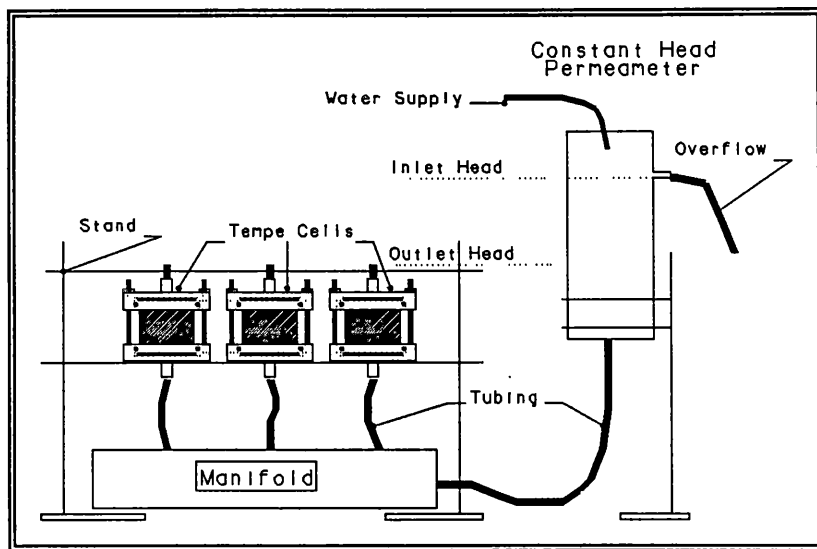


Figure 3.6. Constant head permeameter and Tempe cell configuration used for the saturated hydraulic conductivity tests.

3.3.3 Test Results and Analyses

The saturated hydraulic conductivity values measured for the soil samples are listed in Table 3.3. An important aspect of hydraulic conductivity which most people find hard to understand is the accuracy to which hydraulic conductivity should be reported. Even though the values are reported to two significant digits, it is really the magnitudes of the values which should be used when making comparisons between measured values. The difference in a hydraulic conductivity of 1.5 and 9.5 is insignificant when the full range over which hydraulic conductivity can range is 7 or more orders of magnitude. The measured hydraulic conductivities for the Coast Range soils vary by less than an order of magnitude between similar samples. This amount of variation is acceptable and expected.

Table 3.3. *Measured hydraulic conductivity for the coast range soils.*

19

Sample No.	Test	USCS Class.	Soil Type	Hyd. Cond. (cm/s)	Hyd. Cond. (ft/day)
6-1	A	SP	Bohannon	4.4×10^{-4}	1.2
	B			8.7×10^{-5}	0.2
	C			3.2×10^{-4}	0.9
6-2	A	SW	Bohannon	6.4×10^{-3}	18.3
	B			2.6×10^{-3}	7.3
	C			7.2×10^{-3}	20.5
16-1	A	SP	Umpcoos	8.8×10^{-3}	24.8
	B			5.9×10^{-3}	16.7
	C			9.2×10^{-3}	26.1
16-2	A	GW	Umpcoos	3.0×10^{-4}	0.8
	B			2.2×10^{-4}	0.6
	C			2.3×10^{-4}	0.6
17-1	A	GW	Jason	3.9×10^{-5}	0.1
	B			6.5×10^{-5}	0.2
	C			8.5×10^{-5}	0.2
18-1	A	SW	Preacher	4.9×10^{-3}	13.8
	B			4.4×10^{-3}	12.4
	C			4.3×10^{-3}	12.3
18-2	A	SP	Preacher	1.5×10^{-3}	4.3
	B			1.5×10^{-3}	4.1
	C			1.4×10^{-3}	4.1

BIBLIOGRAPHY

American Society for Testing and Materials, (1988), *Annual Book of ASTM Standards*, Section 4: Construction, Vol. 04.08, Philadelphia, PA.

Baldwin, E. M., (1981), *Geology of Oregon*, (3rd ed.), Dubuque, Iowa, Kendall/Hunt, 170 p.

Bishop, A. W., (1966), *The Strength of Soils as Engineering Materials.*, Sixth Rankine Lecture, Geotechnique, Vol. 16, No. 2, pp. 91-128.

Brunsdon, D. and Prior, D. B., (1984), *Slope Instability*, New York, John Wiley, 620 p.

Burroughs, E. R. and Thomas, B. R., (1977), *Declining Root Strength in Douglas-Fir After Felling as a Factor in Slope Stability*, USDA Forest Service Research Paper INT-190, 28 p.

Chorly, R. J., Schumm, S. A., and Sugden, D. E., (1984), *Geomorphology*, New York, Methuen & Co., p. 605.

Cunny, R. W., Strohm, W. E., and Hadala, P. E., (1964), *Effect of Large-size Particles on the Shear Strength of a Saturated Clay Gravel*, Technical Report S-78-1, US Army Engineer Waterways Experiment Station, Vicksburg, Miss.

Donaghe, R. T., and Cohen, M. W., (1978), *Strength and Deformation Properties of Rock Fill*, Technical Report S-78-1, US Army Engineer Waterways Experiment Station, Vicksburg, Miss.

Franklin, J. F. and Dyrness, C. T., (1988), *Natural Vegetation of Oregon and Washington*, Oregon State University Press, 452 p.

Graham, J. D., (1986), *Mass Movement Dynamics, Geomorphology and Their Relationship to Geology in the North Fork Siuslaw Drainage Basin Oregon Coast Range*, Oregon State University, Department of Forest Engineering, M.S. Thesis, p. 97.

Hammond, C. J., (1988) Unpublished laboratory data.

Harr, R. D. and Yee, C. S., (1975), *Soil and Hydrologic Factors Affecting the Stability of Natural Slopes in the Oregon Coast Range*, Water Resources Research Institute, WRRI-33, Oregon State University, 204 p.

Holtz, R. D. and Kovacs, W. D., (1981), *An Introduction to Geotechnical Engineering*, New Jersey, Prentice-Hall, Inc., p. 733.

Horn, H. M. and Deere, D. U., (1962), *Frictional Characteristics of*

Minerals, Geotechnique, Vol. 12, No. 4, Dec., pp. 319-335.

Istok, J., (1981), *Clay Mineralogy in Relation To Landscape Instability in the Coast Range of Oregon*, Oregon State University, Department of Forest Science, M.S. Thesis, p. 90.

Ketcheson, G. L., (1977), *Hydrologic Factors and Environmental Impacts of Mass Soil Movements in the Oregon Coast Range*, Oregon State University, Department of Forest Engineering, M.S. Thesis, p. 94.

Kirkpatrick, W. M., (1965) *Effects of Grain Size and Grading on the Shearing Behavior of Granular Materials*, Proceedings, 6th International Conference on Soil Mechanics and Foundation Engineering, Montreal, Vol. 1, pp. 273-277.

Lee, K. L., (1970), *Comparison of Plane Strain Triaxial Tests on Sand*, Journal of the Soil Mechanics and Foundation Division, ASCE, Vol. 96, No. SM3, May, pp. 901-923.

Leslie, D. D., (1963), *Large Scale Triaxial Tests on Gravelly Soils*, Proceedings, Second Pan-American Conference on Soil Mechanics and Foundation Engineering, pp. 181-202.

Lovell, J. P. B., (1969), *Tyee Formation: Undeformed Turbidites and their Lateral Equivalents: Mineralogy and Paleogeography*, Geological Society of America Bulletin, Vol. 80, January, pp. 9-22.

Marachi, N. D., Chen, C. K., and Seed, H. B., (1972), *Evaluation of Properties of Rockfill Materials*, Journal of the Soil Mechanics and Foundation Division, ASCE, Vol. 98, No. SM1, Jan., pp. 95-114.

Pierson, C. T., (1977), *Factors Controlling Debris-Flow Initiation on Forested Hillslopes in the Oregon Coast Range*, University of Washington, Department of Geological Sciences, Ph.D. Dissertation, p. 167.

Rowe, P. W., (1962), *The stress Dilatancy for Static Equilibrium of an Assembly of Particles in Contact*, Proceedings of the Royal Society, Series A, Vol. 269, No. 1339, Oct., pp. 500-527.

Schockley, W. G., (1948), *Correction of Unit Weight and Moisture Content for Soils Containing Gravel Sizes*, Technical Data Sheet No. 2, US Army Engineer Waterways Experiment Station, Vicksburg, Miss.

Schroeder, W. L. and Alto, J. V., (1983), *Soil Properties for Slope Stability Analysis; Oregon and Washington Coastal Mountains*, Forest Science, Vol. 29, No. 4, pp. 823-833.

Vallerga, B. A., Seed, H. B., Monismith, C. L., and Cooper, R. S., (1957), *Effect of Shape, Size, and Surface Roughness of Aggregate Particles on the Strength of Granular Materials*, Special Technical Publication No. 212, ASTM.

Whitman, R. V. and Healy, K. A., (1962), *Shear Strength of Sands During Rapid Loading*, Journal of the Soil Mechanics and Foundations Division, ASCE, Vol. 88, No. SM2, April, pp. 99-132.

Section 4

Overview of Rock Slope Pore Pressure Assumptions and Descriptions of Computer Codes PLANE and WEDGE



Where Tradition
Meets the Future

1889-1989

University of Idaho August 7, 1989

College of Mines and
Earth Resources

Rod Prellwitz
Research Engineer
USDA-FS Forestry Sciences Lab
PO Box 8089
Missoula, MT 59807

RE: Response to issue of "water pressure analysis for
rock slope stability assessments"

University of Idaho
Moscow, Idaho
83843

Office of the Dean
208-885-6195

Department of Metallurgical
and Mining Engineering
208-885-6376

Department of Geography
208-885-6216

Department of Geology and
Geological Engineering
208-885-6192

Idaho Mining and
Mineral Resources
Research Institute
208-885-7989

I have looked over the materials Carol Hammond provided regarding your thinking on the calculation of pore pressures in plane-shear and in 3-D wedge stability analyses. This topic has been a major issue in rock slope stability analysis for many years, and simplifications to facilitate engineering calculations have been the rule. Your conclusions and suggestions as of 6-30-89 seem appropriate for the HP-41 codes you plan to distribute, provided that limitations and assumptions are documented clearly for potential users.

The Hoek and Bray concept of hydrostatic stress (triangular distribution) is valid only if the failure mass acts as a one-piece, solid impermeable block that "floats" on a water-filled discontinuity (-ies, for 3-D wedges). If the block is a typically fractured rock mass, then a phreatic surface approach is more appropriate. I tend to favor the latter approach in many cases.

As far as reworking the 3-D wedge analysis, I have algorithms based on vector geometry that would allow a user to compute the volume of a wetted "pyramid" to provide estimates of pore pressure for partially saturated conditions and of the wetted area of the tension crack as well. These methods could be worked into a computer code that might be HP-41 compatible, but more likely would be for PC's. Analytical comparisons should be made between the hydrostatic case and the phreatic case for various failure geometries, and then checked against professional judgment as derived from field observations. If you want to pursue this, I could have a graduate student look into it as part of next year's coop agreement -- estimated cost: \$1.5K to \$3K.

Please contact me if you need additional information.

Sincerely,



Stanley M. Miller, Associate Professor of Geological Engineering

MODELING SHEAR STRENGTH AT LOW NORMAL STRESSES FOR ENHANCED ROCK SLOPE ENGINEERING

Stanley M. Miller

Department of Geology and Geological Engineering
University of Idaho, Moscow, Idaho 83843

ABSTRACT

The engineering design of slope configurations and slope reinforcement systems for highway rock-slope cuts requires estimation of the shear strength along geologic discontinuities, which will control potential failure paths and mechanisms. Because most highway cuts in rock are rarely higher than about 60 m and because geologic structures generally lack continuous lengths on this scale, the effective normal stresses acting on potential sliding surfaces will be less than about 40 tsm (8200 psf). In fact, for most cases these normal stresses are less than 10 tsm (2050 psf). Natural roughness and non-planarity of rock discontinuities induce a nonlinear shear strength envelope that can have a pronounced curvature at low normal stresses. This nonlinear character of rock shear strength has a major influence on slope stability investigations, especially when slope cuts are not very high and the resulting failure modes are small.

Several methods for modeling the nonlinear shear strength of rock discontinuities and for incorporating it into limit-equilibrium slope stability analyses are discussed. These generally can be divided into two groups: 1) those based on the JRC (joint roughness coefficient) used in conjunction with the basic friction angle and 2) those based on least-squares regression models of laboratory direct-shear results for natural discontinuities used in conjunction with a waviness angle measured in the field. Examples of slope stability computations for plane-shear and for three-dimensional wedge failure modes suggest that the safety factor based on JRC methods is very sensitive to the JRC rating. Also, a power regression model generally is preferable to a linear model for describing the shear strength of rock discontinuities. If not used with care when analyzing small potential failure masses, a linear model can result in calculated safety factor values that are unrealistically high.

INTRODUCTION

The concept of a nonlinear shear failure envelope for rock discontinuities, such as joints, bedding, and foliation, is not a new idea in the field of rock mechanics. Curved relationships between the shear strength and normal stress were noted some 20 years ago by a number of investigators, including Lane and Heck (1964), Patton (1966), and Jaeger (1971). Many rockfill materials also tend to have nonlinear shear failure envelopes (Barton and Kjaernsli, 1981). A curved model for rock discontinuity shear strength can predict values of shear strength that are much different than those predicted by a traditional

linear model consisting of c (cohesion) and ϕ (friction angle), particularly for small values of normal stress on the order of 0.1 tsm to 20 tsm (20 psf to 4100 psf). Such values of applied normal stress are common to those experienced in highway rock-slope cuts, both for dry failure masses less than 10 m high found near the slope crest or in benches and for larger wet (i.e., groundwater pore pressures are present) failure masses that may involve an entire slope.

Most of the public-domain and commercially available computer software for conducting limit-equilibrium rock-slope stability analyses rely on a linear c, ϕ model of shear strength. Estimation of the input values for c and ϕ typically relies on laboratory direct-shear tests of 10 cm to 30 cm blocks that contain discontinuities or on pull/tilt tests conducted on larger blocks of rock in the field. Shear strength models based on laboratory tests are quite sensitive to the range of normal loads specified by the responsible technician or engineer. Ideally, these loads should subject the test specimens to normal stresses similar to those expected in the rock slope under study. If a fairly large range of stresses is anticipated, then the selected model for the shear failure envelope should be appropriate over the entire range.

Because limit-equilibrium stability analyses are used to compute factors of safety that lead to design recommendations, the effective normal stresses on the potential failure planes as computed via these stability analyses are really the key levels of normal stress for which the shear strength must be estimated. Thus, a preliminary stability assessment aimed at the identified failure modes (such as plane-shears, 3-D wedges, and step-paths) in the rock slope can provide valuable guidance to the design engineer for the shear-strength testing program. This means that computer programs used for slope stability evaluations should provide output of calculated values of "intermediate" variables, such as the weight and volume of the potential failure mass, the pore pressure, the effective normal stress acting on the sliding plane(s), and the corresponding shear strength.

THE JRC MODEL OF SHEAR STRENGTH

A curved shear strength model for rock discontinuities initially proposed by Barton (1973) relies on three terms besides the effective normal stress: 1) the joint roughness coefficient (JRC), 2) the joint-wall compressive strength (JCS), and 3) the basic friction angle. The JRC is a descriptive measure of surface roughness over lengths of 0.1 m to 10 m and has unitless values that range from 0 to 20. It can be estimated by visual matching of roughness profiles (ISRM, 1978, p. 345) or by measuring the amplitude of asperities on the joint surface (Barton, 1982). The JCS typically is estimated from the measured rebound of a standard Schmidt-L Hammer as prescribed by ISRM (1978, p. 347-350). The most reliable means to obtain a value for the basic friction angle is to conduct direct-shear tests of saw-cut planar surfaces made in rock specimens collected from the field site. Engineers sometimes will rely on a generic, "textbook" value of, say, 30 degrees and will not bother to conduct direct-shear tests. However, basic friction angles can vary widely among even similar rock types, so at least a minimal direct-shear testing program is advisable (results of recent rock shear testing conducted by the author yielded basic friction angles of 22, 29, and 34 degrees for quartzite, gneiss, and granite, respectively).

Barton (1973) relied upon a wide variety of experimental results to develop a formula for describing a curved shear-strength envelope that predicts discontinuity shear strength as

a function of effective normal stress, JRC, JCS, and basic friction angle. This empirical model, which has been accepted widely in the rock mechanics community, can be expressed in the following form:

$$\tau = \sigma'_n \cdot \tan \left[(JRC) \cdot \log_{10} \left(\frac{JCS}{\sigma'_n} \right) + \phi_b \right] \quad (1)$$

where: τ = shear strength, σ'_n = effective normal stress, JRC = joint roughness coefficient, JCS = joint-wall compressive strength, and ϕ_b = basic friction angle.

Of the input terms, JRC generally has the greatest influence on shear strength at low normal stress values. The basic friction angle also is important, but its potential variability (i.e., range of values) is considerably smaller than that of the measured JRC. Figure 1 illustrates the sensitivity of predicted shear-strength envelopes to the JRC value. Therefore, care must be taken to obtain representative, unbiased JRC data/information.

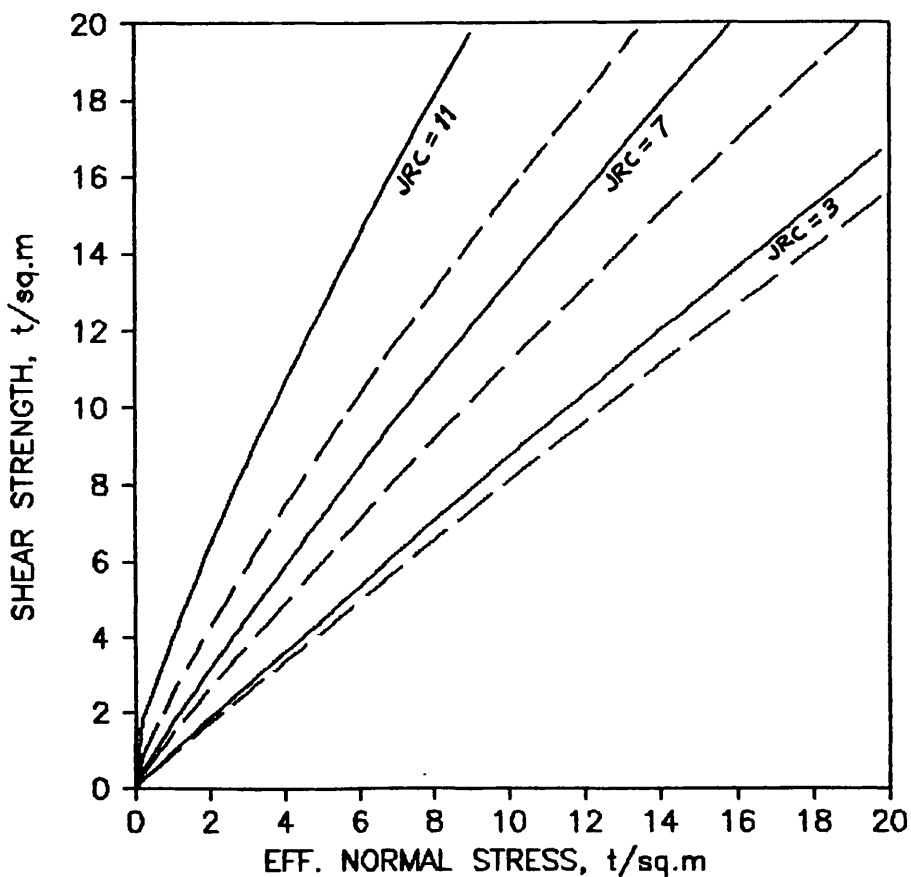


Figure 1. Examples of discontinuity shear-strength envelopes predicted by the JRC model for a given set of granite joints having JCS = 10000 tsm (as derived from a Schmidt-hammer rebound value of 42 and a rock density of 2.66 tcm) and $\phi_b = 32^\circ$ (as derived from direct-shear tests of saw-cut surfaces); the dashed envelopes are for a JCS value of 2000 tsm.

In limit-equilibrium slope stability computations, once the effective normal stress acting on the sliding surface has been calculated, the corresponding shear strength (which contributes to the resisting force) can be obtained directly by using equation (1). Unfortunately, most of the slope-stability computer programs in use today require a c , ϕ linear model of shear strength. A simple modification to such computer codes will allow them to handle the nonlinear JRC shear-strength model via the following expressions that relate c and ϕ to the JRC-predicted shear strength (Kirsten and Moss, 1985, p. 117):

$$c = \frac{\pi}{180} \cdot \sigma'_n \cdot \text{JRC} \cdot \left[1 + \left(\frac{\tau}{\sigma'_n} \right)^2 \right] \cdot \log_{10} e \quad (2)$$

$$\phi = \arctan \left(\frac{\tau}{\sigma'_n} - \frac{c}{\sigma'_n} \right) \quad (3)$$

where: c = cohesion, ϕ = friction angle, and the other terms are as previously defined. Thus, a computer subroutine based on equations (1), (2), and (3) can be incorporated into traditional rock-slope stability programs/codes to produce the necessary c and ϕ values.

SHEAR-STRENGTH MODEL BASED ON PSUEDO-RESIDUAL SHEAR TESTS

Laboratory direct-shear tests of natural rock discontinuities often will provide curved shear-strength envelopes for both the peak strengths and for the psuedo-residual strengths. The term "psuedo-residual" is appropriate in this case, because most investigators doubt whether a true residual strength can be obtained during small-scale shear tests due to dilation that persists even for quite large displacements. The data obtained from such shear tests practically always can be fitted by a power model better than by a linear model when least-squares regression is applied (see the example given in Figure 2). A general power-curve model for the shear-strength envelope is given as: $\tau = a(\sigma_n)^b + c$ (Miller and Borgman, 1984), which provides adequate flexibility to handle cohesionless behavior ($c = 0$) and a linear failure envelope (for $b = 1$, then $a = \tan \phi$ and $c = \text{cohesion}$). Knowledge of scale effects and of pertinent results of back-analyses of rock-slope failures makes it prudent to use the psuedo-residual shear data rather than the peak shear data from small-scale laboratory direct-shear tests.

The power-curve failure envelope obtained from such laboratory shear tests of natural joints is an appropriate model of shear strength on the testing scale (typically 10 to 30 cm) and will incorporate the effects of asperity roughness and joint-wall compressive strength. The effects of undulations/waviness observed over distances of about 1 to 10 m will not be taken into account by the power-curve model. One way to remedy this shortcoming when conducting a limit-equilibrium slope stability analysis is to incorporate this larger-scale waviness into the calculated resisting force (i.e., as an additive term to the shear strength in the numerator of the safety factor ratio: $FS = \text{Resisting Force} / \text{Driving Force}$). This additional resistance should depend on the severity of the waviness and on the effective normal stress acting on the overall sliding surface.

One approach to quantifying this waviness is to measure the average and minimum dips along the rock discontinuity(ies) of interest as part of the field data collection exercise

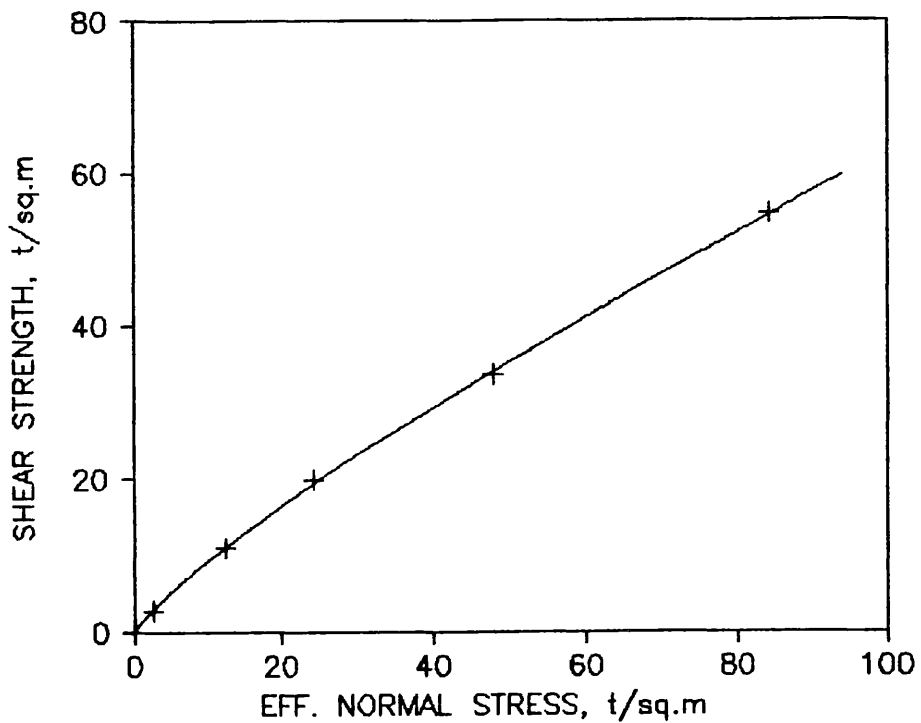


Figure 2. Example of a power-curve failure envelope fitted to direct-shear test results for a natural joint in granite; $\tau = 0.017 + 1.340 \sigma_n^{0.836}$ (in tsm units).

(Call and others, 1976). An estimate of the waviness then is given by: waviness = [average dip] - [minimum dip], and is expressed in units of degrees. The average dip of the sliding surface is used in slope stability analyses to calculate the volume of the potential failure mass (which leads to subsequent determinations of the weight and effective normal stress) and to resolve forces that act on the failure mass. If the discontinuous rock mass were to slide along the identified failure surface, then individual rock blocks with sizes defined by the joint spacings would have to slide along portions of the failure surface having a dip equal to the average dip minus the waviness. Thus, the greater the waviness, the greater the resistance to sliding that is experienced by the potential failure mass.

Based on these considerations, some engineers (among the first was R.D. Call, now with Call & Nicholas, Inc., Tucson, Arizona) rely on a simple means to incorporate waviness into slope stability calculations, as illustrated in Figure 3. The contribution of discontinuity waviness to the resisting force is equal to the effective normal force times the tangent of the waviness angle. This waviness term adds a "large-scale" component to the shearing resistance along a potential failure surface, and when used in conjunction with a curved shear-failure envelope obtained from direct-shear tests of natural discontinuities (which consider small-scale roughness and joint-wall strength), a reasonable mechanism for

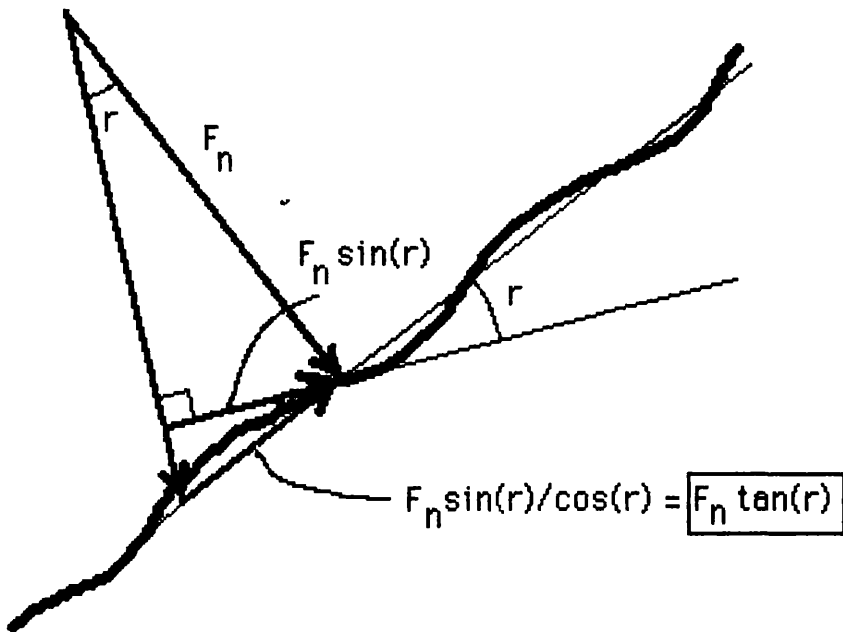


Figure 3. Contribution of the waviness to the resisting force in a rock-slope stability analysis.

incorporating discontinuity shear strength into rock-slope design is possible. One advantage of this method is that waviness is much easier and faster to measure in the field than are the types of data associated with JRC.

When using this model of discontinuity shear-strength, the design engineer should beware of applying a linear c, ϕ failure envelope to the pseudo-residual shear data provided by a laboratory testing program. A linear model may seem appropriate for a large range of normal stresses (and may suffice for values exceeding 30 tsm for most rock types), but such is not the case for many natural discontinuity surfaces subjected to low values of normal stress. As an example, the five shear data presented in Figure 2 can be fitted by a linear model to yield the following expression: $\tau = 2.978 + 0.624\sigma_n$ (envelope 3 in Figure 4), which provides a considerable overestimation of shear strength at normal stresses less than 7 tsm. A more appropriate linear model for slope stability investigations would be based on the three data points having normal stresses less than 30 tsm; this gives $\tau = .938 + 0.783\sigma_n$ (envelope 2 in Figure 4).

EXAMPLES OF SHEAR-STRENGTH INFLUENCE ON CALCULATED SAFETY FACTOR

To illustrate the influence that the selected shear-strength model exerts on the slope design process, safety-factors have been computed for realistic plane-shear and wedge failure modes using the shear strength of granite joints as presented in Figures 1 and 2. The

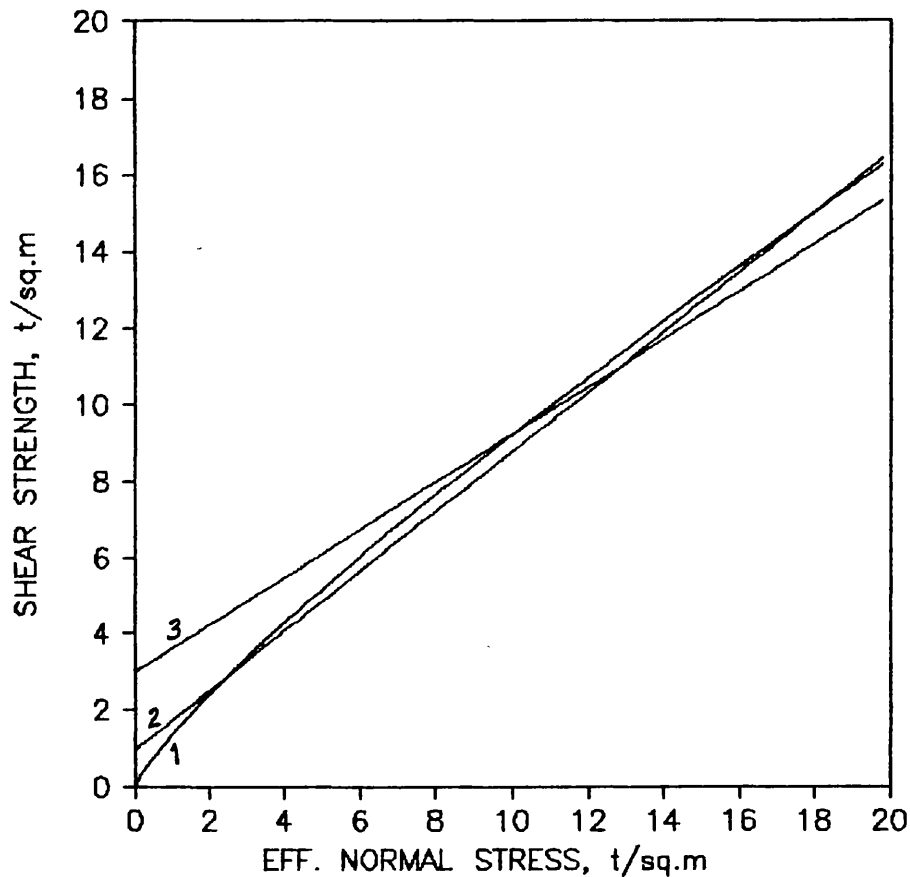


Figure 4. Comparisons of shear-strength envelopes (fitted to data given in Fig. 2) at low values of normal stress; curve 1 is general power model, curve 2 is linear model fitted to three smallest data, curve 3 is linear model fitted to all five data.

results are based on dry conditions and slope cuts of 0.5:1 (i.e., 64°) made in a natural hillslope with a gradient of 4:1 (i.e., a dip of 14°). The failure height in all cases is defined as the vertical distance from the slope crest to the daylight point of the sliding surface in the slope-cut face. Tables 1 and 2 summarize the results of the safety factor calculations. Case B for the plane-shear modes is plotted in Figure 5, and Case A for the 3-D wedge modes is plotted in Figure 6.

These example calculations illustrate the importance of adequately modeling discontinuity shear strength during a rock-slope design project. For the low normal stresses typical to such investigations a simple reliance on traditional c , ϕ shear-strength models can produce unrealistically high safety factor values in a limit-equilibrium slope stability analysis. The problem is even more apparent when groundwater-induced pore pressures are present in the rock slope, because they will reduce further the effective normal stress acting on potential sliding surfaces.

Table 1. Safety factor values computed for example plane-shear failure modes with potential sliding planes dipping at 35° and 50° .

	Failure Height (m)	Safety Factor Values							
		1. Power	2. Linear	3. Linear	4. JRC-Model				
Case A: JRC = 3 Wav. = 3°	30	1.27	0.87	1.27	0.82	1.21	0.93	1.21	0.74
	15	1.42	0.97	1.35	0.93	1.45	1.29	1.25	0.76
	6	1.64	1.12	1.57	1.27	2.17	2.38	1.30	0.80
Case B: JRC = 7 Wav. = 11°	3	1.83	1.26	1.95	1.84	3.38	4.19	1.34	0.82
	30	1.47	0.98	1.47	0.93	1.41	1.05	1.78	1.16
	15	1.62	1.09	1.55	1.05	1.65	1.41	1.92	1.26
Case C: JRC = 11 Wav. = 20°	6	1.84	1.24	1.78	1.39	2.38	2.50	2.13	1.40
	3	2.04	1.38	2.16	1.96	3.58	4.31	2.31	1.52
	30	1.72	1.13	1.71	1.08	1.65	1.19	2.72	1.96
	15	1.86	1.23	1.79	1.19	1.89	1.55	3.15	2.32
	6	2.08	1.38	2.02	1.53	2.62	2.64	3.92	3.02
	3	2.28	1.52	2.40	2.10	3.82	4.45	4.76	3.87

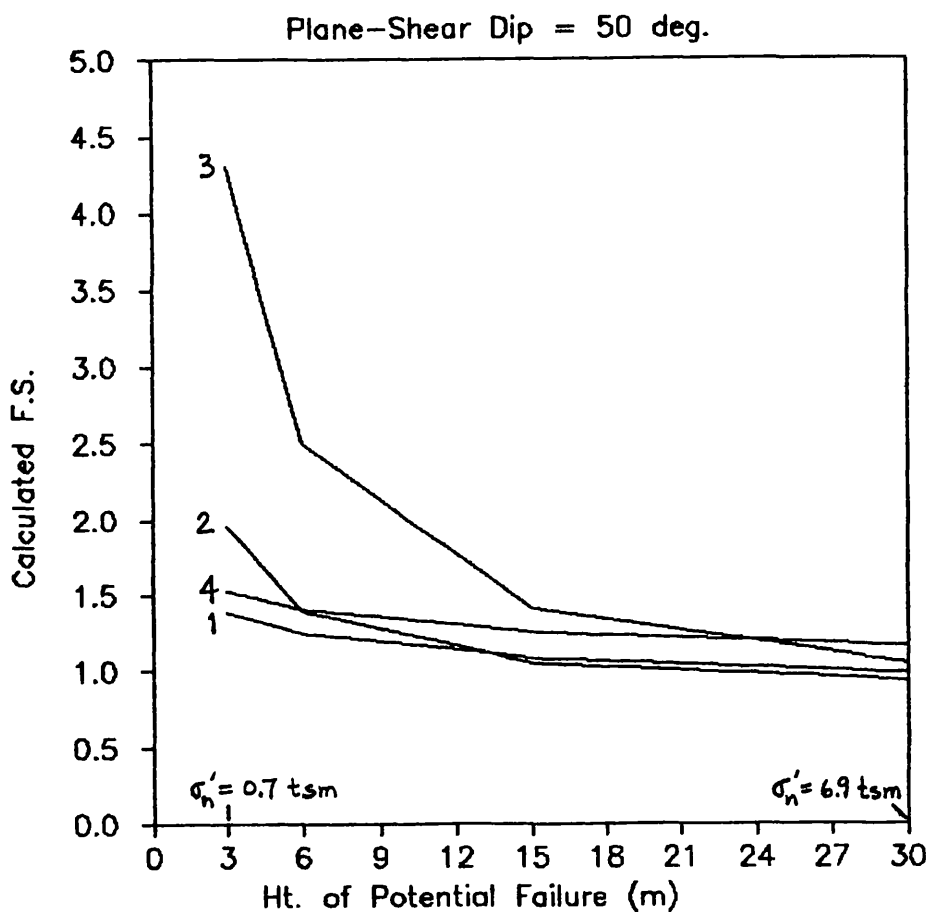


Figure 5. Factor of safety values for 50° plane-shear Case B.

Table 2. Safety factor values computed for example 3-D wedge failure modes for a slope cut with dip dir. = 300° , dip = 64° ; left plane dip dir. = 255° , dip = 57° ; right plane dip dir. = 330° , dip = 48° . The bearing and plunge of the wedge intersection are 304° and 45° , respectively.

	Failure Height (m)	Safety Factor Values			
		1. Power	2. Linear2	3. Linear3	4. JRC-Model
Case A: JRC = 3 Wav. = 3°	30	1.164	1.097	1.257	0.995
	15	1.299	1.253	1.753	1.027
	6	1.508	1.721	3.240	1.071
	3	1.695	2.501	5.718	1.105
Case B: JRC = 7 Wav. = 11°	30	1.321	1.253	1.414	1.558
	15	1.456	1.409	1.910	1.685
	6	1.665	1.878	3.396	1.877
	3	1.851	2.658	5.874	2.044
Case C: JRC = 11 Wav. = 20°	30	1.497	1.429	1.590	2.632
	15	1.632	1.585	2.085	3.119
	6	1.840	2.053	3.572	4.070
	3	2.027	2.834	6.050	5.231

Wedge Intsctn. Brg., Plng. = 304° , 45°

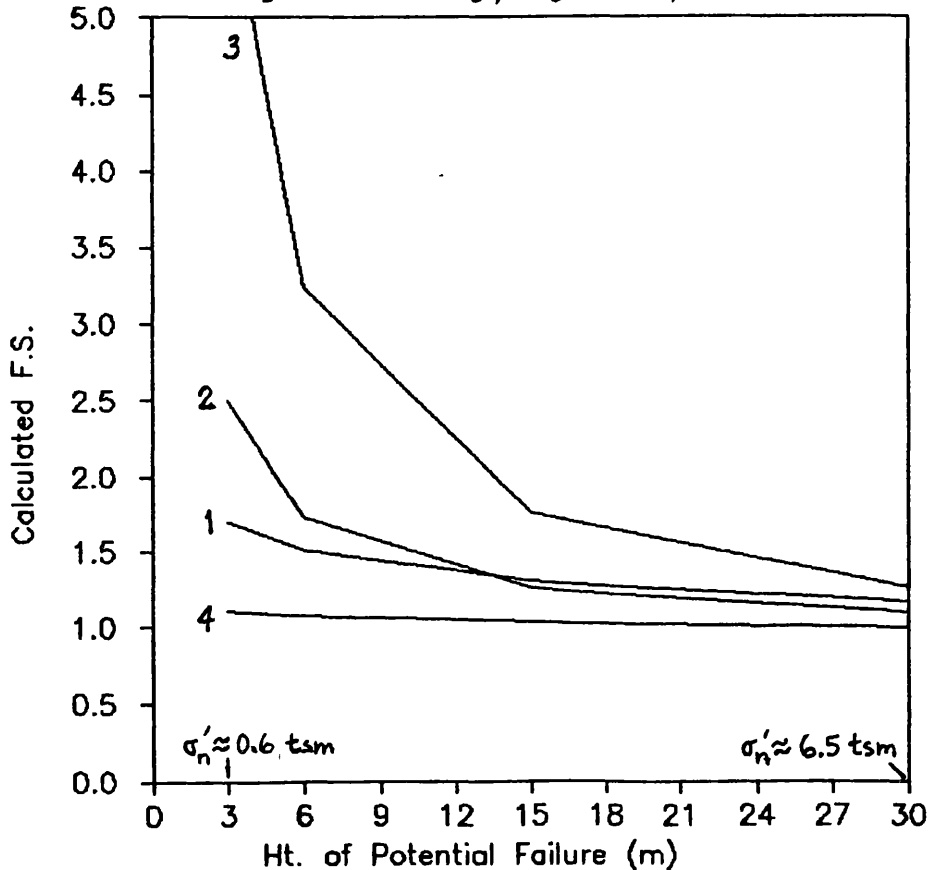


Figure 6. Factor of safety values for 3-D wedge Case A.

CONCLUSIONS

When limit-equilibrium slope stability analyses are used in the design of highway rock-slope configurations or support systems (such as rock bolts, cable tendons, tie-back walls, etc.), the geotechnical engineer must exercise care in estimating the shear strength along rock discontinuities. It is especially critical to model the shear-strength envelope at very low normal stresses (less than 20 tsm), because potential sliding surfaces in road cuts will be subjected to such stresses. The nonlinear JRC Model of shear strength generally is preferred to a traditional c, ϕ linear model, but it predicts shear strengths that are highly sensitive to the estimated value of JRC (joint roughness coefficient). This sensitivity may lead to overly conservative slope designs if the JRC is underestimated and to undesirable nonconservative designs if the JRC is overestimated.

An alternate shear-strength model is based on psuedo-residual shear strengths obtained from laboratory direct-shear tests of natural discontinuities and a waviness angle measured in the field. A general power-curve failure envelope can be fitted to the laboratory shear data and almost always provides a better estimator of shear strength at low normal stresses than does a traditional linear model. The larger-scale waviness effects are added in to the resisting force during the safety-factor calculations in the stability analysis. Experience with this design approach and the results of example calculations of safety factors indicate that a linear model can be appropriate over small ranges of normal stress, but that a power-curve model will provide more reasonable estimates of shear strength in the general case.

A preliminary slope stability assessment of potential failure modes (such as plane-shears, 3-D wedges, and step-paths) can provide valuable guidance to the design engineer for the shear-strength evaluation program. This assessment can be enhanced significantly by computer programs that provide output of calculated values of "intermediate" variables, such as the weight and volume of the potential failure mass, the pore pressure, the effective normal stress acting on the sliding plane(s), and the corresponding shear strength. In particular, knowledge of the pertinent levels of normal stress anticipated in the rock cut is essential to a valid estimation of discontinuity shear strength, and thus, to a prudent rock slope design.

REFERENCES

Barton, N., 1973, Review of a New Shear Strength Criterion for Rock Joints; *Engineering Geology*, v. 7, p. 287-332.

Barton, N., 1982, Shear Strength Investigations for Surface Mining; in Stability in Surface Mining, Vol. 3, C.O. Brawner, ed., SME-AIME, New York, p. 179.

Barton, N. and Kjaernsli, B., 1981, Shear Strength of Rockfill; *Jour. Geotech. Engr. Div., ASCE*, v. 107, p. 873-891.

Call, R.D., Savel, J.P., and Nicholas, D.E., 1976, Estimation of Joint Set Characteristics from Surface Mapping Data; in Proc. of 17th U.S. Symp. on Rock Mech., Salt Lake City, UT, p. 2B2.1 - 2B2.9.

ISRM (International Society for Rock Mechanics), 1978, Suggested Methods for the Quantitative Description of Discontinuities in Rock Masses; *Intl. Jour. Rock Mech. Min. Sci. & Geomech. Abstr.*, v. 15, p. 319-368.

Jaeger, J.C., 1971, Friction of Rocks and Stability of Rock Slopes; *Geotechnique*, v. 21, no. 2, p. 97-134.

Kirsten, H.A.D. and Moss, A.S.E., 1985, Probability Applied to Slope Design - Case Histories; in Rock Masses: Modeling of Underground Openings/ Probability of Slope Failure/ Fracture of Intact Rock, C.H. Dowding, ed., ASCE, New York, p. 106-121.

Lane, K.S. and Heck, W.J., 1964, Triaxial Testing for Strength of Rock Joints; in Proc. of 6th Rock Mech. Symp., Rolla, MO, p. 98-108.

Miller, S.M. and Borgman, L.E., 1984, Probabilistic Characterization of Shear Strength Using Results of Direct Shear Tests; *Geotechnique*, v. 34, no. 2, p. 273-276.

Patton, F.D., 1966, Multiple Modes of Shear Failure in Rock and Related Materials; unpubl. Ph.D. thesis, Univ. of Illinois, 282 p.

Overview of Rock Slope Stability Codes: PLANE and WEDGE

New slope stability computer programs have been developed for the general analysis of plane-shear and 3-D wedge failure modes in a rock slope. The source codes are written in FORTRAN and can be readily compiled on any microcomputer equipped with a FORTRAN compiler (either PC-compatible or Macintosh). Input and output mechanisms are still a bit simplistic, but can be enhanced easily if deemed appropriate by USFS research personnel.

Both programs allow the user to select one of two shear strength protocols: 1) Barton's JRC/JCS method, or 2) a general nonlinear (power curve) model of shear strength. In both cases, a field-scale waviness factor is included (avg. dip minus minimum dip) to account for the larger-scale undulations that influence the shear strength in field situations. In addition, several methods for dealing with groundwater pore pressures can be selected by the user, including total-unit-weight / boundary-pressures and buoyant-unit-weight / seepage forces. This flexibility dictates that engineers using these codes be well-versed in pore-pressure modeling and have a good knowledge of specific field conditions (i.e., a highly fracture rock mass vs. a massive one with well-defined discontinuity patterns). Also, artificial slope support via rock bolt/cable tension can be incorporated into both the Plane and Wedge analyses.

SI units are used consistently throughout the programs with lengths expressed in meters, forces expressed in metric tonnes (i.e., 1000 kg_f), stresses expressed in tonne/sq.m (tsm), and unit weights expressed in tonne/cu.m (tcm). Thus, the unit weight of water is 1.0 tcm (equivalent to 62.4 pcf). Also, 1 tsm is equal to 1.42 psi, or 204.8 psf.

PLANE -- A 2-D analysis that includes vertical tension cracks

Important switches: TYP -- Sets a flag that controls the type of shear strength model

(J = JRC/JCS model; G = General power-curve model)

WTR -- Sets a flag that controls the pore-pressure method

(H = Hydrostatic boundary pressure; S = Seepage force)

Example input data files (see variable list on following pages):

64 14 37 2 15 2.66 0 10	A, AU, B, R, H, DEN, BTEN, BPL
G	TYP
.895 .975 .1	AT, BT, CT (a, b, c for general, power-curve model)
S	WTR
5 2	DW, DWC
<hr/>	
64 14 37 2 15 2.66 0 10	A, AU, B, R, H, DEN, BTEN, BPL
J	TYP
3 9000 32	AT, BT, CT (JRC, JCS, base fric.angle for JRC model)
H	WTR
5 2	DW, DWC

When H is used to select the hydrostatic pressure option (i.e., WTR = H), two methods are used throughout the plane shear computations:

1) The boundary pressure distribution is assumed to originate from water standing in the vertical tension crack and take on the form of a triangular distribution (as proposed by Hoek & Bray, Rock Slope Engineering). Thus, if there is no water in the tension crack, there is no pore pressure acting on the failure plane.

2) The boundary pressure distribution is assumed to take on the shape of a "mirror-image" of that portion of the failure mass below the piezometric surface (i.e., level to which water will rise in a standpipe piezometer). This surface is defined by the user via the variable DW, and is assumed parallel to the upper surface of the ground slope (i.e., natural ground slope prior to making the slope cut).

Computed safety factor values for both situations are listed in the output file when PLANE is executed with WTR = H.

When S is used to select the seepage force option (i.e., WTR = S), the portion of the failure mass below the piezometric surface is assumed to be saturated in the sense that all discontinuities in the rock mass are filled with water and interconnected enough to allow water flow. Again, this surface is defined by DW and is assumed parallel to the natural ground slope. Thus, the gradient and the saturated volume are used to compute the seepage force, and the buoyant unit weight is used in the calculation of a weight of the failure mass.

WEDGE -- A 3-D analysis based on dir. cosines and vector calculations

Important switches: TYP -- Sets a flag that controls the type of shear strength model

(J = JRC/JCS model; G = General power-curve model)

WTR -- Sets a flag that controls the pore-pressure method

(H = Hydrostatic boundary pressure; S = Seepage force)

Example input data files (see variable list on following pages):

300 64 315 14 255 57 330 48 2.66	FDDR, FDIP, UDDR, UDIP, LDDR, LDIP, RDDR, RDIP, DEN
5. 130. 10.	BTEN, BBG, BPL
G	TYP (sets flag for <u>General</u> , power-curve model)
2 1.055 .995 .1 2 1.100 .990 .2	WAVL, ATL, BTL, CTL, WAVR, ATR, BTR, CTR*
S	WTR
15 5	H, DW

300 64 315 14 255 57 330 48 2.66	FDDR, FDIP, UDDR, UDIP, LDDR, LDIP, RDDR, RDIP, DEN
5. 130. 10.	BTEN, BBG, BPL
J	TYP (sets flag for <u>JRC</u> model)
2 4 9000 32 2 5 10000 32	WAVL, ATL, BTL, CTL, WAVR, ATR, BTR, CTR**
H	WTR
15 5	H, DW

* Waviness, a, b, c for general, power-curve model for left and right sides.

** Waviness, JRC, JCS, base fric.angle for left and right sides.

No tension crack is used in these wedge stability analyses. The piezometric "mirror-image" approach is used when WTR = H, whereas seepage force calculations result when WTR = S. As with the PLANE code, the piezometric surface is assumed parallel to the natural ground surface.

PLANE. FOR

```

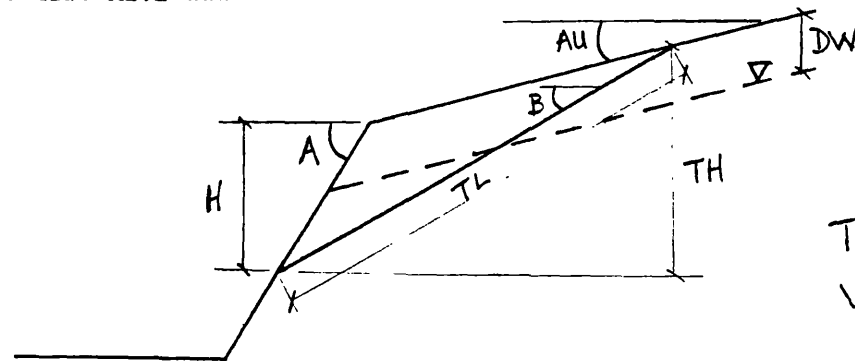
C
C*** FORTRAN77 PROGRAM TO CALCULATE FACTOR OF SAFETY FOR
C*** PLANE-SHEAR FAILURE MODE IN A ROCK SLOPE.
C Code by S.M. Miller, Geological Engrg., Univ. of Idaho, March, 1987.
C Modified November, 1989. Modified again September, 1990.
C This version includes a tension crack (vertical) and bolt loading.
C

      PROGRAM PLANEFS

C
C***** VARIABLE LIST
C

C      H = HT. FROM FAILURE TOE TO CUT CREST          A = CUT FACE ANGLE
C      B = AVG. DIP OF DISCONTINUITY                   AU = UPSLOPE ANGLE
C      R = AVG. WAVINESS OF DISCONTINUITY              TL = FAILURE LENGTH
C      TAU = SHEAR STRENGTH ALONG DISCONTINUITY       TH = FAILURE HEIGHT
C      DW = DEPTH TO WATER FROM GR. SURFACE          DEN = ROCK DENSITY
C      AREA = 2-D AREA OF POTEN. FAILURE MASS         U = UPLIFT WATER FORCE
C      ASAT = 2-D WATER EFF. AREA OF FAIL. MASS        HTCK = HT. OF T.CRK.
C      W = EFF. WEIGHT OF POTEN. FAILURE MASS          HWTK = HT. WATER IN T.CRK.
C      TDIS = HORZ.DIST. FROM CUT CREST TO T.CRK.     BPL = PLUNGE OF BOLT
C      TLT = FAIL.LENGTH FOR T.CRK. CASE              BTEN = EFF.TENSION ON BOLT
C      THT = FAIL.HEIGHT FOR T.CRK. CASE              SEEP = SEEPAGE FORCE
C      HBTK = HT.FROM FAIL.TOE TO BOTTOM OF T.CRK.    V = T-CRK WATER FORCE
C      DWC = DEPTH TO T.CRACK WATER FROM G.S.         RF = RESISTING FORCE
C      SB = WET (SATUR.) SLIDING LENGTH               DF = DRIVING FORCE
C      SBT = SB FOR TENSION CRACK CASE               SF = SAFETY FACTOR
C      UM = WATER UPLIFT FOR MOD./MIRROR CASE        SFM = SF FOR MOD./MIRROR CASE
C***** REAL RAD,H,A,AR,AU,AUR,B,R,BR,RR,TL,TH,AT,BT,CT,TAU,BTEN,BPL,DEN
REAL RAD,H,A,AR,AU,AUR,B,R,BR,RR,TL,TH,AT,BT,CT,TAU,BTEN,BPL,DEN
REAL TLT,THT,TDIS,TDMIN,TDMAX,HBTK,HTCK,HWTK,TANRR,TANUR,COSBU
REAL TANAR,TANBR,SINAR,SINBR,COSAR,COSBR,CO$UR,AREAM,ASATM,HWEX
REAL DW,DWC,T1,AREA,W,ENS,DTF,SA,SB,ASAT,HVC,U,V,DF,RF,SF
REAL WM,UM,SFM
CHARACTER*1 MOI,TYP,SWI,WTR
CHARACTER*18 IFILE,OFILE
COMMON AT,BT,CT,RAD
COMMON COSBR,SINBR,COSBU,SINBU,COSBB,SINBB
C
RAD=45./ATAN(1.)
C
      WRITE(*,100)
100 FORMAT(//, ' *** Stability Analysis for Plane-Shear Mode ***')
C
*** TINPUT NECESSARY DATA ***

```



TYPICAL R (WAVINESS)
VALUES :

0° (planar) - 10° (und)

WEDGE FOR

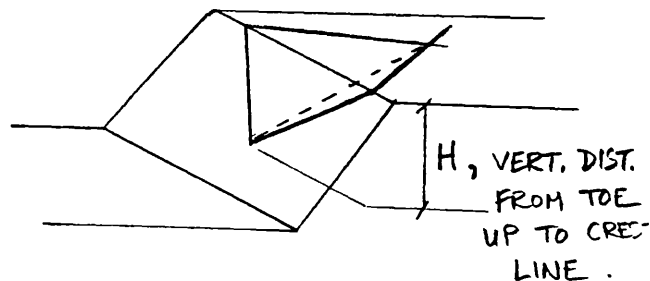
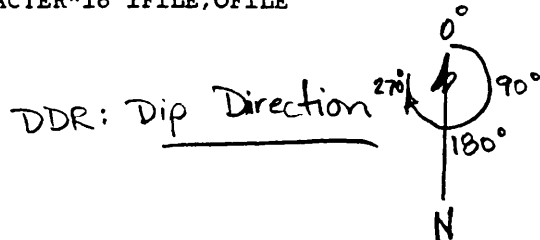
C
 C*** FORTRAN77 PROGRAM FOR SAFETY FACTOR CALC. OF 3-D WEDGE ***
 C Code by S.M. Miller, Geological Engrg., Univ. of Idaho, April, 1987.
 C Modified for more general wedge geometries in March, 1988.
 C Modified to include discontinuity waviness in July, 1988; and to
 C include seepage calcs. & bolt tension as options, September, 1990.
 C

PROGRAM WEGFS

C
 C*****
 C VARIABLE LIST
 C

C FDDR = SLOPE CUT (FACE) DIP DIR. FDIP = SLOPE CUT (FACE) DIP
 C UDDR = UPPER SLOPE DIP DIR. UDIP = UPPER SLOPE DIP
 C LDDR = DIP DIR. OF LEFT WEG. PLANE LDIP = DIP OF LEFT WEG. PLANE
 C RDDR = DIP DIR. OF RIGHT WEG. PLANE RDIP = DIP OF RIGHT WEG. PLANE
 C*NOTE: LEFT AND RIGHT PLANES DEFINED BY VIEWING UP THE WEG. INTERSECTION
 C WAVL = WAVINESS ANG. OF LEFT PLANE WAVR = WAVINESS ANG. OF RIGHT PLANE
 C H = TOE-TO-CUTCREST WEDGE HT. (m) DW = DEPTH TO WATER FROM GR. SURFACE (m)
 C DEN = ROCK DENSITY (t/cm) BTEN = ROCK BOLT TENSION (t)
 C BBG = ROCK BOLT BEARING (0-360) BPL = ROCK BOLT PLUNGE (0-90)
 C AF,BF,CF = DIR.COS.NORM.TO SLOPE CUT AU,BU,CU = DIR.COS.NORM.TO UPPER SLOPE
 C AL,BL,CL = DIR.COS.NORM.TO LEFT PL. AR,BR,CR = DIR.COS.NORM.TO RIGHT PL.
 C AI,BI,CI = DIR.COS.OF WEG. INTERSECT. ABLT,BBLT,CBLT = DIR.COS. OF BOLT
 C BRGI = BEARING OF WEG. INTERSECTION PLNI = PLUNGE OF WEG. INTERSECTION
 C WIL = LENGTH OF WEG. INTERSECT. (m) WILW = LENGTH OF WET WEG. INTERSECT. (m)
 C VOL = VOLUME OF WEDGE (cu.m) VOLW = "SATUR." VOL. OF WEDGE (cu.m)
 C VOLD = DRY VOL. OF WEDGE (cu.m) GRAD = GRADIENT FOR SEEPAGE CALCS.
 C ALFT = AREA OF LEFT PLANE (sq.m) ARHT = AREA OF RIGHT PLANE (sq.m)
 C ALTW = WET AREA OF LEFT PL. (sq.m) ARTW = WET AREA OF RIGHT PL. (sq.m)
 C SEEP = TOTAL SEEPAGE FORCE ACTING ON WEDGE (t) SEEPR = SEEP. FORCE NORM.TO RIGHT PL.
 C SEEPL = SEEP. FORCE NORM.TO LEFT PL. SNR = NORM. STRESS ON RIGHT PL. (t)
 C SNL = NORM. STRESS ON LEFT PL. (t) SF = SAFETY FACTOR
 C WT = WEIGHT OF WEDGE (t) RF = RESISTING FORCE ON WEG. (t)
 C DF = DRIVING FORCE ON WEG. (t)

C
 REAL RAD,FDDR,FDIP,UDDR,UDIP,LDDR,LDIP,RDDR,RDIP,DEN,H,DW
 REAL AF,BF,CF,AU,BU,CU,AL,BL,CL,AR,BR,CR,AI,BI,CI,ANGL,ANGR
 REAL HW,BRGI,PLNI,SINA,COIF,FLW,WIL,ALFT,ARHT,WILW,ALTW,ARTW
 REAL VOL,VOLW,WT,FWAT,AIBR,AIBL,ALBR,FNL,FNR,SNL,SNR,DF,RF,SF
 REAL WAVL,WAVER,ATL,BTL,CTL,ATR,BTR,CTR,TAUL,TAUR,AV,BV,CV
 REAL VIDDR,AVI,BVI,CVI,DIPLW,DIPRW,ALW,BLW,CLW,ARW,BRW,CRW
 REAL SILW,SIRW,CLWI,CRWI,ALWAV,ARWAV,WAVLE,WAVRE
 REAL PLNW,ANGUF,ANGVF,SIUF,SIVF,DCLEN,DWDY,UPROJ,DCUP
 REAL BTEN,BBG,BPL,BPDDR,BPDIP,ABLT,BBLT,CBLT,BICK,T
 REAL VOLD,GRAD,SEEP,SPDDR,SPDIP,SEEPL,SEEPR
 CHARACTER*1 MOI,OUT,TYP,WTR,SWI
 CHARACTER*18 IFILE,OFILE



TYPICAL WAVINESS VALUES: 0° (planar) - 10° (undulating)

Section 5

Geostatistics Workshop Notes

Geostatistics Notes

USDA-FS Workshop

Eugene, Oregon

March, 1990

Let's begin with a few questions:

Question: What is the difference between statistics and probability? Or is there a difference?

Yes, there is a difference!

Statistics is the science that deals with the analysis of data and the processes of making inferences and decisions about the populations or systems from which the data were obtained. Thus, data are required for a statistical analysis.

Probability theory is an internally consistent branch of mathematical logic based on a systematic statement and formulation of principles that allow for meaningful descriptions of random variations in populations or systems. Although data may be helpful, they are not required for a probabilistic analysis.

Question: Given a set of data collected from a spatial population (e.g., in a study area we might be interested in thickness of soil cover over bedrock or t.d.s. in ground water), how can I best predict what the data value would be at an unsampled location?

What you are after is a "spatial estimate", which can be obtained in several different ways, the most common being:

1) simple averaging of regional or local values (i.e., if you had no knowledge about the spatial patterns of the data, the local mean would be a reasonable guess for the unknown value)

2) multiple regression (least-squares, best-fit), or trend surface modeling to describe a "best" surface through the data values; thus, the estimated data value would lie on this surface.

3) interpolation via some defined algorithm that uses data in the spatial neighborhood (proximity) of the location where the estimate is to be made.

Question: What is geostatistics?

It is not the application of statistics to geological problems! Geostatistics is a branch of applied statistics that focuses on the characterization of spatial dependence in attributes and the use of that dependence to predict values of the attributes at unsampled locations. Spatial dependence implies that two data values from nearby locations will be more alike than two values from distant locations.

Question: How many data values are needed for a geostatistical analysis that leads to spatial estimates?

Oftentimes, it is not a question of, "how many?", but rather a question of, "where are they?" Prudently located sampling sites can help reduce data requirements, but a set of about 25-30 observations (300-435 pairs) is a realistic minimum in most cases.

Question: Can geostatistical tools provide any advantages over other spatial interpolation procedures?

Yes, but only if there is an identifiable spatial dependence in the data set. This indicates that adequate characterization of the spatial dependence is essential for the implementation of geostatistical estimation procedures.

An excellent new introductory text on geostatistics:

Isaaks, E.H. and Srivastava, R.M., 1989, An Introduction to Applied Geostatistics; Oxford Univ. Press, New York, 561 p.

Random Variables and Probability Distributions

A "random variable" is a variable (e.g., a physical property, attribute, or characteristic) that takes on different values according to the outcomes of repeated experiments or sampling events.

These values cannot be predicted with any certainty, and consequently each value or range of values has an associated probability of occurrence. For this reason, random variables often are called stochastic variables to indicate the stochastic, or probabilistic, nature of their values.

The term "random" here does not imply that the variable itself is random or has randomly distributed values, but rather that the values occur in a probabilistic manner.

A probability distribution is a function (discrete or continuous) that defines probabilities of occurrence for values of a random variable. Two common ways to represent such a distribution are:

1) Cumulative distribution function (cdf):

$$F(x) = \text{Probability}(X \text{ takes on a value } \leq x) = P(X \leq x)$$

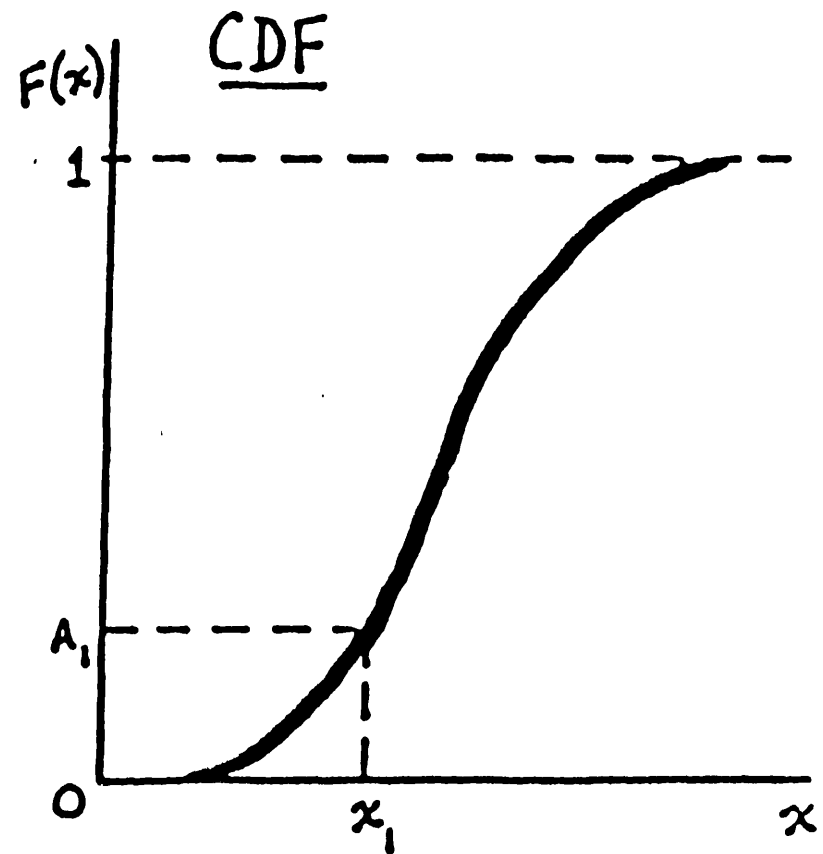
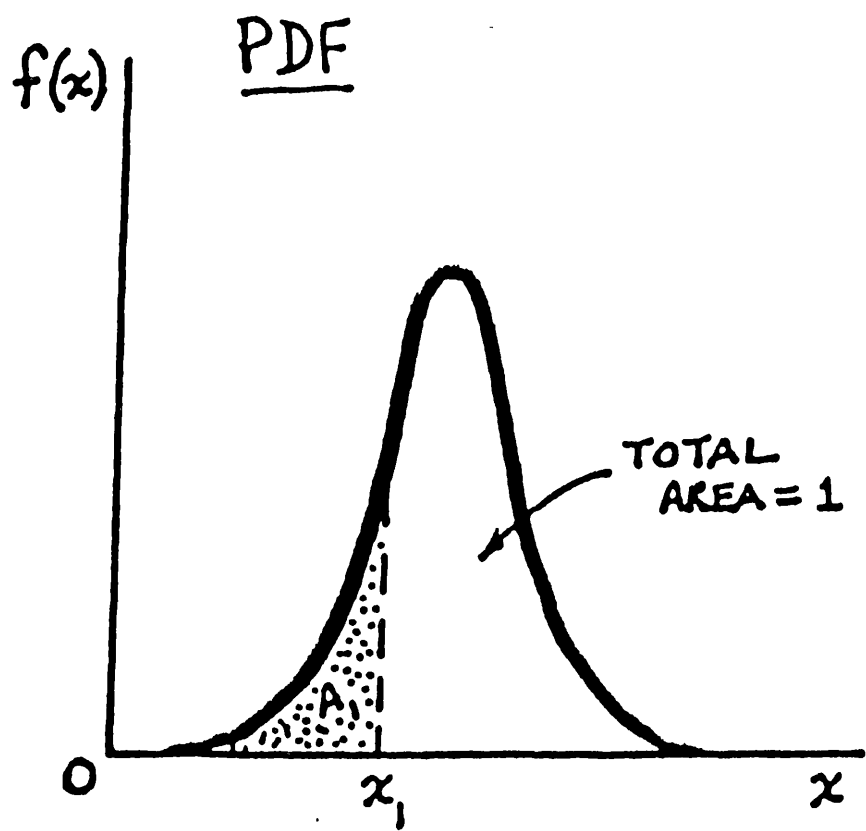
Properties of the cdf: a) has values between 0 and 1 inclusive, b) is a non-negative, non-decreasing function, and c) for two values $a < b$ of a random variable, $P(a < X \leq b) = F(b) - F(a)$

2) The probability density function (pdf) is given by:

$$f(x) = \frac{d[F(x)]}{dx}$$

Properties of the pdf: a) is a non-negative function such that:

$$\int_{-\infty}^{\infty} f(x) dx = 1, \text{ and } b) P(a < X \leq b) = \int_a^b f(x) dx$$

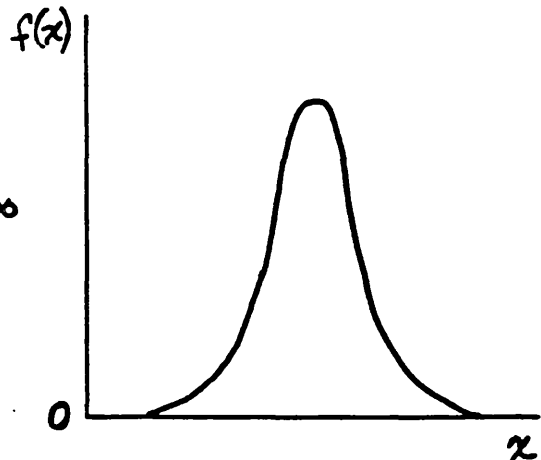


NORMAL (GAUSSIAN) DISTRIBUTION

$$f(x) = \frac{e^{-\frac{1}{2}(\frac{x-\mu}{\sigma})^2}}{\sigma\sqrt{2\pi}}, \text{ for } -\infty < x < \infty$$

$$m(X) = \mu$$

$$v(X) = \sigma^2$$



LOGNORMAL DISTRIBUTION
(for a RV X such that
 $\ln X$ has a normal distr.)

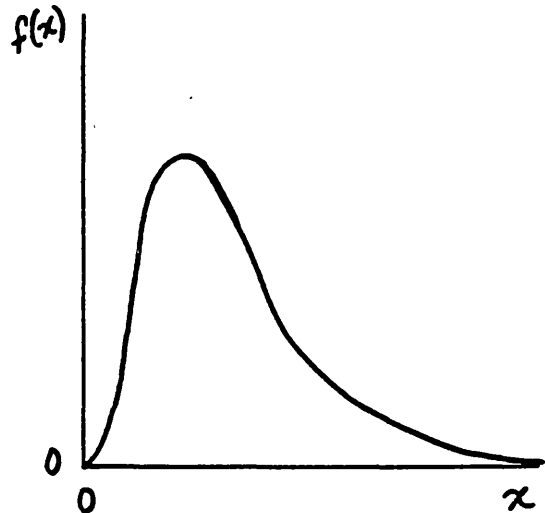
$$f(x) = \begin{cases} \frac{e^{-\frac{1}{2}(\frac{\ln x - \mu}{\sigma})^2}}{x\sigma\sqrt{2\pi}}, & \text{if } x > 0 \\ 0, & \text{otherwise} \end{cases}$$

$$m(X) = e^{\mu + \frac{\sigma^2}{2}}$$

$$v(X) = [m(X)]^2(e^{\sigma^2} - 1)$$

$$\text{Also, } \mu = \ln[m(X)] - \frac{\sigma^2}{2}$$

$$\sigma^2 = \ln \left\{ \frac{v(X)}{[m(X)]^2} + 1 \right\}$$



Expectation Operator

The expectation of a random variable (RV) X is defined as:

$$E[X] = \int_{\text{all } x} x f(x) dx$$

This expectation defines the centroidal axis of the pdf of X and also is known as the mean of X , $m(X) = E[X]$.

A common measure of the dispersion (i.e., spread) of the distribution of X about its mean is the variance of X :

$$\text{var}[X] = E\{[X - m(X)]^2\} = \int_{\text{all } x} [x - m(X)]^2 f(x) dx$$

Important Relationships:

For a RV X and a constant c :

$$\begin{aligned} E[cX] &= cE[X] & \text{var}[cX] &= c^2\text{var}[X] & \text{var}[X+c] &= \text{var}[X] \\ \text{var}(X) &= E(X^2) - [E(X)]^2 \end{aligned}$$

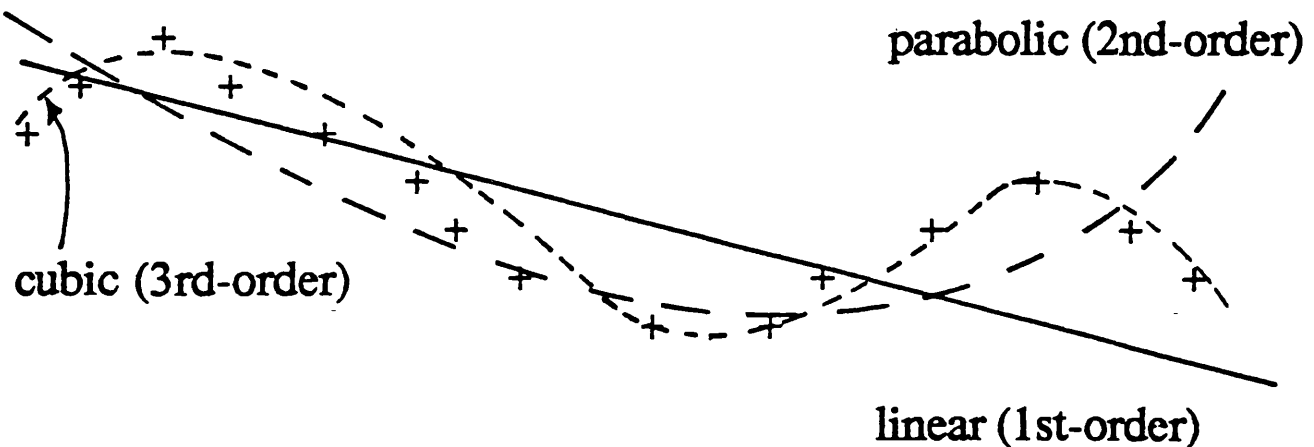
The standard deviation of X is the positive square root of the variance of X : $sd(X) = \sqrt{\text{var}(X)}$

The covariance of two RV's X and Y is :

$$\text{Cov}(X, Y) = E\{[X - m(X)][Y - m(Y)]\} = E[XY] - m(X)m(Y)$$

Trend Surface Modeling (a special case of multiple regression)

Goal: To describe a regional, best-fit trend and use it to estimate attribute values at unsampled locations. The fit is obtained via a least-squares linear (multiple) regression.



Trend Fit: A linear function of geographic coordinates of a set of observations defined such that the squared deviations (of the dependent variable) from the trend are minimized.

1st-order model:

$$y = b_0 + b_1 x_1 + b_2 x_2 = T_1$$

2nd-order model:

$$y = T_1 + b_3 x_1^2 + b_4 x_1 x_2 + b_5 x_2^2 = T_2$$

3rd-order model:

$$y = T_2 + b_6 x_1^3 + b_7 x_1^2 x_2 + b_8 x_1 x_2^2 + b_9 x_2^3$$

Typically, X_1 is easting coord. and X_2 is northing coord.

An m -th order trend model will have $(m+1)(m+2)/2$ coefficients.

If we let n = number of data points, and k = number of trend model coefficients excluding b_0 , then an ANOVA (Analysis of Variance) table for a given model can be set up as follows:

<u>Source of Variation</u>	<u>Sum of Squares</u>	<u>Degrees of Freedom</u>	<u>Mean Square</u>	<u>F-Statistic</u>
Regression	SS_R	k	$MS_R = SS_R/k$	$F = MS_R/MS_E$
Error	SS_E	$n-k-1$	$MS_E = SS_E/(n-k-1)$	
Total	SS_T	$n-1$		

If the regression effect is not significantly different from the random (error) effect, then 1) the spatial distribution of the dependent variable is random and independent of location, or 2) the distribution of the dependent variable may be dependent on location, but the wrong regression model was used. We can use a statistical F-test to evaluate this "significance of fit."

Hypothesis test: $H_0 : b_1 = b_2 = \dots = b_k = 0$

$H_a : b_1 \neq 0, b_2 \neq 0, \dots b_k \neq 0$

Reject H_0 if the computed "test" value of F ($F = MS_R/MS_E$) exceeds the tabled value of F for k d.f. in numerator and $n-k-1$ d.f. in denominator. A rejection implies that the regression fit is significant (i.e., it is meaningful and provides a reasonable model for the regional trend of the data set).

Example from data file TRENEX.DAT (2nd-order fit):

Calc. $F = 12.23$; Tabled $F_{.05, 5/5} = 5.05$; Therefore, Reject!

We conclude that the 2nd-order model is reasonable.

Notes: $n > k+1$; data set should avoid clusters; extrapolation poor

C:\MAIN>TRENFIT

*** FORTRAN PROGRAM FOR TREND SURFACE FIT ***

ENTER NAME OF INPUT DATA FILE: TRENEX.DAT

ENTER NAME OF OUTPUT FILE: DUMT

ENTER ORDER OF DESIRED SURFACE: 1 2 3 OR 4: 2

MSR, MSE, F: 102.1903 8.3552 12.231

DO YOU WANT TO EST. A POINT NOW--Y,N? Y

ENTER COORD. PAIR AT WHICH EST. IS DESIRED: 250 275

TREND-FIT ESTIMATE [X1,X2,Y]: 250.0000 275.0000 10.7607

DO YOU WANT ANOTHER PT. ESTIMATED--Y,N? N

Stop - Program terminated.

C:\MAIN>

C:\MAIN>

C:\MAIN>

C:\MAIN>TYPE DUMT

RESULTS OF TREND SURFACE FIT OF ORDER 2 FOR DATA FILE: TRENEX.DAT

NUMBER OF DATA PTS. = 11

B 0 -.632267E+02
 B 1 .506494E+00
 B 2 .403805E+00
 B 3 -.280125E-03
 B 4 -.210000E-02
 B 5 -.237983E-04

TREND MODEL, BY ORDER, IS:

$$Y = B_0 + B_1 \cdot X_1 + B_2 \cdot X_2 + B_3 \cdot X_1^{**2} + B_4 \cdot X_1 \cdot X_2 + B_5 \cdot X_2^{**2} + B_6 \cdot X_1^{**3} + B_7 \cdot X_2 \cdot X_1^{**2} + B_8 \cdot X_1 \cdot X_2^{**2} + B_9 \cdot X_2^{**3} + B_{10} \cdot X_1^{**4} + B_{11} \cdot X_2 \cdot X_1^{**3} + B_{12} \cdot X_1^{**2} \cdot X_2^{**2} + B_{13} \cdot X_1 \cdot X_2^{**3} + B_{14} \cdot X_2^{**4}$$

SOURCE OF VAR.	SUM OF SQS.	DEG. OF FR.	MEAN SQ.	F
REGRESSION	510.9515	5.	102.1903	12.231
ERROR	41.7758	5.	8.3552	
TOTAL	552.7273	10.		

COEF. OF MULTIPLE CORREL., R = .96147

TREND-FIT ESTIMATE [X1,X2,Y]: 250.0000 275.0000 10.7607

TABLE V Percentage Points of the *F* Distribution (continued) $F_{0.05, \nu_1, \nu_2}$

		Degrees of freedom for the numerator (ν_1)																		
ν_1	ν_2	1	2	3	4	5	6	7	8	9	10	12	15	20	24	30	40	60	120	∞
Degrees of freedom for the denominator (ν_2)	1	161.4	199.5	215.7	224.6	230.2	234.0	236.8	238.9	240.5	241.9	243.9	245.9	248.0	249.1	250.1	251.1	252.2	253.3	254.3
	2	18.51	19.00	19.16	19.25	19.30	19.33	19.35	19.37	19.38	19.40	19.41	19.43	19.45	19.45	19.46	19.47	19.48	19.49	19.50
	3	10.13	9.55	9.28	9.12	9.01	8.94	8.89	8.85	8.81	8.79	8.74	8.70	8.66	8.64	8.62	8.59	8.57	8.55	8.53
	4	7.71	6.94	6.59	6.39	6.26	6.16	6.09	6.04	6.00	5.96	5.91	5.86	5.80	5.77	5.75	5.72	5.69	5.66	5.63
	5	6.61	5.79	5.41	5.19	5.05	4.95	4.88	4.82	4.77	4.74	4.68	4.62	4.56	4.53	4.50	4.46	4.43	4.40	4.36
	6	5.99	5.14	4.76	4.53	4.39	4.28	4.21	4.15	4.10	4.06	4.00	3.94	3.87	3.84	3.81	3.77	3.74	3.70	3.67
	7	5.59	4.74	4.35	4.12	3.97	3.87	3.79	3.73	3.68	3.64	3.57	3.51	3.44	3.41	3.38	3.34	3.30	3.27	3.23
	8	5.32	4.46	4.07	3.84	3.69	3.58	3.50	3.44	3.39	3.35	3.28	3.22	3.15	3.12	3.08	3.04	3.01	2.97	2.93
	9	5.12	4.26	3.86	3.63	3.48	3.37	3.29	3.23	3.18	3.14	3.07	3.01	2.94	2.90	2.86	2.83	2.79	2.75	2.71
	10	4.96	4.10	3.71	3.48	3.33	3.22	3.14	3.07	3.02	2.98	2.91	2.85	2.77	2.74	2.70	2.66	2.62	2.58	2.54
	11	4.84	3.98	3.59	3.36	3.20	3.09	3.01	2.95	2.90	2.85	2.79	2.72	2.65	2.61	2.57	2.53	2.49	2.45	2.40
	12	4.75	3.89	3.49	3.26	3.11	3.00	2.91	2.85	2.80	2.75	2.69	2.62	2.54	2.51	2.47	2.43	2.38	2.34	2.30
	13	4.67	3.81	3.41	3.18	3.03	2.92	2.83	2.77	2.71	2.67	2.60	2.53	2.46	2.39	2.35	2.31	2.27	2.22	2.18
	14	4.60	3.74	3.34	3.11	2.96	2.85	2.76	2.70	2.65	2.60	2.53	2.46	2.39	2.35	2.31	2.27	2.22	2.18	2.13
	15	4.54	3.68	3.29	3.06	2.90	2.79	2.71	2.64	2.59	2.54	2.48	2.40	2.33	2.29	2.25	2.20	2.16	2.11	2.07
	16	4.49	3.63	3.24	3.01	2.85	2.74	2.66	2.59	2.54	2.49	2.42	2.35	2.28	2.24	2.19	2.15	2.11	2.06	2.01
	17	4.45	3.59	3.20	2.96	2.81	2.70	2.61	2.55	2.49	2.45	2.38	2.31	2.23	2.19	2.15	2.10	2.06	2.02	1.97
	18	4.41	3.55	3.16	2.93	2.77	2.66	2.58	2.51	2.46	2.41	2.34	2.27	2.19	2.15	2.11	2.06	2.03	1.98	1.93
	19	4.38	3.52	3.13	2.90	2.74	2.63	2.54	2.48	2.42	2.38	2.31	2.23	2.16	2.11	2.07	2.03	1.98	1.94	1.88
	20	4.35	3.49	3.10	2.87	2.71	2.60	2.51	2.45	2.39	2.35	2.28	2.20	2.12	2.08	2.04	1.99	1.95	1.90	1.84
	21	4.32	3.47	3.07	2.84	2.68	2.57	2.49	2.42	2.37	2.32	2.25	2.18	2.10	2.05	2.01	1.96	1.92	1.87	1.81
	22	4.30	3.44	3.05	2.82	2.66	2.55	2.46	2.40	2.34	2.30	2.23	2.15	2.07	2.03	1.98	1.94	1.89	1.84	1.78
	23	4.28	3.42	3.03	2.80	2.64	2.53	2.44	2.37	2.32	2.27	2.20	2.13	2.05	2.01	1.96	1.91	1.86	1.81	1.76
	24	4.26	3.40	3.01	2.78	2.62	2.51	2.42	2.36	2.30	2.25	2.18	2.11	2.03	1.98	1.94	1.89	1.79	1.73	1.70
	25	4.24	3.39	2.99	2.76	2.60	2.49	2.40	2.34	2.28	2.24	2.16	2.09	2.01	1.96	1.92	1.87	1.82	1.77	1.71
	26	4.23	3.37	2.98	2.74	2.59	2.47	2.39	2.32	2.27	2.22	2.15	2.07	1.99	1.95	1.90	1.85	1.80	1.75	1.69
	27	4.21	3.35	2.96	2.73	2.57	2.46	2.37	2.31	2.25	2.20	2.13	2.06	1.97	1.93	1.88	1.84	1.79	1.73	1.67
	28	4.20	3.34	2.95	2.71	2.56	2.45	2.36	2.29	2.24	2.19	2.12	2.04	1.96	1.91	1.87	1.82	1.77	1.71	1.65
	29	4.18	3.33	2.93	2.70	2.55	2.43	2.35	2.28	2.22	2.18	2.10	2.03	1.94	1.90	1.85	1.81	1.75	1.70	1.64
	30	4.17	3.32	2.92	2.69	2.53	2.42	2.33	2.27	2.21	2.16	2.09	2.01	1.93	1.89	1.84	1.79	1.74	1.68	1.62
	40	4.08	3.23	2.84	2.61	2.45	2.34	2.25	2.18	2.12	2.08	2.00	1.92	1.84	1.78	1.74	1.69	1.64	1.58	1.51
	60	4.00	3.15	2.76	2.53	2.37	2.25	2.17	2.10	2.04	1.99	1.92	1.84	1.75	1.70	1.65	1.59	1.53	1.47	1.39
	120	3.92	3.07	2.68	2.45	2.29	2.17	2.09	2.02	1.96	1.91	1.83	1.75	1.66	1.61	1.55	1.55	1.43	1.35	1.25
	∞	3.84	3.00	2.60	2.37	2.21	2.10	2.01	1.94	1.86	1.83	1.75	1.67	1.57	1.52	1.46	1.40	1.32	1.22	1.00

 $F_{0.05, \nu_1, \nu_2}$

		Degrees of freedom for the numerator (ν_1)																		
ν_1	ν_2	1	2	3	4	5	6	7	8	9	10	12	15	20	24	30	40	60	120	∞
Degrees of freedom for the denominator (ν_2)	1	4052	4999.5	5403	5625	5764	5859	5928	5982	6022	6056	6106	6157	6209	6235	6261	6287	6313	6339	6366
	2	98.50	99.00	99.17	99.25	99.30	99.33	99.36	99.37	99.39	99.40	99.42	99.43	99.45	99.46	99.47	99.47	99.48	99.49	99.50
	3	34.12	30.82	29.46	28.71	28.24	27.91	27.67	27.49	27.35	27.23	27.05	26.87	26.69	26.00	26.50	26.41	26.32	26.22	26.13
	4	21.20	18.00	16.69	15.98	15.52	15.21	14.98	14.80	14.66	14.55	14.37	14.20	14.02	13.93	13.84	13.75	13.65	13.56	13.46
	5	16.26	13.27	12.06	11.39	10.97	10.67	10.46	10.29	10.16	10.05	9.89	9.72	9.55	9.47	9.38	9.29	9.20	9.11	9.02
	6	13.75	10.92	9.78	9.15	8.75	8.47	8.26	8.10	7.98	7.87	7.72	7.56	7.40	7.31	7.23	7.14	7.06	6.97	6.88
	7	12.25	9.55	8.45	7.85	7.46	7.19	6.99	6.84	6.72	6.62	6.47	6.31	6.16	6.07	5.99	5.91	5.82	5.74	5.65
	8	11.26	8.65	7.59	7.01	6.63	6.37	6.18	6.03	5.91	5.81	5.67	5.52	5.36	5.20	5.12	5.03	4.95	4.86	4.76
	9	10.56	8.02	6.99	6.42	6.06	5.80	5.61	5.47	5.35	5.26	5.11	4.96	4.81	4.73	4.65	4.57	4.48	4.40	4.31
	10	10.04	7.56	6.55	5.99	5.64	5.39	5.20	5.06	4.94	4.85	4.71	4.56	4.41	4.33	4.25	4.17	4.08	4.00	3.91
	11	9.65	7.21	6.22	5.67	5.32	5.07	4.89	4.74	4.63	4.54	4.40	4.25	4.10	4.02	3.94	3.86	3.78	3.69	3.60
	12	9.33	6.93	5.95	5.41	5.06	4.82	4.64	4.50	4.39	4.30	4.16	4.01	3.86	3.78	3.70	3.62	3.54	3.45	3.36
	13	9.07	6.70	5.74	5.21	4.86	4.62	4.44	4.30	4.19	4.10	3.96	3.82	3.66	3.51	3.43	3.35	3.27	3.18	3.09
	14	8.86	6.51	5.56	5.04	4.69	4.46	4.28	4.14	4.03	3.94	3.80	3.66	3.51	3.43	3.35	3.27	3.18	3.09	3.00
	15	8.68	6.36	5.42	4.89	4.36	4.32	4.14	4.00	3.89	3.80	3.67	3.52	3.37	3.29	3.21	3.13	3.05	2.96	2.87
	16	8.53	6.23	5.29	4.77	4.44	4.20	4.03	3.89	3.78	3.69	3.55	3.41	3.26	3.18	3.10	3.02	2.93	2.84	2.75
	17	8.40	6.11	5.18	4.67	4.34	4.10	3.93	3.79	3.68	3.59	3.46	3.31	3.16	3.08	3.00	2.92	2.83	2.75	2.65
	18	8.29	6.01	5.09	4.58	4.25	4.01	3.84	3.71	3.54	3.41	3.30	3.21	3.07	2.93	2.78	2.70	2.62	2.54	2.45
	19	8.18	5.93	5.																

Regionalized Variables and Spatial Dependence

A regionalized variable is a type of random variable that is distributed over space and, as such, it must be sampled over space at various locations. Let u be a location vector defined by the 3-D cartesian coordinates (u, v, w) , which is analogous to an (x, y, z) coordinate. Then:

$X(u)$ is a regionalized variable (ReV),
 $X(u_i)$ is a random variable at location u_i , and
 $x(u_i)$ is a data value for the ReV at location u_i .

A spatial random function is a set or collection of ReV's (i.e., an indexed ReV). Thus, a ReV is one realization of the random function (RF). In the general case, the spatial attribute of interest is modeled as a random function (e.g., soil thickness, gold grade, piezometric head, contaminant concentration).

Consider a pair of locations u_i and u_i+h , where h is the separation distance between the two locations. Then, the corresponding $X(u_i)$ and $X(u_i+h)$ usually are not independent but are related by some type of spatial dependence. A shorter separation distance results in a greater dependence. This behavior is common to spatial attributes in natural systems, as well as in man-made constructed systems (e.g., highway subgrades & pavements, earth fills, clay liners).

In a traditional statistical sense many realizations of the pair, $[X(u_i), X(u_i+h)]$ are required to make statistical inferences. However, this is impractical!! Instead, we must depend on the averaging of pairs over the region, pairs separated by a defined h . To "trust" this averaging, we must accept stationarity assumptions.

Types of Stationarity Assumptions:

1. Strict stationarity -- A random function is stationary if its spatial law is invariant under translation. That is, its pdf and spatial covariance are independent of location.
2. Second-order stationarity (covariance stationarity) -- A random function is 2nd-order stationary if its mathematical expectation exists and does not depend on location, and if the covariance exists for each pair of RV's $[X(u_i), X(u_i+h)]$ and depends only on the separation distance h .
3. Weak second-order stationarity (intrinsic hypothesis) -- A random function follows the intrinsic hypothesis if its mathematical expectation exists and does not depend on location, and if for all h the increment $[X(u_i) - X(u_i+h)]$ has finite variance that does not depend on location.
4. Local stationarity -- A restriction of 2nd-order or weak 2nd-order stationarity to a local neighborhood in which $h \leq$ some limit. Almost all natural phenomena can be modeled as RF's with at least a locally stationary hypothesis.

IMPORTANT : Stationarity is a property/characteristic of the model, not of the actual data set.

Because proper identification of averaging areas is critical to a geostatistical evaluation, the first step in the study should be an exploratory data analysis, where the data set is investigated for spatial trends, discontinuities, and patterns.

Exploratory Data Analysis

1. Consider the scale of measurements and the size of areas over which spatial averaging should occur.

Tools: contour plots
 profiles and fence diagrams
 moving-window statistics (mean, median, s.d.)

Look for trends and discontinuities. If data are abundant, then averaging over smaller areas is appropriate. However, if data are sparse, then one single area may be appropriate.

2. Generate means, variances, histograms, cumulative frequency plots, etc., for each of the selected averaging areas. If data locations are clustered in preferentially low-valued or high-valued areas, then simple equal-weighted averaging or histogram development produces biased estimates.

One way to decluster the data set and account for data redundancy is:

$$\text{est. of mean: } \bar{x}_A = \frac{1}{|A|} \sum_{j=1}^N w_j x(u_j)$$

$$\text{est. of cum freq. fnc.: } \hat{F}_A(x) = \frac{1}{|A|} \sum_{j=1}^N w_j i(u_j ; x)$$

where: $|A|$ = Area under study, w_j = area of infl. polygon at j ,

$$\sum_{j=1}^N w_j = |A| \quad \text{and} \quad i(u_j ; x) = \begin{cases} 1, & \text{if } x(u_j) \leq x \\ 0, & \text{if } x(u_j) > x \end{cases}$$

3. Data transforms may be helpful. Highly skewed data have statistics that are influenced heavily by the extreme values in the data set. One way to mitigate that influence is to use monotonous data transforms (i.e., maintain the data ranks).

Examples: log, ln, rank, uniform-rank, normal-score transforms

Description of Spatial Dependence

Spatial covariance function:

$$\begin{aligned} C(h) &= E[(X(u) - E[X(u)])(X(u+h) - E[X(u+h)])] \\ &= E[X(u)X(u+h)] - \{E[X(u)]\}^2 \quad (\text{assume constant mean}) \end{aligned}$$

$$\widehat{C}(h) = \frac{1}{N(h)} \sum_{i=1}^{N(h)} x_i x_{i+h} - \left[\frac{1}{n} \sum_{i=1}^n x_i \right]^2 \quad \text{This is a biased est.!}$$

$$\widehat{C}(h) = \frac{1}{N(h)} \sum_{i=1}^{N(h)} x_i x_{i+h} - m(x_{-h}) m(x_{+h}) \quad \text{This is preferred!}$$

where: n = total number of data

$N(h)$ = number of data pairs with locations h apart

$m(x_{-h})$ = mean of data values located $-h$ from others

$m(x_{+h})$ = mean of data values located $+h$ from others

Variogram function:

$$\gamma(h) = \frac{1}{2} E[(X(u) - X(u+h))^2] \quad \text{Often called "semivariogram"}$$

$$\widehat{\gamma}(h) = \frac{1}{2N(h)} \sum_{i=1}^{N(h)} (x_i - x_{i+h})^2$$

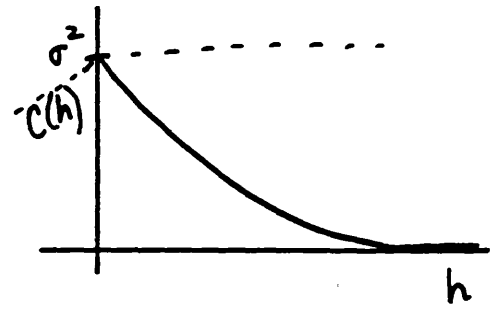
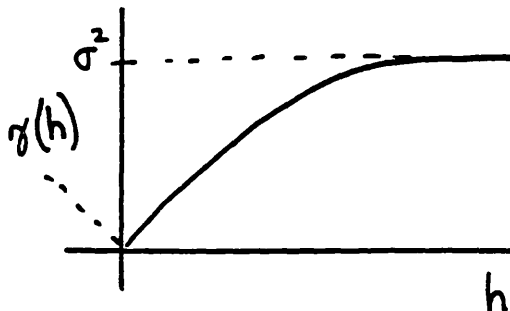
Under an assumption of covariance stationarity, the variogram and covariance functions are related as follows:

$$\begin{aligned}
 \gamma(h) &= \frac{1}{2} E[\{X(u) - X(u+h)\}^2] \\
 &= \frac{1}{2} E[\{X(u) - m - [X(u+h) - m]\}^2] \\
 &= \frac{1}{2} E[\{X(u) - m\}^2 + \{X(u+h) - m\}^2 - 2\{X(u) - m\}\{X(u+h) - m\}] \\
 &= \underbrace{\frac{1}{2} \left[E\{[X(u) - m]^2\} + E\{[X(u+h) - m]^2\} \right]}_{\sigma^2} - \underbrace{2E\{[X(u) - m][X(u+h) - m]\}}_{C(h)}
 \end{aligned}$$

where $\sigma^2 = \text{Var}[X(u)]$

$$\gamma(h) = \frac{1}{2} [2\sigma^2 - 2C(h)]$$

$$\gamma(h) = \sigma^2 - C(h)$$



ESTIMATION OF THE VARIOGRAM FUNCTION

16

GENERAL CASE FOR IRREGULARLY SPACED DATA :

FOR h MEASURED IN A GIVEN DIRECTIONAL WINDOW,

$$\hat{\gamma}(h) = \frac{\sum_{\text{ALL PAIRS}} w(|u_i - u_j| - h) * \frac{1}{2} [\chi(u_i) - \chi(u_j)]^2}{\sum_{\text{ALL PAIRS}} w(|u_i - u_j| - h)}$$

WHERE i, j denote a unique pair of data locations
for each increment of i or j

$w(\cdot)$ = weighting fnc. to appropriately
average contributions from the
irregularly spaced data pairs

EXAMPLES OF WEIGHTING FNC.'S :

1. inverse square - $w(y_i - h) = \frac{1}{(y_i - h)^2}$

2. uniform - $w(y_i - h) = \begin{cases} 1, & \text{if } |y_i - h| < \frac{\text{CLASS SIZE}}{2} \\ 0, & \text{otherwise} \end{cases}$

3. Gaussian - $w(y_i - h) = e^{-\frac{(y_i - h)^2}{2c^2}}$

NOTE : GEOEAS software
uses a lag-mean approach
rather than a lag-centered approach.

where c
is a constant
so that the
effective averaging
width = $2.5c$.

RULES OF THUMB :

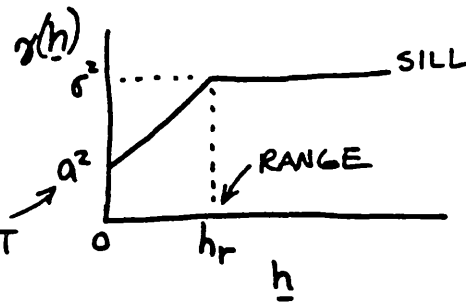
1. No. of pairs used at any computational lag ≥ 25 or 30 .
2. Maximum lag $\lesssim \frac{L}{2}$, where L is max. dimen. of study region.

COMMONLY USED VARIOGRAM MODELS

17

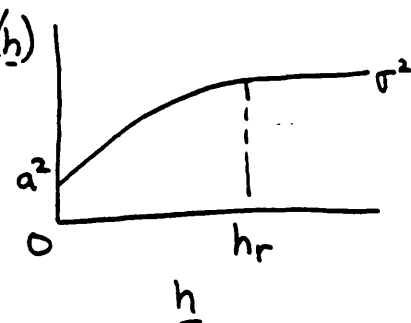
A. MODELS WITH A SILL (COV. STATIONARITY)

SIMPLE TRANSITIVE MODEL (LINEAR WITH SILL) NUGGET



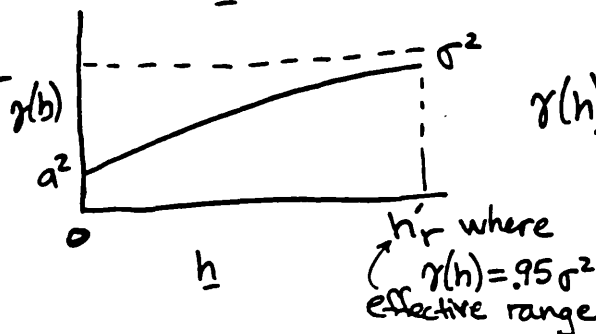
$$\gamma(h) = \begin{cases} a^2 + (\sigma^2 - a^2) \frac{h}{h_r}, & \text{if } 0 \leq h \leq h_r \\ \sigma^2, & \text{if } h \geq h_r \end{cases}$$

SPHERICAL MODEL



$$\gamma(h) = \begin{cases} a^2 + (\sigma^2 - a^2) \left[\frac{3h}{2h_r} - \frac{1}{2} \frac{h^3}{h_r^3} \right], & \text{if } 0 \leq h \leq h_r \\ \sigma^2, & \text{if } h > h_r \end{cases}$$

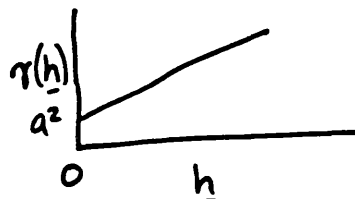
EXPONENTIAL MODEL



$$\gamma(h) = a^2 + (\sigma^2 - a^2) (1 - e^{-\frac{h}{c}}), \quad \text{for } h \geq 0 \quad \& \quad c = \text{constant related to } h_r$$

B. MODELS WITHOUT A SILL (INTRINSIC HYPOTHESES)

LINEAR MODEL



$$\gamma(h) = a^2 + ch, \quad \text{for } h \geq 0 \quad \& \quad c = \text{constant}$$

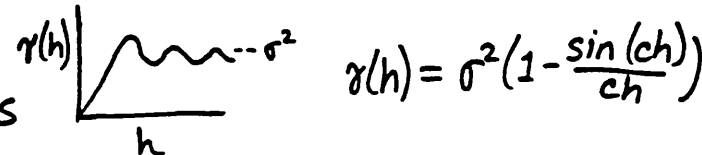
LOGARITHMIC MODEL



$$\gamma(h) = a^2 + c \ln(h), \quad \text{for } h \geq 0 \quad \& \quad c = \text{constant}$$

C. SPECIAL MODELS

HOLE-EFFECT (PERIODIC) MODELS



$$\gamma(h) = \sigma^2 \left(1 - \frac{\sin(ch)}{ch} \right)$$

EXAMPLE VARIOGRAM COMPUTATION

LET THE NUMBER OF FRACTURES PER 10' CORE RUN BE CONSIDERED AS A REGIONALIZED VARIABLE

DATA VALUES COLLECTED AT REGULAR 10' INTERVALS ARE GIVEN AS FOLLOWS:

(18
(16
(14
(15
(19
(17
(21
(20

FOR $h = 10$ ft :

$$\hat{\gamma}(10) = \frac{1}{2} \cdot \frac{1}{7} [2^2 + 2^2 + 1^2 + 4^2 + 2^2 + 4^2 + 1^2] = \underline{\underline{3.3}}$$

FOR $h = 20$ ft :

$$\hat{\gamma}(20) = \frac{1}{2} \cdot \frac{1}{6} [4^2 + 1^2 + 5^2 + 2^2 + 2^2 + 3^2] = \underline{\underline{4.9}}$$

FOR $h = 30$ ft :

$$\hat{\gamma}(30) = \frac{1}{2} \cdot \frac{1}{5} [3^2 + 3^2 + 3^2 + 6^2 + 1^2] = \underline{\underline{6.4}}$$

FOR $h = 40$ ft :

$$\hat{\gamma}(40) = \frac{1}{2} \cdot \frac{1}{4} [1^2 + 1^2 + 7^2 + 5^2] = \underline{\underline{9.5}}$$

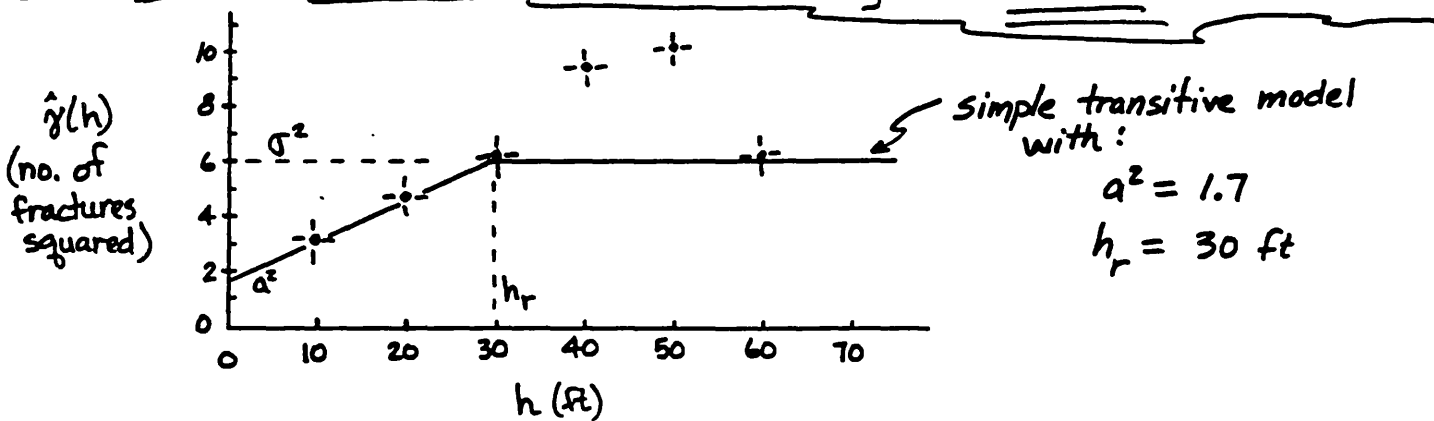
$$\begin{aligned} n &= 8 \\ \bar{x} &= 17.5 \\ s^2 &= 6.0 \end{aligned}$$

FOR $h = 50$ ft :

$$\hat{\gamma}(50) = \frac{1}{2} \cdot \frac{1}{3} [1^2 + 5^2 + 6^2] = \underline{\underline{10.3}}$$

FOR $h = 60$ ft :

$$\hat{\gamma}(60) = \frac{1}{2} \cdot \frac{1}{2} [3^2 + 4^2] = \underline{\underline{6.3}}$$



As part of a geotechnical site investigation, SPT blow counts in 11 drill holes are recorded for a known layer of SW soil (Unif. Soil Classif. System). The drilling pattern and the measured blow counts are given below. Compute the omnidirectional variogram for lags less than 150 m.

+17
○^A | 100 m |
+34 +23 +8

+22 +23 +19

+11 +25 +27

+27

Characteristics of Spatial Interpolation Schemes

1. Should use a distance measure -- +
 - IAD (inverse absolute distance) +
 - IDS (inverse distance squared) ○
 - Polygonal/triangulation +
 - Moving-Window Average +
 - Linear Krigings (general set of linear least-sq. schemes) ○
 - Conditional Krigings (non-least-sq.) ○

2. Should apply to specific phenomenon -- +
 - "Intelligent" IAD or IDS +
 - Customized Moving-Window Average +
 - All Krigings ← →
spatial continuity

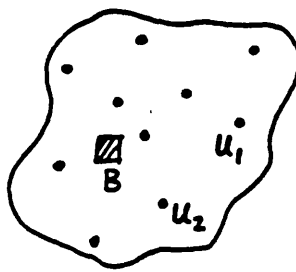
3. Should account for data redundancy -- +
 - All Krigings ○
 - + ← → ○

4. Should account for data values, as well as for their locations, when used to derive the weights -- +
 - Conditional Krigings (Indicator Kriging, Probability Kriging, Multigaussian Kriging) ○
 - + ← → +

5. Should provide a measure of local accuracy (reliability of estimate) that depends on data values, as well as on data configuration. +
 - Conditional Krigings ○

ORDINARY LINEAR KRIGING (COV. STATIONARITY ASSUMED)

REGION OF
INTEREST :



Let:

u_i = location

$x(u_i)$ = sample value at
location u_i

n = no. of sample values
(data)

GOAL: TO PREDICT THE AVERAGE VALUE OF THE
BLOCK B , WHICH CAN BE A VOLUME, AREA,
OR POINT.

↳ PUNCTUAL KRIGING, or
POINT KRIGING

DEFINE THE FOLLOWING:

1. "TRUE" AVERAGE VALUE
OF B $\rightarrow \bar{V}_B = \frac{1}{B} \int_B X(u) du$

2. ESTIMATED AVERAGE VALUE
OF B $\rightarrow \hat{V}_B = \sum_{i=1}^n a_i x(u_i)$

subject to $\sum_{i=1}^n a_i = 1$

(a_i = weights with values based on the
 x_i locations relative to B)

3. ESTIMATION VARIANCE

$$\sigma_E^2 = E \left[(\bar{V}_B - \hat{V}_B)^2 \right]$$

KRIGING IS A GEOSTATISTICAL PROCEDURE TO ESTIMATE
THE VALUE OF A BLOCK BY USING A WEIGHTED,
LINEAR COMBINATION OF DATA VALUES SUCH THAT THE
ESTIMATE IS UNBIASED AND HAS MINIMUM ESTIMATION VARIANCE.

DEVELOPMENT OF KRIGING EQUATIONS

$$\sigma_E^2 = E[(\hat{V}_B - \hat{\hat{V}}_B)^2] = E\left\{\left[\frac{1}{B} \int_B X(u) du - \sum_{i=1}^n a_i x(u_i)\right]^2\right\}$$

$$\sigma_E^2 = E\left\{\left[\frac{1}{B} \int_B X(u) du - \sum_{i=1}^n a_i x(u_i)\right]^2\right\} + 2\lambda \left(\sum_{i=1}^n a_i - 1\right)$$

•
•
•
•

Lagrange Multiplier
(a "slack" term to allow for
the subject condition $\sum a_i = 1$)

$$\sigma_E^2 = C_{BB} + \sum_{i=1}^n \sum_{j=1}^n a_i a_j C_{ij} - 2 \sum_{i=1}^n a_i C_{Bi} + 2\lambda \left(\sum_{i=1}^n a_i - 1\right)$$

MINIMIZE σ_E^2 BY TAKING THE PARTIAL DERIVATIVE
WITH RESPECT TO a_i AND SETTING IT EQUAL TO ZERO.

$$\frac{\partial (\sigma_E^2)}{\partial a_i} = 0$$

$$2 \sum_{j=1}^n a_j C_{ij} - 2 C_{Bi} + 2\lambda = 0$$

where: C_{BB} = covar. between pts. in B

C_{ij} = covariance between values
at locations u_i & u_j

$$= \text{Cov}[X(u_i), X(u_j)]$$

C_{Bi} = covariance between values
at the block and
location x_i

$$\sum_{j=1}^n a_j C_{ij} + \lambda = C_{Bi}$$

$$\sum_{i=1}^n a_i = 1$$

← SYSTEM OF $n+1$ EQUATIONS
USED TO SOLVE FOR
THE KRIGING WEIGHTS.

KRIGING EQUATIONS IN MATRIX NOTATION:

$$\left[\begin{array}{cccccc} C_{11} & C_{12} & C_{13} & \cdots & C_{1n} & 1 \\ C_{21} & C_{22} & C_{23} & \cdots & C_{2n} & 1 \\ \vdots & \vdots & \vdots & \ddots & \vdots & \vdots \\ C_{n1} & C_{n2} & C_{n3} & \cdots & C_{nn} & 1 \\ 1 & 1 & 1 & \cdots & 1 & 0 \end{array} \right] \left[\begin{array}{c} a_1 \\ a_2 \\ \vdots \\ a_n \\ \lambda \end{array} \right] = \left[\begin{array}{c} C_{B1} \\ C_{B2} \\ \vdots \\ C_{Bn} \\ 1 \end{array} \right]$$

$\underbrace{\phantom{C_{11} \quad C_{12} \quad C_{13} \quad \cdots \quad C_{1n} \quad 1}}_{C} \quad \underbrace{}_{A} \quad \underbrace{\phantom{C_{B1} \\ C_{B2} \\ \vdots \\ C_{Bn} \\ 1}}_{C_{Bi}}$

$$CA = C_{Bi}$$

$$\hat{A} = C^{-1} C_{Bi}$$

AFTER SOLVING FOR THE WEIGHTS, THE ESTIMATED VALUE OF THE BLOCK IS GIVEN BY:

$$\begin{aligned} \hat{V}_B &= \sum_{i=1}^n \hat{a}_i x(u_i) \\ &= \hat{a}_1 x(u_1) + \hat{a}_2 x(u_2) + \cdots + \hat{a}_n x(u_n) \end{aligned}$$

THE ESTIMATION VARIANCE FOR THE BLOCK CAN ALSO BE CALCULATED:

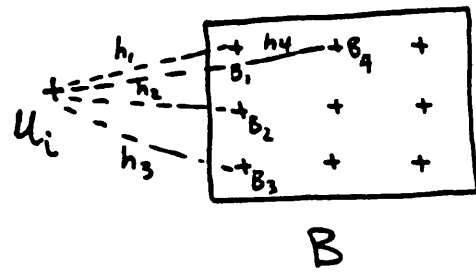
$$\hat{\sigma}_E^2 = \sigma_k^2 = C_{BB} - \sum_{i=1}^n \hat{a}_i C_{Bi} - \hat{\lambda}$$

\uparrow KRIGING VARIANCE

$$\sigma_k^2 = C_{BB} - \hat{A}^T C_{Bi} \quad (\text{matrix form})$$

IN PRACTICE, THE NUMBER OF DATA (n) USED IN THE KRIGING ESTIMATION IS LIMITED SO THAT ONLY THOSE DATA LOCATIONS WITHIN A RANGE OF INFLUENCE OF THE BLOCK LOCATION ARE USED.

- * C_{ij} values are obtained from the estimated variogram or spatial covariance fnc.
- * C_{Bi} values are obtained by averaging the covariances between 9, 16, or 25 points in the block with each i -th data point



$$\hat{C}_{Bi} = \frac{1}{q} \sum_{j=1}^q \text{Cov}(x_i, B_j)$$

- * C_{BB} is a constant value for all blocks of identical dimensions; it is obtained by averaging the covariances between 9, 16, or 25 points within the block.

Example : $\hat{C}_{BB} = \frac{1}{81} \sum_{i=1}^9 \sum_{j=1}^9 \text{Cov}(B_i, B_j)$

The mean covariance of all lags contained in B.

FOR POINT KRIGING, $\hat{C}_{BB} = \hat{\sigma}_{\text{pop}}^2 = \hat{C}(0)$

KRIGING IS AN EXCELLENT MAPPING TOOL BECAUSE IT PROVIDES INTERPOLATED ESTIMATES THAT ARE UNBIASED AND HAVE MINIMUM ESTIMATION VARIANCE; IT ALSO PROVIDES A PREDICTION OF HOW GOOD THE ESTIMATES ARE VIA THE σ_k^2 VALUES.

POINT KRIGING EXAMPLE

25

REGIONALIZED VARIABLE TO BE ESTIMATED: YOUNG'S MODULUS (E) OF INTACT ROCK

THE AVAILABLE DATA SET OF E VALUES IS USED TO ESTIMATE A VARIOGRAM WHICH IS WELL FITTED BY A SIMPLE TRANSITIVE MODEL WITH:

Use equation $\gamma(h) = \begin{cases} a^2 + (\sigma^2 - a^2) \frac{h}{h_r}, & \text{for } h \leq h_r \\ \sigma^2, & \text{for } h > h_r \end{cases}$

for 2-D case

$$= \begin{cases} 18 + 47\left(\frac{h}{h_r}\right), & \text{for } h \leq 30 \text{ m} \\ 65, & \text{for } h > 30 \text{ m} \end{cases}$$

NOTE:
 $C(h) = \sigma^2 - \gamma(h)$

THREE NEARBY DATA VALUES WILL BE USED TO KRIGE A VALUE AT LOCATION $x_0 (20, 20)$.

NOTE:
 $E(y) = 51 \text{ GPa}$

$$\begin{array}{c} x_2 = 43 \text{ GPa} \\ u_2 (15, 25) \\ x_0 = ? \\ u_0 (20, 20) \\ x_3 = 58 \text{ GPa} \\ u_3 (40, 15) \\ u_1 (10, 10) \\ x_1 = 52 \text{ GPa} \end{array}$$

$$\begin{array}{l} h_{01} = \sqrt{10^2 + 10^2} = 14.1 \text{ m} \quad C(h_{01}) = 24.9 \\ h_{02} = \sqrt{5^2 + 5^2} = 7.1 \text{ m} \quad C(h_{02}) = 35.9 \\ h_{03} = \sqrt{20^2 + 5^2} = 20.6 \text{ m} \quad C(h_{03}) = 14.7 \\ h_{12} = \sqrt{5^2 + 15^2} = 15.8 \text{ m} \quad C(h_{12}) = 22.2 \\ h_{13} = 30.4 \text{ m} \quad C(h_{13}) = 0 \\ h_{23} = 26.9 \text{ m} \quad C(h_{23}) = 4.9 \end{array}$$

KRIGING EQUATIONS:

$$\begin{bmatrix} 65 & 22.2 & 0 & 1 \\ 22.2 & 65 & 4.9 & 1 \\ 0 & 4.9 & 65 & 1 \\ 1 & 1 & 1 & 0 \end{bmatrix} \begin{bmatrix} a_1 \\ a_2 \\ a_3 \\ \lambda \end{bmatrix} = \begin{bmatrix} 24.9 \\ 35.9 \\ 14.7 \\ 1 \end{bmatrix}$$

SOLUTION:

$$\begin{array}{l} a_1 = .265 \\ a_2 = .495 \\ a_3 = .240 \\ \lambda = -3.326 \end{array}$$

$$V_0 = .265(52 \text{ GPa}) + .495(43 \text{ GPa}) + .240(58 \text{ GPa}) = \underline{\underline{49 \text{ GPa}}}$$

$$\sigma_k^2 = 65 - [.265(24.9) + .495(35.9) + .240(14.7) - 3.326] = \underline{\underline{40.4 \text{ (GPa)}^2}}$$

CONDITIONAL TYPES OF KRIGING

Indicator Kriging (IK)

A reasonable approach to modeling the uncertainty about any spatial $X(\underline{u})$ estimate is to obtain an estimate of the CDF at \underline{u} , given the available information or data set :

$$F[(\underline{u}; x) | \text{Info}(n)] = \text{Prob}[X(\underline{u}) \leq x | \text{Info}(n)]$$

It can be shown that this local conditional/ CDF is equivalent to the expectation of the indicator function:

$$E[I(\underline{u}; x) | \text{Info}(n)] = F[(\underline{u}; x) | \text{Info}(n)]$$

where: n is the number of data

x is a value taken on by $X(\underline{u})$

$I(\underline{u}; x)$ takes on values according to the indicator transform of $x(\underline{u})$:

$$i(\underline{u}; x) = \begin{cases} 1, & \text{if } x(\underline{u}) \leq x \\ 0, & \text{if } x(\underline{u}) > x \end{cases} \quad \begin{matrix} \text{(i.e., } x \text{ is a} \\ \text{threshold value)} \end{matrix}$$

We estimate this CDF at location \underline{u} for a given value x according to:

$$\hat{F}[(\underline{u}; x) | \text{Info}(n)] = I^*[(\underline{u}; x) | \text{Info}(n)] = \sum_{j=1}^N a_j(\underline{u}; x) \cdot i(\underline{u}_j; x)$$

where the a_j 's are weights assigned to N surrounding indicator-transformed data values.

To solve for these weights we must:

1. Transform original data values to indicator (0 or 1) values using threshold x .
2. Compute the estimated indicator variogram, $\hat{\gamma}_i(h; x)$
3. Use the indicator data and indicator variogram in a kriging system to solve for the indicator weights

We can repeat steps 1 - 3 for several different x threshold values and thus provide a discretized estimate of the local conditioned CDF of X .

Notes:

1. Remember: $\sum a_j = 1.0$
2. For K thresholds (x_k for $k = 1, 2, \dots, K$) we need to model K indicator variograms and conduct K indicator krigings